Optimal Multi-Year Management of Regional Water Resources Systems under Uncertainty

Mashor Housh

Optimal Multi-Year Management of Regional Water Resources Systems under Uncertainty

Research Thesis
In Partial Fulfillment of the
Requirements for the
Degree of Doctor of Philosophy

Mashor Housh

Submitted to the Senate of
the Technion – Israel Institute of Technology

Av, 5771 Haifa July, 2011

Dedication

I dedicate this dissertation

to all my teachers, my parents, my beloved wife Suzanne and my dearest daughter Julia

Acknowledgments

This research was conducted under the joint-supervision of Professor Avi Ostfeld and Professor Uri Shamir at the Faculty of Civil and Environmental Engineering.

I am deeply grateful to Professor Avi Ostfeld and Professor Uri Shamir, my teachers, advisors, mentors, and friends. Their support, advice, and encouragement were crucial to my research in general and to this dissertation in particular.

Avi and Uri, I cannot thank you enough.

Special place in my heart is reserved to my first role model – Jihad Zoubi, from Kfar-Manda high-school, for providing me not only with knowledge, but also with tools to educate myself.

I am indebted to all my teachers at Kfar-Manda high-school for providing me the education to success and excel at the Technion's undergraduate studies and to my teachers at the Technion for their contribution and support over the duration of my undergraduate and PhD studies.

The generous financial help of the Technion is gratefully acknowledged. I am obliged to Professor Yakov Ben-Haim for his advice on the Info-Gap method, to Professor Aharon Ben-Tal for his valuable advice on the Robust Optimization method, and to Mr. Miki Zaide for providing the data on the Israeli National Water System.

My thanks to my friends, Dr. Jack Hadad, Eng. Waseem Khouri, Dr. Robert Ishaq and and Dr. Lina Sela. Not forgetting my friend and office partner Jonathan Arad for the very interesting conversations we had over lunch, the insights he provided for the dissertation and publications, helping me understand how to trade options, and much more.

I also wish to express my love and gratitude to my beloved family for their understanding and support throughout the duration of my studies; my parents, brothers, and sisters for their endless love and encouragement. But most importantly, to my dearest wife Suzanne, whose love and support I treasure more than anything in the world.

Table of Contents

Abstract 1

List of Symbols 3

List of Abbreviation 7

1. Introduction 9
    - 1.1. Motivation 9
    - 1.2. Objectives and Contribution 11
    - 1.3. Dissertation Outline 13
2. Literature Survey and Methodology 15
    - 2.1. Deterministic Models 15
        - 2.1.1. Introduction 15
        - 2.1.2. Water management models 15
        - 2.1.3. The Israeli National Water System (INWS) 21
        - 2.1.4. Management models applied to the INWS 24
    - 2.2. Models that consider Uncertainty 25
        - 2.2.1. Introduction 25
        - 2.2.2. Optimization under uncertainty 26
        - 2.2.3. Water systems under uncertainty 33
        - 2.2.4. Infrastructure management under uncertainty 41
3. Deterministic Model 46
    - 3.1. Introduction 46
    - 3.2. Background and Motivation 46
    - 3.3. Model Outline 48
    - 3.4. Model Components 48
        - 3.4.1. Objective Function 50
        - 3.4.2. Constraints 51
    - 3.5. Optimization Plan 56
        - 3.5.1. Eliminating Dependent Variables 57
        - 3.5.2. Resultant Variables 59
    - 3.6. Evaluating the Objective Function and the Constraints 62
    - 3.7. The Optimization Solver 63
        - 3.7.1. Optimization Software 63
    - 3.8. Illustrative Example 63

3.9. Large WSS Example 72
3.10. The Time Chain Method (TCM) 80
3.10.1. Gradient estimation 80
3.10.2. Estimating the Jacobian of the nonlinear constraints 82
3.10.3. Efficiency of the TCM scheme 85
3.11. Scaling 87
3.12. Model User Interface 87
4. Scenario based Stochastic Programming 89
4.1. Introduction 89
4.2. General stochastic model 89
4.2.1. The Expected Value approach 91
4.2.2. The Penalty approach: 91
4.2.3. The Worst Case approach 92
4.2.4. The Value at risk approach: 92
4.2.5. The Mean-Variance approach 93
4.3. Scenarios based Stochastic Programming 93
4.3.1. Generation of scenario trees 94
4.4. Wait-and-See approach 95
4.4.1. Example 1 96
4.4.2. Example 2 99
4.5. Mean-Variance tradeoff 100
4.5.1. Example 102
4.6. External problem for tradeoff generation 105
4.6.1. Example 106
4.7. The Here-and-Now approach 107
4.7.1. Example 108
4.8. Two stage Stochastic Programming 109
4.9. Multi-stage Stochastic Programming (MSP) 110
4.9.1. Implementation of MSP 112
4.10. Limited Multistage Stochastic Programming (LMSP) 113
4.10.1. LMSP vs. Scenarios reduction 115
4.10.2. K-means clustering 117
4.10.3. Illustrative example 118
4.10.4. Example 1 120

4.10.5. Example 2 122
4.10.6. Example 3 (Large scale example) 125
4.11. Generalized LMSP (GLMSP) 128
5. Robust Optimization 130
5.1. Introduction 130
5.2. Robust Counterpart (RC) approach 131
5.2.1. Robust counterpart of an uncertain linear program 132
5.2.2. Why ellipsoidal uncertainty? 134
5.2.3. Probability guarantees of RC 135
5.3. Management model of a Water Supply System (WSS) 136
5.3.1. Mathematical model 138
5.4. Applying the RC approach 141
5.4.1. Constructing the uncertainty set 141
5.4.2. Formulation of the RC 142
5.5. Examples 144
5.5.1. Problem data 144
5.5.2. RC solution and Simulation results 145
5.6. Folding Robust Counterpart (FRC) 150
5.6.1. Multistage Stochastic Programming (MSP) 150
5.6.2. Folding horizon simulation 152
5.6.3. Simulation results 153
5.7. Ambiguous chance constraints (Example) 154
5.8. Application to the large WSS system 156
6. Info-Gap model 158
6.1. Introduction 158
6.2. One year model 158
6.2.1. Robustness functions 159
6.2.2. Example 1 162
6.2.3. Optimization 164
6.2.4. Example 2 164
6.2.5. Example 3 167
6.3. Multi-year model 169
6.3.1. Robustness functions 169
6.3.2. Example 171

6.4. Discussion 1 174
6.5. Discussion 2 176
7. Conclusions 179
7.1. Research Contributions 179
7.1.1. Water Supply System (WSS) model 179
7.1.2. Optimization 179
7.1.3. Optimization under uncertainty 180
7.2. Summary and Conclusions 180
7.2.1. Deterministic Model 180
7.2.2. Stochastic Models 182
7.2.3. RC Methodology 183
7.2.4. Info-Gap Methodology 183
7.2.5. Main Conclusions 185
7.3. Future Research 186
7.3.1. Deterministic Model 186
7.3.2. Stochastic Models 186
7.3.3. Robust Optimization 187
7.3.4. Info-Gap Model 188
8. Appendix 1 189
9. Appendix 2 205
10. References 207

List of Tables

Table 3.1: Junction node connectivity matrix.....52
Table 3.2: Definition of the matrix A^0 53
Table 3.3: Reduced row echelon form of the matrix A 59
Table 3.4: Aquifer data 65
Table 3.5: Flow and salinity distribution in the network (MCM), $(mgcl/lit)$ respectively. The values in the parentheses are the salinities. (All the values have been rounded to one decimal place). * W.Level = the aquifer water level (m), values in the parentheses are the aquifer salinity at the end of the season.....70
Table 3.6: Operation costs (M$) of the illustrative example, Base Run and 5 Sensitivity Analysis runs. (All values have been rounded to two decimal places). * *S*- is the season index, *S*=1+2 represents the entire year. 70
Table 3.7: Demand data for the large WSS. 73
Table 3.8: Aquifer data for the large WSS. *The recharge salinity is 150 $(mgcl/lit)$, recharge in the second season is 0. 73
Table 3.9: Flow and salinity from the sources (MCM), $(mgcl/lit)$ respectively. The values in the parentheses are the salinities. (All values have been rounded to one decimal place). * Aquifer water levels (m) , and salinities (in parentheses) $(mgcl/lit)$ at the end of the season. 74
Table 3.10: Component and total costs (M$) of the large WSS - base run and 4 sensitivity analyses. (All the values have been rounded to two decimal places).....74
Table 3.11: The recharge in the three aquifers.....79
*The second season recharge is 0 79
Table 4.1: Probability Mass Function (PMF) of the recharge, example 1 97
Table 4.2: Probability Mass Function (PMF) of the recharge, example 2 99
Table 4.3: Optimal solution for each scenario (MCM), illustrative example.....118
Table 4.4: Aggregated nodes' values (MCM).....118
Table 4.5: MSP solution, example 1. Flow (MCM), removal ratio (%).....120
Table 4.6: LMSP, step 1 results of example 1. Flow (MCM), removal ratio (%). 121
Table 4.7: LMSP, step 2 results of example 1. Flow (MCM), removal ratio (%). 121
Table 4.8: LMSP, step 3 results of example 1. Flow (MCM), removal ratio (%). 122

Table 4.9: Comparison between the MSP and the LMSP optimal decision, example 1. Flow (MCM), removal ratio (%). 122
Table 4.10: PMF of the recharge, example 2..... 123
Table 4.11: Clustering scheme, example 2. 123
Table 4.12: Comparison between the MSP and the LMSP decision, example 2..... 124
Table 4.13: PMF of the recharge, example 3..... 125
Table 4.14: Clustering scheme, example 3. 127
Table 4.15: Comparison between the MSP and the LMSP with different extraction levy, example 3. 128
Table 5.1: The junction node connectivity matrix for the network in Figure 5.1..... 139
Table 5.2: Simulation results for the static polices. std=standard deviation. 147
Table 5.3: Discrete approximation of the multivariate normal distribution. 152
Table 5.4: Simulation results for the dynamic polices. std=standard deviation. 154
Table 5.5: Simulation results for the ambiguous chance constraints example. 155

List of Figures

Figure 2.1: Recharge record in INWS.....23
Figure 2.2: Israel Water Sources 23
Figure 2.3: Main Water Systems and Desalination Plants 24
Figure 2.4: Implicit (left) vs. Explicit (right) stochastic programming.....27
Figure 3.1: Demonstration WSS 49
Figure 3.2: Linkage between seasons and years through state variables 49
Figure 3.3: Definition of the matrix D_Q^S 53
Figure 3.4: Definition of the matrix B^0 54
Figure 3.5: Dependent flows, definitions and values.....59
Figure 3.6: General network topology 60
Figure 3.7: Definition of the matrix K^S 62
Figure 3.8: Scheme for evaluation of the constraints and objective function with a given set of flow decision variables Q_{indep} and RR 62
Figure 3.9: Evaluation scheme of the illustrative example.....66
Figure 3.10: (a) Seasonal recharge: for each year, the recharge of season 1 is uniformly distributed from $\{0,50,100\}$ and in season 2 it is always 0. (b) The optimal trajectory of the water level in the aquifer. 71
Figure 3.11: Large WSS layout and conveyance capacity in season 1 and 2. (MCM, rounded to one decimal place) 73
Figure 3.12: Base run Season 1 results - flow (MCM) and salinity $(mgcl/lit)$ distribution. (All values have been rounded to one decimal place).....76
Figure 3.13: Water level trajectories with and without extraction levy 79
Figure 3.14: Tradeoff curves of desalination + conveyance cost vs. final storage; each curve has points corresponding to four values of the maximum specific extraction levy (from bottom to top on each curve) [0,0.4,0.7,1] $(M\$/MCM)$. 79
Figure 3.15: Scheme of the TCM for 3 stages (objective function).....81
Figure 3.16: Scheme of the TCM for 3 stages (constraints) 83
Figure 3.17: Paths for the chain rule implementation.....84
Figure 3.18: Computation time as a function of planning horizon, comparing with and without the TCM procedure (on an Intel Core i7 M620 2.67 GHz laptop) 86
Figure 3.19: Snapshot of the *.html report 88

Figure 4.1: Cumulative Density Function of the objective 93
Figure 4.2: Scenario trees: (a) fan (b) feather-duster (c) balanced tree 94
Figure 4.3: Probability Mass Functions (PMFs) for example 1: (a) objective (total cost) (b) final water level (c) aquifer withdrawal first year (d) aquifer withdrawal last year 97
Figure 4.4: Total cost (B$) and aquifers withdrawal (MCM) for each scenario. 99
Figure 4.5: Mean-Variance tradeoff 102
Figure 4.6: Aquifers withdrawal (MCM) comparison 103
Figure 4.7: PMFs of Aquifers withdrawal corresponding to expected cost of 370 (M$) and 392 (M$), respectively. 104
Figure 4.8: Operation cost range along the Mean-Variance tradeoff 105
Figure 4.9: Validation of the external problem tradeoff 106
Figure 4.10: PMF of the aquifer water level at the end of the horizon 108
Figure 4.11: Layout of the illustrative example 116
Figure 4.12: K-means clustering process 117
Figure 4.13: Optimal solution (MCM) of the illustrative example. 119
Figure 4.14: Unbalanced scenario tree of the recharge, example 1. 120
Figure 4.15: schematic description of the GLMSP scope 129
Figure 5.1: Network layout 138
Figure 5.2: Desalination amount over years for each static policy 146
Figure 5.3: Simulation results of the NP 148
Figure 5.4: Simulation results of the RP3 policy 148
Figure 5.5: Reliability vs. Cost 149
Figure 5.6: Desalination amount over years for each dynamic policy 154
Figure 5.7: Distributions support for different Pmax values 156
Figure 5.8: Aquifers water levels in the large system 157
Figure 6.1: Example 1, robustness for: (a) budget (b) maximum water level (c) minimum water level (d) overall system. 163
Figure 6.2: Example 2, WSS layout 164
Figure 6.3: Example 2, robustness as a function of the aquifer withdrawal with different values of budget. 166
Figure 6.4: Example 2, maximum robustness tradeoffs: (a) maximum robustness vs. aquifer withdrawal (b) maximum robustness vs. budget 166
Figure 6.5: Example 3, maximum robustness vs. budget 168

Figure 6.6: Example 3, maximum robustness vs. budget: (a) influence of the network parameters (b) influence of the aquifer parameters 169
Figure 6.7: Multi-year example, robustness for budget violation.....172
Figure 6.8: Multi-year example, robustness for: (a) minimum water level, decision 1 (b) maximum water level, decision 1 (c) minimum water level, decision 2 (d) maximum water level, decision 2. 173
Figure 6.9: Multi-year example, maximum robustness for: (a) 1 year horizon (b) two years horizon (c) three years horizon (d) 4 years horizon. 174
Figure 6.10: Schematic presentation of the Info-Gap formulation 177
Figure 6.11: Schematic presentation of the RO formulation.....178

Abstract

This thesis deals with management of water resources systems under uncertainty, concentrating on seasonal multi-year management of water quantities and salinities in regional water supply systems (WSS), where water is taken from sources, which include aquifers, reservoirs, and desalination plants, and delivered through a distribution system to consumers who require prescribed quantities of water under salinity constraints. Within this framework the natural replenishment into the aquifers is uncertain, while the desalination plants can produce a large and reliable amount of water, but at greater cost. A deterministic optimization model has been developed. In which the uncertain variables are represented by some deterministic values. The objective function and some of the constraints in this model are non-linear and therefore a non-linear optimization method was used. The model determines the optimal operational plan of the supply system of reservoirs, aquifers, desalination plants and the conveyance system.

A number of approaches for optimization under uncertainty of the aquifers' recharge have been developed and applied, including: (a) probabilistic (stochastic) approaches in which the aquifers recharge is modeled as a stochastic process and (b) non-probabilistic approaches in which no probabilistic assumption is made about the aquifers' recharge.

A key issue when formulating stochastic models is the sequence in which decisions alternate with observations. Various stochastic models were developed in this thesis, which considered different alternations between decisions and observations of the recharge stochastic process. These models include two-stage and multi-stage stochastic programming along with the two extreme cases: a) the Wait-and-See approach, in which decisions are made *after* all the realizations are known b) the Here-and-Now approach, in which decisions are made *before* the realizations are known.

In addition to these approaches a Limited Multi-stage Stochastic Programming (LMSP) approach was developed. The LMSP is an approximation of the Multi-stage Stochastic Programming (MSP) approach which was developed in the current work. The Robust Optimization (RO) methodology and the Info-Gap decision theory (non-probabilistic approaches) were applied.

A small "made up" system was used for testing the algorithms and for demonstrating and explaining the results; a real scaled system which represents the central part of the Israeli National Water System (INWS) was solved by all models, and the results are presented to demonstrate the efficacy of the tools used and efficiency of the models as proof of their practicality. The results of the large system show the importance for models with uncertainty incorporation over deterministic models. The solution can change dramatically when recharge uncertainty is imposed.

The results show that the LMSP provides a good approximation for the stochastic approaches. The quality of the LMSP was verified by several examples which show the emphasis and the justification of the LMSP approximation. The results of the non-probabilistic methods are very promising, since they result in smaller mathematical problems and they obtain competitive results in terms of robustness and tractability compared to the classical probabilistic methods.

List of Symbols

Sections 3.1-3.9

p,a,d - Pipe, Aquifer and Desalination Plant, respectively.

z,S,Y - Demand Zone, Season and Year, respectively

$CC_p^{S,Y}$ - Conveyance Cost ($\$ / season$)

$X_p^{S,Y}$ - Head Loss (m)

$Q_p^{S,Y}$ - Pipe Discharge ($m^3 / season$)

$w^{S,Y}$ - Number of Pumping Hours ($hr / season$)

$KWHC^{S,Y}$ - Pumping Cost ($\$ / kwhr$)

ΔZ_p - Topographical Difference (m)

$\Delta Hf_p^{S,Y}$ - Energy Head Loss (m)

c_p^Y - Hazen Williams coefficient ($-$)

D_p - Link Diameter (cm)

L_p - Link Length (km).

$\overline{\overline{CE}}_a^{S,Y}$ - Specific Extraction Levy ($\$ / m^3$)

$h_a^{S,Y}$ - Water Level (m)

$(h_{\min})_a^{S,Y}$ - Minimum Allowed Water Level (m)

$(h_{\max})_a^{S,Y}$ - Maximum Allowed Water Level (m)

$\left(\overline{CE}^{\max}\right)_a^{S,Y}$ - Maximum Extraction Levy ($\$ / m^3$)

$CE_a^{S,Y}$ - Extraction Levy ($\$ / season$)

$Q_a^{S,Y}$ - Pumping Amount from Aquifers ($m^3 / season$)

$CD_d^{S,Y}$ - Desalination Cost ($\$ / season$)

α_d - Desalination Cost Coefficient ($\$ / m^3$)

β_d -Desalination Cost Coefficient ($-$)

$Q_d^{S,Y}$ - Desalination Amount ($m^3 / season$)

$RR_d^{S,Y}$ - Removal Ratio ($\%$)

Q_{Source} / C_{source} - Vector of discharges/salinity leaving source nodes

Q_{pipes} / C_{pipes} - Vector of discharges/salinity in the links

Q_{demand} / C_{demand} - Vector of discharges/salinity at demand nodes.

$R_a^{S,Y}$ - Recharge (MCM)

SA_a - Storativity Multiplied by Area (m^2)

$h_a^{S,Y} / C_a^{S,Y}$ - Water Level/Salinity in Aquifers (m) /($mgcl / lit$)

$h_a^{(S,Y)-1} / C_a^{(S,Y)-1}$ - Water Level/Salinity in Aquifers (m) /($mgcl / lit$)

$(C_R)_a^{S,Y}$ Salinity of the Recharge Water ($mgcl / lit$)

$C_d^{S,Y}$ - Desalinated Water Salinity ($mgcl / lit$)

C_{sea} - Sea Water Salinity ($27000\, mgcl / lit$)

$\left(\#_{\max}\right)_{p,a,d}^{S,Y}$ - Maximum Allowed Value

$(\#_{\min})_{p,a,d}^{S,Y}$ - Minimum Allowed Value

$(\#)_{dep}$ - Vector of dependent decision variables

$(\#)_{indep}$ - Vector of independent decision variables

Sections 3.10-3.12 and Chapter 4

t - Stage Index $t \in [1, T_f]$

u^t - Vector of Decision Variables

x^t, y^t - Two Vectors of State Variables

p^t - Vector of Parameters

$f, W, V, g_j \ \forall j$ - Nonlinear Functions

A^t - Rectangular Coefficient Matrix

b^t - RHS Vector

LB^t, UB^t - Lower and Upper Bounds, respectively

F - Overall Objective Function

$U = [u^1, ..., u^{T_f}]$ - Vector of Multi-Year Decision Variables

δ_v - Perturbation Step of Variable v

e_v - Unit Vector in Direction v

ϕ - Statistical Operator

λ - Penalty Per-Unit Deviation of Constraints

α - Pre-Specified Reliability

VaR_β - value associated with risk β

ω - Weighting Parameter

E - Expectation Operator

Σ - Variance Operator

R - Stochastic Process of the Recharge

$R^s = (r_1^s \cdots r_{T_f}^s)$ - Recharge Scenario s

p^s - Probability of Recharge Scenario s

Chapter 5

a, d, l - Aquifer, Desalination Plant and Link, respectively

z, t - Demand Zone and Year, respectively

$des_{d,t}$ - Cost of Desalinated Water Per MCM ($\$ / MCM$)

$Q_{d,t}$ - Desalinated Water Amount (MCM / $year$)

$C_{l,t}$ - Cost of Transportation Per MCM ($\$ / MCM$)

$Q_{l,t}$ - Flow in Link (MCM / $year$)

$h_{a,t}$ - Water Level in the Aquifer (m)

$\hat{h}_a$ - Prescribed Final Water Level (m)

E_a - Penalty Per-Unit Deviation ($\$ / m$)

G - Junction Node Connectivity Matrix

$Q_{natural,t}$ - Vector of Elements $Q_{a,t}$ $\forall a$

$Q_{desalination,t}$ - Vector of Elements $Q_{d,t}$ $\forall d$

$Q_{links,t}$ Vector of Elements $Q_{l,t}$ $\forall l$

$Q_{z,t}$ - Water Demand (MCM / $year$)

$Q_{demand,t}$ - Vector of Elements $Q_{z,t}$ $\forall z$

$Q_{a,t}$ - Aquifers Extraction Amount (MCM / $year$)

$R_{a,t}$ - Uncertain Recharge (MCM / $year$)

$\#_{i,t}^{\max}$ - Maximum Allowed Value

$\#_{i,t}^{\min}$ - Minimum Allowed Value

μ_R - Expected Value of the Uncertain Recharge

Σ_R - Covariance matrix of the Uncertain Recharge

Δ - Square Root Matrix of the Covariance

$U(\theta)$ - Ellipsoidal Uncertainty Set Radius θ

Chapter 6

x - Decision Rule

$U(\alpha)$ - Info-Gap Uncertainty Set

α – Uncertainty parameter

$\tilde{R}$ - Estimated Recharge (MCM / $year$)

Q_{aq} - Aquifer Extraction (MCM / $year$)

h_0 - Initial Water Level (m)

h_f - Final Water Level (m)

$M_i(\alpha)$ - Inner Maximum/Minimum in Robustness Function i

$\hat{\alpha}_i$ - Robustness for Failure i

List of abbreviation

AARC-Affine Adjustable Robust Counterpart

BOT-Build Operate Transfer

BR-Base Run

Breadth-First-Search algorithm (BFS)

CA-Coastal Aquifer

CCP-Chance Constraints Programming

CP-Conservative Policy

DP-Dynamic Programming

FMSPP- Folding Multi-Stage Stochastic Programming policy

FNP-Folding Nominal Policy

FRC-Folding Robust Counterpart

FRP-Folding Robust Policy

GA-Genetic Algorithm

GLMSP-Generalized Limited Multi-Stage Stochastic Programming

GMP-Grey Mathematical Programming

GRG-Generalized Reduced Gradient

INWSS-Israel National Water Supply System

IS-Implicit Stochastic

IWA-Israel Water Authority

LK-Lake Kinneret

LMSP-Limited Multi-Stage Stochastic Programming

LP-Linear Programming

MA-Mountain Aquifer

MCM-Million Cubic Meter

MIP-Mixed Integer Programming

MSP- Multi-Stage Stochastic Programming

NA-Not Applicable

NP-Nominal Policy

NWC- National Water Carrier

PMF-Probability Mass Function

RC-Robust Counterpart

RHS-Right Hand Side

RO-Robust Optimization

RP-Robust Policy

SA-Sensitivity Analysis

SDP-Stochastic Dynamic Programming

SLP-Sequential Linear Programming

SMBO-Search Method for Box-Constrained Optimization

SQP-Sequential Quadratic Programming

ST-Spanning Tree

SWDP-Sea Water Desalination Plants

TBS-Three Basin System

TCM-Time Chain Method

TSP-Two-Stage Stochastic Programming

WSS-Water Supply System

1. Introduction

1.1. Motivation

Management of water resources systems is aided by models of various types, ranging from those used for long-term development of large systems, to detailed operation of smaller parts, for example annual operation of an aquifer. It does not seem feasible to create a single tool which deals with all levels in time and space simultaneously. A possible option is to use a suite of models, inter-connected in a loose hierarchy [Shamir, 1971].

This work concentrates on management of the Israeli National Water Supply System (INWSS) that comprises several aquifers, a surface reservoir - Lake Kinneret, large sea-water desalination plants, a central conveyance system, and numerous local distribution systems. Several sea-water desalination plants have been constructed and began operation in 2006, 2007 and 2009. Their current combined annual capacity is 285 MCM/year, already about 25% of the current average annual replenishment of all natural sources (~1,300 MCM/year). By 2013 this will rise to about 50% and by 2050 it is expected to be 150% (i.e., 1.5 times today's average natural recharge).

The various consumers have different requirements regarding the quantity and the quality of the water supplied to them. The consumers are urban, agriculture, and industry, plus commitments under bilateral agreements with the Hashemite Kingdom of Jordan and the Palestinian Authority.

The models developed herein are aimed to support/guide INWSS managers (also referred to as the decision makers) in making decisions on operation of the system over a time horizon of several years, and also in evaluating proposed plans for system changes and capacity expansion. The INWSS is not very large and still quite challenging to manage and optimize, as a result of its complex structure and conditions, and the requirements for reliable service. An important aspect of this complexity is associated with hydrological uncertainty, including the effects of climate change, in addition to population growth, inclusion of desalination plants and the deterioration of water quality in the sources.

As the INWSS shares many characteristics with regional water supply systems (WSS) elsewhere, the models in this work were formulated in a general form and format, to

facilitate application to regional systems with similar elements and characteristics as the INWSS. A central part of the INWSS was used as a case study for the generalized model.

The research presented in this thesis has been aimed to develop a multi-year model for managing regional WSS under conditions of hydrological uncertainty. As the research progressed, several modeling philosophies, strategies and methodologies for optimization under uncertainty were developed and tested.

Models for water systems management deal with quantities of water delivered from sources to demand zones. More recently, there are models that consider water quality as well, in particular salinity throughout the system, so that the objectives and constraints of management consider both quantity and quality (salinity) [Draper et al., 2003; Jenkins et al., 2004; Zaide 2006]. With the inclusion of desalination plants (as is the case in the INWSS), water quality considerations are now a vital part of the modeling procedure. It is important to consider both quantity and salinity in the water sources, in the water supplied to consumers, and at each node of the supply system itself. With salinity consideration becoming a key factor of the management model, the complexity of the model evidently increases.

Another consideration is the sustainability of the management plan. This implies meeting the needs of the present without reducing the ability of the next generation to meet its needs [Loucks, 2000]. This requires a perspective with a relatively long time-horizon, and assigns a value for leaving the system at the end of the planning horizon with reservoirs that have not been depleted nor have high salinity. An associated aspect of multi-year water supply management relates to hydrological uncertainty [Ajami et al., 2008] and climate change [Grantz et al., 2007], which is the main focus of this work.

In light of the above, there is a challenge to develop a **multi-quality, multi-year** model for management of water quantities and salinities in a regional WSS **under uncertainty**.

Most models developed so far (including models for the INWSS) are essentially deterministic. This means that the amount of natural replenishment is known and changes from year to the next in a known sequence (which can be "shuffled" to test different possible future sequences, in an "ensemble" mode). The historical time series

of replenishment is used to test the performance of capacity development and operational plans, thus generating estimated future distributions of system states and performance. Still, this is not considered to be an explicit inclusion of system reliability and performance under hydrological uncertainty. A main objective of the current research is to incorporate explicit considerations of uncertainty, both at the conceptual level – i.e., what are the best ways to formulate the objectives and constraints for long-term management in view of uncertainties – as well as the technical level – i.e., what techniques and methodologies can and should be used in modeling, so that the results are usable in the real world.

This research presents a seasonal multiyear model for management of both water quantity and salinity, using optimization methods with an emphasis on management uncertainty associated with replenishment. The objective that drives the decision is to minimize the present value of system operation cost, subject to technological, administrative, and environmental constraints, and possibly include social implications as well.

Models of regional water systems are large and complex hence, simplifications and aggregation must be made in order to obtain a solvable model. This is particularly true when uncertainty is introduced, since it significantly expands the dimension of the model.

1.2. Objectives and Contribution

The objective of this research is to develop a water management model using optimization under uncertainty conditions in order to guide long-term water supply system operation. The model can then be used to evaluate directions for capacity expansion of the WSS.

There may be more than one suitable model for optimization under uncertainty, based on different approaches. Several methodologies/models for decision making under uncertainty were used in determining the optimal management of a regional WSS under hydrological uncertainty associated with the replenishment of the natural resources. In fact there are other sources of uncertainty that will influence the development and management plan (in particular in the INWSS), including demands uncertainty, agreements with neighboring countries, new and improved technologies for desalination at lower cost, rising (or dropping) prices of oil, international trade

agreements on agricultural and other products, etc. However, this research did not account for all these uncertainties; it considers only hydrological uncertainty.

Decisions under uncertainty involve a subjective attitude. Decision makers may be risk-averse, risk-neutral or risk-tolerant (risk loving/risk seeking), and their decisions will be accordingly influenced. In management of resources for the public good, it is not the individual decision maker's attitude to risk that is the dominant feature (although it definitely plays a role!) but rather the policy of the governing body: the Water Authority, the Ministry of National Infrastructure, the Ministry of Finance, ultimately the Government. It is therefore not possible to anticipate the attitude that will be taken by the decision makers at decision times. Furthermore, statements and decisions regarding risk-management which are made ahead of the actual risky situation do not predict well the decision when the actual risky situation materializes. The Ministry of Finance and the Government's decisions on desalination for the INWSS demonstrate such a case: in the dry spell leading up to summer of 2002 the Government approved a plan for constructing seawater desalination plants with a capacity of 400 MCM/year; then there was a very wet year in 2002/2003 - and the amount was reduced to 260 MCM/year (!); the recent dry spell led to another reversal, and a decision to increase to 600 MCM/year by 2013 and 750 MCM/year by 2020.

The conclusion to be drawn from this is that the tools required to support decision making in the face of uncertainty must be flexible enough to allow testing tradeoffs between various characteristics of future outcomes, efficient enough to be run quickly for different inputs, and transparent enough to convey to the decision makers the full range of consequences of different possible decisions. So the developed models will quantify the following:

1. Indications regarding the best capacities of production and conveyance facilities.

2. The optimal 'salinity map' of the supply system for each season over years.

3. The optimal conveyance map of the supply system for each season over years.

This work is connected to the Water Authority through Miki Zaide, Strategic Planner at the Government Authority for Water and Sewage. This was aimed to achieve two goals: (a) information and advice regarding the INWSS which can be obtained (however: there is no claim that the model will be completely realistic), and (b) if the

methodology is successful it will have a chance of being adopted and used by the Water Authority.

1.3. Dissertation outline

The remainder of the thesis is organized as follows:

Chapter 2 includes literature review and theoretical background of the methodologies used in the research. The first part (Section 2.1) introduces a comprehensive review for deterministic WSS models. This part also includes a special Section that describes the INWSS and the models used for its management.

The second part includes a review of methodologies for optimization under uncertainty (Section 2.2.2). Several applications of these methodologies for water resources models are reviewed in Section 2.2.3. A review of some models from other fields are presented in Section 2.2.4.

Chapter 3 presents the deterministic formulation of the seasonal multi-year model for management of water quantities and salinity in regional water supply systems. Next, the optimization framework for solving the nonlinear optimization problem is presented. It includes a set of manipulations for reducing the model size, and an efficient finite differences scheme for calculating the derivatives required by the optimization algorithm. This is followed by application of the methodology to a small demonstration system (Section 3.8) and to the central part of the INWSS (Section 3.9).

Chapter 4 introduces various scenario based stochastic models based on the deterministic model developed in Chapter 3. In Section 4.10, the Limited Multi-stage Stochastic Programming (LMSP) which is an approximation of the MSP developed in this work is introduced. Several examples were run to validate the quality of the solution obtained by the LMSP.

Chapter 5 introduces the Robust Optimization (RO) methodology and its application for optimizing the operation of a WSS. A new WSS model, that differs from the model developed in Chapter 3 is introduced, due to restriction of convexity for application of the RO methodology. It is a linear model and does not consider salinity. The results obtained from the RO were compared to the solution from other methodologies, such as MSP.

Chapter 6 introduces the Info-Gap methodology and its application for the WSS model developed in Chapter 3. This application is preliminary, to demonstrate the methodology, thus the examples included are only the small network.

Chapter 7 is a general summary, discussion, conclusions, and recommendations for further research.

Appendix 1 presents a Search Method for Box Optimization (SMBO) which was developed as a byproduct of this thesis as an attempt to solve the optimization model in Chapter 3. SMBO is a heuristic population based search methodology which solves global optimization problems by representing the population as Probability Density Functions (PDF) within the problem bounds. The performance of SMBO is compared with old and recent genetic algorithms (GA). The results show that SMBO performs equally or better than the GAs in both comparisons.

Appendix 2 graphical results for the large scale example in Chapter 3

Appendix 3 includes the list of references.

2. Literature survey and methodology

2.1. Deterministic models

2.1.1. Introduction

Management of water resources systems is characterized by inter-dependent hydrological, physical, environmental, ecological economic and social aspects, and therefore determining the optimal design and operational management policies for water systems poses complex challenges for decision makers. Planning and management decisions for water resources systems are determined according to the effects expected to arise as a result of these decisions. These effects can be predicted by expert opinion and/or by quantitative information generated by mathematical and computational models. The past four decades have witnessed significant advances in the ability to model engineering, economic, ecological, hydrological and political aspects of large complex water resources systems. Today, quantitative mathematical optimization models are considered essential tools to assist design and management of water resources systems.

In the planning phase, models assist in determining the topological layout and the size of the system components to meet specified requirements while optimizing for specified objectives. Operational management models determine the operation over a given time horizon, divided into specified periods, given the system components and capabilities, the required service, and the objective function. The two model categories are inter-related, since the system’s layout and component sizes obviously affects the optimal operation, while operational models can help in detecting system deficiencies and "bottlenecks" whose solution will improve system performance and whose cost is justified by the improved performance.

2.1.2. Water management models

Water resources systems are distributed in space and operate over a time horizons that range from short (minutes, hours, days) to long (months, a year) to very long (multi-year) and are subdivided into time-periods. The spatial and temporal resolution of a model has to be selected judiciously – to capture the essential features and performance measures while avoiding excessive and costly detail. Thus, models range from highly aggregated versions of an entire water system with annual periods to

much more detailed models in space and time. It does not seem feasible to create a single management model that covers all levels in time and space simultaneously and the preferred option is therefore to use a suite of models, inter-connected in a hierarchy. Shamir, [1971] analyzed the management of the Israeli National Water Supply System and proposed an approach to its optimization by using a “Hierarchy of Models”. This approach recommends using a series of inter-connected models, which have different scales in time and space; the models supply each other with information and results that relate to their constraints and objective functions. Close to the top of the hierarchy an aggregate model is designed to determine the general plan of the system, its major topology and addresses the capacity expansion of its main components. At this level, the model does not have to consider the detailed hydraulics; therefore it treats the conveyance system as a transportation network. Once the first level model’s results are obtained, new models with detailed components of the network are used, with the results of the first aggregate model spread out and detailed in space and time. These models have to consider the detailed hydraulics more explicitly. Selecting the proper aggregation in time and space for a particular application is one of the most important challenges of modeling.

For short-term (weekly to monthly) or longer-term (years to decades) operation of a large scale water supply system a medium aggregation is used to manage simultaneously both the sources and the network [Fisher et al., 2002; Draper et al., 2003, 2004; Jenkins et al., 2004; Watkins et al., 2004]. Fisher et al., [2002] developed and applied, in a combined US, Dutch, Palestinian, Jordanian and Israeli team, a model called Water Allocation System (WAS) under the framework of the Middle East Water Project. WAS is a benefit-maximizing model driven by consumers' willingness-to-pay (demand functions), with constraints representing physical laws and administrative regulations. It considers water sources and consumers in districts and a physical conveyance system that connects them. WAS recognizes that one cannot use competitive markets to insure efficient allocations since at least the following basic properties needed for a free market to function are often absent: (a) A competitive market must have a large number of independent small sellers and buyers, which is not true in water markets. (b) In a competitive market we assume that social costs and benefits must coincide with private ones, which is not the case in the presence of externalities that affect the social optimal results. Thus the objective

function is maximization of total social net benefit, over all consumers in all districts, i.e. the difference between the total benefit generated by water-based activities and the cost of supplying it. WAS is a single-year model, which accepts a defined water supply system and determines the annual operation of the sources and conveyance systems under fixed hydrological conditions; a multi-year model MYWAS is under development. The model generates the optimal water use pattern and helps in analyzing the cost-benefit of proposed infrastructure projects. WAS is developed to promote and facilitate cooperation in water in order to obtain win-win situations in disputes over water. Application by Israeli, Palestinian and Jordanian teams to their water sectors showed that the value of the water in dispute is very small while the potential gains from cooperation are relatively large.

Draper et al., [2004] developed a simulation model for planning and management of the State Water Project and the Federal Central Valley Project in California. The model is called California Water Resources Simulation Model (CALSIM). It couples a simulation language with a mixed integer linear programming (MIP) solver for efficient water allocation decisions. The model is a single time step optimization (the optimization does not include long term considerations) while simulation is used to link the system operation over a sequence of monthly periods. For each time step a set of objectives and constraints are considered in the optimization problem, different objectives can be added using a combination of weights which construct the overall monthly objective. The weights are subjective factors that indicate the decision maker's preferences. The monthly constraints can be formulated as hard or soft constraints with associated penalties for deviating from a specified target. The MIP solver enables CALSIM to represent nonlinear ‘if-then’ constraints and piecewise linearization of nonlinear functions. However, the MIP problem is much more difficult to solve than LP, hence the number of the binary integer variables has to be limited. Water quality considerations are not included explicitly in CALSIM; still, it uses an external module which consists of an Artificial Neural Network (ANN) to estimate the water quality in the system.

Jenkins et al., [2004] and Draper et al., [2003] developed and applied a large-scale economic-engineering optimization model of California’s water supply system called CALVIN. The model combines economic benefit and loss functions in its objectives. It manages surface sources, groundwater sources, and allocates water using a 72 year

record of historical hydrologic data. The model maximizes the economic value of agricultural and urban water uses, within specified physical, environmental, and operational constraints. Incorporating the economic performance in the objective function facilitates maximizing net economic benefit to the entire system, which leads to optimal balance between supply and demand. The optimization algorithm is a linear network flow formulation where convex economic functions are replaced by piecewise linear functions. CALVIN runs with historical time series of monthly inflows with a single demand condition to prescribe monthly system operation. Agricultural and urban water demands are represented by economic value functions for 2020 levels of development. CALVIN is solved for water quantities; water quality is represented by flow constraints and elimination of some water sources as potential water supplies.

Watkins et al., [2004] developed a screening model called the South Florida Systems Analysis Model (SFSAM) that uses optimization to reduce the large number of alternatives and operating polices to a few that can then be simulated and evaluated in greater detail. The model seeks minimum cost within specified physical, environmental, and operational constraints, to manage surface and groundwater resources and allocate water using 25 years of historical hydrologic record. The mathematical optimization model is a linear network flow formulation where the water conveyance and storage facilities are represented as arcs in the network. The objective functions and some of the constraints are expressed by piecewise linear functions. SFSAM runs with monthly time series of inflows and a single demand condition to prescribe monthly system operation. The demand condition is set equal to the maximum demand observed over the 25-year of the historical record study record. There is no reference to water quality neither in the network nor in the sources.

Many models deal only with quantities of water to be delivered from sources to demand zones. More recently, there are models that consider water quality as well, in particular salinity [Yates et al., 2005; Tu et al., 2005]. Yates et al., [2005] developed WEAP21, which is a simulation model comprised of watershed-scale hydrologic processes, physical network of reservoirs, canals demand sectors and environmental requirements. The hydrologic module of WEAP21 considers evapotranspiration, surface runoff, subsurface runoff and percolation. It includes the interconnections between an aquifer and the surface of the watershed. It also includes a temperature-

index snow-melt model and heat budget equations. The water quality module in WEAP21 includes constituents that are conservative or decay according to an exponential decay function such as: Dissolved Oxygen (DO) and Biological Oxygen Demand (BOD). Demand allocation is determined by a linear programming optimization module in which the priorities are entered by the user. The consumers are divided into equity groups, and the objective function is formulated such that demand zones with the same priority are supplied equally as percentage of their total demand. The optimization module does not reflect fully all of the model's components: (a) It only considers the water quantity allocation among the different demand zones, the water quality in the watershed, the aquifers and the network is not considered in the optimization phase (b) The water allocations are made according to user-specified input that are independent of source state and of conveyance costs.

Tu et al., [2005] developed a quality-quantity flow model to optimize water distribution in a regional water supply system with multi-quality sources. The model is a nonlinear optimization model with monthly operation units and a six month management horizon, which considers water and quality parameters balance in the system but does not consider hydraulic laws. The nonlinear mathematical model is solved by a hybrid genetic algorithm (GA) using the optimization software LINGO. The GA is first used to globally search for the directions of all undirected arcs in the network. Then a generalized reduced gradient algorithm (GRG) embedded in the GA is used to optimize the objective function for fitness evaluation. The methodology was applied to the regional water distribution system of the Metropolitan Water District of Southern California twice; the first objective function was to minimize the total shortage in water supply and the second objective function was to minimize the deviations of reservoir storage from the preset target.

The network representation in a model can be classified according to the physical laws that are considered explicitly in the model constraints [Ostfeld and Shamir, 1993; Cohen et al., 2000]. Ostfeld and Shamir, [1993], solved for optimal operation policy of a multi-quality water supply system, which consists of the following elements: sources, reservoirs, pipes, pumping stations, treatment plants and consumption nodes. The objective function was to minimize the total operational cost. Three types of models were developed: steady-state, quasi-steady-state and an approximate unsteady state. The solution was obtained with GAMS/MINOS (General Algebraic Modeling

System). Cohen et al., [2000] determined the optimal operation of a multi-quality network under steady-state flow conditions. This work was developed in 3 parts: (a) Q-C is the flow-quality transport model (b) Q-H is the hydraulic model which represents the network hydraulic (c) Q-C-H which uses the shared flow vector Q of the two partial models to represent the hydraulics and the water quality simultaneously. The Q-C-H is divided into the two sub-problems which are solved separately and then combined into a comprehensive Q-C-H model. The purpose of this decomposition is to tackle the nonlinearities that appear in the Q-C-H problem.

According to this classification the proposed models of Tu et al., [2005] and Yates et al., [2005] are flow-quality models which consider the balance of the flows and mass of quality parameters, but without explicit inclusion of the hydraulics. The inherent assumption of these models is that the hydraulic operation with the quantities prescribed by the model would be feasible. With the inclusion of desalination plants as an important source in water supply systems, as is the case in Israel, water salinity consideration must be included explicitly in the management scheme. It is important and necessary to consider both quantity and salinity in the water sources, in the water supplied to consumers and at nodes of the supply system itself, with due consideration to the hydraulic performance of the system. With the salinity considerations becoming an important part of management models, the complexity of the model evidently increases.

An important consideration is sustainability of the operational management plan. This implies meeting the needs of the present without reducing the ability of the next generation to meet its needs [Loucks, 2000]. Sustainable management requires a perspective with a relatively long time-horizon. Zaide, [2006] developed a model for Multi-Year Combined Optimal Management of Quantity and Quality in the Israeli National Water Supply System (MYCOIN). This model is aimed to consider long-term (years) allocation optimization with various components of water supply, water quality and water system and demand zones for national level decision makers. It is a deterministic seasonal (two seasons per year) multi-year model for management (operation and implications for development) of both water quantity and salinity in the Israeli National Supply System (INWSS). Both quantity and salinity considerations (in the water sources, supply system and demand zones) are optimized simultaneously for a long time horizon. The objective function is defined as minimum

total cost of multi-year operation subject to physical, environmental and operational constraints. The optimization model is solved by the generalized reduced gradient algorithm (GRG) with an off-the-shelf software that uses Excel for model formulation.

In this Section we presented some of the deterministic water management models which are relevant to our work. This work introduces a model for optimal multi-year management of regional water resources systems under hydrological uncertainty. It is a seasonal multi-year model for optimal management of both water quantity and salinity, which minimizes the overall cost of the system operation subject to technological, administrative, and environmental constraints. The model does not include hydraulic constraints and does not guarantee required heads at consumer nodes, yet the objective function takes into account the cost of conveyance as a function of the hydraulics properties of the network. This is appropriate when it can be assumed that the resulting operation plan will be feasible hydraulically [Cohen et al., 2000].

We next provide some information about the Israeli National Water System (INWS), whose central part is used in demonstrating the application of the models developed in this research.

2.1.3. The Israeli National Water System (INWS)

Israel is located in a semi-arid to arid region. The annual rainfall ranges from over 1,000 mm in the north to 150 mm and less in the south, over a distance of some 500 km, with an average annual rainfall of 500 mm. The average annual replenishment of fresh water in all sources for the 77 year historical record (Figure 2.1) is 1,391 (MCM/year). The main sources (Figure 2.2) are Lake Kinneret (LK, average annual replenishment 580 MCM), the Mountain Aquifer (MA, 360 MCM) and the Coastal Aquifer (CA, 310 MCM). Most of the water supply in the INWS depends on these three sources, and hence this main part of the national system is called the Three Basin System (TBS). The replenishment has been declining in recent decades, due to a variety of causes, and the total is now estimated at around 1,100 (MCM/year). In the last decades the Israeli water managers are facing difficulties to supply a reliable quantity of fresh water from the TBS due to the high variability of annual replenishment where the standard deviation of the 77 year historical record of the

annual replenishment reached to 460 (MCM), i.e. 32% of the average. Another aspect is the frequent long sequences of below average replenishment which can result in cumulative deficits of 1,500 (MCM) and more. In addition, there is the quality issue, since large parts of the aquifers, especially in the Coastal Aquifer, are no longer suitable for direct potable purposes because of contamination due to human activities and over-extraction that caused intrusion of saline water bodies.

At the beginning of this study (2007) the total annual consumption of all sectors for all types of water was 2060 (MCM), of which 1,435 (MCM) (70%) is potable and the rest non-potable, reclaimed wastewater and brackish waters. The urban consumption exceeded 50% of the total potable water use and the potable water use by agriculture was set by the Government to 560 (MCM/year) to maintain agriculture that can use only potable quality water. Other consumers are industry, nature, and commitments under agreements with the Hashemite Kingdom of Jordan with the Palestinian.

Following the Water Sector (Interim) Master Plan for the years 2002-2010 [Water Commission, 2002], the government of Israel decided to construct sea water desalination plants (SWDP) with an installed capacity of 400 (MCM/year). The first SWDP, located in Ashkelon (Figure 2.3), was inaugurated in 2005, and produces 115 (MCM/year) of very high-quality water, the second plant, at Palmachim, with a capacity of 45 (MCM/year), began operation in 2007, and the third plant, at Hedera, with a capacity of 127 (MCM/year), was inaugurated in late 2009. The product of all plants – a total of 287 (MCM/year) - is injected into the National Carrier (Figure 2.3), and blended with water from the natural sources. Two additional SWDP plants are added: under construction at Sorek, with a capacity of 150 (MCM/year), and at Ashdod, with a capacity of 100 (MCM/year), whose contract is being finalized with Mekorot.

The INWS is highly integrated; the National Water Carrier (NWC) which connects the three main water sources, most of the other sources and some 30 regional systems by a conveyance network that covers most of the country’s area and supplies water to some 4,000 primary consumers. The consumers are urban, industry, agriculture, nature, and commitments under bilateral agreements with the Hashemite Kingdom of Jordan and the Palestinian Authority. The various consumers have different requirements concerning the reliability and quality of supplied water. The complexity

of management, operation and design of the INWS will increase as quality considerations become more important, primarily due to the inclusion of desalinated water with its high quality that allows blending with lower quality waters.

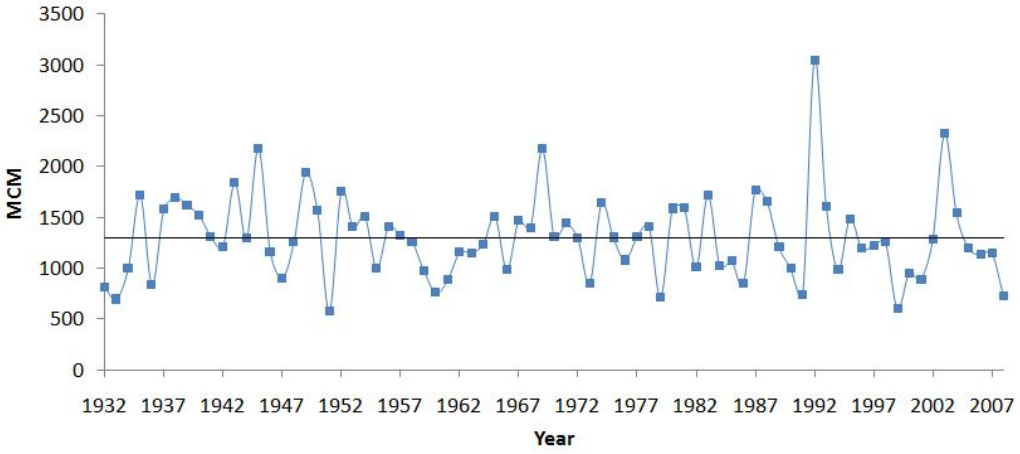

Figure 2.1: Recharge record in INWS

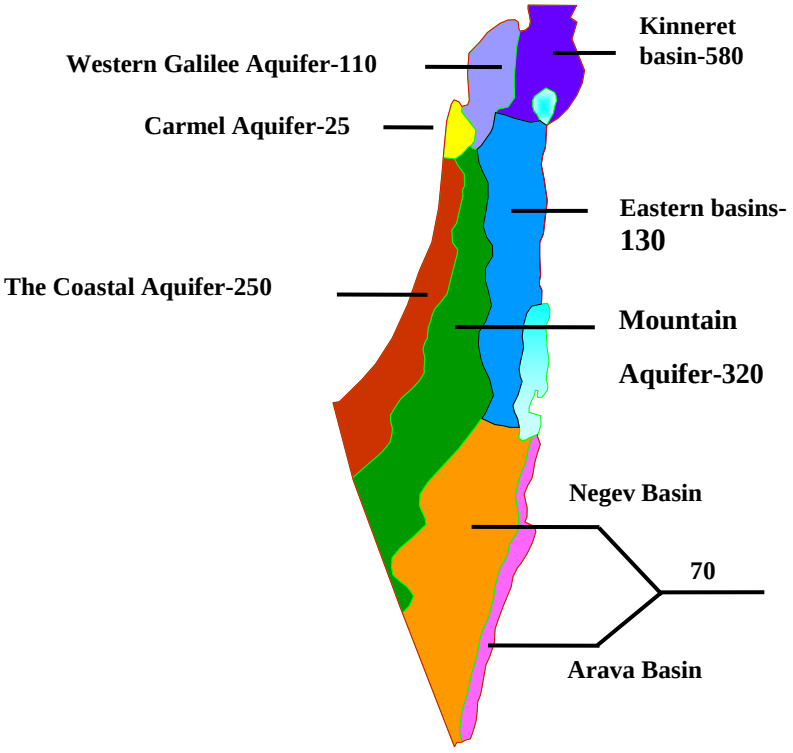

Figure 2.2: Israel Water Sources

Figure 2.3: Main Water Systems and Desalination Plants

2.1.4. Management models applied to the INWS

The INWS may not be very large by international standards, yet it is a complex system to manage and optimize. The complexity and difficulty of modeling for management of the NWSS are due to: the large number and variety of components in the system, the need to consider operation under uncertain conditions, and the introduction of quality into the model, which creates non-linearities and amplifies the difficulty of solving a large optimization model.

The Israeli Water Authority (IWA) uses a suite of models which support decision making including: “National Balance Generator” developed by TAHAL (1998) to perform simulations of the total national water balance, considering 12 regions connected by a conveyance network; “Aggregative Model” [Water Commission, 2003] in which all the potable water quantities in the Three Basin System (TBS = Kinneret, Coastal and Mountain Aquifers) are aggregated into a single combined source which serves the total demand. This model is driven by a simulation scheme which considers many multi-year replenishment time series. Based on these series the model produces statistical reports concerning the supply reliability and storage capacity. Schwarz et al., [1986] developed an LP transportation model (TKUMA) for the INWS management. Water quality was incorporated by successive linearizations

of the non-linear quality equations. The annual optimization model considers the quantities provided from 8 natural sources and 4 desalination plants to 8 demand zones. TKUMA was used in a multi-year simulation framework where the state variables in the natural sources connect the successive years. Zaide, [2006] developed a Multi-Year Combined Optimal Management of Quantity and Quality in the Israeli National Water Supply System (MYCOIN), which is an optimization model that considers long-term (years) allocation optimization with various components of water supply, water quality and water system and demand zones for national level decision makers. At Mekorot (Israel National Water Company) and the IWA there are several models which are aimed to manage and operate a single source, which was not included in this short review as they have less relevance to those developed in this study.

Among all the models which were developed for the INWS there is no management model which considers multi-year optimization of quantity-quality of the system under hydrological uncertainty. This explains the need for a model that considers these aspects especially in the inclusion of new components such as desalination plants and hydrological uncertainty which is expected to increase.

2.2. Models that consider Uncertainty

2.2.1. Introduction

Planning and management of infrastructure projects is always conducted under conditions of uncertainty. Typically, uncertainty results from the two aspects: (a) The loads/demands placed on the system, and (b) The capability/capacity of the planned system to meet the loads/demands. The system fails whenever the load exceeds the capacity. In the domain of water, future demands are those imposed by the consumers (even when demand management is exercised), while the capacity to meet the demands depends on the uncertain hydrology and system delivery capacity. The uncertainties can be classified into two types: (a) Objective (external) uncertainty, which results from an uncontrolled or unknown phenomenon, and (b) Subjective (internal) uncertainty, which results from lack of adequate knowledge of the system and its parameters [Wendt et al., 2002].

One way to deal with uncertainty is to practically ignore it. In this approach, the nominal or expected value of the uncertainty is usually used in a deterministic

formulation, while it is well understood that in reality the uncertain variables will certainly deviate from this value.

Another standard way to deal with uncertainties is by overdesign of the infrastructure project at the design stage and by operating rules based on overestimation of the uncertainties at the operation stage. This approach can work well when the number of uncertain parameters is small; otherwise it can lead to design and operation that are much too expensive. Since, uncertainties in different parameters have different effects on the system; overdesign may present conservative solution [Babayan, 2007].

Given this generic situation, a required next step in the development of management models is optimization under uncertainty. A major difficulty in optimization under uncertainty is in dealing with an uncertainty space that is very large which leads to very large-scale optimization models. Decision-making under uncertainty is further complicated when the problem being is multi-period and/or multi-stage [Sahinidis, 2004].

2.2.2. Optimization under uncertainty

Decisions must often be taken in the face of the unknown, for example precipitation and evaporation variability that affect availability of water, on the supply side, and the urban and irrigation water requirements, on the other. The consequences of the decision taken at time now cannot be known until the unknown data are revealed. Still, some corrective decisions may be taken in the future as more and more data become known.

In the deterministic optimization the uncertainty plays no role and some selected values of the unknown parameters are used in determining the decisions. In stochastic optimization [Birge and Louveaux, 1997] the uncertain parameters are modeled as random variable with a known probability distribution. Generally, there are two types of stochastic programming: implicit and explicit stochastic programming.

Implicit stochastic programming (Figure 2.4) uses a (sufficiently long) sequence of data corresponding to random variables. Using forecasting methods which are based on existing knowledge and the history of the system (or by using Monte Carlo simulation) this data are used to simulate the possible future values of the uncertain variables. In this approach, the stochastic aspects of the problem are implicitly

included and each forecast is used as input for deterministic optimization. The optimal solution obtained by each optimization problem is unique to that forecast, and the range of outcomes is analyzed to arrive at the decision rules.

Explicit stochastic programming (Figure 2.4) incorporates the probability distribution of the random variables inside the optimization problem, and as a result both the objective and the constraints are stochastic in nature. Hence, statistical operations (e.g. expectation) should be applied to the objective and the constraints. There are many options to apply the explicit stochastic programming approach, for example different objective functions could be considered which differ by the statistical operator applied to the stochastic objective function. Regarding the constraints, one could use: (a) Chance constraints which depend on a specified levels of risk of violating these constraints (b) Penalizing the constraints violation by adding penalty term to the objective (c) Combination of chance constraints and violation penalty.

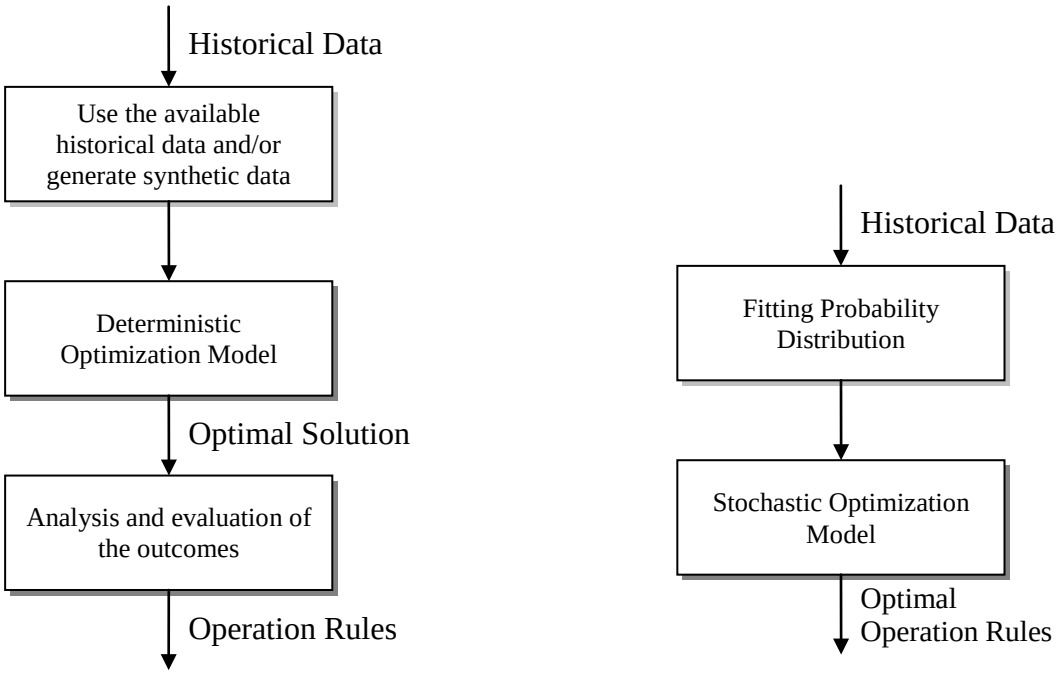

Figure 2.4: Implicit (left) vs. Explicit (right) stochastic programming

A key question which should be answered before formulating the stochastic model is the sequence in which decisions alternate with observations. To explain the concepts of the stochastic programming let us first consider the unconstrained optimization problem: $f(x,R) \rightarrow \min$ where x is vector of decision variables and R is the stochastic process.

A common tool to present the stochastic process is to work with scenarios [Dupacova, 2000], which are particular representations of how the process might be realized in the future. We approximate the stochastic process R by a finite set of scenarios $R^s \in \Omega$ $\forall s$ with probability p^s. In general, some kind of probabilistic model or simulation is used to generate a batch of such scenarios out of the continuous process. The challenge then, is how to make good use of the scenarios in coming up with an effective decision.

In the deterministic formulation of this optimization problem the uncertainty is treated through the replacement of the random elements of R by some particular estimate $\hat{R}$. The problem solved is: $f(x,\hat{R}) \to \min$ the optimal solution of this problem does not involve any hedging of decisions since only the single realization $\hat{R}$ is considered. The implicit approach implies that decision can be taken after the value of R becomes known. Hence, we have an optimization problem which depends on R^s as a fixed parameter: $f(x,R^s) \to \min \ \forall s$, after solving this optimization problem for each s we obtain the decision corresponding to each scenario x^s, these decisions construct the objective value set $\min_{x^s} f(x^s,R^s) \in \Omega_f \quad \forall s$ and the optimal solution set $\arg\min_{x^s} f(x^s,R^s) \in \Omega_x \ \forall s$. Both sets need to be analyzed in their dependence on the stochastic process R. The optimal value and the optimal solution sets are treated as stochastic elements and their probabilistic behavior is used to derive decision rules for implementation.

When the decision has to be taken in advance, before any realization of the stochastic process is revealed, then the probability distribution of the process should be explicitly included in the problem. The extreme case is when all the decisions have to be made in advance, i.e. all the problem is considered as a single stage. In this formulation each possible decision has stochastic value $f(x,R)$ with its own Probability Density Function (PDF). Since we cannot minimize a probability density function of $f(x,R)$ we have to apply a statistical operator on the PDF before the optimization. Some of the common operators which are used are:

(a) The Worst case approach, $\max_R f(x,R) \to \min$ in which we minimize the worst outcome which may results from the decision. This corresponds to a pessimistic attitude. It does not distinguish between the outcomes according to their probability of

occurrence; hence it could give poor results when the worst outcome has small probability as it the case many real word problems.

(b) The Expectation approach, $E_R[f(x,R)] \to \min$ in which we minimize the expectation of the PDF, hence, this approach emphasize the average outcome.

(c) The Variance approach, $\sum_R[f(x,R)] \to \min$, in which we minimize the variance of the PDF, hence, this approach emphasizes the variability of the outcome.

(d) The Value at Risk approach, $VaR_\alpha[f(x,R)] \to \min$ in which we minimize the quantile value associated with confidence level α.

(e) Any combination of the above approaches is also applicable. For instance the Mean-Variance approach, $\psi(E_R[f(x,R)], \sum_R[f(x,R)]) \to \min$ where ψ provides a way to balance between the expectation and variance. This approach is quite traditional in financial applications, where the outcomes variance is considered a measure of risk [Markowitz, 1959].

When we need to consider not just one decision and one observation, but possible interactions between decisions and observations in stages, then multi-stage stochastic programming (MSP) should be used [Dupacova, 1995]. The MSP distinguishes between decisions that have to be made now before any information is reveled and decisions at later stages where part of the information becomes available. However, the decisions of the first stage (present) are made with recognition that there are opportunities for modification and corrections at later stages (recourse decisions). In the T_f stages problem the expectation formulation of the MSP is:

$$E_R\left[f\left(x_0, x_1(R_1), x_2(R_1,R_2), ..., x_{T_f}(R_1, ..., R_{T_f}), R\right)\right] \to \min \qquad (2.1)$$

Where for example $x_2(R_1,R_2)$ show that decision at stage two depends on the information revealed up to this stage. A special case of the MSP is the two stage stochastic programming; this formulation involves an initial decision (present), receiving reveled information and then a single recourse decision.

Recourse decisions (future decisions taken after some information is realized) can react to the past, but they cannot be based on knowing the future before it happens. In the MSP terminology, the decision space X consists of all function $x(\cdot)$ that are

nonanticipative. The MSP solves for an optimal policy defined as the first stage decision (values) and the recourse decisions (functions). Minimization over a function space confronts us with a more advanced level of mathematics to which conventional optimization methodology in not applicable.

This problem is overcome by solving the MSP with discrete probability distribution of the stochastic process, which was introduced earlier by the scenarios representation of the process. When the process is given by scenarios, to specify the function $x(\cdot)$ we replace it by a finite number of vectors equal to the different possibilities which the function $x(\cdot)$ takes as its input. For example, the function $x_1(R_1)$ is replaced by k_f vectors $x_1(R_1^k)$ where $k = 1..k_f$ and k_f is the different values which R_1 takes in the scenario set.

Up to this point we presented the methodologies for unconstrained optimization. When dealing with constrained optimization problems, some of the constraints may also depend on the stochastic process. In general the problem constraints could be classified as follows: (a) constraints which are not affected by the stochastic process which we can represent by the feasibility set $x \in C$ (b) inequality constraints depend on stochastic process $g(x,R) \le 0$ (c) equality constraints $m(x,R) = 0$.

An inequality constraint will be satisfied for all the realization of the stochastic process by replacing it with its worst-case counterpart $\max_R g(x,R) \le 0$, representing a conservative approach that is costly.

By an equality constraint we are asking for a decision which makes the random left side of the constraint $m(x,R)$ equal to zero. Namely, the requirement on the decision is that it has to make the random variable to be not random at all but have the constant value of zero. In many cases such a decision does not exist. Modeling uncertain equality constraints should therefore be avoided, and uncertain inequality constraints should be replaced by their worst-case counterpart only if the constraint in question is a hard constraint which cannot be violated under any circumstances. However, when the constraints are soft and can be violated with no collision in the model these constraints can be substituted by penalty terms in the objective function [Dupacova et al., 1991]. Whenever the constraint is violated, the penalty term invokes an additional

cost that is proportional to the amount of violation. For example, the so-called linear penalty function is: $p = \lambda \cdot \max\left(g(x,R),0\right)$ where λ is the penalty per unit deviation.

Soft constraints can also be modeled as chance constraints [Wendt et al., 2002] in which they are relaxed probabilistically. Using the chance constraints approach one may specify the required level of risk of violating the constraint. The chance constraint is defined as $\text{prob}\{g(x,R) \le 0\} \ge$ pre-specified probability that this inequality holds.

For instance, requiring this probability to equal one is the same as making the constraints hard constraints, which have to be satisfied for all the realization of the stochastic process. In contrast when requiring the probability to equal 0.9 the constraints are satisfied for only 90% of the realizations.

The size of the optimization problem results from the explicit stochastic model is greatly affected by the future branching and the scenarios' number considered in the model. The challenge of solving large scale optimization problems with many variables and constraints is one of the main concerns of stochastic programming.

To overcome the difficulty of the large scale optimization model various decomposition methods have been suggested [Rockafellar and Wets, 1991; Mulvey and Ruszczynsk, 1995].

Another optimization technique which is also applied to stochastic models is Stochastic Dynamic Programming (SDP). As opposed to the MSP, the decisions at each stage do not depend on the information we may infer from the directly on underlying stochastic process, instead, the decisions at each stage depends on the observed state of the system which is a function of the stochastic process. Dupacova and Sladky, [2002] discussed the similarities and the differences of MSP and SDP. To explain the concept of SDP we shall first explain the deterministic Dynamic Programming (DP) in which we define the objective function as a recursive formula and decompose the original problem into sub-problems that are solved sequentially over each stage. In the sub-problems solution we translate the state variable into a finite number of levels and then perform conditional optimization over all possible discrete combinations of state levels. For all the discrete combinations the objective function is optimized recursively over each time period in a backwards sequence. The

SDP models attempt to solve the recursion relation adapted to stochastic problems by applying statistical operator (such as expectation) on the recursive objective.

Beside the stochastic approach, there is another class of optimization under uncertainty, methods in which the uncertainty is not probabilistic, but rather deterministic and set-based. Namely, instead of seeking to immunize the solution in some probabilistic sense to stochastic uncertainty, the decision maker seeks a solution that is optimal for any realization of the uncertainty in a given set. We review three variants of these methods:

(a) Inexact programming [Soyster, 1973] in which the model incorporates the uncertain parameters as ranges $R \in [R^-, R^+]$. The objective is to maintain feasibility against whatever might happen when the actual values are realized from the intervals. Another way to deal with interval uncertainty is the Grey Mathematical Programming (GMP) developed by Huang, [1994] for linear models. The model is transformed into two deterministic sub-models, which correspond to the upper and lower bounds for the desired objective function value, through this transformation we obtain two sub-models that provide interval solutions e.g. $x_{opt} \in [x_{opt}^-, x_{opt}^+]$ and decision alternatives can be chosen within these intervals.

(b) Robust Optimization [Ben-Tal et al., 2009], a more recent approach to optimization under uncertainty, in which there is no limitation on the uncertainty to be represented by intervals, but rather any set could be chosen to represent the uncertain parameters. However, the use of convex sets, such as an ellipsoidal set $U = \left\{ R : \hat{R} + \Delta\varsigma, \|\varsigma\| \le \theta \right\}$, makes it possible to formulate a tractable optimization problem. The Robust Optimization (RO) associates with the uncertain problem its robust counterpart where the constraints are satisfied for every realization within the prescribed set while the worst case value of the objective function is minimized.

This method was applied in different fields such as portfolio models [Ben-Tal et al, 2000b; Lobo and Boyd, 2000], inventory theory [Bertsimas and Thiele, 2006; Bienstock and Ozbay 2008], process scheduling [Li and Ierapetritou, 2008] and network models [Mudchanatongsuk et al., 2005].

(c) The Info-gap decision theory [Ben-Haim, 2006] seeks decisions which maximize robustness to failure instead of minimizing the objective function. The optimization

problem is to find the decision x such that it would be feasible with as many as possible realization in the uncertain parameters set. When the uncertainty set is defined as: $U = \left\{ R : \left| R - \hat{R} \right| \le \alpha \right\}$ where R deviates from the expected function $\hat{R}$ by an unknown amount α. The greater the value of α, the greater the possibilities of R, so α, the uncertainty parameter, expresses the information gap between what is known and what needs to be known for an ideal solution of the exact function. The methodology expresses the idea that uncertainty may be either pernicious or propitious, that is, an uncertain variation may be either adverse or favorable: the robustness function is the greatest level of uncertainty consistent with no failure, while the opportunity function is the least level of uncertainty, which entails the possibility of sweeping success. Consequently, the robustness and opportunity functions can be expressed as the maximum or minimum of a set of α values: $\hat{\alpha}$ = max $\{\alpha$: minimal requirements are satisfied$\}$, $\hat{\beta}$ = min $\{\alpha$: sweeping success is obtained$\}$. An application of the Info-Gap on water resources model is presented in the next Section.

2.2.3. Water systems under uncertainty

Planning and management of real-life water resources projects are always conducted under uncertainty, such as uncertain demands, flows, yields, costs and benefits, etc. A common approach is to neglect the uncertainty in the mathematical model by replacing them with deterministic estimator. However, Philbrick and Kitanidis, [1999] show the limitation of this approach for reservoirs management. They present three models for reservoirs managements and demonstrate that the deterministic formulation does not perform as well as a stochastic formulation in which the uncertain parameters considered as random parameters with known PDF.

Recently, consideration of uncertainties is becoming a standard step in water resources modeling. Numerous models were developed in the past for management optimization of reservoirs, in which, inflows, net evaporation, hydrologic, and economic parameters and system demands are considered as random variables [Labadie, 2004]. Hiew et al., [1989] and Crawley and Dandy, [1993] applied the Implicit Stochastic (IS) approach for optimal management of multi-reservoirs system with uncertain inflows. However, since implicit approach requires solving many large scale deterministic problems, Hiew et al., [1989] formulated a linear model and Crawley and Dandy, [1993] formulated piecewise linear approximation of the

nonlinear model which can be solved efficiently by available linear programming methods.

In many applications of multi-reservoirs management, linear techniques are not applicable due to the existence of nonlinear and non-separable functions in objective functions and constraints. In these cases, various nonlinear algorithms are used, such as Successive Linear Programming (SLP), Successive Quadratic Programming (SQP), Generalized Reduced Gradient (GRG), interior-point algorithms and Genetic Algorithms (GA). Barros et al., [2003], compared the performance of SQP and SLP on a large scale Brazilian hydropower system. Peng and Buras, [2000] applied the GRG to nonlinear model within IS optimization framework. Cai et al., [2001] presented a framework for solving large-scale nonlinear water management model by GA which can be used within the IS approach.

Dynamic programming is also a popular optimization technique within the IS scheme applied to reservoirs management. The earliest application of IS and dynamic programming has its roots in Young, [1967]. The difficulty in using dynamic programming is the curse of dimensionality, which makes it impractical in large-scale systems. To overcome this drawback in the context of IS approach, some versions of discrete dynamic with various approximations were proposed. Among them the incremental dynamic programming and the discrete differential dynamic programming which were applied to reservoir management models in the last decades. For more details and applications of these methods we refer the reader to Labadie, [2004] and the references therein. Vasiliadis and Karamouz, [1994] explicitly incorporate the stochastic inflows of a single reservoir into the optimization model and solved it by the stochastic dynamic approach to minimize the expectation of the cost function.

Similar to stochastic dynamic programming, the scenario based Multi-stage Stochastic Programming (MSP) is also explicitly includes the random parameters in the optimization model. The MSP had wide applications in water resources modeling. Kracman et al., [2006] developed a multi-stage linear programming model which considers stochastic inflows given as scenario tree for a system of reservoirs in the Colorado River in Texas. The model seeks maximum total expected benefit of the system over a five year horizon. Where the first stage decision is water quantity to

contract for the coming years and the future decisions are monthly reservoirs releases to meet specified requirements. The main disadvantage of this scenario based method is that the size of the optimization problem will increase with the number of scenarios and result in an extremely large scale optimization problem. However, the model is linear, and therefore large scale problems can be solved efficiently by decomposition methods such as Bender's decompositions [Benders, 1962].

A special variant of the MSP is the Two-stage Stochastic Programming (TSP) in which the problem is formulated to optimize the actual objective value of the first stage plus the total expected value of future decisions (recourse), which depend on the first stage decisions and future random realizations. Seifi and Hipel, [2001] applied the TSP for a linear model of multi-reservoir operation with stochastic inflows specified by set of scenarios. In this model the two stages are decision making stages and not time period stages as in Kracman et al., [2006]. In the first decision stage the model decides on the releases for the entire period to minimize the sum of deviation from given targets for the storage and the releases. The second stage is considered as surplus and shortage variables corresponding to each scenario along with the expected value of the shortage and spill penalty. This formulation leads to a large scale linear program which is solved efficiently by an interior-point algorithm that exploits the structure of the problem being considered.

One of the more common objectives is to optimize expected value of the objective as it the case in Vasiliadis and Karamouz [1994], Kracman et al. [2006] and Seifi and Hipel [2001]. However, decision makers are always interested in risk measures together with or instead of the expected value. Yamout et al., [2007] considered a water resource allocation problem over a region of East Central Florida. The available water is considered random and represented by finite number of scenarios. The paper studies the effect of incorporating a new objective, termed Conditional Value at Risk in analyzing a water allocation problem by comparing the results with various frequently used models and objectives for stochastic optimization, such as: deterministic expected value model, scenario analysis model and STP model with recourse. The new objectives which incorporate a risk measure provides an objective value with a confidence level associated with it.

Watkins and McKinney, [1997] incorporated different risk measures in their optimization models. They considered two water resources planning problems with stochastic parameters represented by scenarios. The first is for screening a water supply plan with stochastic future demand, and the second considers the problem of hydraulically containing a ground water contaminant when aquifer parameters are stochastic given by scenarios. In the first model they modeled the cost variance as a measure of risk and minimized an objective function defined as a weighted sum of the expected value of the cost and the standard deviation of the cost. In the second model they used the upper partial mean, i.e., the expected positive deviation from the mean cost as a measure of risk and minimized an objective function defined as a weighted between the expected value of the cost and the upper partial mean of the cost.

Chance Constrained Programming (CCP), is a common and popular technique in the modeling of stochastic problems. Several researchers developed chance constraints optimization schemes to design water distribution systems under demand and roughness coefficients stochastic conditions, modeled as PDFs. Lansey et al., [1989], Xu and Goulter, [1998] and Babayan et al., [2005] formulated a chance constrained minimization problem for least cost design of water supply systems. The model is formulated as minimization of the network cost of a nonlinear function of the pipe diameters in the network, under constraints of water balance, energy conservation and minimum head requirement at the nodes, where the discharge in each pipe is expressed by the Hazen-Williams equation. This formulation implies that the objective function is deterministic, since the objective function does not depend on the stochastic parameters (the demand and the roughness coefficients). The constraints in the demand nodes and the minimum required head constrain are stochastic and hence formulated as chance constraints. Lansey et al., [1989] modeled the stochastic demands and roughness coefficients as independent normally distributed random variables, and showed that the stochastic constraints are also normally distributed, which facilitates the formulation of a closed form of the chance constraints. For a pre-determined confidence level of the chance constraints, the deterministic equivalent of the chance constraints model was solved using the Generalized Reduced Gradient 2 (GRG2).

In practice, demands in the certain area may be highly correlated, as they are affected by the same causes, e.g., hot and dry weather conditions. Xu and Goulter, [1998],

solved the same formulation, but the stochastic parameters were modeled by correlated normally distributed variables. Incorporating the correlation in the model makes it more difficult to evaluate the chance constraints so they suggested a Monte Carlo simulation and linearization of the model equations to facilitate the chance constraints evaluations. The GRG2 optimization method requires that decision variables (e.g., pipe diameters) to be continuous variables, which is unrealistic. Recently, Babayan et al., [2005] overcame this drawback by using GA linked to an integration based technique for evaluating the probabilities associated with the chance constraints. The minimum cost design formulated previously is a chance constraint problem with deterministic objective function which depends only on the pipe diameters of the networks. In contrast to this formation Kapelan et al., [2005] proposed a multi-objective optimization approach for solving design problem under stochastic demand which was modeled as normal PDF and roughness coefficient modeled as uniform PDF. This approach is aimed to minimize the total design cost and the failure probability. Hence, the chance constraints in the former formulation are contained in the multi-objective optimization scheme. The multi-objective optimization problem was solved by multi-objective GA to obtain the whole Pareto front in a single run. The Pareto front identifies the trade-off between the total cost and the failure probability. In contrast, the single objective formulation, e.g. Lansey et al. [1989], only solves for one point on the Pareto front, the point that corresponds to the pre-determined failure probability.

Filion et al. [2007] proposed a new formulation which considers not only the hydraulic performance of the system but also the economical damages and losses arising from death and human injury during low and high pressure failures. For instance, a low pressure failure can affect residential and commercial users, cause pipes to collapse, and in the event of a fire, it can cause the loss of property and human life. A high pressure failure can cause pipes to burst with flooding damage to surrounding property. The suggested formulation accounts for this damage by minimizing two objective optimization problems comprised of expected annual cost and expected damage minimization.

In addition to the many applications of the CCP for optimal design problems, several researchers applied this approach for management problems. Wagner [1999] applied the CCP to model the least cost pumping model for remediating the ground water

contamination. This model is a part of a framework for analyzing the optimal position of ground water sampling for ground water projects. The least cost pumping module is formulated as chance constraints in which the concentrations as a function of the stochastic parameters are normally distributed.

Sankarasubramanian et al. [2009] presented an optimization model for water allocation from a reservoir to users, where the optimization is performed under stochastic inflow forecasts given as scenarios. The optimization model seeks maximum utility of water use with feasible water allocation policy. The expectation operator was applied to the objective function and the stochastic constraints were replaced by chance constraints. Generally, there is one stochastic constraint in a reservoir management model, which is associated with the continuity equation of the storage, while in this model a second constraint is added, which is associated with the maximum deviation allowed for the water users from predetermined (contracted) amount.

In real world problems, the information is frequently not sufficient to cast the uncertain variables as PDFs or scenarios. Instead, the available information may be used to present the uncertain variables as intervals or uncertainty sets. This is reasonable, because planners and engineers typically find it more difficult to specify distributions than to define value intervals/sets. Hipel et al. [1999] demonstrate the information gap methodology for three models for three systems arising in watershed management: (a) Hydroelectric generation system in which water flows from the watershed into a reservoir, then through the generating plant back out into the environment. If the reservoir is unable to store all the inflow, then water is diverted past the generating plant directly to the environment, with consequent loss of electricity generation. (b) Irrigation system in which water polluted with pesticides and/or fertilizers flows from farmland to a collection facility before treatment, and then to the environment. If the collection capacity is too small, some polluted water flows directly into the environment. (c) Urban sewage system where sewage flows to a large primary treatment facility, then to a second facility and then back to the environment. Overflow of untreated sewage directly into the environment occurs if the primary plant capacity is too small.

The drainage of the watershed over time is considered uncertain, while the only information is given by the nominal value of the drainage. In the three models the decision maker must choose the storage capacity of the collection facility and the treatment/process rate which is assumed to be constant over time. The inlflow in each case is unknown and given by the uncertainty set:

$$U(\alpha,\tilde{r}) = \left\{ r(t) : r(t) \geq 0 \; and \int_0^T \left[r(t) - \tilde{r}(t) \right]^2 dt \leq \alpha \right\} \qquad (2.2)$$

which constrains the integrated squared deviation of the actual drainage over time from the nominal drainage. Each model was solved for maximum robustness, defined as the maximum deviation allowed without violating the failure criteria which states that the stored volume cannot exceed the storage capacity.

Water planning and management decisions face increasing challenges to satisfy a variety of water demands, exacerbated by the recent droughts, climate variability and climate change. Therefore, a framework for incorporating large-scale climate information into the water resources planning and decision-making process is needed in order to accommodate forecasts of the future scenarios. Grantz at el. [2007] developed a framework for incorporating large-scale climate information into the water resources planning and decision making process, and demonstrated it to the semiarid Truckee-Carson Basin in Nevada. The framework consists of: (a) Identification of climate signals that are relevant to the area of interest, (b) Development of probabilistic forecasts for stream flow based on the climate signals, and (c) Incorporation of the forecasts into the decision support system. In this study a simplified seasonal management model was developed for the Truckee-Carson basin to demonstrate the utility of the climate based stream flow forecasts in water resources decision making. The model is based on the conservation of mass, subject to the supply and demand constraints of the system. In this case, the supplies are the Truckee and Carson forecasts, the demands are irrigation and fish requirements. The decision variables are the storage available for irrigation, Truckee River water available for fish and the Truckee Canal diversion. The results of the climate based stream flow forecast were compared to the results from historical record, in order to investigate the benefit of including climate information in the stream flow forecast.

The result show that that incorporating climate information into the stream flow forecast improves the overall skill in forecasting the decision variables.

Minville et al. [2010] used several climate projections from five general circulation models with two greenhouse gas scenarios to evaluate the uncertainty of these future potential climates on floods and hydroelectric production. The climate change projections were used to produce synthetic series using a stochastic weather generator for the climate variables: minimum temperature, maximum temperature, and precipitation. To account to for the natural variability of the climate, thirty stochastic series for each climate variable were generated for each of the climate projections, which then served as input for a hydrological model which simulates the watershed response (inflow to river or reservoir) for each of the thirty series. Given the simulated inflows and reservoir simulation model the climate change impacts are evaluated by entering each of the thirty series of the future inflows for all the climate projections into the reservoir simulation model which includes hydropower system and spilled flows. Hence, for predetermined operating rules, performance measures of the reservoirs (reliability and vulnerability) are evaluated and compared to simulation results of a historical control period. The results show that classical management policy of the reservoir should be re-considered in order to incorporate the new hydrological conditions.

In contrast to Grantz at el. [2007] and Minville et al. [2010], Ajami et al. [2008] used only climatological historical data in their analysis. The climatological data were used as input for the hydrological model. However, they consider not only the climatological uncertainty but also uncertainty of parameter values and in the structure of the hydrological model. In this paper integrated Bayesian uncertainty estimator framework was used to incorporate parameters and model structural of the hydrological model. This framework consists of using three different models with variety of model parameters.

Like in Minville et al. [2010], different operational rules were considered in examining how hydrological uncertainties impact reliability, resilience, and vulnerability for reservoir management. Uncertainty in climate change was used as input in forecasting the future scenarios discussed in Grantz at el. [2007] and Minville et al. [2010]. For instance: uncertainty in forecasting the effect of green house gases

(GHGs) on climate change, amount of the GHGs, the technologies available for the treatment, and the decisions of future policy makers.

Tol [1998] demonstrated an uncertain model that deals with decisions which affect climate change, through the emission of GHGs. A part of that uncertainty that is often ignored is the behavior of future policy makers. For example, a present day policy maker wants to stabilize the concentration of GHGs, but this is unlikely to be a welfare maximizing policy, therefore future policy makers have an incentive to switch to less ambitious emission controls, as a result the costs substantially increase if current policy makers want to set long-term goals without the full cooperation of future policy makers. Tol, [1998] attempts to advise a current policy maker what he should do, given a long-term goal for climate policy while he does not know what future policy makers will do. The only uncertainties considered are those regarding the motives of future policy makers, with only two types of policy makers: stabilizers and optimizers who are seeking to maximize net present welfare. When the current policy maker is a stabilizer, successive policy makers will either follow his strategy or switch to a policy which maximizes the net present welfare. The probability of a switch (conditional probability) is considered constant over time. The objective of the current policy maker is to minimize the net present costs of emission reduction, given certain conditions on the chance of meeting the stabilization target. The model is demonstrated with a numerical example which shows that if current policy makers want to meet a cumulative emission constraint in expectation, then the preferred policy does not qualitatively deviate from one suggested by a standard cost-effective policy. If, however, the constraint is to be met with a certain probability, then the importance of early action is enhanced relative to that of postponed action and the costs substantially increase.

2.2.4. Infrastructure management under uncertainty

Uncertainty in planning and management of infrastructure projects has been tackled by various approaches, including probabilistic and non-probabilistic. In the former approach, two methods have been used for representing uncertain variables: discrete and continuous distributions. González et al. [2006] suggests a methodology for maintenance of railway infrastructure (called RCM) under uncertainty regarding the deterioration rate of the railway infrastructure. The model formulation assumes that

the management under facility deterioration is a discrete Markov decision process, with a known matrix of transition probabilities. In contrast, Jido et al. [2008] developed an infrastructure Maintenance and Rehabilitation (M&R) model for maintenance of railway infrastructure, under uncertainty of the deterioration rate, without neglecting the inspection cost that has trade-off with the M&R cost. The introduction of the inspection cost into the model adds more uncertainty to the model, for instance: how to inspect the facility and which technology to use? Usually, infrastructure management is presented as a Markov decision process in which the state of facilities is defined in discrete states to represent the uncertain deterioration. However, in Jido et al. [2008] continuous states are defined instead, in order to avoid "the curse of dimensionality". Both models developed by González et al. [2006] and Jido et al. [2008] are designed to minimize the expected value of the facility's lifecycle cost. However, if the optimality is based only on cost expectation (i.e. risk neutral attitude) this may not meet the requirement of reliability in the sense that system failure may have a significant probability.

Zhao at el. [2006] demonstrated an improved approach for optimal decision making for infrastructure development and expansion decisions based on the decision maker's risk preference. The decision making process is modeled as a multistage stochastic problem with uncertainty modeled by a binomial tree. As a result of the binomial lattice representation of the uncertainty the random outcome is subject to a normal distribution, i.e. the optimal risk averse decision has analytical terms depending on the risk preference factor, variance and expectation of the normal distribution. The risk factor is an input for the model, the expectation and the variance are formulated as a recursive relation that can be solved by a SDP which applies backwards calculations to determine the optimal values and decisions.

When the uncertain variables are represented as continuous distribution, this leads to a stochastic programming problem, in which special treatments are applied to the objective function and the constraints, so the problem can be re-stated as an equivalent deterministic one.

Chan at el. [2006] presented a study on selecting electricity contracts for a large-scale chemical production plant, which requires electricity importation under uncertainty regarding the electricity demand. Two common types of electricity contracts are

considered: (a) Time zone (TZ) contract where electricity price depends on the time during the day (b) Loading curve (LC) contract where restrictions are employed in the contract, and if any of these restrictions is violated penalties will be charged on the customers. The customers, however, are rewarded in the second contract by a lower electricity price compared to the first one. Chan at el. [2006] considered only demand uncertainty which is assumed to be normally distributed. The problem is formulated as a multi-period probabilistic linear programming and modeled as a chance constrained linear program. This approach seeks to satisfy the constraints involved by a predetermined confidence level based on the known PDF of the uncertain variables, and thus the problem can be restated as an equivalent deterministic one. The essential challenge lies in the computation of the probabilities of satisfying the constraints, but in the paper this is an easy task as a result of the fact that the demand is normally distributed and is the only uncertainty. Furthermore, there is only one chance constraint in the model, namely that related to the amount of the product being produced, which must satisfy the market demand with the predefined confidence level. The objective is to determine the best electricity contract and the optimal imported electricity amount in each shift which maximize the net-profit of chemical production plant according to the desired confident level.

In case that traditional stochastic programming is not applicable because of lack of sufficient information to construct the PDFs the uncertain variables can be presented as intervals. One alternative for dealing with this type of uncertainty is to use methods of optimality analysis i.e. sensitivity analysis or to formulate best/worst case models [Liik at el., 2004]. However, sensitivity analysis is generally suitable for problems with few uncertain variables. The best/worst case analysis solved only for the two extremes possibilities which may not necessarily construct a set of stable intervals for generating decision alternatives. To overcome these drawbacks when many uncertain variables are given as intervals, one must test a number of combinations for deterministic values within the intervals. However, for large-scale problems, this number may become extremely large [Huang at el., 2005].

Liik at el., [2004] presented a model for long-term optimization of electricity generation capacity. In the deterministic formulation of the problem, the objective is to minimize the total costs in the planning period considering the reliability and environmental constraints. The model assumes that the set of existing power plant

units and a set of units which can be build in the future are given. The optimization task is to determine the optimal unit commitment and the economic scheduling of units' active power and energy production during the planning period. Liik at el. [2004] consider the uncertain problem in which the load duration curve (which is the cumulative probability of load magnitudes) and the cost function are uncertain. Each of the uncertain functions is given in the form of intervals, i.e. the load function is bounded within an interval that changes over time along the planning horizon and the same for the cost function. Instead of the cost function the authors suggest to define a new function representing the risk or the possible losses caused by uncertainty factors. A min-max approach was applied to the uncertain risk function to obtain the deterministic equivalent model which was solved by dynamic programming.

Huang at el. [2005] developed a model for long-term planning of the integrated solid waste management system under uncertainty (ISWM), i.e. management of municipal solid waste, which includes programs that reduce or reuse the waste produced, and/or divert wastes from traditional disposal facilities to recycling, composting, and/or incineration. The suggested model can effectively reflect uncertain characteristics of the waste management systems, such as the amounts of solid waste generated in cities and towns, the costs for various waste transportation routes, and the capacities and operating costs of waste management facilities. Economically, the model considers costs related to waste collection, transfer, transportation, processing and disposal, capital investments for developing and expanding waste management facilities, and revenues from recycled materials, finished compost, and residual facility values. Its solutions provide bases for answering questions of siting, timing, and sizing for new and expanded waste management facilities in relation to a variety of waste-diversion targets. The problem is modeled as an inexact mixed integer linear programming model which minimizes the net system cost, related to four groups of costs and revenues: (a) Waste collection and transportation costs (b) Facility operating costs (c) Capital costs for new and expanded facilities and (d) Revenues from the sale of composting products and recyclable materials, and the facilities' residual market values. Under the constraints of: (a) Capacity limitation (b) Mass balance, and (c) Technical constraints.

Models for infrastructure planning and management uncertainties may have probabilistic and non- probabilistic characteristics. The former can be formulated with

stochastic approaches and the latter can be expressed as intervals with known lower and upper bounds but unknown distributions. Namely, it is possible to incorporate probabilistic and non-probabilistic approaches in one model in order to represent different kinds of uncertainties.

Li at el. [2006] demonstrated a two-stage chance constrained mixed integer linear programming method for an integrated municipal solid waste (IMSW) management under uncertainty. In the (IMSW) management there are different kind of uncertainties, such as costs of waste transportation and facility operation and revenues from waste management facilities, which can be presented by intervals. In comparison, uncertainties such as waste generation rates may be better presented as random variables with known PDFs. The cost function in Li at el. [2006] covers expenses for handling fixed allowable waste flows, probabilistic excess flows, expansions of the waste management facilities, and revenues from waste treatment facilities, therefore the model is attending to minimize the expected cost. The system constraints are related to all of the relationships between the decision variables and the waste generation management conditions. The first-stage decision variables represent allowable waste flows from district to waste management facility. The second-stage decisions are related to probabilistic excess flows from district to facility under varied waste generation, capacity expansion schemes for the landfill and waste treatment facilities. The constraints on the existing landfill capacity are formulated as chance constraints. All other uncertainties like the cost coefficient and some other parameters in the constraints are formulated as interval uncertainties. The integrated final mathematical model which includes interval uncertainties inexact programming is needed in order to obtain the optimal solution.

3. Deterministic model

3.1. Introduction

The main objective of this work, as indicated by its title, is to develop and test a model for seasonal multi-year management of water quantities and salinity in regional water supply systems (WSS) under uncertain hydrological condition. As one step towards this meeting this objective we formulate, implement and test the performance of a deterministic model. Computational efficiency of this model is a guiding principle, since the deterministic model will constitute a kernel of a stochastic optimization tool.

The details of the model and the solution technique are given in the next Sections. The model's objective function and the constraints are presented in Section 3.4. Sections 3.5, 3.6 and 3.7 contain the optimization plan and the optimization tools, namely structuring the model for the optimization solver. Sections 3.8 and 3.9 present numerical examples and sensitivity analysis. Section 3.10 presents the Time-Chained-Method (TCM), and its performance measure.

3.2. Background and Motivation

Management of water resources systems (WSS) is aided by models of various types, ranging from long-term development of large systems, to detailed operation of smaller parts such as a distribution system or an aquifer. Thus models range from highly aggregate versions of an entire water system to much more detailed models in space and time. It does not seem feasible to create a single tool that covers all levels in time and space simultaneously and the preferred option is therefore to use a suite of models, inter-connected in a hierarchy [Shamir, 1971; Zaide, 2006]. Selecting the proper aggregation in time and space for a particular application is one of the most important aspects of modeling. The short-term (weekly to annual) or long-term (years, decades) operation of a large scale WSS can be captured in a model of medium aggregation that is used to manage simultaneously both the sources and the network [Fisher et al., 2002; Draper et al., 2003, 2004; Jenkins et al., 2004; Watkins et al., 2004]. Many models deal with quantities of water to be delivered from sources to demand zones. Some models consider water quality as well, in particular salinity [Mehrez et al.1999; Tu et al., 2005; Yates et al., 2005; Zaide, 2006].

The network representation in the model can be classified according to the physical laws that are considered explicitly in the model constraints [Ostfeld and Shamir, 1993; Cohen et al., 2000]. According to this classification the models of Tu et al. [2005], Yates et al. [2005] and Zaide [2006] are flow-quality models which consider the balance of the flows and mass of quality parameters, but without explicit inclusion of the hydraulics. The inherent assumption of these models is that the hydraulic operation with the quantities prescribed by the model would be feasible hydraulically. With the inclusion of desalination plants as an important source in WSS, as is the case in Israel, water salinity consideration must be included in the management. It is important and necessary to consider both quantity and salinity in the water sources, in the water supplied to consumers and at nodes of the supply system itself. With the salinity considerations becoming an important part of management models, the complexity of the model evidently increases.

A further consideration is sustainability of the management plan. This implies meeting the needs of the present without reducing the ability of the next generation to meet its needs [Loucks, 2000]. Sustainable management requires a perspective with a relatively long time-horizon, and hence the need to develop multi-year flow-quality models for WSS management. The multi-year models insure that the final state of the system at the end of the operating horizon is considered, either as a constraint or having a value in the objective function.

An associated aspect of multi-year water supply management relates to hydrological uncertainty [Ajami et al., 2008], climate change [Grantz et al., 2007], population growth [Kasprzyk et al., 2009], and the decline of water quality in the sources. The model described in this Chapter is deterministic; however, as will be demonstrated below, our model is developed with structural adaptability and high computational efficiency in mind, so it can be a building-block for a model that takes uncertain considerations into account by sensitivity or uncertainty analysis [Lal et al., 1997; Wong et al., 2002; Wu et al., 2006]; an Ensemble or Scenario-based Optimization [Seifi and Hipel, 2001; Kracman et al., 2006] or by Implicit Stochastic Optimization [Crawley and Dandy, 1993; Labadie, 2004].

Water resources management models have been solved by a variety of optimization techniques. Evolutionary Algorithms, including Genetic Algorithms and others, have

gained popularity in recent years, as detailed in a recent review paper [Nicklow et al., 2010]. During the first stages of this research we developed our own Evolutionary Algorithm titled “Search Method for Boxed-Constrained Optimization” as a candidate solver for the optimization problem (for details and application of this method to WSS problems see Appendix 1).

3.3. Model Outline

A seasonal multi-year model for management of water quantities and salinity in regional water supply systems (WSS) has been developed; water is taken from sources, which include aquifers, reservoirs and desalination plants, conveyed through a distribution system to consumers who require certain quantities of water under specified salinity constraints. The year is divided into seasons, and the operation is subject to technological, administrative and environmental constraints such as water levels and water quality in the aquifers, capacities of the pumping and distribution system, capacity of the desalination plants and their maximum salinity removal ratio. The objective is to operate the system over a period of several years, each year divided into two seasons, with minimum total cost of desalination, pumping, delivery and an extraction levy in the aquifers. The objective function and some of the constraints in the model are nonlinear, leading to a nonlinear optimization problem. The model does not include hydraulic constraints and does not guarantee required heads at consumer nodes, yet the objective function takes into account the cost of conveyance as a function of the hydraulic properties of the network. This is appropriate when it can be assumed that the resulting operation plan will be feasible hydraulically [Cohen et al., 2000].

3.4. Model Components

In the seasonal multi-year model for management of water quantity and salinity, water is taken from sources, which include aquifers, reservoirs and desalination plants, conveyed through a distribution system to consumers who require certain quantities of water with specified salinity limits. The small WSS shown in Figure 3.1 was used for model development, testing and demonstration; results will be shown also (in Section 3.9) for the WSS shown in Figures 3.11, which is a central part of the Israeli National WSS. The year is divided into seasons (two seasons in the examples, but there could be more, since the computational cost rises only linearly with the number of seasons,

as detailed in Section 3.10) and the operation is subject to constraints on water levels and water quality (salinity) in the aquifers, capacities of the pumping and distribution system, capacity of the desalination plants and their salinity removal ratio. Therefore the decision variables in each season are: desalinated water production and salinity removal ratio in the desalination plants, and the water flow and water salinity distribution throughout the network. Two sets of state variables describe the state of the system at the end of each season: water levels and water salinities in the natural resources (aquifers and reservoirs).

The model was developed in two forms, first as an annual model and then it was expanded into a multi-year model. The annual model served as the building block for the multi-year with the state variables linking the seasons and the years (Figure 3.2). The annual model has value in itself, as it can be used to determine the coming year's operation with the known initial condition and the desired end-of-year state prescribed. It is also valuable for developing and debugging when new system expansions/modifications are considered.

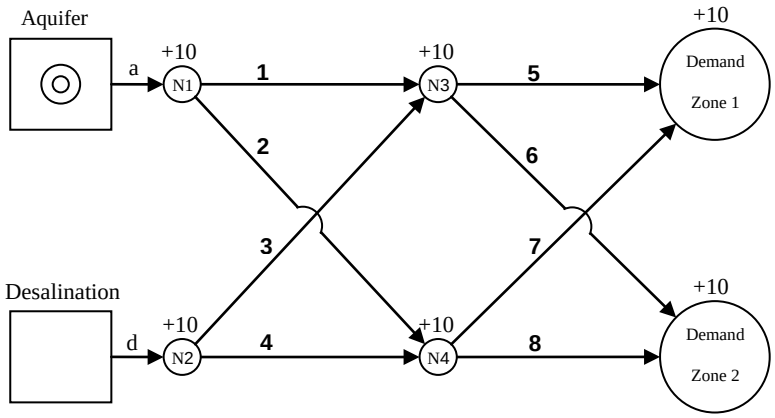

Figure 3.1: Demonstration WSS

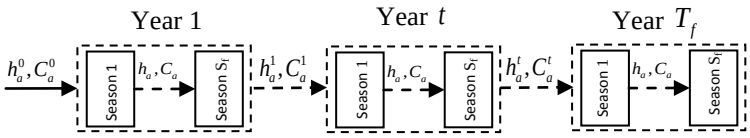

Figure 3.2: Linkage between seasons and years through state variables

3.4.1. Objective function

The objective is to operate the system with minimum total cost of desalination CD, extraction levy from the natural sources CE and conveyance costs CC over the planning horizon T_f.

In the next Sections p,a,d,z,S,Y denote pipe, aquifer, desalination plant, demand zone, season and year, respectively.

Conveyance Cost

The conveyance cost in a pipe is related to the head loss, given by the Hazen-Williams equation, and the topographical difference between its ends (assuming the same hydraulic head at both ends, a reasonable assumption for a seasonal model).

$$\begin{aligned} CC_p^{S,Y} &= \frac{X_p^{S,Y} \cdot \left(\frac{Q_p^{S,Y}}{w^{S,Y}} \right)}{200} \cdot 0.736 \cdot w^{S,Y} \cdot KWHC^{S,Y} \\ X_p^{S,Y} &= \Delta Z_p + \Delta Hf_p^{S,Y} \\ \Delta Hf_p^{S,Y} &= 1.526 \cdot 10^7 \cdot \left(\frac{Q_p^{S,Y}}{w^{S,Y} c_p^Y} \right)^{1.852} \cdot D_p^{-4.87} \cdot L_p \end{aligned} \tag{3.1}$$

where $CC_p^{S,Y}$ is conveyance cost ($\$ / season$); $X_p^{S,Y}$ is head loss (m); $Q_p^{S,Y}$ is discharge ($m^3 / season$); $w^{S,Y}$ is number of pumping hours ($hr / season$); $KWHC^{S,Y}$ is pumping cost ($\$ / kwhr$); ΔZ_p is topographical difference (m); $\Delta Hf_p^{S,Y}$ is energy head loss (m); c_p^Y is Hazen Williams coefficient ($-$); D_p is link diameter (cm); L_p is link length (km).

Extraction Levy

The extraction levy depends on the water level in the natural resource. The levy is higher at low water levels, to indicate the increasing value (cost of scarcity) of the resource. The specific levy is expressed as a value per unit volume, so the cost of the extraction levy is:

$$\begin{aligned} \overline{CE}_a^{S,Y} &= \left(1 - \frac{h - h_{\min}}{h_{\max} - h_{\min}} \right)_a^{S,Y} \cdot \left(\overline{CE}^{\max} \right)_a^{S,Y} \\ CE_a^{S,Y} &= \overline{CE}_a^{S,Y} \cdot Q_a^{S,Y} \end{aligned} \tag{3.2}$$

which is a quadratic relationship between of extraction levy and the amount pumped, where $\overline{CE}_a^{S,Y}$ is specific levy ($\$/m^3$); $h_a^{S,Y}$ is water level (m); $(h_{\min})_a^{S,Y}$ is minimum allowed water level (m); $(h_{\max})_a^{S,Y}$ is maximum allowed water (m); $\left(\overline{CE}^{\max}\right)_a^{S,Y}$ is maximum levy ($\$/m^3$); $CE_a^{S,Y}$ is extraction levy ($\$/season$); $Q_a^{S,Y}$ is pumping amount ($m^3/season$).

Desalination Cost

The desalination cost includes a constant price per unit of desalinated water plus a variable cost of the salinity removal ratio:

$$CD_d^{S,Y} = \left(\alpha_d + \frac{1}{(100 - RR_d^{S,Y})^{\beta_d}} \right) \cdot Q_d^{S,Y} \tag{3.3}$$

where $CD_d^{S,Y}$ is desalination cost ($\$/season$); α_d is constant ($\$/m^3$); $Q_d^{S,Y}$ is desalination amount ($m^3/season$); $RR_d^{S,Y}$ is removal ratio ($\%$); β_d is constant ($-$).

Overall Cost

The objective of the multi-year model is to minimize the present value of the total cost of operation over the planning horizon.

$$cost = \sum_Y \frac{\sum_S \left(\sum_p CC_p^{S,Y} + \sum_d CD_d^{S,Y} + \sum_a CE_a^{S,Y} \right)}{(1+r)^Y} \tag{3.4}$$

where $cost$ is the total operation cost ($\$$); r is the annual discount rate ($-$). Since the objective function is nonlinear, it can easily be converted into benefit maximization by including the value of the quantity and salinity of the water supplied to consumers (within the specified constraints), if the relevant cost/benefit coefficients are available.

3.4.2. Constraints

Water Conservation Law

This law holds for all nodes in the network; source nodes, intermediate nodes and demand nodes. A WSS can be represented as a directed graph consisting of N nodes connected by M edges. The nodes can be grouped into two sub-groups: N_1 are source nodes, such as desalination plant and aquifers, with one outgoing link for each

source node and N_2 are junction nodes where two or more edges join i.e., intermediate nodes and demand node. The M edges represent the links between two nodes; links in which the direction of flow is not fixed are represented by two edges, one in each direction. The topology of the network is represented by the junction node connectivity matrix A, where $A \in \mathbf{R}^{N_2 \times M}$ has a row for each node and a column for each edge. The nonzero elements in each row are $+1$ and -1 for incoming and outgoing edges respectively. The first columns in A correspond to the links which leave source nodes (aquifers and desalination plants), while the last rows correspond to the demand nodes. For each season S in year Y the following linear equation system insures water conservation at the network nodes.

$$A \cdot Q = b \tag{3.5}$$

where $Q = [Q_{source}, Q_{pipes}]^T$; $b = [0, Q_{demand}]^T$; Q_{Source} is the vector of discharges leaving source nodes; Q_{pipes} is the vector of discharges in the links which are connected to intermediate nodes excluding the links which are connected to source nodes; Q_{demand} is the vector of outgoing discharges at demand nodes.

The water supply network shown in Figure 3.1 has 2 source nodes, 4 intermediate nodes and 2 demand nodes. The junction node connectivity matrix for this network $A \in \mathbf{R}^{6\times10}$ is given in Table 3.1 and the vectors Q and b are $Q = [Q_a, Q_d, Q_1, ..., Q_8]^T$; $b = [0, ..., 0, Q_{z=1}, Q_{z=2}]^T$.

Node	Source		Pipe							
	a	**d**	**1**	**2**	**3**	**4**	**5**	**6**	**7**	**8**
1	1	0	-1	-1	0	0	0	0	0	0
2	0	1	0	0	-1	-1	0	0	0	0
3	0	0	1	0	1	0	-1	0	-1	0
4	0	0	0	1	0	1	0	-1	0	-1
5	0	0	0	0	0	0	1	1	0	0
6	0	0	0	0	0	0	0	0	1	1

Table 3.1: Junction node connectivity matrix

Mass Conservation Law

For each season S of year Y the following linear equation system insures salt mass conservation at network nodes:

$$
\begin{aligned}
&A^0 \cdot D_Q \cdot C^0 = 0, \qquad A^0 \in \mathbf{R}^{N_2 \times (M+n_3)} \\
&A^0 = \left(\begin{array}{c|c} A & 0 \\ & -I \end{array} \right) \\
&C^0 = [C_{source}, C_{pipes}, C_{demand}]^T \\
&D_Q \in \mathbf{R}^{(M+n_3)\times(M+n_3)} \ \text{diagonal matrix} \\
&D_Q = \mathbf{diag}\left([Q_{source}, Q_{pipes}, Q_{demand}]\right)
\end{aligned}
\tag{3.6}
$$

where C_{source} is salinity leaving source nodes; C_{pipes} is the salinity in the links which are connected to intermediate nodes excluding the links which are connected to source nodes; C_{demand} is salinity supplied at demand nodes; n_3 number of demand nodes; $I \in \mathbf{R}^{n_3 \times n_3}$ is the identity matrix.

For the network in Figure 3.1, the matrix $A^0 \in \mathbf{R}^{6\times12}$ is given in Table 3.2, $D_Q \in \mathbf{R}^{12\times12}$ is given in Figure 3.3 and the vector C^0 is defined as $C^0 = [C_a, C_d, C_1, ..., C_8, C_{z=1}, C_{z=2}]^T$.

Node	Source		Pipe								Demand	
	a	d	1	2	3	4	5	6	7	8	z=1	z=2
1	1	0	-1	-1	0	0	0	0	0	0	0	0
2	0	1	0	0	-1	-1	0	0	0	0	0	0
3	0	0	1	0	1	0	-1	0	-1	0	0	0
4	0	0	0	1	0	1	0	-1	0	-1	0	0
5	0	0	0	0	0	0	1	1	0	0	-1	0
6	0	0	0	0	0	0	0	0	1	1	0	-1

Table 3.2: Definition of the matrix A^0

$$
D_Q^S \in \mathbf{R}^{12\times12}
$$

$$
D_Q^S = \begin{pmatrix}
Q_a^S & & & & & & & & & & & \\
& Q_d^S & & & & & & & 0 & & & \\
& & Q_1^S & & & & & & & & & \\
& & & \ddots & & & & & & & & \\
& & & & & & Q_8^S & & & & & \\
& 0 & & & & & & & Q_{z=1}^S & & & \\
& & & & & & & & & & Q_{z=2}^S &
\end{pmatrix}
$$

Figure 3.3: Definition of the matrix D_Q^S

Hydrological Balance for Natural Resources

The hydrological water and salinity mass balances insure that the change in aquifer storage equals the difference between the recharge and withdrawal during the season:

$$
R_a^{S,Y} - Q_a^{S,Y} = SA_a \cdot (h_a^{S,Y} - h_a^{(S,Y)-1}) \tag{3.7}
$$

$$\left(C_R\right)_a^{S,Y} \cdot R_a^{S,Y} - C_a^{(S,Y)-1} \cdot Q_a^{S,Y} = SA_a \cdot \left(C_a^{S,Y} \cdot h_a^{S,Y} - C_a^{(S,Y)-1} \cdot h_a^{(S,Y)-1}\right) \quad (3.8)$$

where $R_a^{S,Y}$ is recharge (m^3); SA_a is the storativity multiplied by area (m^2); $h_a^{S,Y}, C_a^{S,Y}$ are water level and salinity respectively (m), ($mgcl/lit$); $h_a^{(S,Y)-1}, C_a^{(S,Y)-1}$ are water level and salinity in the previous season respectively (m), ($mgcl/lit$); $(C_R)_a^{S,Y}$ is salinity of the recharge water ($mgcl/lit$). Each natural source (aquifer, reservoir) is viewed as a single entity. If an aquifer is to be subdivided into cells with hydraulic connections between them then a finite difference representation of the aquifer or a simulation tool can be substituted for equations (3.7) and (3.8).

Desalinated Water Salinity

$$C_d^{S,Y} = C_{sea} \cdot \left(\frac{100 - RR_d^{S,Y}}{100}\right) \quad (3.9)$$

where $C_d^{S,Y}$ is desalinated water salinity ($mgcl/lit$); C_{sea} is sea water salinity (27000 $mgcl/lit$); $RR_d^{S,Y}$ is the removal ratio (%).

Dilution Condition

The model assumes total mixing at all nodes, so the salinity in all links leaving a node is the same. This dilution condition is given by the linear equation system:

$$B^0 \cdot C^0 = 0 \quad (3.10)$$

Each row of B^0 indicates equal salinity for two outgoing edges which share the same inflow node, i.e. each row has only two non-zero elements $+1$ and -1; when three links leave the same node there are two rows, each with two non-zero elements $+1$ and -1. In the demonstrated example (Figure 3.1), the matrix $B^0 \in \mathbf{R}^{4\times 12}$ is given in Figure 3.4, each of the 4 intermediates nodes has 2 outgoing edges, and therefore each of the 4 nodes has 1 row in the matrix B^0.

$$B^0 \in \mathbf{R}^{4\times 12}$$

$$B^0 = \begin{pmatrix} 0 & 0 & -1 & 1 & 0 & 0 & 0 & 0 & 0 & 0 & 0 & 0 \\ 0 & 0 & 0 & 0 & -1 & 1 & 0 & 0 & 0 & 0 & 0 & 0 \\ 0 & 0 & 0 & 0 & 0 & 0 & -1 & 0 & 1 & 0 & 0 & 0 \\ 0 & 0 & 0 & 0 & 0 & 0 & 0 & -1 & 0 & 1 & 0 & 0 \end{pmatrix}$$

Figure 3.4: Definition of the matrix B^0

Conveyance Capacity Constraints

The model deals with balance of water and salt mass and does not consider explicitly the hydraulic energy balance of the system. However, in order to prevent infeasibilities of hydraulic conditions, the discharges in the pipes are limited by capacity constraints which are calculated from the maximum hourly conveyance capacity of the pipe, multiplied by the number of hours in the season. The lower bound is set to zero since the flow direction in the pipes is fixed.

$$0 < Q_p^{S,Y} < (Q_{\max})_p^{S,Y} \tag{3.11}$$

where $(Q_{\max})_p^{S,Y}$ is the maximum discharge allowed ($m^3 / season$). If the flow direction in a link is not set in advance then two pipes with opposite directions are introduced, and the solution will determine for each season the direction of flow.

Extraction Capacities from the Natural Sources

The amount from each natural resource may be restricted by an upper bound, reflecting various hydrological and hydraulic considerations. The lower bound is set to zero as the flow from the source is one-directional.

$$0 < Q_a^{S,Y} < (Q_{\max})_a^{S,Y} \tag{3.12}$$

where $(Q_{\max})_a^{S,Y}$ is the maximum admissible/feasible withdrawal ($m^3 / season$).

Desalination Capacity

The amount of desalinated water from each plant is limited by an upper bound which represents plant capacity and by a lower bound (which may be zero) that represents a condition of the contract with the plant concession.

$$(Q_{\min})_d^{S,Y} < Q_d^{S,Y} < (Q_{\max})_d^{S,Y} \tag{3.13}$$

where $(Q_{\max})_d^{S,Y}$ is maximum supply ($m^3 / season$); $(Q_{\min})_d^{S,Y}$ is minimum supply ($m^3 / season$).

Removal Ratio Limits

Salinity removal limits reflect the plant technology and its overall system design:

$$(RR_{\min})_d^{S,Y} \le RR_d^{S,Y} \le (RR_{\max})_d^{S,Y} \quad (3.14)$$

where $RR_d^{S,Y}$ is removal ratio (%); $(RR_{\min})_d^{S,Y}$ is minimum removal ratio (%); $(RR_{\max})_d^{S,Y}$ is maximum removal ratio (%).

Water Levels in the Sources

Constraints on water levels in the natural resources reflect policy and operational limits.

$$(h_{\min})_a^{S,Y} < h_a^{S,Y} < (h_{\max})_a^{S,Y} \quad (3.15)$$

where $h_a^{S,Y}$ is water level (m); $(h_{\min})_a^{S,Y}$ is minimum allowed water level (m); $(h_{\max})_a^{S,Y}$ is maximum allowed water level (m).

Salinity Levels in the Sources

Constraints on admissible source salinity reflect source management policies, especially for preventing excessive water salinity.

$$(C_{\min})_a^{S,Y} < C_a^{S,Y} < (C_{\max})_a^{S,Y} \quad (3.16)$$

where $C_a^{S,Y}$ is water salinity in ($mgcl/lit$); $(C_{\min})_a^{S,Y}$ is minimum salinity ($mgcl/lit$) (which may be zero); $(C_{\max})_a^{S,Y}$ is maximum admissible salinity ($mgcl/lit$).

Demand Salinity Constraints

Ensuring salinity of supply water within bounds:

$$(C_{\min})_z^{S,Y} < C_z^{S,Y} < (C_{\max})_z^{S,Y} \quad (3.17)$$

where $C_z^{S,Y}$ is water salinity supplied for demand zone z ($mgcl/lit$); $(C_{\min})_z^{S,Y}$ is minimum salinity ($mgcl/lit$); $(C_{\max})_z^{S,Y}$ is maximum admissible salinity ($mgcl/lit$).

3.5. Optimization Plan

The mathematical formulation of the optimization model determines its suitability for solution by an optimization algorithm and the resultant computational efficiency. Since we intend to run the model many times, in interactive mode with decision making, and later as a kernel of models for management under uncertainty, we have

developed a set of manipulations that improve substantially the solvability and efficiency of the model.

3.5.1. Eliminating Dependent Variables

To reduce the model size we extract one dependent decision variable from each equality constraint. Then the dependent variables are substituted in the objective function and the inequality constraints to obtain a smaller model (fewer decision variables) without equality constraints.

In the linear equality constraints set obtained from the water balance requirement (Equation 3.5):

$$A \cdot Q = b \tag{3.18}$$

the reduction is achieved by solving the linear equation system. This system is most likely underdetermined since we have more edges than nodes $M > N_2$, and the rank of the matrix A is therefore N_2 [Boulos and Altman, 1991].

The general solution of the underdetermined system (3.18) is given by:

$$Q_{dep} = A_1^{-1} \cdot \left(b - A_2 \cdot Q_{indep} \right) \tag{3.19}$$

where A_1 is a matrix of N_2 independent columns of A; A_2 is a matrix of $M - N_2$ dependent columns of A; $(\,)_{dep}$ is the vector of dependent decision variables; $(\,)_{indep}$ is the vector of independent decision variables.

In graph theory this is related to the spanning tree (ST); a ST of a connected graph is defined as a maximal set of edges that contains no cycle, i.e. the graph matrix of the ST has full rank. Thus finding the dependent columns of the matrix A is equivalent to finding the non-ST edges of the graph. In a connected graph there are many STs, and any of these can indicate which columns in A are dependent and which are not. To generate a ST one can use the Breadth-First-Search algorithm (BFS) [Boulos et al., 2006], or simply by calculating the reduced echelon form of A using Gauss Jordan elimination with partial pivoting. In the reduced echelon form the columns which are related to ST edges construct the standard basis.

The inequality constraints (3.11)-(3.13) define lower and upper bounds for the vector Q. Substituting the dependent variables in the inequality constraints (3.11)-(3.13) leads to:

$$\begin{aligned} &\left(Q_{\min}\right)_{dep} \le A_1^{-1}\cdot\left(b - A_2\cdot Q_{indep}\right) \le \left(Q_{\max}\right)_{dep} \\ &b - A_1\cdot\left(Q_{\max}\right)_{dep} \le A_2\cdot Q_{indep} \le b - A_1\cdot\left(Q_{\min}\right)_{dep} \end{aligned} \tag{3.20}$$

Constraint (3.20) with the following bounds replaces constraints (3.11)-(3.13):

$$\left(Q_{\min}\right)_{indep} < Q_{indep} < \left(Q_{\max}\right)_{indep} \tag{3.21}$$

Another way to extract the dependent decision variables from the underdetermined system is to calculate the null space of A, $Null(A)$. The solution of the underdetermined system is given by the sum of a particular solution of the system and a vector in the null space of A.

$$Q = Q_{particular} + Null\left(A\right)\cdot\Delta Q \tag{3.22}$$

In graph theory the null space of A is related to the loops and pseudo-loops of the network, and the solution is achieved by considering the circular flows ΔQ in loops and pseudo-loops as decision variables [Boulos et al., 2006]. The size of the decision vector ΔQ is $M - N_2$ - exactly the same as Q_{indep} in the previous approach. In our model we have used the first approach i.e. equations (3.19)-(3.21) because it keeps the decision variables bounded.

For the water supply system model shown in Figure 3.1, the reduced row echelon form of the graph matrix is given in Table 3.3. Recalling that in the reduced echelon form the columns related to ST edges construct the standard basis, i.e. the ST edges are $\{a, d, 1, 2, 5, 7\}$. Hence the non-ST edges are $\{3, 4, 6, 8\}$ and their corresponding flows in each season present the independent decision variables; thus A_2 contains columns $\{3, 4, 6, 8\}$ while A_1 contains columns $\{a, d, 1, 2, 5, 7\}$. The definitions of Q_{dep}, Q_{indep}, A_1 and A_2 are given in Figure 3.5.

Node	Source		Pipe							
	a	d	1	2	3	4	5	6	7	8
1	1	0	0	0	1	1	0	0	0	0
2	0	1	0	0	-1	-1	0	0	0	0
3	0	0	1	0	1	0	0	1	0	1
4	0	0	0	1	0	1	0	-1	0	-1
5	0	0	0	0	0	0	1	1	0	0
6	0	0	0	0	0	0	0	0	1	1

Table 3.3: Reduced row echelon form of the matrix A

$Q^S_{indep} = [Q^S_3, Q^S_4, Q^S_6, Q^S_8]^T$

$Q^S_{dep} = [Q^S_a, Q^S_d, Q^S_1, Q^S_2, Q^S_5, Q^S_7]^T$

$(Q_{\min})^S_{indep} = [0,0,0,0]^T$

$(Q_{\max})^{S=1}_{indep} = [57.6,57.6,57.6,57.6]^T$

$(Q_{\max})^{S=2}_{indep} = [18.8,18.8,18.8,18.8]^T$

$(Q_{\min})^S_{dep} = [0,0,0,0,0,0]^T$

$(Q_{\max})^{S=1}_{dep} = [50,50,57.6,57.6,57.6,57.6]^T$

$(Q_{\max})^{S=2}_{dep} = [50,50,18.8,18.8,18.8,18.8]^T$

$b^S = [0,0,0,0,25,25]^T$

$$A_1 = \begin{pmatrix} 1 & 0 & -1 & -1 & 0 & 0 \\ 0 & 1 & 0 & 0 & 0 & 0 \\ 0 & 0 & 1 & 0 & -1 & -1 \\ 0 & 0 & 0 & 1 & 0 & 0 \\ 0 & 0 & 0 & 0 & 1 & 0 \\ 0 & 0 & 0 & 0 & 0 & 1 \end{pmatrix}$$

$$A_2 = \begin{pmatrix} 0 & 0 & 0 & 0 \\ -1 & -1 & 0 & 0 \\ 1 & 0 & 0 & 0 \\ 0 & 1 & -1 & -1 \\ 0 & 0 & 1 & 0 \\ 0 & 0 & 0 & 1 \end{pmatrix}$$

Figure 3.5: Dependent flows, definitions and values

3.5.2. Resultant Variables

A special and useful property of our model is that equality constraints (3.6), (3.9), (3.10) and the hydrological constraints (3.7), (3.8) imply that for fixed values of the flows and removal ratios the salinity variables C and the state variables of the natural resources h_a, C_a are also fixed (resultant variables). This property insures the ability to evaluate the objective function and all the constraints for predetermined Q_{indep} and RR, since the remaining flows are dependent and the other variables are resultant variables which can be evaluated directly.

By using the equality constraints (3.7) and (3.8) we can extract the state variables of the natural resources h_a, C_a as a function of Q_{indep}.

$$h_a^{S,Y} = \frac{R_a^{S,Y} - Q_a^{S,Y}}{SA_a} + h_a^{(S,Y)-1} \qquad (3.23)$$

$$C_a^{S,Y} = \frac{1}{h_a^{S,Y}} \left(\frac{\left(C_R\right)_a^{S,Y} \cdot R_a^{S,Y} - C_a^{(S,Y)-1} \cdot Q_a^{S,Y}}{SA_a} + C_a^{(S,Y)-1} \cdot h_a^{(S,Y)-1} \right) \quad (3.24)$$

The salinity variables of the desalination plants nodes given in (3.9) can also be calculated by given Q_{indep} and RR. Hence, C_{source} is a function of Q_{indep} and RR. After calculating the state variables of the natural resources the objective function and the inequality constraints (3.15) and (3.16) can also be evaluated.

Note that in our formulation the objective function does not depend directly on water salinity in the system (it does, however, reflect the cost of desalination, which is required in order to meet salinity constraints). Constraint (3.15) is linear in the given formulation, but if the aquifers were represented by a finite differences model or a simulation program this constraint would be nonlinear.

Given a network with the structure depicted in Figure 3.6, water quantity distribution in the network for all the edges and the sources salinity vector C_{source}. One can formulate the salinity balance equation at each node $j = 1...J$ and $k = 1...K$. Hence we can formulate $eq\_bal = J + K$ equations with $un = \sum_{j=1}^{J} MID\_OUT_j + K$ unknowns.

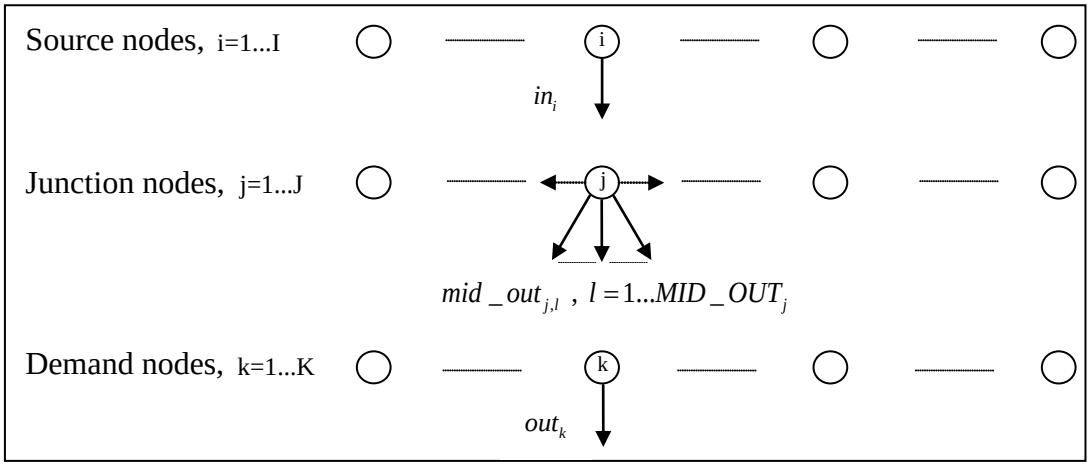

Figure 3.6: General network topology

By applying the full dilution condition in the network nodes, we obtain that for each $j = 1...J$ the edges $mid\_out_{j,l}$, $l = 1...MID\_OUT_j$ have the same salinity, hence we can formulate $\sum_{j=1}^{J} \left(MID\_OUT_j - 1 \right) = \sum_{j=1}^{J} MID\_OUT_j - J$ equations of the form

$$\text{salinity of link}[mid\_out_{j,l}] = \text{salinity of link}[mid\_out_{j,l+1}] .$$

From the salinity balance we have $eq\_bal = J + K$ equations and from the dilution condition we have $eq\_dil = \sum_{j=1}^{J} MID\_OUT_j - J$ equations. The total number of equation is $eq = \sum_{j=1}^{J} MID\_OUT_j + K$, which is equal to the total number of the salinity unknowns.

To extract the salinity variables, constraints (3.6) and (3.10) can be joined to form the following:

$$K \cdot C^0 = 0 \tag{3.25}$$

where K is a block matrix defined as $K = \left(\frac{A^0 \cdot D_Q}{B^0} \right)$. When C_{source} is determined using the salinity state variables C_a and the desalination plants salinity C_d given in (3.9), the first columns corresponding to the sources are moved to the RHS of the equation system to form the following:

$$K_1 \cdot C = -K_2 \cdot C_{source} \tag{3.26}$$

where $C = [C_{pipes}, C_{demand}]^T$, K_1 is a square and full rank matrix, hence the resultant salinity variables are:

$$C = -K_1^{-1} \cdot K_2 \cdot C_{source} \tag{3.27}$$

The matrices K_1, K_2 are functions of the flows, i.e. functions of the independent decision variables Q_{indep}. Since the salinity variables are a product of the inverse of K_1 and K_2, this creates a nonlinear relationship between the salinity variables and Q_{indep}. As a consequence, the inequality constraint (3.17) is nonlinear.

Regarding the WSS shown in Figure 3.1, for predetermined $Q_{indep} = [Q_3, Q_4, Q_6, Q_8]^T$ and RR_d; the vector $C_{source} = [C_a, C_d]^T$ is determined using (3.24) and (3.9). Hence, the vector $C = [C_1, ..., C_8, C_{z=1}, C_{z=2}]^T$ can be obtained by (3.27). Where $K_2 \in \mathbf{R}^{2\times 10}$ is the matrix combining the first columns (corresponding to the sources) of the matrix K and $K_1 \in \mathbf{R}^{10\times 10}$ is the matrix of the remaining columns of K; the matrix K is given in Figure 3.7.

$$K^S \in \mathbf{R}^{10\times 12}$$

$$K^S = \left(\begin{array}{cccccccccccc}
Q_a^S & 0 & -Q_1^S & -Q_2^S & 0 & 0 & 0 & 0 & 0 & 0 & 0 & 0 \\
0 & Q_d^S & 0 & 0 & -Q_3^S & -Q_4^S & 0 & 0 & 0 & 0 & 0 & 0 \\
0 & 0 & Q_1^S & 0 & Q_3^S & 0 & -Q_5^S & 0 & -Q_7^S & 0 & 0 & 0 \\
0 & 0 & 0 & Q_2^S & 0 & Q_4^S & 0 & -Q_6^S & 0 & -Q_8^S & 0 & 0 \\
0 & 0 & 0 & 0 & 0 & 0 & Q_5^S & Q_6^S & 0 & 0 & -Q_{z=1}^S & 0 \\
0 & 0 & 0 & 0 & 0 & 0 & 0 & 0 & Q_7^S & Q_8^S & 0 & -Q_{z=2}^S \\
\hline
0 & 0 & -1 & 1 & 0 & 0 & 0 & 0 & 0 & 0 & 0 & 0 \\
0 & 0 & 0 & 0 & -1 & 1 & 0 & 0 & 0 & 0 & 0 & 0 \\
0 & 0 & 0 & 0 & 0 & 0 & -1 & 0 & 1 & 0 & 0 & 0 \\
0 & 0 & 0 & 0 & 0 & 0 & 0 & -1 & 0 & 1 & 0 & 0
\end{array}\right)$$

Figure 3.7: Definition of the matrix K^S

3.6. Evaluating the Objective Function and the Constraints

The dependent variables Q_{dep} and the resultant variables are functions of the decision variables Q_{indep} and RR. Hence, the objective function and all the constraints can be evaluated for predetermined decision variables Q_{indep} and RR. The seasonal evaluation scheme is depicted in Figure 3.8, where: (a) The flow distribution in the network and the source limitations (3.5) and (3.11)-(3.13) are integrated by the inequality linear constraints (3.20) and the bounds (3.21), (b) Evaluation of the objective function does not require the salinity calculations in the system, since it depends only on the removal ratios of the desalination plants, and (c) The remaining inequality constraints (3.15)-(3.17) are nonlinear in the general case (discussed in the previous Section).

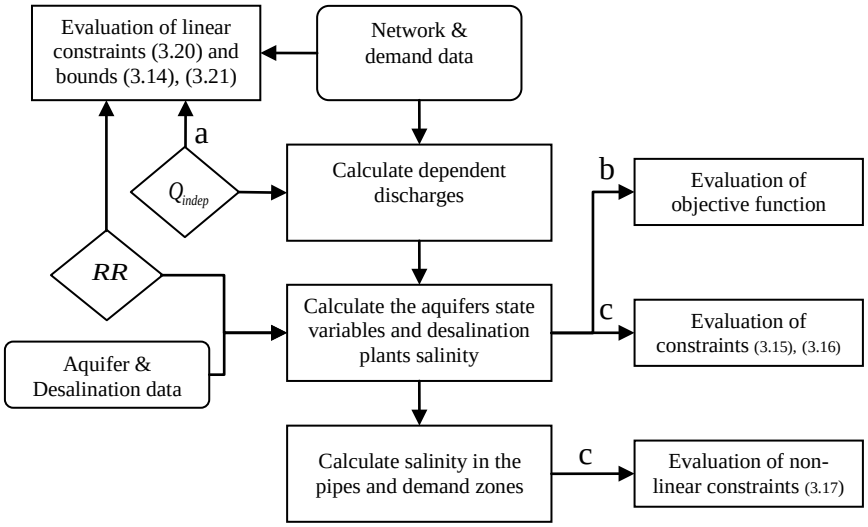

Figure 3.8: Scheme for evaluation of the constraints and objective function with a given set of flow decision variables Q_{indep} and RR

3.7. The Optimization Solver

The steps described in the previous Sections result in a general nonlinear optimization, which can be solved with one of the existing general nonlinear programming solvers, such as SQP [Fletcher, 1985] or an interior point algorithm [Waltz et al., 2006; Byrd et al., 2000]. These solvers use the gradient of the objective and the Jacobian matrix of the nonlinear constraints. When calculation of the analytical derivatives is computationally demanding, a finite differences scheme can be used to give an estimation of the derivatives. However, for a water supply network of practical size the optimization model becomes very large, particularly for long-term multi-stage operation problems, so this numerical approximation is very cumbersome.

We have therefore developed the Time-Chained-Method (TCM), an efficient finite differences scheme designed for our model's multi-stage structure, which reduces the computation time from $O(T_f^2)$ *to* $O(T_f)$ where T_f is the number of stages. Nonlinear optimization solvers are sensitive to scaling [Betts, 2001], which means that the solver may encounter difficulties when decision variables have different scale. To overcome these difficulties a transformation of variables is used. Details of the TCM appear in Section 3.10.

3.7.1. Optimization Software

Due to the general structure of the objective function and constraints in our model a general nonlinear optimization solver is required. Our model was programmed in MATLAB and uses the interior-point algorithm with conjugate gradient of the FMINCON nonlinear optimization suite.

We developed a special-purpose pre-processor that generates the data for the optimizer and a post-processor that displays the results in tabular and graphic forms (see Section 3.12). These tools facilitate greatly the use of the software for creating models of any system and for ease of making topological and data changes for sensitivity analysis and/or testing alternatives. Scaling is applied to model data to improve convergence (see Section 3.11).

3.8. Illustrative Example

A water supply system model (Figure 3.1) has been solved in this example; minimum cost of operating a system which is fed from a one cell aquifer and a desalination

plant to supply two customers over a year. The year has two seasons: the first has 265 days ("winter" with low demands) and the second 90 days ("summer" with high demands). The daily pumping hours in each season is 20 (hr/day), hence the seasonal pumping hours are $w^{S=1}=5300\ (hr/season)$, $w^{S=2}=1800\ (hr/season)$.

Problem Parameters

Pipes and Conveyance Cost Data

The network layout is presented by the junction node connectivity matrix A, given in Table 3.1. The pipes 1-8 all have the same parameters: diameters $D_p=50\ (in)$, lengths $L_p=1(km)$, Hazen Williams coefficients $c_p=110\ (-)$, and no topographic difference between their ends $\Delta Z_p=0\ (m)$. The pipes seasonal capacities are based on a hydraulic loss of 4 ‰. The resulting capacities for all pipes are $(Q_{\max})_p^{S=1}=57.6(MCM/season)$ and $(Q_{\max})_p^{S=2}=18.8(MCM/season)$ for season 1 and the season 2 respectively. The energy cost for both seasons is $KWHC^S=0.1\ (\$/kwhr)$.

Sources and Demand Data

The demand data for the two demand zones are identical for both demand zones and both seasons, that is the water demand $(Q_{demand})_z^S=25\ (MCM/season)$ and the water salinity requirements are $(C_{\min})_z^S=0\ (mgcl/lit)$, $(C_{\max})_z^S=190\ (mgcl/lit)$. The system is fed from two sources; the first is an aquifer with initial water level $h_a^0=11\ (m)$, initial water salinity $C_a^0=180\ (mgcl/lit)$, recharge in the first season $R_a^{S=1}=50\ (MCM)$ and in the second season $R_a^{S=2}=0\ (MCM)$. The operational limits and additional parameters of the aquifer are given in Table 3.4. The second source is a sea-water desalination plant (sea water is $C_{Sea}=27000\ (mgcl/lit)$); the plant is large enough to supply the entire seasonal demand in both seasons, hence $(Q_{\max})_d^S=50\ (MCM)$. The plant has no obligation for a minimal supply requirement (which is often a constraint in actual practice) i.e. $(Q_{\min})_d^S=0\ (MCM)$. The removal ratio of the plant is between $(RR_{\min})_d^S=99\ (\%)$ and $(RR_{\max})_d^S=99.9\ (\%)$, yielding a product salinity in the range 270-27 $(mgcl/lit)$. The desalination cost parameters are $\alpha_d=0\ (\$/MCM)$ and $\beta_d=1\ (-)$.

$\left(h_{\max}\right)_a^S\ (m)$	100	$\left(C_{\max}\right)_a^S\ (mgcl/lit)$	210
$\left(h_{\min}\right)_a^S\ (m)$	1	$\left(C_{\min}\right)_a^S\ (mgcl/lit)$	0
$\left(C_R\right)_a^S\ (mgcl/lit)$	200	$\left(Q_{\max}\right)_a^S\ (MCM)$	50
$SA_a\ (-)$	1	$\left(\overline{CE}^{\max}\right)_a^S\ (\$/MCM)$	0

Table 3.4: Aquifer data

Extracting Dependant Variables

According to Section 3.5.1, the flow constraints (3.5) and (3.11)-(3.13) are substituted by constraints (3.20) and (3.21) where the dependent flows are given by (3.19):

$$\underbrace{b^S - A_1 \cdot \left(Q_{\max}\right)_{dep}^S}_{\underline{U}^S} \le A_2 \cdot Q_{indep}^S \le \underbrace{b^S - A_1 \cdot \left(Q_{\min}\right)_{dep}^S}_{\overline{U}^S} \tag{3.28}$$

$$\left(Q_{\min}\right)_{indep}^S < Q_{indep}^S < \left(Q_{\max}\right)_{indep}^S \tag{3.29}$$

$$Q_{dep}^S = A_1^{-1} \cdot \left(b^S - A_2 \cdot Q_{indep}^S\right) \tag{3.30}$$

Section 3.5.1 presents the definitions of these constraints for the network layout considered in this example (Figure 3.1). The values and the definitions are given in Figure 3.5.

Extracting Resultant Variables

For given values of Q_{indep}^S and RR_d^S, the aquifer state variables are given by (3.23) and (3.24) while the desalinated water salinity is given by (3.9):

$$h_a^S = \frac{R_a^S - Q_a^S}{SA_a} + h_a^{S-1} \tag{3.31}$$

$$C_a^S = \frac{1}{h_a^S}\left(\frac{\left(C_R\right)_a^S \cdot R_a^S - C_a^{S-1} \cdot Q_a^S}{SA_a} + C_a^{S-1} \cdot h_a^{S-1}\right) \tag{3.32}$$

$$C_d^S = C_{sea} \cdot \left(\frac{100 - RR_d^S}{100}\right) \tag{3.33}$$

Once these values have been calculated, the salinity distribution is given by (3.27):

$$C^S = \left(-K_1^{-1}\right)^S \cdot \left(K_2\right)^S \cdot C_{source}^S \tag{3.34}$$

Section 3.5.2 presents the definitions of the RHS in (3.34) for the network layout considered in this example (Figure 3.1).

Evaluating the Objective Function and the Constraints

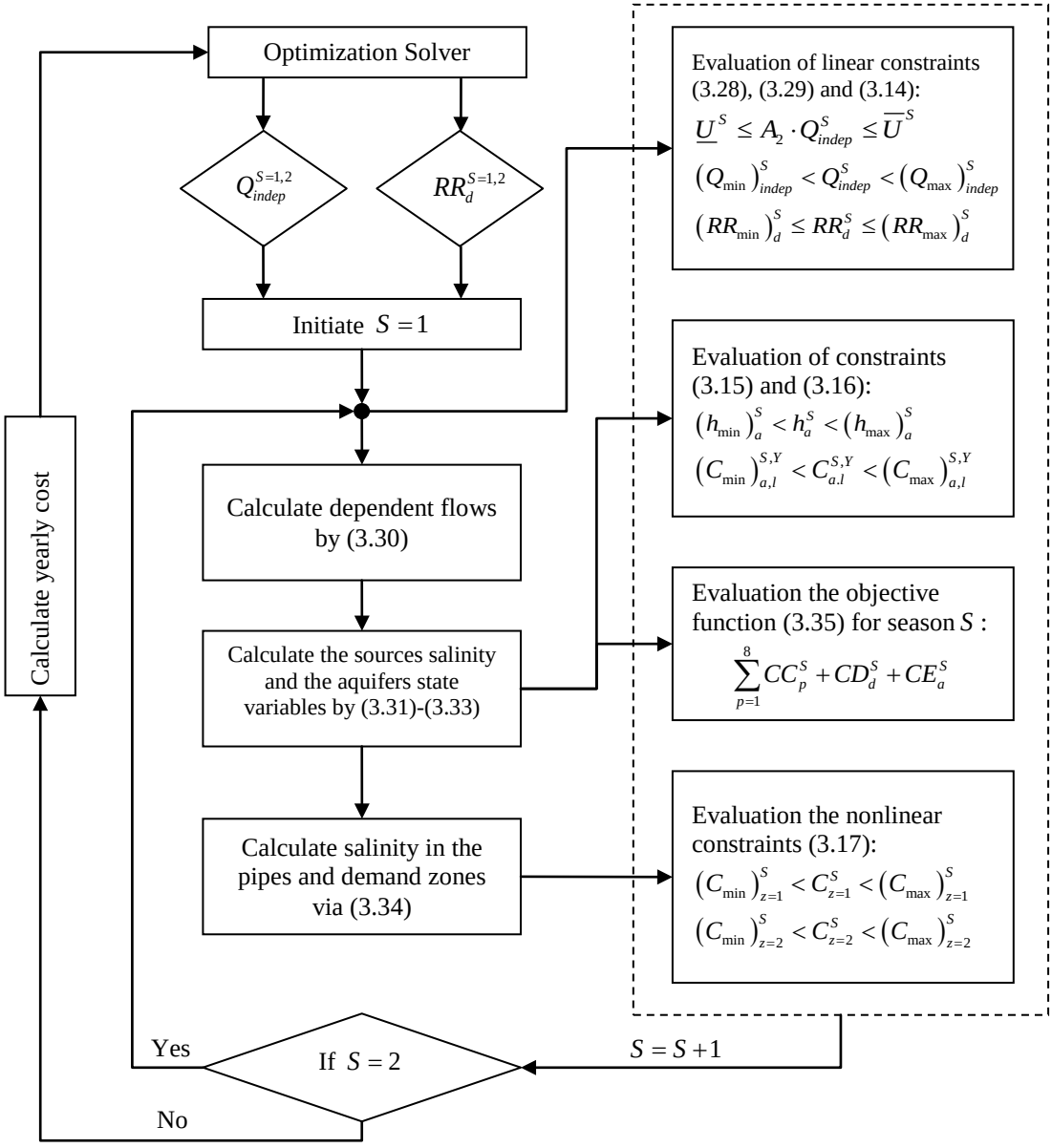

Figure 3.9: Evaluation scheme of the illustrative example

The overall cost of the annual operation cost is given by (3.4):

$$\text{cost} = \sum_{S=1}^{2}\left(\sum_{p=1}^{8} CC_p^S + CD_d^S + CE_a^S\right) \tag{3.35}$$

where CE_a^S is the extraction levy given by (3.2); in this example $CE_a^S = 0$ since $\left(\overline{CE}^{\max}\right)_a^S = 0$. CD_d^S is the desalination cost given by (3.3):

$$CD_d^S = \left(\frac{1}{(100 - RR_d^S)}\right) \cdot Q_d^S \cdot 10^6 \tag{3.36}$$

CC_p^S is the conveyance cost of pipe p which is given by (3.1):

$$\begin{aligned} CC_p^S &= \frac{X_p^S \cdot Q_p^S \cdot 10^6}{200} \cdot 0.736 \cdot KWHC^S \\ X_p^S &= \Delta Hf_p^S \\ \Delta Hf_p^S &= 1.526 \cdot 10^7 \cdot \left(\frac{Q_p^S \cdot 10^6}{w^S c_p}\right)^{1.852} \cdot D_p^{-4.87} \cdot L_p \end{aligned} \tag{3.37}$$

The evaluation scheme of this example is described in Figure 3.9.

Base Run and Sensitivity Analysis

Table 3.5 and 3.6 show detailed results for the base run (BR) and 5 sensitivity analysis (SA) runs.

Base Run (BR)

The optimal decision variables, obtained from the optimization solver are:

$$\begin{aligned} Q_{indep}^{S=1} &= \left[Q_3^{S=1}, Q_4^{S=1}, Q_6^{S=1}, Q_8^{S=1}\right]^T = [11.2, 11.2, 12.5, 12.5]^T \\ RR_d^{S=1} &= 99.25 \\ Q_{indep}^{S=2} &= \left[Q_3^{S=2}, Q_4^{S=2}, Q_6^{S=2}, Q_8^{S=2}\right]^T = [8.8, 8.8, 12.5, 12.5]^T \\ RR_d^{S=2} &= 99.43 \end{aligned} \tag{3.38}$$

with minimum objective value (total cost) of 61 $(M\$)$ which comprises conveyance cost of 0.1 $(M\$)$ and desalination cost of 60.9 $(M\$)$, there is no extraction levy cost since the extraction levy has been set to 0. As a result, the optimal solution preferred water from the aquifer to desalinated water and hence the level in the aquifer is reduced to its minimum allowed level at the end of the year $\left(h_{\min}\right)_a^S = 1\,(m)$ and the water salinity in the aquifer rises to its maximum value $\left(C_{\max}\right)_a^S = 210\,(mgcl/lit)$. To minimize the cost the model set the salinity at the demand nodes to the maximum allowed value $C_z^S = 190\ (mgcl/lit)$ in both seasons. The full solution is shown in Tables 3.5 and 3.6.

Sensitivity Analysis

Five sensitivity analysis runs were carried out in order to test the model's response to changes in the parameters of the objective function and the constraints. The solutions of all runs are shown in Tables 3.5 and 3.6.

The purpose of sensitivity analysis 1 (SA1) is to explore the influence of the recharge salinity on the optimal solution. Therefore the recharge water salinity is modified to $\left(C_R\right)_a^S = 180\,(mgcl/lit)$ instead of 200 $(mgcl/lit)$ in (BR). The extraction levy is left at 0, hence the optimal solution preferred water from the aquifer to desalinated water and the level in the aquifer was reduced to its minimum allowed level at the end of the year. The annual available water from the aquifer is $60\,(MCM)$ (50 from recharge and 10 from initial storage); hence the model needed annual desalination of $40\,(MCM)$ to supply the 100 (MCM) demand. The optimal solution of (SA1) is almost identical for both seasons. It is not perfectly identical since the seasons' lengths are not equal; this results in different conveyance costs. However, the conveyance costs are not a significant part of the objective function (two orders of magnitude smaller than the desalination cost as shown in Table 3.6) and for this reason the conveyance cost did not change the optimal solution significantly. If the difference in the conveyance cost were neglected, then the optimal seasonal solution would be perfectly identical at both seasons, resulting in $Q_a^S = 30\,(MCM)$ and $Q_d^S = 20\,(MCM)$. The aquifer water is equally distributed in pipes 1, 2 since these are identical pipes (the same parameters) i.e. $Q_{1,2}^S = 30/2 = 15\,(MCM)$. In the same manner, the desalinated water is equally distributed $Q_{3,4}^S = 20/2 = 10\,(MCM)$. Each of the intermediate nodes 3 and 4 passes $15+10 = 25\,(MCM)$, recalling that pipes 5-8 have identical parameters results in $Q_{5-8}^S = 12.5\,(MCM)$

To insure minimum cost the model set the salinity at the demand nodes to the maximum admissible value $C_z^S = 190\,(mgcl/lit)$ and to insure salinity of 190 $(mgcl/lit)$ at the demand nodes, the desalinated water salinity at the plant has been set to $C_d^S = 205\,(mgcl/lit)$ i.e., $RR_d^S = 99.24\,(\%)$. The aquifer water salinity remains as the initial salinity i.e., $C_a^S = 180\,(mgcl/lit)$, since the recharge salinity is equal to the initial salinity. As stated previously, the solution in Table 3.5 is slightly different from the solution discussed above since the seasons do not have identical lengths.

Sensitivity analysis 2 (SA2) introduces an extraction levy with maximum specific levy $\left(\overline{CE}^{\max}\right)_a^S$ $(M\$/MCM)$ equal to the desalination cost of 1 (MCM) from 27000 $(mgcl/lit)$ down to 190 $(mgcl/lit)$ i.e. 1.42 $(M\$/MCM)$. As a result, the model takes less water from the aquifer and the total cost higher than in the (BR). The final water level in the aquifer 24.2 (m) did not reach the minimum limit and the final aquifer salinity 205.9 $(mgcl/lit)$ did not reach the maximum value, as was the case in (BR).

In (SA3) we set the prices so the aquifer and the desalination to have the same water cost per (MCM) at the beginning of the year. To do this we set the maximum specific levy $\left(\overline{CE}^{\max}\right)_a^S$ $(M\$/MCM)$ equal to the desalination cost of 1 (MCM) from 27000 $(mgcl/lit)$ down to 180 $(mgcl/lit)$ i.e. 1.5 $(M\$/MCM)$. Furthermore, we set the aquifer initial water level to its minimum value $h_a^0 = 1\,(m)$, the recharge salinity to $\left(C_R\right)_a^S = 180\,(mgcl/lit)$ and the maximum salinity requirement in the demand zones to $C_z^S = 180\ (mgcl/lit)$. As a result, both of the sources supply water with salinity of 180 $(mgcl/lit)$, the initial water level is at its minimum value, thus at the beginning of the year the specific extraction cost is equal to the specific desalination cost. The results show almost identical values for both seasons. The model uses less water from the aquifer and the total cost is higher than in (BR) and (SA1). The final water level in the aquifer did not reach the minimum limit, as in (BR) and (SA1). As explained previously the conveyance cost is relatively low compared to the extraction and desalination cost as shown in Table 3.6, for this reason the conveyance aspect did not influence the optimal solution significantly.

(SA4) modifies (SA3) by increasing of the conveyance cost in the system. To increase the conveyance cost of the system to the same order of magnitude of extraction and desalination costs, all the pipes' diameters have been set to $D_{1-8} = 12\ (in)$. The optimal solution for (SA4) takes more water from the aquifer compared to (SA3). Since the conveyance cost became significant the model avoids taking too much water from desalination because of the high conveyance cost. In (SA5) we change to even smaller set of pipes diameters $D_{1-8} = 5\ (in)$ which results in conveyance cost two orders of magnitude larger than the extraction and desalination costs; we obtain approximately the same water amount taken from both sources which is distributed equally in the

network. Table 3.5 contains the flow and salinity results of the runs BR and SA1-SA5. Table 3.6 includes the cost components and totals for these runs.

Run	S	Aquifer	Desalination	Pipe 1-2	Pipe 3-4	Pipe 5-8	Zone 1, 2	W.Level *
(BR)	1	27.7(180)	22.3(202.4)	13.8(180)	11.2(202.4)	12.5(190)	25(190)	33.3(210)
	2	32.3(210)	17.7(153.4)	16.2(210)	8.8(153.4)	12.5(190)	25(190)	1(210)
SA1	1	30.3(180)	19.7(205.4)	15.2(180)	9.9(205.4)	12.5(190)	25(190)	30.7(180)
	2	29.7(180)	20.3(204.6)	14.9(180)	10.2(204.6)	12.5(190)	25(190)	1(180)
SA2	1	22.4(180)	27.6(198.1)	11.2(180)	13.8(198.1)	12.5(190)	25(190)	38.6(205.9)
	2	14.4(205.9)	35.6(183.6)	7.2(205.9)	17.8(183.6)	12.5(190)	25(190)	24.2(205.9)
SA3	1	16.6(180)	33.4(180)	8.3(180)	16.7(180)	12.5(180)	25(180)	34.4(180)
	2	16.8(180)	33.2(180)	8.4(180)	16.6(180)	12.5(180)	25(180)	17.6(180)
SA4	1	19.7(180)	30.3(180)	9.8(180)	15.2(180)	12.5(180)	25(180)	31.3(180)
	2	24.1(180)	25.9(180)	12.1(180)	12.9(180)	12.5(180)	25(180)	7.2(180)
SA5	1	24.9(180)	25.1(180)	12.4(180)	12.6(180)	12.5(180)	25(180)	26.1(180)
	2	25(180)	25(180)	12.5(180)	12.5(180)	12.5(180)	25(180)	1.2(180)

Table 3.5: Flow and salinity distribution in the network (MCM), $(mgcl/lit)$ respectively. The values in the parentheses are the salinities. (All the values have been rounded to one decimal place). * W.Level = the aquifer water level (m), values in the parentheses are the aquifer salinity at the end of the season.

		Cost (M$)			
Run	S *	Extraction	Desalination	Conveyance	Total
BR	1	0.00	29.79	0.01	29.80
	2	0.00	31.10	0.08	31.17
	1+2	0.00	60.89	0.09	60.98
SA1	1	0.00	25.90	0.01	25.91
	2	0.00	26.78	0.07	26.86
	1+2	0.00	52.68	0.08	52.76
SA2	1	19.77	37.58	0.01	57.36
	2	15.66	52.37	0.09	68.12
	1+2	35.43	89.96	0.09	125.48
SA3	1	16.53	50.06	0.01	66.60
	2	20.93	49.85	0.08	70.86
	1+2	37.46	99.91	0.09	137.46
SA4	1	20.48	45.48	9.63	75.59
	2	33.89	38.84	72.03	144.76
	1+2	54.37	84.32	81.66	220.35
SA5	1	27.83	37.71	645.70	711.23
	2	37.42	37.53	5109.76	5184.70
	1+2	65.24	75.23	5755.46	5895.93

Table 3.6: Operation costs (M$) of the illustrative example, Base Run and 5 Sensitivity Analysis runs. (All values have been rounded to two decimal places). * *S*- is the season index, *S*=1+2 represents the entire year.

Multi-Year Run

This Section presents a 20-year run with zero discount rate based on the (BR) parameters, except for the maximum conveyance in season 2 which have been changed to $\left(Q_{\max}\right)_p^{S=2} = 25\ (MCM / season)$ instead of 18.8 in order to insure the ability to supply all the demand from the desalination plants in case the aquifer is empty. The maximum water level in the aquifer is also changed to a fictitiously high value $\left(h_{\max}\right)_a^S = 300\ (m)$, in order to insure no spill/overflow from the aquifer. The same data are repeated year after year for 20 years (40 seasons) except the recharge values in the first season $R_a^{S=1}(MCM)$ which have been generated randomly in each year from a uniform discrete probability function with three values $\{0,50,100\}$, the resulting sample is shown in Figure 3.10a and the resulting optimal trajectory of the water level in the aquifer is shown in Figure 3.10b. The results show that the model adapts the water extraction from the aquifer according to the behavior of the recharge. The extraction levy is 0 (as in BR), so the minimum level in the aquifer is reached at the end of the time horizon.

(a) Seasonal recharge

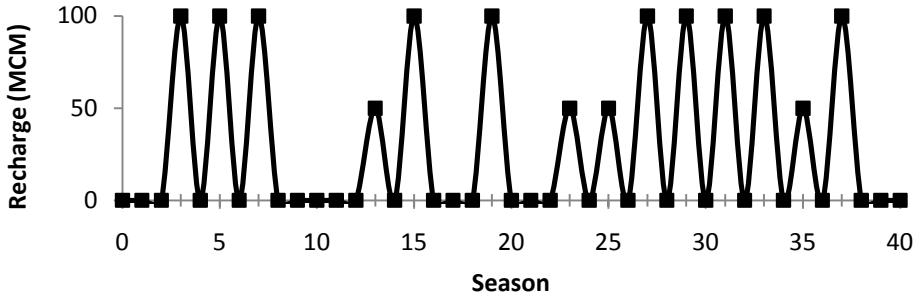

(b) Optimal trajectory

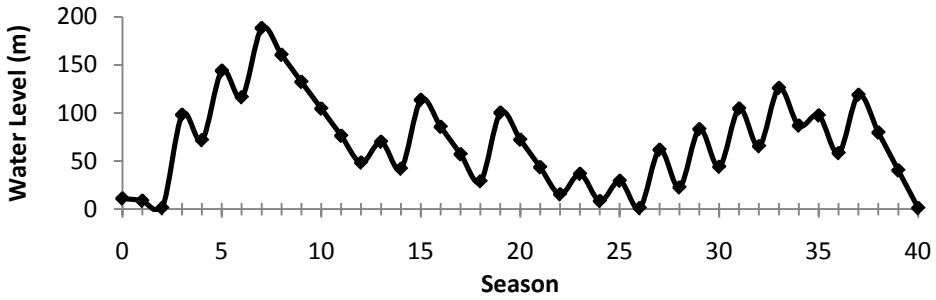

Figure 3.10: (a) Seasonal recharge: for each year, the recharge of season 1 is uniformly distributed from $\{0,50,100\}$ and in season 2 it is always 0. (b) The optimal trajectory of the water level in the aquifer.

3.9. Large WSS Example

The small system shown in Figure 3.1 was used in the development phase of the research. Extensive sensitivity analysis was used to test and verify the model's performance, which was then applied to a larger and more realistic WSS.

Problem Parameters

A water system with 9 demand zones, 3 aquifers, 5 desalination plants and 49 pipes (Figure 3.11, generated by the post-processor (Section 3.12), which shows system topology and link carrying capacities in the two seasons) has been solved in this example; the structure of this system mimics a part of the Israeli National Water System. The year is divided into two seasons, which can be called "winter" (lower demands, 265 days) and "summer" (high demands, 90 days).

The daily pumping hours are 14, 16 (hr/day) respectively for the first and the second season, hence the seasonal pumping hours are $w^{S=1}=3710\ (hr/season)$, $w^{S=2}=1440\ (hr/season)$. The seasonal capacities of the pipes are shown in Figure 3.11, based on pipe diameters, lengths, Hazen Williams coefficients, topographic difference and a hydraulic loss of 4 ‰. The energy cost for the first season is $KWHC^{S=1}=0.09\ (\$/kwhr)$ and for the second season is $KWHC^{S=2}=0.11\ (\$/kwhr)$.

The seasonal demands for the 9 demand zones are given in Table 3.7. The maximum allowed water salinity in all zones is set to 220 $(mgcl/lit)$. The maximum desalination amount of plants 1 to 5 are $(Q_{\max})_d^S=[30,100,100,200,100]\ (MCM)$ respectively, while all the desalination plants have no obligation for a minimal supply requirement i.e. $(Q_{\min})_d^S=0\ (MCM)$. The removal ratio of the plants is between $(RR_{\max})_d^S=99.95\ (\%)$ and $(RR_{\min})_d^S=99.75\ (\%)$, yielding a product salinity in the range 13.5-67.5 $(mgcl/lit)$. The desalination cost parameters are $\alpha_d=0.7\ (M\$/MCM)$ and $\beta_d=-10^6\ (-)$ which implies constant desalination cost per (MCM) in all the plants. Data for the three aquifers are given in Table 3.8. The maximum allowed salinity in all aquifers is set to 350 $(mgcl/lit)$.

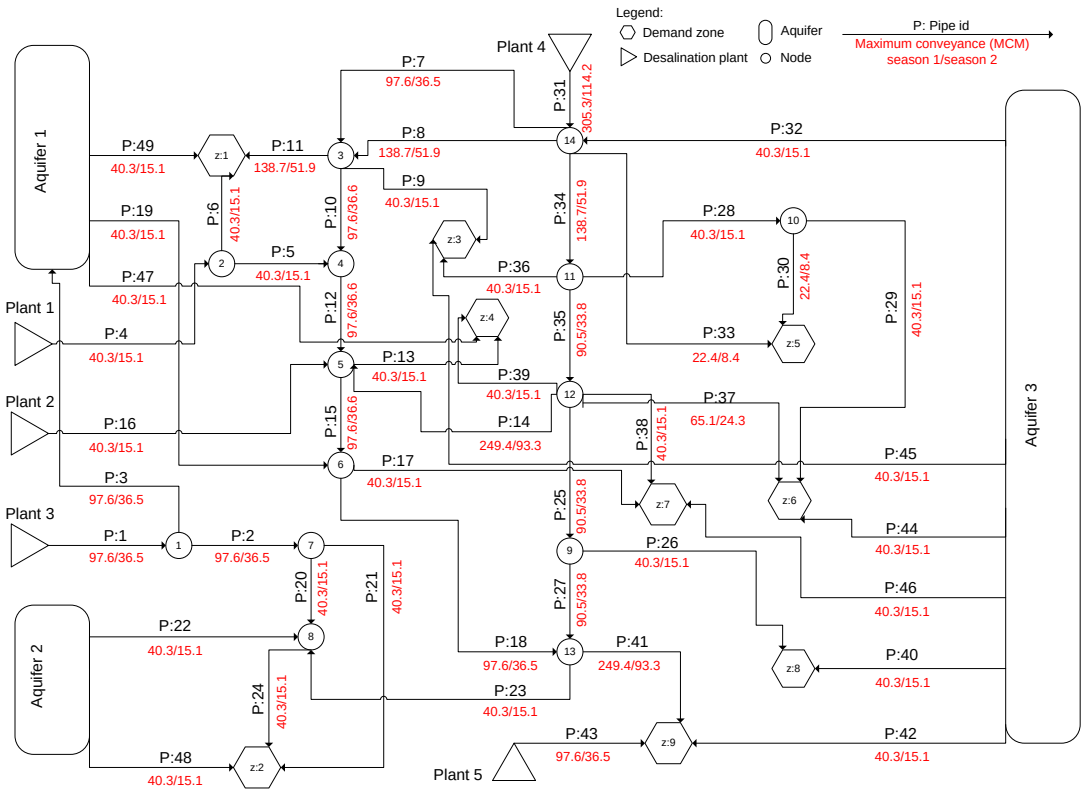

Figure 3.11: Large WSS layout and conveyance capacity in season 1 and 2. (MCM, rounded to one decimal place)

Demand z	season 1 (MCM)	season 2 (MCM)
1	116.9	50.1
2	9.1	3.9
3	53.9	23.1
4	36.4	15.6
5	18.2	7.8
6	90.3	38.7
7	9.1	3.9
8	18.2	7.8
9	198.1	84.9

Table 3.7: Demand data for the large WSS.

Aquifer a=1..3	$(Q_{\max})_a^S$ (MCM)	$(h_{\max})_a^S$ (m)	$(h_{\min})_a^S$ (m)	h_a^0 (m)	C_a^0 $(mgcl/lit)$	SA (MCM/m)	$R_a^{S=1}*$ (MCM)
1	130	33	1	2	300	65	210
2	111	50	1	3	300	37	100
3	290	50	17	19	150	25	360

Table 3.8: Aquifer data for the large WSS. *The recharge salinity is 150 $(mgcl/lit)$, recharge in the second season is 0.

Base Run and Sensitivity Analysis

The model was run for a single year: a Base Run (BR) and four Sensitivity Analysis runs (SA1-SA4), each with certain data modified, to examine its performance under various conditions (detailed below). Table 3.9 shows the quantities taken from sources, aquifer levels and salinities. Table 3.10 shows the cost components and the total cost for each run.

Run	S	Aquifer Extraction, a=1..3			Aquifer Water Level*, a=1..3			Desalination Plants, d=1..5				
		1	2	3	1	2	3	1	2	3	4	5
(BR)	1	106.8(300)	6.6(300)	188.5(150)	3.6(164.9)	5.5(226.6)	25.9(150)	7.5(28.4)	33.5(13.5)	2.5(13.5)	110.7(30.5)	94.2(40.5)
	2	45.2(164.9)	3.8(226.6)	72(150)	2.9(164.9)	5.4(226.6)	23(150)	5.3(41.3)	15.1(40.2)	0.1(14.3)	57.8(44.6)	36.5(41)
SA1	1	84.3(220)	6.6(300)	168.9(150)	3.9(176.8)	5.5(226.6)	26.6(150)	7.7(40.2)	24.3(38.6)	35.2(13.5)	130(43.5)	93.2(41)
	2	45.2(176.8)	3.8(226.6)	72(150)	3.2(176.8)	5.4(226.6)	23.8(150)	5.3(40.8)	15.1(40.2)	0.1(19.4)	57.8(44.8)	36.5(41.3)
SA2	1	53.8(220)	4.5(300)	142.1(150)	4.4(189.9)	5.6(227.4)	27.7(150)	0(36.5)	0(37.3)	22.2(13.5)	305.3(180.9)	22.2(40)
	2	30.1(189.9)	3.5(227.4)	72(150)	3.9(189.9)	5.5(227.4)	24.8(150)	0(39.4)	0(40.2)	0.1(38.1)	114.2(180.9)	15.9(41)
SA3	1	84.3(220)	6.5(300)	169(150)	3.9(176.8)	5.5(226.6)	26.6(150)	11.3(40.2)	0(67.5)	35.2(13.5)	146.3(42.1)	97.6(40.8)
	2	45.2(176.8)	3.8(226.6)	72(150)	3.2(176.8)	5.4(226.6)	23.8(150)	10(40.5)	0(67.5)	0.1(28.1)	68.2(44)	36.5(41)
SA4	1	106.8(300)	6.5(300)	168.9(150)	3.6(164.9)	5.5(226.6)	26.6(150)	7.7(37.8)	33.4(13.5)	2.5(14)	130.1(38.1)	94.2(39.1)
	2	45.2(164.9)	3.8(226.6)	72(150)	2.9(164.9)	5.4(226.6)	23.8(150)	5.3(41.6)	15.1(40.8)	0.1(19.2)	57.8(43.5)	36.5(41.3)

Table 3.9: Flow and salinity from the sources (MCM), $(mgcl/lit)$ respectively. The values in the parentheses are the salinities. (All values have been rounded to one decimal place). * Aquifer water levels (m), and salinities (in parentheses) $(mgcl/lit)$ at the end of the season.

	Annual Cost (M$)			
Run	**Extraction**	**Desalination**	**Conveyance**	**Total**
(BR)	0.00	238.69	56.43	295.12
SA1	135.48	266.39	54.97	456.84
SA2	89.55	39.76	67.47	196.78
SA3	135.49	266.38	56.08	457.95
SA4	149.98	251.61	56.41	458.00

Table 3.10: Component and total costs (M$) of the large WSS - base run and 4 sensitivity analyses. (All the values have been rounded to two decimal places)

Base run

In the base run we solve the model for one year with the data given in Figure 3.11, Tables 3.7 and 3.8 and no extraction levy from the aquifers. The optimal quantity and salinity distribution in the network for the 1st season are shown in Figure 3.12. The objective value (total cost) is 295 $(M\$)$ comprised of 56 $(M\$)$ conveyance and 239 $(M\$)$

desalination Since there is no extraction levy cost the optimal solution preferred water from the aquifers to desalinated water. However, the extractions from the aquifers did not reach the maximum allowed amounts stated in Table 3.8 since there are other constraints that became binding. The results for season 1 (Figure 3.12) are used to explain the logic of the optimal solution that has been reached, concentrating especially on the role of salinity in determining the outcome.

The flow capacities of the pipes leading from aquifer 1 are all $40.3 \cdot 3 = 120.9\ (MCM)$ but the flow in pipe 47 cannot reach 40.3 (MCM) since this is a direct pipe to demand zone 4 and the initial water salinity in the aquifer does not meet the water salinity requirement in demand zone 4. Hence the need for some desalinated water in order to meet the salinity requirement, which is brought via pipes 13 and/or 39. The optimal solution is expected to result in maximum allowed salinity in demand zone 4 (to reduce cost), so the three flows and salinities to demand zone 4 are set to match the demand 36.4 (MCM) and maximum salinity of 220 $(mgcl/lit)$. The optimal flow pattern is: pipe 39 carries no flow, pipe 13 carries 10.2 (MCM) with salinity 13.5 $(mgcl/lit)$, while pipe 47 carries 26.2 (MCM) with the salinity of aquifer 1, i.e. 300 $(mgcl/lit)$.

Aquifer 2, with salinity 300 $(mgcl/lit)$, is connected directly to demand node 2, whose demand is 9.1 (MCM), and supplies to it only 6.6 (MCM) while pipes 20 and 21 brings the remainder, which is desalinated water, to meet the salinity limit in demand zone 2.

In aquifer 3 the initial water salinity is 150 $(mgcl/lit)$ which is below the demand requirement, hence the only limitation is the conveyance capacity of the pipes leaving the aquifer i.e. 40.3 (MCM). The flows reached the maximum conveyance in pipes 32, 42, 44 and 45, while in pipes 40 and 46 that are connected directly to demand zones the flows are 18.2 and 9.1 (MCM).

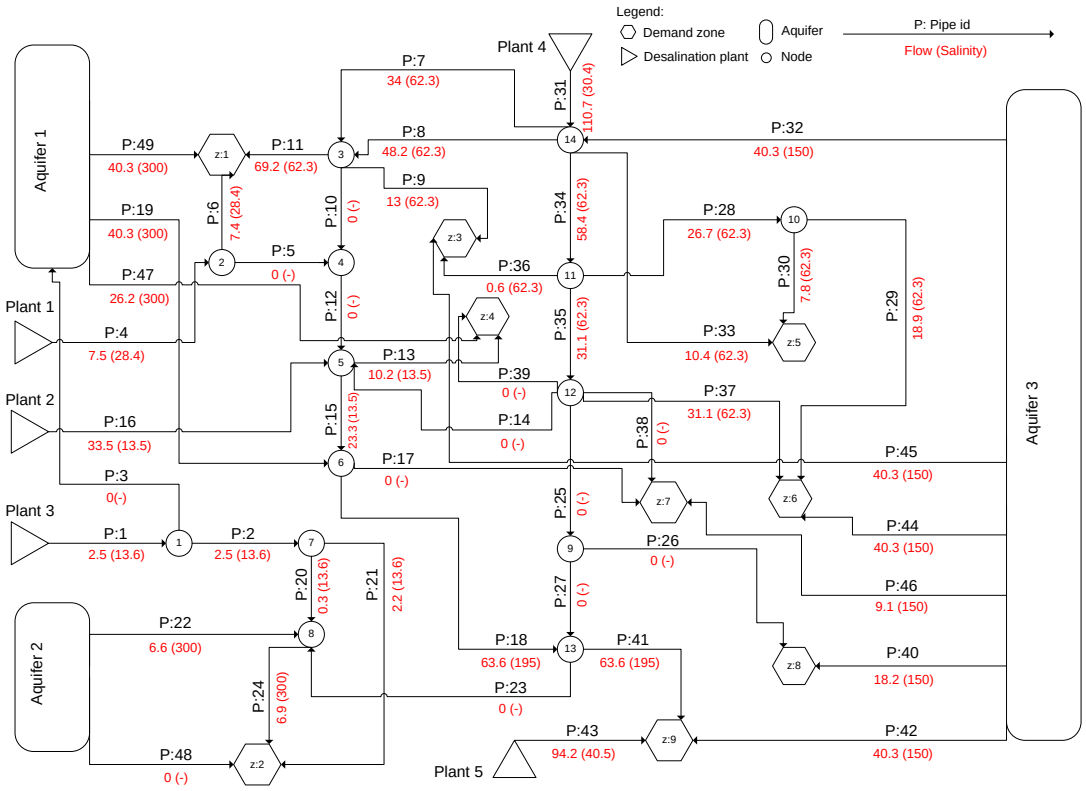

Figure 3.12: Base run Season 1 results - flow (MCM) and salinity $(mgcl/lit)$ distribution. (All values have been rounded to one decimal place)

Sensitivity Analysis

Of the many sensitivity runs that have been conducted we show here four, selected to demonstrate the response of the model to changes in the parameters of the objective function and the constraints. The optimal quantity and salinity distribution in the network for the 1st season is shown in Appendix 2 for each of the sensitivity runs.

Sensitivity analysis SA1 introduces an extraction levy as defined in Equation 2 with maximum specific levy $\left(\overline{CE}^{\max}\right)_a^S$ $(M\$/MCM)$ equal to the desalination cost of 1 (MCM) i.e. 0.7 $(M\$/MCM)$. As a result, the model takes less water from aquifers 1 and 3 and the total cost is increased compared to the BR, as seen in Table 3.10. Because of the extraction levy, the optimal solution keeps more water in aquifers 1 and 3, while the same amount is extracted from aquifer 2 with and without the extraction levy, hence the state of the this aquifer remains as in the BR. Another notable characteristic of this run is the flow in pipe 3 that takes desalinated water from node 1 to aquifer 1. Desalinated water is brought via pipe 3 to dilute the aquifer water

down to the allowed 220 $(mgcl/lit)$. In this case, demand node 4 takes all its needs through pipe 47 with salinity of 220 $(mgcl/lit)$.

In sensitivity analysis SA2 we modify SA1 by modeling desalination plant 4 as a large and free–of-charge water source with fixed salinity of 180 $(mgcl/lit)$. This is accomplished by: (a) fixing the maximum production of plant 4 to a high value of 1000 (MCM), (b) fixing its removal ratio bound to 99.33 (%) and (c) fixing the desalination cost parameter $\alpha_4 = 0\ (M\$/MCM)$. The total cost decreases compared to BR and SA1, as seen in Table 3.10. The results show that the model keeps more water in aquifer 1 and 3, while in aquifer 2 the same amount is extracted and the state of the this aquifer does not change compared to BR and SA1. Pipe 3 conveys low salinity water in order to dilute the aquifer water to the required level. Moreover, some of the pipes out of aquifer 1 carry no flow, since supply from the free plant 4 is preferred to extraction from the aquifers.

Sensitivity analysis SA3 and SA4 demonstrate how to eliminate parts of the model in order to use it as a tool to check planning alternatives. SA3 modifies SA1 by eliminating desalination plant 2, this is achieved by fixing its maximum flow to 0. In SA1 plant 2 produced 24.3 (MCM) which was conveyed through pipes 16, 15, 18 and 41 to demand node 9. After eliminating plant 2 the model produces more water in desalination plants 4 and 5. The additional water from plant 4 is distributed in the network through different routes to demand node 9 in order to minimize the conveyance cost. SA4 modifies SA1 by eliminating pipe 3 which connects desalination plant 3 with aquifer 1; this is done by fixing the maximum conveyance capacity to 0. In SA1 the model used pipe 3 to dilute aquifer 1 water from salinity of 300 $(mgcl/lit)$ to the required 220 $(mgcl/lit)$. After elimination of pipe 3, aquifer 2 and plant 3 can only convey water to demand node 2, hence the extraction in aquifer 1 and the production in plant 2 has to increase significantly compared to SA1, as seen in Table 3.9. Appendix 2 includes graphical output for the first season operation to each one of the four sensitivity analysis.

Multi-Year Run

Two 10-year runs with 6.5% discount rate are compared, with and without extraction levy. The first is based on the BR parameters and the second on SA1 parameters, and

the maximum water level in the aquifers is changed to $(h_{\max})_a^S = 100\ (m)$ to insure no spill/overflow from the aquifers. The same data are repeated year after year for 10 years in both runs, except that the aquifer recharges in the first season ("winter") $R_a^{S=1}(MCM)$ are the last 10 years' recharge data from the hydrological data of Israel (Table 3.11). The water level trajectories in the three aquifers for both runs are shown in Figure 3.13. The results demonstrate that the extraction levy encourages preserving high water levels in aquifer 1 and 3. In aquifer 2 practically the same trajectory is obtained in both runs, since aquifer 2 is limited to supplying demand zone 2 and therefore the same amount is extracted with and without the extraction levy.

The extraction levy is a value assigned to water in storage, representing a policy of sustainable management. Runs with different extraction levy values can be used to show the tradeoff between storage in the aquifers at the end of the management horizon and the costs of desalination and conveyance, which rise as less water is taken from the aquifers with increasing values of the levy. Figure 3.14 shows this tradeoff between storage in the aquifers at the end of 10 year horizon and the desalination and conveyance cost, for different maximum specific levy values $\left(\overline{CE}^{\max}\right)_a^S = [0, 0.4, 0.7, 1]$ $(M\$/MCM)$. The tradeoff shows that increasing the maximum specific levy from 0 to 0.4 $(M\$/MCM)$ (lowest two points on each curve) does not change the optimal solution markedly, resulting in small changes in the cost and the final total storage. While by increasing the maximum specific levy from 0.4 to 0.7 $(M\$/MCM)$ the model preserves 30% more water in storage with a 16% increment of desalination and conveyance costs.

The linear tradeoff of the total storage indicates that each additional (MCM) of storage at the end of year 10 costs almost the same as the present value cost of 1 (MCM) desalinated water. This is particularly true because the conveyance cost did not change significantly among the runs with different levy values. The tradeoff of aquifer 2 shows a small change in storage, due to the limited conveyance network in the vicinity of aquifer 2. The allocation of additional storage between aquifers 1 and aquifer 3 changes for different values of the maximum specific levy. For 0.4-0.7 the allocation is 54% in aquifer 1 and 46% in aquifer 3, while for 0.7-1 the allocation is 67% in aquifer 1 and 33% in aquifer 3.

	Recharge (MCM)		
Year	Aquifer 1	Aquifer 2	Aquifer 3
1	117	58	139
2	188	94	304
3	172	86	264
4	195	97	409
5	252	126	520
6	182	91	262
7	200	100	340
8	200	100	260
9	222	111	292
10	174	87	230

Table 3.11: The recharge in the three aquifers.

*The second season recharge is 0

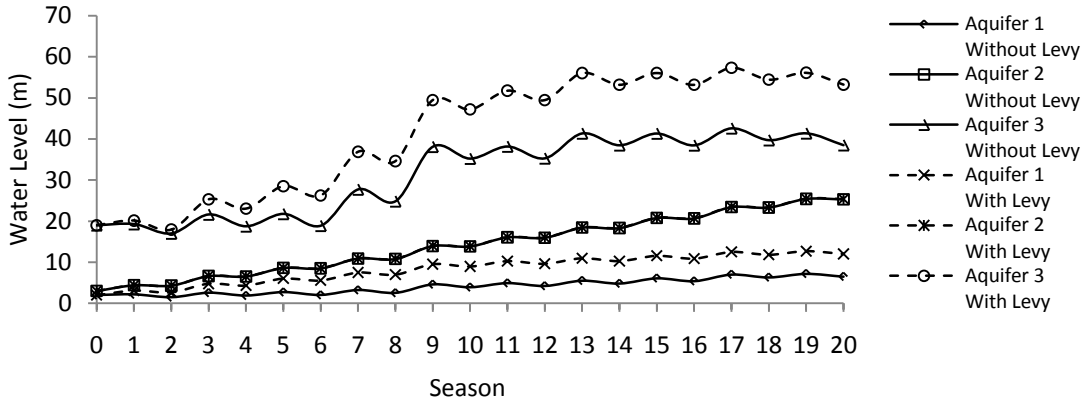

Figure 3.13: Water level trajectories with and without extraction levy

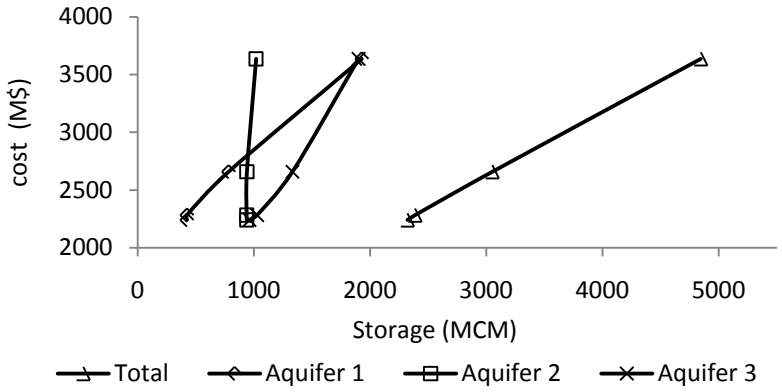

Figure 3.14: Tradeoff curves of desalination + conveyance cost vs. final storage; each curve has points corresponding to four values of the maximum specific extraction levy (from bottom to top on each curve) [0,0.4,0.7,1] $(M\$/MCM)$.

3.10. The Time Chain Method (TCM)

The model can be formulated as the following nonlinear optimization problem:

$$\begin{aligned}
&\min_{u^t\,\forall t} \; F = \sum_{t=1}^{T_f} f(x^{t-1}, u^t, p^t) \\
&s.t. \\
&\left.\begin{aligned}
&x_r^t = W(x_r^{t-1}, u^t, p^t) && \forall r = 1..n_1 \\
&y_r^t = V(y_r^{t-1}, x_r^{t-1}, u^t, p^t) && \forall r = 1..n_1 \\
&A^t \cdot u^t \le b^t \\
&g_j(y^{t-1}, x^{t-1}, u^t, p^t) \le 0 && \forall j = 1..m \\
&LB_i^t \le u_i^t \le UB_i^t && \forall i = 1..n
\end{aligned}\right\} \forall t = 1..T_f
\end{aligned} \tag{3.39}$$

where t is the stage index $t \in [1, T_f]$; $u^t \in \mathbf{R}^n$ is the vector of decision variables; $x^t \in \mathbf{R}^{n_1}, y^t \in \mathbf{R}^{n_1}$ are two vectors of state variables corresponding to the aquifers state variables (n_1 is number of aquifers); p^t is a vector of parameters; $f, W, V, g_j \; \forall j$ are nonlinear functions; A^t is a rectangular coefficient matrix; b^t is RHS vector; $LB^t \in \mathbf{R}^n, UB^t \in \mathbf{R}^n$ are lower and upper bounds respectively.

Each of the T_f stages has its contribution to the objective function f^t, set of constraints $g^t_{j=1..m} \le 0$, decision variables $u^t_{i=1..n}$ and state variables $x^t_{r=1..n_1}$, $y^t_{r=1..n_1}$.where f^t, g^t denote $f(x^{t-1}, u^t, p^t)$ and $g(y^{t-1}, x^{t-1}, u^t, p^t)$ respectively. The overall objective is to minimize $F = \sum_{t=1}^{T_f} f^t$ satisfying the constraints $\forall t = 1..T_f$ while the decision variables are $u_{i=1..n}^{\forall t=1..T_f}$.

3.10.1. Gradient estimation

A finite difference scheme provides estimations for $\nabla F \in \mathbf{R}^{1 \times n \cdot T_f}$. The central finite differences scheme to calculate an approximation of ∇F is:

$$\frac{\partial F}{\partial U_v} \approx \frac{F(U + \delta_v \cdot e_v) - F(U + \delta_v \cdot e_v)}{2 \cdot \delta_v} \quad \forall v = 1..n \cdot T_f \tag{3.40}$$

where U is the multi-year vector of decision variables that contains the annual decision vectors $u^t \; \forall t$ i.e. $U = [u^1, ..., u^{T_f}]$; δ_v is a perturbation step of variable v; e_v is the unit vector in direction v.

Estimation of ∇F requires $2 \cdot n \cdot T_f$ evaluations of the function F and the state equation of x, each evaluation needs the computation for all T_f stages. Suppose S_{time} is the computation time for one stage, therefore the total computation time is:

$$\begin{aligned} Time &= 2 \cdot n \cdot T_f^2 \cdot S_{time} \\ Time &= O(T_f^2) \end{aligned} \tag{3.41}$$

Efficient Estimating of ∇F

Each stage t is linked to the previous stages through the state variable so that the derivatives of the objective function with respect to (w.r.t.) former decisions can be calculated using the derivative of the objective function w.r.t. its own input state variable and the derivatives of these state variable w.r.t. previous decisions. For example, to calculate the derivative of the objective function of stage 3 f^3 with respect to the decisions of stage 1, u^1, we can use the derivatives of f^3 w.r.t. x^2, derivatives of x^2 w.r.t. x^1 and derivatives of x^1 w.r.t. u^1 as depicted in Figure 3.15.

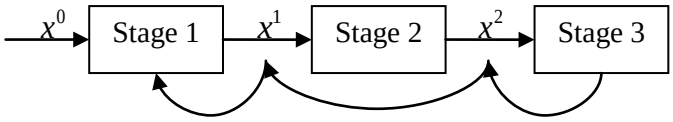

Figure 3.15: Scheme of the TCM for 3 stages (objective function)

The following steps take advantage of two properties of the model: (a) $\nabla F = \sum_{t=1}^{T_f} \nabla f^t$ i.e., the objective function is additive, (b) the functions of stage t do not depend (obviously) on decision variables of later stages thus:

$$\frac{\partial f^t}{\partial u_i^k} = 0 \quad \forall k = t+1..T_f \quad \forall i = 1..n \tag{3.42}$$

For each function f^t we have to estimate $\frac{\partial f^t}{\partial u_i^k} \quad \forall k = 1..t \quad \forall i = 1..n$

For the n derivatives $\frac{\partial f^t}{\partial u_i^t} \quad \forall i = 1..n$:

$$\frac{\partial f^t}{\partial u_i^t} \approx \frac{f(x^{t-1}, u^t + \delta_i e_i, p^t) - f(x^{t-1}, u^t - \delta_i e_i, p^t)}{2\delta_i} \quad \forall i = 1..n \tag{3.43}$$

We can also estimate the derivatives $\frac{\partial f^t}{\partial x_r^{t-1}}$, $\frac{\partial x_r^t}{\partial u_i^t}$ and $\frac{\partial x_r^t}{\partial x_r^{t-1}}$

$$\frac{\partial f^t}{\partial x_r^{t-1}} \approx \frac{f(x^{t-1}+\delta_r e_r, u^t, p^t) - f(x^{t-1}-\delta_r e_r, u^t, p^t)}{2\cdot\delta_r} \quad \forall r = 1..n_1 \tag{3.44}$$

$$\frac{\partial x_r^t}{\partial u_i^t} \approx \frac{W(x_r^{t-1}, u^t+\delta_i e_i, p^t) - W(x_r^{t-1}, u^t-\delta_i e_i, p^t)}{2\cdot\delta_i} \quad \forall r = 1..n_1 \ \forall i = 1..n \tag{3.45}$$

$$\frac{\partial x_r^t}{\partial x_r^{t-1}} \approx \frac{W(x_r^{t-1}+\delta_r, u^t, p^t) - W(x_r^{t-1}-\delta_r, u^t, p^t)}{2\cdot\delta_r} \quad \forall r = 1..n_1 \tag{3.46}$$

The component r of x^t (i.e. x_r^t) is only dependent on x_r^{t-1}, then $\frac{\partial x_{r=r'}^t}{\partial x_{r=r''}^{t-1}} = 0 \quad \forall r' \neq r''$.

The remaining derivatives $\frac{\partial f^t}{\partial u_i^k} \quad \forall k = 1..t-1 \quad \forall i = 1..n$ are given by the chain rule:

$$\frac{\partial f^t}{\partial u_i^k} = \sum_{r=1}^{n_1} \left(\frac{\partial f^t}{\partial x_r^{t-1}} \underbrace{\left(\prod_{j=k+1}^{t-1} \frac{\partial x_r^j}{\partial x_r^{j-1}} \right)}_{(k=t-1)\to 1} \frac{\partial x_r^k}{\partial u_i^k} \right) \quad \forall k = 1..t-1 \ \forall i = 1..n \tag{3.47}$$

Thus we need $2\cdot(n+n_1)$ evaluations of the function f^t and the state equation of x in order to estimate ∇f^t and the linking derivatives, each of these evaluations needs only the computation of stage t.

Suppose S_{time} is the stage computation time, then the computation time for ∇f^t and the linking derivatives is $2\cdot(n+n_1)\cdot S_{time}$.

Recalling that $\nabla F = \sum_{t=1}^{T_f} \nabla f^t$ hence the computation time for ∇F is:

$$\begin{aligned} Time &= 2\cdot(n+n_1)\cdot S_{time}\cdot T_f \\ Time &= O(T_f) \end{aligned} \tag{3.48}$$

This procedure has been termed the Time-Chained-Method (TCM).

3.10.2. Estimating the Jacobian of the nonlinear constraints

A finite difference scheme provides estimations for the Jacobian matrix of the nonlinear constraints $J \in \mathbf{R}^{m\cdot T_f \times n\cdot T_f}$.

To estimate the finite differences of the constraints $g_{j=1..m}^{t=1..T_f} \le 0$, the same methodology (TCM) is applied. However, in this case two state variables are involved in the constraints x and y, where the state variable y is a function of the state variable x, since $y_r^t = V(y_r^{t-1}, x_r^{t-1}, u^t, p^t)$. This dependency makes it harder to estimate the gradient of each constraint. For example, to calculate the derivative of a constraint of stage 3 g_j^3 with respect to the decisions of stage 1, u^1, we should use the derivatives of g_j^3 w.r.t. x^2 and y^2, derivatives of x^2 w.r.t. x^1, derivatives of x^2 w.r.t. y^1, derivatives of y^2 w.r.t. x^1, derivatives of y^2 w.r.t. y^1 and derivatives of x^1 and y^1 w.r.t. u^1 as depicted in Figure 3.16.

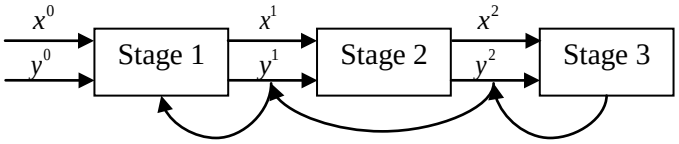

Figure 3.16: Scheme of the TCM for 3 stages (constraints)

In the general case calculation the derivatives $\frac{\partial g_j^t}{\partial u_i^k} \quad \forall k = 1..t-1 \quad \forall i = 1..n$ is given by applying the chain rule for all the paths given in the Figure 3.17.

However, in the formulation (3.39) the state variable x does not depend on the state variable y, hence $\frac{\partial x_r^{k+1}}{\partial y_r^k} = 0, \forall k$ and only part of the paths are relevant.

Out of the paths which start from the root $\frac{\partial y_r^k}{\partial u^k}$ only one path can have a non-zero derivative which is given by:

$$\text{Path } 1 = \sum_{r=1}^{n_1} \left(\frac{\partial g_j^t}{\partial y_r^{t-1}} \underbrace{\left(\prod_{j=k+1}^{t-1} \frac{\partial y_r^j}{\partial y_r^{j-1}} \right)}_{(k=t-1)\to 1} \frac{\partial y_r^k}{\partial u_i^k} \right) \quad \forall k = 1..t-1 \quad \forall i = 1..n \tag{3.49}$$

The first path which does not include the state variable y also could have non-zero derivative

$$\text{Path } 2 = \sum_{r=1}^{n_1} \left(\frac{\partial g_j^t}{\partial x_r^{t-1}} \underbrace{\left(\prod_{j=k+1}^{t-1} \frac{\partial x_r^j}{\partial x_r^{j-1}} \right)}_{(k=t-1)\to 1} \frac{\partial x_r^k}{\partial u_i^k} \right) \quad \forall k = 1..t-1 \quad \forall i = 1..n$$

(3.50)

From all the paths which start from the root $\frac{\partial x_r^k}{\partial u^k}$ and end by $\frac{\partial g_i^t}{\partial y_r^{t-1}}$ only $t-k-1$ paths which include only one member of the form $\frac{\partial y_r^{k+1}}{\partial x_r^k}$ can have non-zero derivatives.

$$\text{Path } l = \sum_{r=1}^{n_1} \left(\frac{\partial g_j^t}{\partial y_r^{t-1}} \underbrace{\left(\prod_{j=l+k+1}^{t-1} \frac{\partial y_r^j}{\partial y_r^{j-1}} \right)}_{(l=t-k-1)\to 1} \frac{\partial y_r^{l+k}}{\partial x_r^{l+k-1}} \underbrace{\left(\prod_{j=k+1}^{l+k-1} \frac{\partial x_r^j}{\partial x_r^{j-1}} \right)}_{(l=1)\to 1} \frac{\partial x_r^k}{\partial u_i^k} \right) \qquad (3.51)$$

$\forall k = 1..t-1 \quad \forall i = 1..n \quad \forall l = 1..t-k-1$

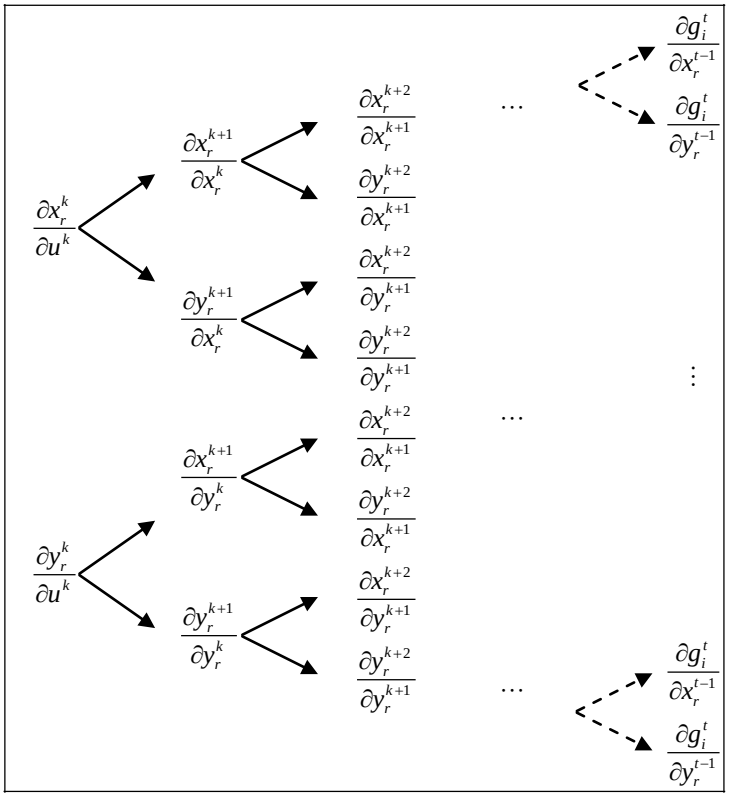

Figure 3.17: Paths for the chain rule implementation

The sum of all the non-zero paths gives the derivatives $\frac{\partial g_j^t}{\partial u_i^k} \quad \forall k = 1..t-1 \quad \forall i = 1..n$

For each of the functions g_j^t we perform this procedure to construct the Jacobian matrix $J \in \mathbf{R}^{m \cdot T_f \times n \cdot T_f}$, which is a lower triangular block matrix, where each element in this block matrix is $\mathbf{R}^{m \times n}$

$$J = \begin{array}{c} \\ g_{j\forall j}^1 \\ g_{j\forall j}^2 \\ \vdots \\ g_{j\forall j}^{T_f} \end{array} \begin{array}{c} \begin{array}{cccc} u_{i\forall i}^1 & u_{i\forall i}^2 & \cdots & u_{i\forall i}^{T_f} \end{array} \\ \begin{pmatrix} \times & 0 & \cdots & 0 \\ \otimes & \times & \ddots & \vdots \\ \vdots & \ddots & \times & 0 \\ \otimes & \cdots & \otimes & \times \end{pmatrix} \end{array} \tag{3.52}$$

The zero entries reflect the fact that the functions of stage t do not depend (obviously) on decision variables of later stages.

The entries marked $\times$ are derivatives which are directly calculated by the finite differences scheme, $\frac{\partial g_j^t}{\partial u_i^t} \quad \forall i = 1..n$:

$$\frac{\partial g_j^t}{\partial u_i^t} \approx \frac{g_j(y^{t-1}, x^{t-1}, u^t + \delta_i e, p^t) - g_j(y^{t-1}, x^{t-1}, u^t - \delta_i e, p^t)}{2\delta_i} \quad \forall i = 1..n \tag{3.53}$$

The calculation of the entries marked $\otimes$ relies on the entries marked $\times$ by applying the chain rule, i.e. the sum of all the paths, Equations (3.49)-(3.51).

3.10.3. Efficiency of the TCM scheme

This Section presents the computational efficiency of the Time-Chained-Method (TCM) compared with the conventional approach of calculating the derivatives at each stage separately. The results are shown for the multi-year base run from Section 3.9 where for the single year run we use the first year's recharge value, for two years the first two, and so on. Each year in the planning horizon has 62 decision variables, 124 linear inequalities and 60 nonlinear inequalities, and a nonlinear objective function. Figure 3.18 presents the computational time to reach an optimal solution for a planning horizon ranging from 1 to 10 years. Each additional year expands the problem size, so that for 10 years it has 620 variables, 1240 linear inequalities, and 600 nonlinear inequalities.

Two model forms are compared, one with the standard gradient calculations of the objective function and Jacobian, the other with the TCM scheme. These results show

the linear rise with TCM versus the quadratic rise with the conventional method, as predicted by Equations (3.41) and (3.48).

Each run was started from the same initial guess of the decision variables and exactly the same final solution was obtained. The results demonstrate the dramatic reduction in computation time achieved by the TCM. For a 10 year operation horizon the ratio is 11200/1750=6.4 and it would rise further for a longer horizon. For 2-5 years the ratio is less significant, but still ranges between 2.5 and 4.5 .This computational efficiency will be most significant when the model is extended to deal with uncertainty, where optimal solutions are required for a large number of realizations of future conditions.

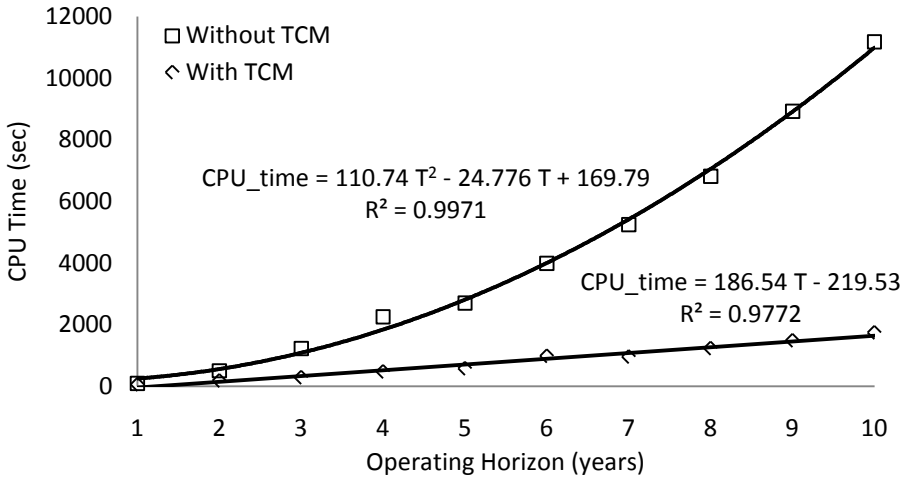

Figure 3.18: Computation time as a function of planning horizon, comparing with and without the TCM procedure (on an Intel Core i7 M620 2.67 GHz laptop)

3.11. Scaling

Solvers of nonlinear optimization are sensitive to scaling; one way to scale a problem is to introduce a linear transformation of the decision variables, of the form

$$\tilde{u}_i^t = a_i^t \cdot u_i^t + b_i^t \tag{3.54}$$

where $a_{i=1..n}^{\forall t=1..T_f}$ are the scale weights and $b_{i=1..n}^{\forall t=1..T_f}$ are the shifts. In our problem the decisions variables are bounded, so we can normalize to the range $[0\ 1]$ by

$$\tilde{u}_i^t = \frac{u_i^t - LB_i^t}{UB_i^t - LB_i^t} \tag{3.55}$$

As a result of this transformation the linear constraints $A^t \cdot u^t \le b^t$ should also be scaled. The scaled linear constraints are:

$$A^t \cdot D^t \cdot \tilde{u}_i^t \le b^t - A^t \cdot LB^t \tag{3.56}$$

where D^t is a diagonal $n \times n$ matrix, $D^t = \mathbf{diag}(UB^t - LB^t)$.

3.12. Model User Interface

The model was programmed in MATLAB. A user friendly GUI (Graphic User Interface) to enter the model parameters was developed. Tabular and graphic final reports are automatically generated by the model.

The model software incorporates a spreadsheet input tool for defining the system layout, components and parameters. The model automatically generates he corresponding input data for the MATLAB code, which is used in the optimization solver FMINCON within the optimization toolbox in MATLAB.

For a large-scale WSS, each model run has the potential to overwhelm users with information, especially when performing multi-year runs. Therefore, we had also developed different tools to display model results and compare results from different model runs. An automatic report generator module which was programmed by MATLAB to produce *.html file format (Figure 3.19) which includes tabular information for the specific run. The report classifies each year from the multi-year run as separate Chapter which include four Sections (a) Run parameters, (b) The solution of season 1, (c) The solution of season 2, and (d) Annual costs. The last

Chapter in the reports includes costs summary for all the years together. Along with the *.html report a schematic network can be generated in *.pdf file format which displays the run results such as discharges and salinities (Figure 3.12) or the network parameters such as pipes diameters, lengths and capacities (Figure 3.11).

Figure 3.19: Snapshot of the *.html report

Note:

Refer to Section 7.2.1 for Summary and Conclusion.

4. Scenario based Stochastic Programming

4.1. Introduction

Chapter 3 introduces a seasonal multi-year model for management of both water quantity and salinity. The model is deterministic, in the sense that the amounts of water that are available in the sources over time (the natural replenishment), on the one hand, and the demands which have to be met, on the other, are prescribed and fixed. An important aspect of multi-year water supply management relates to hydrological uncertainty [Ajami et al., 2008] and climate change [Grantz et al., 2007]. In this Chapter we present a stochastic version of the deterministic model, in which the replenishment into the aquifers/reservoirs is given as stochastic process.

The objective is to operate the system with minimum total cost of desalination, pumping and delivery, subject to technological, administrative, and environmental constraints. In this case, the operation cost and some of the constraints are in fact stochastic, as they depend on the realization of the replenishment into the aquifers/reservoirs.

Using the model of Chapter 3 as a basis, several stochastic models were developed using different stochastic approaches and techniques. Section 4.2 presents a general stochastic formulation. Section 4.3 presents scenario based stochastic programming. Sections 4.4-4.9 demonstrate the application of various scenario based stochastic programs including: Wait-and-See, Here-and-Now, two-stage, and multi-stage approach. Section 4.10 presents the Limited Multi-stage Stochastic Programming (LMSP) which is an approximation of MSP approach that was developed in the current research.

4.2. General stochastic model

As discussed in Section 3.10 the seasonal multi-year management of quantities and salinities in a WSS model for minimizing total present value cost can be formulated as the following nonlinear optimization problem:

$$
\begin{aligned}
&\min_{u^t\ \forall t}\ F=\sum_{t=1}^{T_f} f(x^{t-1},u^t,p^t)\\
&s.t.\\
&\left.\begin{aligned}
&x_r^t = W(x_r^{t-1},u^t,p^t) && \forall r=1..n_1\\
&y_r^t = V(y_r^{t-1},x_r^{t-1},u^t,p^t) && \forall r=1..n_1\\
&A^t\cdot u^t \le b^t\\
&g_j(y^{t-1},x^{t-1},u^t,p^t)\le 0 && \forall j=1..m\\
&LB_i^t \le u_i^t \le UB_i^t && \forall i=1..n
\end{aligned}\right\}\forall t=1..T_f
\end{aligned}
\tag{4.1}
$$

See the notations for Equation (3.39). A concise form of Equation (4.1) is:

$$
\begin{aligned}
&\min_{U}\ F(U,R)\\
&s.t.\\
&m_1(U,R)=0\\
&m_2(U,R)\le 0\\
&\underline{U}\le U\le \bar{U}
\end{aligned}
\tag{4.2}
$$

where U is the multi-year vector of decision variables that contains all decision vectors $u^t\ \forall t$ i.e. $U=[u^1,...,u^{T_f}]$; R is the stochastic replenishment process; m_1, m_2 are vectors of function; $\underline{U}$, $\bar{U}$ are lower and upper bounds, respectively.

In Section 2.2.2 we have reviewed stochastic programming tools for optimization under stochastic conditions. All of these tools can be joined to form a single general formulation of the stochastic model, which can then be used to define special cases for common stochastic models.

As discussed in Section 2.2.2, the equality constraints require the decision to take on values which make the random left side of the constraint $m_1(x,R)$ equal to zero. In other words, this places a requirement on the decision to make the random variable to be not random at all but have the constant value of zero. In many cases such decisions does not exist. To overcome this problem, it is important to avoid solving stochastic equality constraints. Following the optimization procedure in Section 3.5, we extract the dependent variables from the equality constraints:

$$
\begin{aligned}
&\min_{U_{indep}}\ F(U_{indep},R)\\
&s.t.\\
&m_2(U_{indep},R)\le 0\\
&\underline{U}_{indep}\le U_{indep}\le \bar{U}_{indep}\\
&\underline{U}_{dep}\le U_{dep}(U_{indep},R)\le \bar{U}_{dep}
\end{aligned}
\tag{4.3}
$$

If the constraints are hard, i.e., must always be respected, then in the stochastic inequality constraints should be replaced by their worst case values. When the constraints are soft they can be substituted by penalty terms in the objective function, which introduces an additional cost proportional to the amount of violation. Another approach is to model these soft constraints as chance constraints with pre-defined reliability. Since the objective function is stochastic, we have to apply a statistical operator on the objective before the minimization. Some of the operators which are commonly used are discussed in Section 2.2.2, such as: the Worst Case approach, and the Expected Value approach.

The general formulation is given by:

$$\begin{aligned}
&\min_{U_{indep}} \ \phi[F(U_{indep}, R) + \lambda \cdot \max\left(m_2(U_{indep}, R), 0\right)] \\
&s.t. \\
&\text{Prob}[m_2(U_{indep}, R) \le 0] \ge \alpha \\
&\text{Prob}[\underline{U}_{dep} \le U_{dep}(U_{indep}, R) \le \bar{U}_{dep}] \ge \alpha \\
&\underline{U}_{indep} \le U_{indep} \le \bar{U}_{indep}
\end{aligned} \tag{4.4}$$

where ϕ is a statistical operator, such as: max, expectation, variance or combination of operators; λ is the penalty per unit deviation ; α is pre-specified reliability. Some of the special cases of this general formulation are:

4.2.1. The Expected Value approach

In which we minimize the expectation of the objective, and the constraints are modeled as chance constraints: ϕ is the expectation operator and $\lambda = 0$.

$$\begin{aligned}
&\min_{U_{indep}} \ E[F(U_{indep}, R)] \\
&s.t. \\
&\text{Prob}[m_2(U_{indep}, R) \le 0] \ge \alpha \\
&\text{Prob}[\underline{U}_{dep} \le U_{dep}(U_{indep}, R) \le \bar{U}_{dep}] \ge \alpha \\
&\underline{U}_{indep} \le U_{indep} \le \bar{U}_{indep}
\end{aligned} \tag{4.5}$$

This approach emphasizes the average outcome, with pre-specified reliability.

4.2.2. The Penalty approach:

The penalty method is obtained by setting $\alpha = 0$ and $\lambda > 0$.

$$
\begin{aligned}
&\min_{U_{indep}} \; E[F(U_{indep}, R) + \lambda \cdot \max\left(m_2(U_{indep}, R), 0\right)] \\
&s.t. \\
&\text{Prob}[m_2(U_{indep}, R) \le 0] \ge 0 \\
&\text{Prob}[\underline{U}_{dep} \le U_{dep}(U_{indep}, R) \le \bar{U}_{dep}] \ge 0 \\
&\underline{U}_{indep} \le U_{indep} \le \bar{U}_{indep} \\
&\Updownarrow \\
&\min_{U_{indep}} \; E[F(U_{indep}, R) + \lambda \cdot \max\left(m_2(U_{indep}, R), 0\right)] \\
&s.t. \\
&\underline{U}_{indep} \le U_{indep} \le \bar{U}_{indep}
\end{aligned}
\tag{4.6}
$$

4.2.3. The Worst Case approach

In which we minimize the worst possible outcome which may result from the decision and the constraints are hard. This formulation is given by choosing the maximum operator in the objective function and by setting $\alpha = 1$ and $\lambda = 0$ to satisfy the constraints for all the realizations of the stochastic process.

$$
\left.
\begin{aligned}
&\min_{U_{indep}} \; \max_{R}[F(U_{indep}, R)] \\
&s.t. \\
&\text{Prob}[m_2(U_{indep}, R) \le 0] \ge 1 \\
&\text{Prob}[\underline{U}_{dep} \le U_{dep}(U_{indep}, R) \le \bar{U}_{dep}] \ge 1 \\
&\underline{U}_{indep} \le U_{indep} \le \bar{U}_{indep}
\end{aligned}
\right\}
\Leftrightarrow
\begin{cases}
\min\limits_{U_{indep}} \; \max\limits_{R}[F(U_{indep}, R)] \\
s.t. \\
\max\limits_{R}[m_2(U_{indep}, R)] \le 0 \\
\max\limits_{R}[U_{dep}(U_{indep}, R)] \le \bar{U}_{dep} \\
\min\limits_{R}[U_{dep}(U_{indep}, R)] \ge \underline{U}_{dep} \\
\underline{U}_{indep} \le U_{indep} \le \bar{U}_{indep}
\end{cases}
\tag{4.7}
$$

This approach does not distinguish between the outcomes according to their probability of occurrence; hence it can give poor results when the worst outcome has low probability, as is the case many real word problems.

4.2.4. The Value at risk approach:

In the value at risk approach (VaR_β), we minimize the quantile value associated with risk β.

$$
\begin{aligned}
&\min_{U_{indep}} \; VaR_\beta \\
&s.t. \\
&\text{Prob}[F(U_{indep}, R) \le VaR_\beta] \ge 1 - \beta \\
&\text{Prob}[m_2(U_{indep}, R) \le 0] \ge \alpha \\
&\text{Prob}[\underline{U}_{dep} \le U_{dep}(U_{indep}, R) \le \bar{U}_{dep}] \ge \alpha \\
&\underline{U}_{indep} \le U_{indep} \le \bar{U}_{indep}
\end{aligned}
\tag{4.8}
$$

This approach considers only one value of the stochastic objective, namely, the quantile associated with risk β. To demonstrate its drawback consider two decisions U' and U'' which have Cumulative Density Functions (CDFs) of the objective, shown in Figure 4.1.

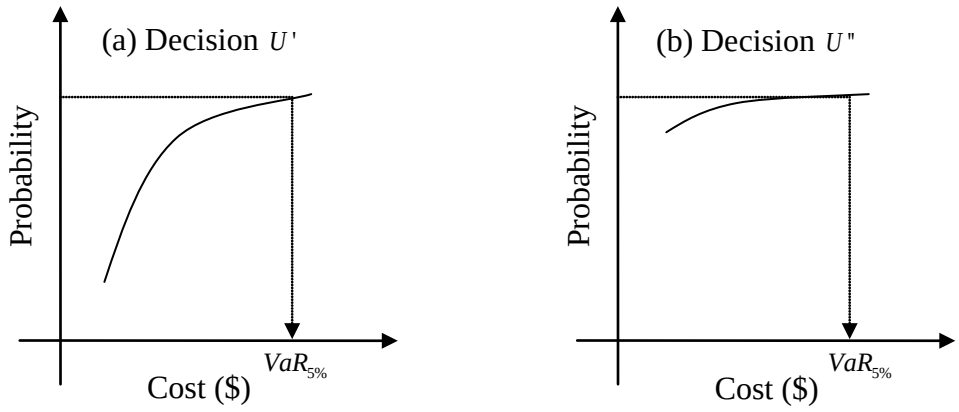

Figure 4.1: Cumulative Density Function of the objective

Both decisions give the same value-at-risk, however it is obvious that the second decision, U'' is preferred since it give more probability to low costs realizations.

4.2.5. The Mean-Variance approach

Combination of different statistical operators is also possible. For example, a commonly used objective is the combination of the expectation and the variance.

$$\begin{aligned} &\min_{U_{indep}} \; E[F(U_{indep}, R)] + \omega \cdot \Sigma[F(U_{indep}, R)] \\ &s.t. \\ &\text{Prob}[m_2(U_{indep}, R) \le 0] \ge \alpha \\ &\text{Prob}[\underline{U}_{dep} \le U_{dep}(U_{indep}, R) \le \bar{U}_{dep}] \ge \alpha \\ &\underline{U}_{indep} \le U_{indep} \le \bar{U}_{indep} \end{aligned} \qquad (4.9)$$

where ω is a weighting parameter and Σ is the variance operator. This approach is quite traditional in financial applications, where the outcomes variance is considered a measure of risk [Markowitz, 1959].

4.3. Scenarios based Stochastic Programming

The scenarios based stochastic programming assumes that the distribution of the stochastic process R is a finite discrete probability space, which is the particular representation of how the process might be realized. The stochastic process R is

approximated by a finite set of scenarios $R^s \in \Omega \quad \forall s$ with probabilities p^s where $\sum_{s=1}^{S_f} p^s = 1$.

If a given problem naturally involves "continuous" random variables, it can be discretized in various ways. When the stochastic process R is represented by a finite number of scenarios $R^s \in \Omega \quad \forall s$, the process can be represented by a scenario tree. A scenario tree consists of nodes and arcs; each node represents a possible realization of the stochastic process, the root node represents the present state, and each node has a unique ancestor (except the root node which has no ancestor). The arcs represent the links between the nodes and are associated with a conditional probability. Along the tree the uncertainty unfolds with the stages, where each path from the root to a leaf represents a scenario. An illustration of scenario trees is shown in Figure 4.2, with four stages and two branches at each node; accordingly we have eight scenarios at the end of the four stages horizon.

The number of branches of all nodes at a given level in the scenario tree can be equal, if this occurs for all stages, the scenario tree is balanced (Figure 4.2c). A special case of the scenario tree is when all the nodes after the first stage have only one branch. This means that the scenario tree is only a "fan" of individual scenarios R^s which occur with probabilities p^s (Figure 4.2a). In this case the entire future is reveled after the first stage, since each node after the root only has only one possible continuation. Hence, the stochastic process is given as two stages; the first is before any realization and the second is after the first realization of the process.

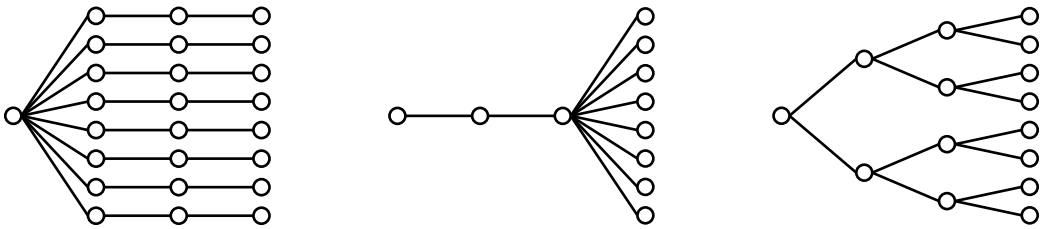

Figure 4.2: Scenario trees: (a) fan (b) feather-duster (c) balanced tree

4.3.1. Generation of scenario trees

For water resources management models we are often able to generate a large number of scenarios, which may be obtained by simulation with stochastic models, historical

data and expert forecasting for extreme scenarios. The most common ways for generating individual scenarios are:

(a) Simulation: in which stochastic models which are calibrated with historical data (e.g. multivariate auto-regression models) are used to produce a set of scenarios to present the stochastic process.

(b) Monte Carlo Sampling: in which the random variables are generated from their known (or assumed) distribution and thus replace the given probability space with a finite space consisting of the samples.

(c) Moment Matching: this uses a finite number of samples that match as closely as possible to the first few moments of the stochastic process.

(d) Bootstrapping: in which the scenarios are generated from the historical data without the need to make any distributional assumptions regarding the process.

A survey of methods for generating sets of scenarios that form an approximation of the underlying random data process is given in Dupačová et al. [2000].

The generated individual scenarios form a scenario fan tree (Figure 4.2a) where the root node corresponds to the present state (initial information). Hence, the generated individual scenarios (data paths) must construct a scenario tree which preserves the correlation structure present in the stochastic process.

Many schemes have been developed for bundling and reduction in order to generate balanced and unbalanced scenario trees out of a fan scenario tree. See for example [Dupačová et al., 2003; Gulpinar et al., 2004 and Heitsch and Römisch, 2005]

4.4. Wait-and-See approach

An important aspect of solving stochastic models is the sequence in which decisions alternate with observations. The implicit stochastic programming (IS) or Wait-and-See approach seeks an optimal solution for each scenario individually. Hence, the Wait-and-See approach assumes that the decision maker is somehow able to wait until the uncertainty is revealed before making the decision, i.e. delaying all decisions until the last possible moment, after all uncertainties have been resolved. The optimal solution relies upon perfect information about the future for each scenario; therefore this approach provides a set of scenario solutions. Because of this assumption such

approach cannot be implemented and is known as the “passive approach”. The optimal solution (solution for each scenario) of the Wait-and-See constructs the objective value set which contains the optimal objective value for each scenario individually and the optimal solution set which contains the optimal decisions for each scenario individually. These sets can be analyzed probabilistically and a heuristic subjective rule is then used to aggregate these solutions to a single one that is selected for implementation.

In this approach one must solve many deterministic problems (one deterministic problem for each scenario) hence, the deterministic model developed in Chapter 3 constitutes an efficient module since it was solved with structural adaptability and high computational efficiency to serve as a building-block for stochastic approaches which consist of solving many deterministic problems. For more details see the TCM method and the optimization plan in Chapter 3.

The corresponding problem is stated as:

$$\left.\begin{array}{l} \min\limits_{U^s_{indep}} \; F(U^s_{indep}, R^s) \\ s.t. \\ m_2(U^s_{indep}, R^s) \le 0 \\ \underline{U}_{dep} \le U_{dep}(U^s_{indep}, R^s) \le \overline{U}_{dep} \\ \underline{U}_{indep} \le U^s_{indep} \le \overline{U}_{indep} \end{array}\right\} \forall s \qquad (4.10)$$

It is solved for each scenario individually to construct the objective value set $\min\limits_{U^s_{indep}} F(U^s_{indep}, R^s) \in \Omega_F \;\; \forall s$ and the optimal solution set $\arg\min\limits_{U^s_{indop}} F(U^s_{indep}, R^s) \in \Omega_U \;\; \forall s$.

4.4.1. Example 1

In this example we solve the multi-year problem with a five years horizon, with the same parameters set defined in the multi-year run (Section 3.8) and a maximum specific levy $\left(\overline{CE}^{\max}\right) = 1 \;\; (M\$/MCM)$.

The yearly aquifers recharges $R\;(MCM)$ (which, we recall, occur only in Season 1, while Season 2 they are zero) are considered stochastic, given by a balanced scenario tree with three branches at each stage. The conditional discrete probability at each

year is given by the Probability Mass Function (PMF) in Table 4.1, where r_t is the recharge in year t, and R^t is the vector of recharges up to year t.

	Low Recharge	Medium Recharge	High Recharge
r_t (MCM)	0	50	100
Prob$(r_t \mid R^t)$	1/3	1/3	1/3

Table 4.1: Probability Mass Function (PMF) of the recharge, example 1

The scenario tree in this case has 243 scenarios (paths in the tree). After solving (4.10) for each scenario individually we can construct the two sets Ω_F and Ω_U, to be analyzed probabilistically to derive a heuristic rule which can be implemented. The PMFs of the multi-year costs (objective values), the water level at the end of the five years and the extraction from the aquifer at the first/last year, are given in Figure 4.3.

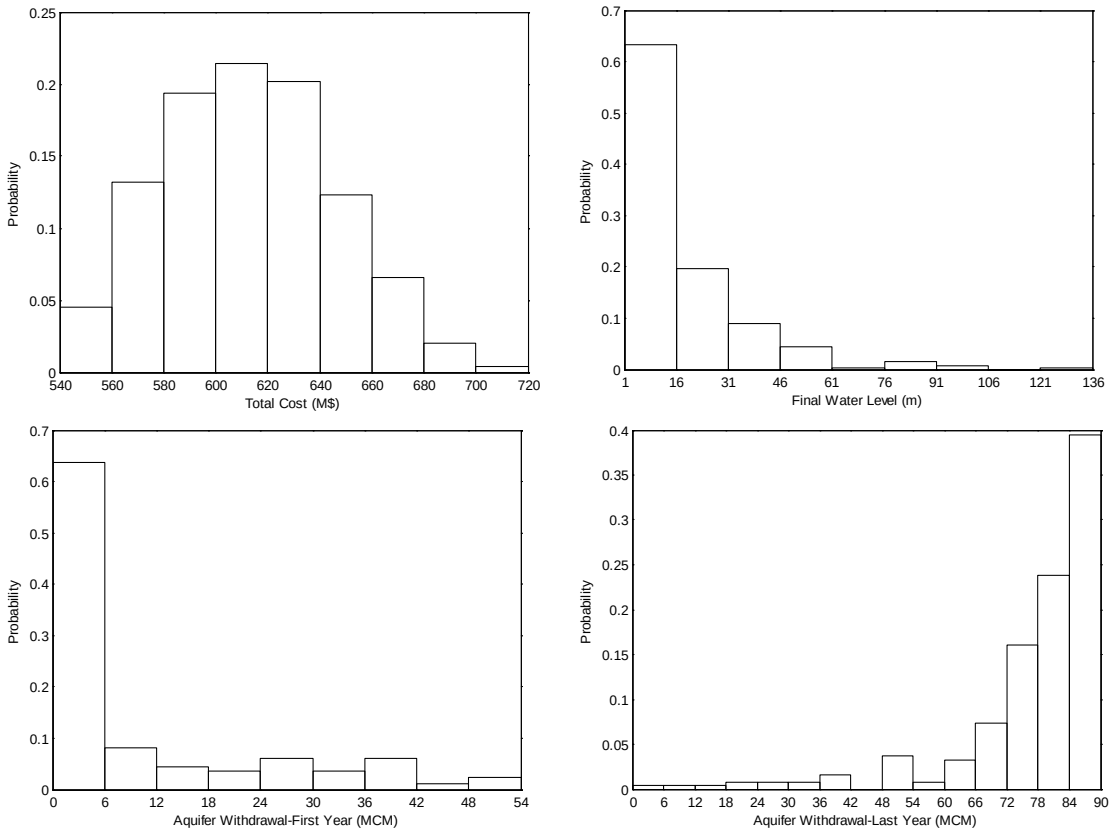

Figure 4.3: Probability Mass Functions (PMFs) for example 1: (a) objective (total cost) (b) final water level (c) aquifer withdrawal first year (d) aquifer withdrawal last year

As seen in Figure 4.3 the solution given by the Wait-and-See approach cannot be implemented, since all decisions are given as PMFs which means that there is no specific solution to be implemented. Still, the PMFs can be used to derive a heuristic rule which guides to a near optimal solution for a wide range of possible realizations.

For example, as seen in Figure 4.3c, the optimal value of the first year withdrawal is between 0-6 (MCM) in 64% of the scenarios and the range of the optimal objective value is between 540-720 $(M\$)$, but there is no theoretical guidance about the compromise between the different values in the PMFs that should actually be adopted.

In practice, such approach may result in poor solutions [Labadie, 2004]. For instance, the last year withdrawal in the example is spread over a wide range which increases the difficulty of choosing a "good" heuristic operation rule. More difficult situations are when we have a uniform distribution which gives no preference for one value over the others.

Note that the above analysis (Figure 4.3) neglects any relationship between one decision variable to the other, and also neglects the relationship between the decision variables and state variables since each PMF was created independently. This dependency should not be neglected, especially when dealing with constrained optimization problems, in which neglecting dependency may result in constraint violations. For example, neglecting the correlation between the total desalination amount and the total withdrawal may lead to unsatisfied demand constraints.

More complex analysis regarding the correlation of the state variable PMF in Figure 4.3b and decision variables PMF in Figure 4.3c&d may be performed to derive operation rules based on the system state. In general, this approach is not considered as an adequate approach for deriving decision for implementation. It is closer to a scenarios analysis or what-if-analysis as it was called by some researchers. Using this approach for preliminary understanding of the model behavior under the stochastic process, such as the ranges of decisions and the objective value, may help develop the appropriate stochastic model. For instance, using this approach may help answering crucial questions for formulating an explicit stochastic model, such as: what is the proper statistical operator which should be applied on the objective function?

Back to the example above, we can see that the worst case value of the objective have low probability which indicates that we should be cautious before implementing the max operator i.e. solving the worst case problem. However, the diversity of the objective value is small, meaning that the expected value of the distribution is close to many outcomes of the objective function, hence choosing the expectation operator may be justified. In contrast, when encountering an outcome with high diversity, the

expectation alone will not be a good representation of the outcomes, and another operator which considers variability of the objective values should be considered.

4.4.2. Example 2

The large scale network presented in Section 3.9 is solved in this example. The multi-year problem of three years horizon is considered with the same parameters set defined in the multi-year run (Section 3.9) and a maximum specific levy $\left(\overline{CE}^{\max}\right)_a = 0.2$ $(M\$/MCM)$.

The yearly aquifers recharges $R_{a=1..3}(MCM)$ are considered stochastic, given by a balanced scenario tree (Figure 4.2c) with two branches at each stage. The conditional probability in each year is given in Table 4.2, where $r_{a,t}$ is the recharge in aquifer a at year t, and R_a^t is vector of recharges up to year t.

	Low Recharge	High Recharge
$r_{1,t}$, $r_{2,t}$, $r_{3,t}$ (MCM)	60, 10 ,110	360, 280, 550
Prob$(r_{a=1..3,t} \mid R^t_{a=1..3})$	0.5	0.5

Table 4.2: Probability Mass Function (PMF) of the recharge, example 2

The scenario tree (Figure 4.2c) in this case has 8 scenarios (paths in the tree), where each of the nodes $2\ldots15$ takes the values of the low recharge if the node index is an odd number, and if even the node takes the values of the high recharge. The objective value for each scenario is given in Figure 4.4a.

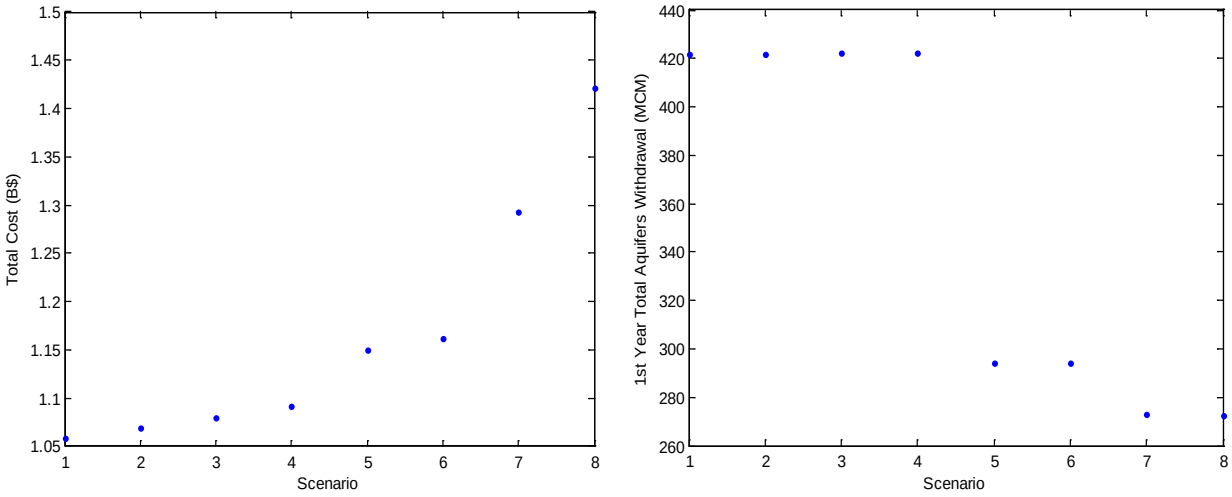

Figure 4.4: Total cost (B$) and aquifers withdrawal (MCM) for each scenario.

For instance, Figure 4.4a shows that scenario 4, with High-Low-Low recharge, costs less than scenario 5, a Low-High-High recharge scenario, despite the fact that scenario 5 has available more aquifer water. Since the high recharge value in scenario 4 at the first year is above the total required demand, aquifers water can be stored for later years. On the other hand, in scenario 5 the low recharge is in the first year, hence despite knowing that the future holds high recharge we must use more from the desalination water in the first year, which leads to high cost in the first year and consequently to a higher total cost.

Again we see from Figure 4.4b that the Wait-and-See solution cannot be implemented, since the decisions have different optimal values for different scenarios. Among the 8 scenarios we have 3 different values for the optimal withdrawal from the aquifers in the first year. The first value (420 MCM) corresponds to the scenarios beginning with a high recharge, while remaining scenarios, which all start with low recharge, are further classified according to the recharge in the second year.

4.5. Mean-Variance tradeoff

The formulation in (4.10) can be solved for predefined objective on the optimal objective set Ω_F. For example, the expectation of the objective values can be minimized. In such a problem all the decisions corresponding to each scenario are determined in the same optimization problem as follows:

$$
\begin{aligned}
&\min_{U^{s\,\forall s}_{indep}} \; E[F(U^s_{indep}, R^s)] \\
&s.t. \\
&m_2(U^s_{indep}, R^s) \le 0 && \forall s \\
&\underline{U}_{dep} \le U_{dep}(U^s_{indep}, R^s) \le \bar{U}_{dep} && \forall s \\
&\underline{U}_{indep} \le U^s_{indep} \le \bar{U}_{indep} && \forall s
\end{aligned}
\qquad (4.11)
$$

However, the optimal solution for each scenario obtained from problem (4.11) would be the same as that obtained from (4.10) since we can obtain the minimum expectation also by minimizing each scenario individually and utilizing the efficiency of solving deterministic model which was developed in Chapter 3. In the general case, this would not always be true. Consider for example if the objective to be minimized is the variance of the set Ω_F. In this case the optimal solution cannot be solved by each scenario individually; we must rather solve the following optimization problem:

$$
\begin{aligned}
&\min_{U^{s\,\forall s}_{indep}} \ \Sigma[F(U^{s}_{indep}, R^{s})] \\
&s.t. \\
&m_2(U^{s}_{indep}, R^{s}) \le 0 \qquad \forall s \\
&\underline{U}_{dep} \le U_{dep}(U^{s}_{indep}, R^{s}) \le \overline{U}_{dep} \qquad \forall s \\
&\underline{U}_{indep} \le U^{s}_{indep} \le \overline{U}_{indep} \qquad \forall s
\end{aligned}
\tag{4.12}
$$

The minimum variance would be zeros which is obtained when all members of Ω_F have the same value, i.e. all the scenarios have the same objective value. Since, each scenario has its own decision vector, the model is capable to increase the costs in order to obtain Ω_F which has the minimum variance, zero.

A zero variance can be obtained by an infinite number of solutions. For instance, suppose that we have the same objective value of for all scenarios, and recalling that the model is capable of increasing costs, a solution that increases the objective values of the scenarios by a constant is also optimal and produces zero variance. Among all optimal solutions which produce zero variance, one may be interested in the solution which produces minimum expectation and have zero variance, this solution can be obtained by increasing the cost of all scenarios to match the minimum cost of the severe scenario. In this case the cost expectation would equal the minimum cost of the severe scenario and have a zero variance.

Using a multi-objective approach for the Mean-Variance is also applicable within the Wait-and-See approach. The Pareto Frontier between the variance and the mean covers the interval from the point of minimum expectation until the point of minimum expectation with variance zero. The minimum expectation with variance zero is equal to the minimum cost of the most severe scenario.

We can obtain the bounds of the tradeoff interval from the solution of (4.10) which implies solving each scenario individually, because the mean of the objective values gives the minimum expectation ($E_{\min}$, left point) and the maximum of the objective values gives the severe scenario cost ($E_{\max}$, right point). For each E_i inner point in the tradeoff interval we can solve the following model and obtain one point on the tradeoff curve:

$$
\begin{aligned}
&\min_{U^{s\,\forall s}_{indep}} \ \Sigma[F(U^s_{indep}, R^s)] \\
&s.t. \\
&E[F(U^s_{indep}, R^s)] \le E_i \\
&m_2(U^s_{indep}, R^s) \le 0 \qquad \forall s \\
&\underline{U}_{dep} \le U_{dep}(U^s_{indep}, R^s) \le \bar{U}_{dep} \qquad \forall s \\
&\underline{U}_{indep} \le U^s_{indep} \le \bar{U}_{indep} \qquad \forall s
\end{aligned}
\tag{4.13}
$$

This model is the same as minimum variance model with the addition of a constraint on the expectation to be below the inner point E_i.

4.5.1. Example

To obtain a point on the tradeoff curve, one should solve formulation (4.13) in which all the decisions corresponding to each scenario are determined in the same optimization problem. Hence, for the stochastic example 1 considered previously (5 years), for each year there are 243 different decision vectors, each decision vector has 10 variables, and we have an optimization problem with $243 \cdot 5 \cdot 10 = 12{,}150$ decision variables. Each decision vector is subject to 24 linear constraint and 16 non-linear constraints, which means that for each point on the tradeoff, an optimization problem with 29,160 linear and 19,440 nonlinear constraints has to be solved. Even for this small example the optimization problem size is too large. In the next Section we present an equivalent external optimization problem which gives the optimal frontier without the need to consider formulation (4.13).

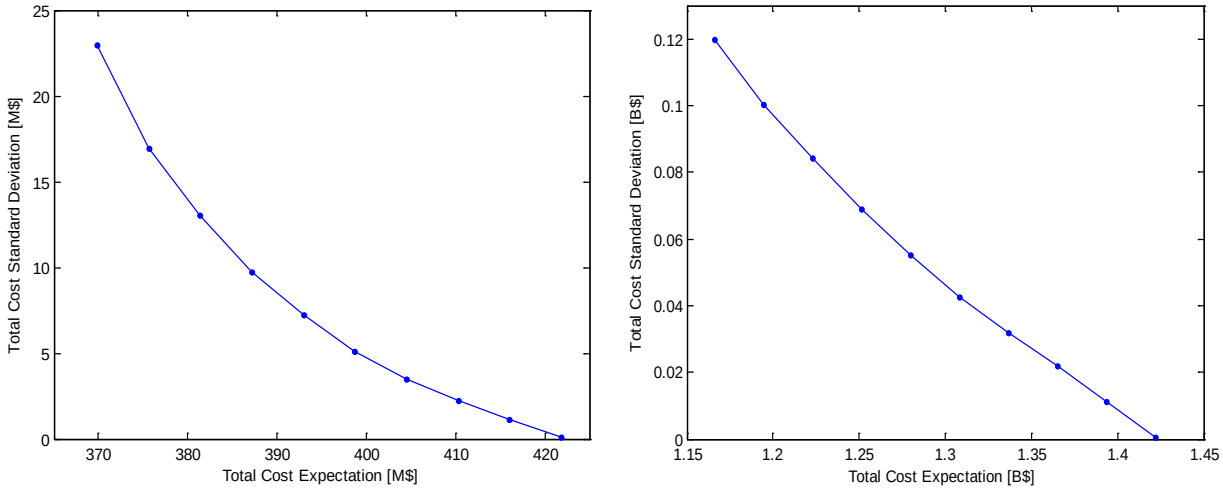

Figure 4.5: Mean-Variance tradeoff

To validate the results obtained from the external problem in the next Section, we solve the formulation (4.13) for the stochastic example 1 with 3 years horizon and

stochastic example 2 with the same parameters considered previously. Figure 4.5, shows the tradeoff for the problem considered in implicit stochastic example 1 (3 years) and example 2, respectively.

For the problem in example 2, the minimum expectation cost can be obtained by averaging the optimal objective values of each scenario individually as explained earlier in this Section, hence the tradeoff interval is from $E_{\min} = 1.17$ to the severe scenario cost which is $E_{\max} = 1.42$, as shown in Figure 4.5b. The tradeoff between the expected value of the cost and its variability (standard deviation) shows that as the cost rises (corresponding to less water taken from the stochastic source and more from desalination) the variability decreases. For instance, Figure 4.6 compares the first point (1.17 B$) and the middle point (1.28 B$) in the tradeoff.

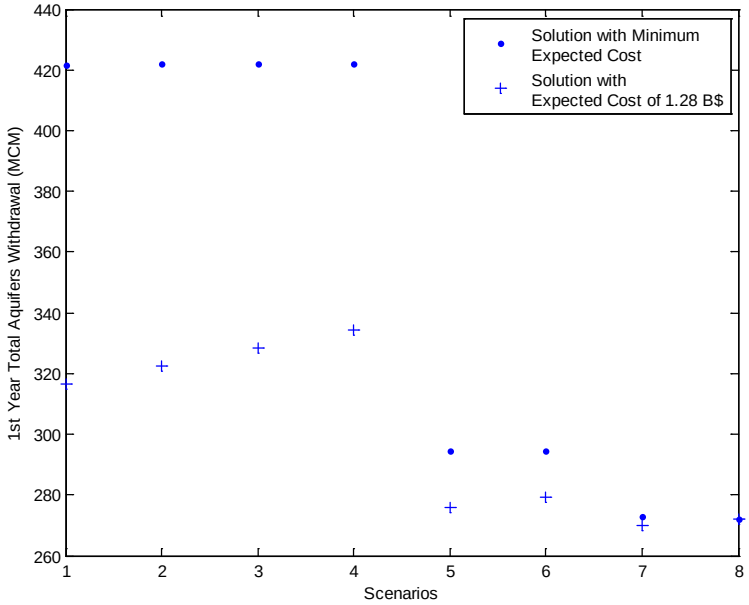

Figure 4.6: Aquifers withdrawal (MCM) comparison

By requesting less variability in the solution we asked to increased the costs in the "good" scenarios e.g. when we ask for zero variability of the cost, each of the scenarios should have the same cost as the severe scenario.

In example 2, the increments in the cost are expressed by less water taken from the stochastic source and more from the desalination, so in this case as we move to the right along the points on the tradeoff the solutions become more robust, as they decrease the reliance on the stochastic source. Hence, the cost variability in this example can be a measure for the solution robustness. However, this is not always true. There is no guarantee that the costs increments is always expressed by less water

taken from the stochastic source (aquifers) and more water taken from the reliable source (desalination), so called robust solution. Basically, it is possible to have larger costs by ineffective water distribution or by ineffective water allocation among the years. So with same water amount taken from the stochastic source we have less cost variability.

To demonstrate this let us consider again the tradeoff of example 1 (Figure 4.5a), and compare the first point (370 M$) and the middle point (392 M$) in the tradeoff. Figure 4.7 shows an opposite behavior between these points, i.e. more aquifer water is taken in the middle point (the point with less cost variability). So we cannot say that low cost variability solution is robust in which we have less reliance on the stochastic process. However, the PMF's variance and the PMF's range of the middle point is less than in the first point - which could also be considered a desired property of if it was selected as the solution.

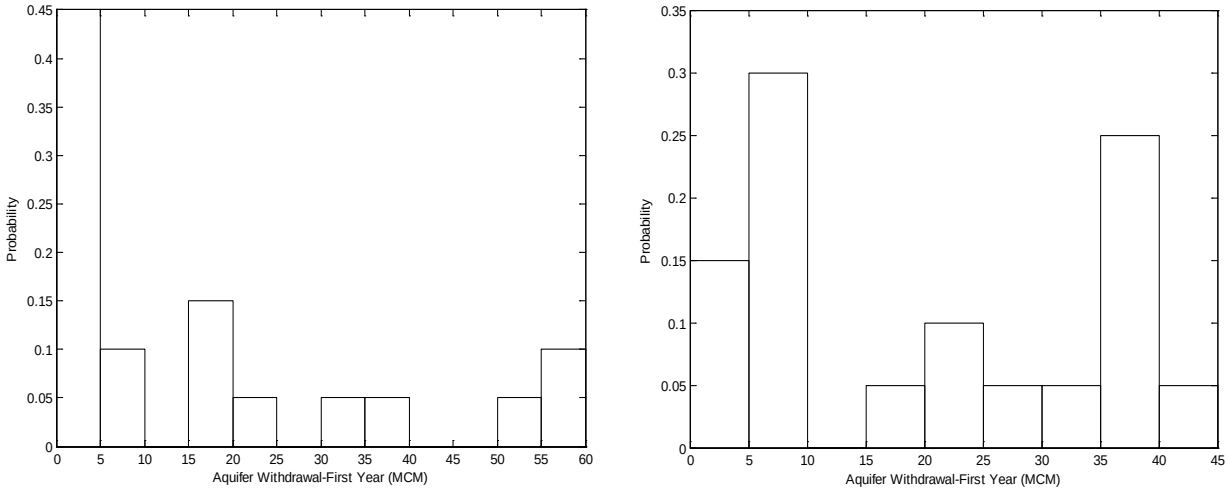

Figure 4.7: PMFs of Aquifers withdrawal corresponding to expected cost of 370 (M$) and 392 (M$), respectively.

The conclusion to be drawn from this example is that we need to understand the consideration of cost variability solutions in making decisions. Choosing the variance/standard deviation as a measure of robustness in the Wait-and-See approach may lead to bad results in the cases where less variability requirement artificially/inefficiently increases the cost of the scenarios to bring them closer to each other, thereby providing the appearance of less variability. In example 1, because of the high extraction levy (which is still lower than desalination cost) there is a preference to preserve water in the first year (Figure 4.7a), but when we asked for less

cost variability the solution inefficiently allocates the aquifer water (high withdrawal in the first year, Figure 4.7b) to artificially increase the costs of the scenarios.

For each point on the tradeoff we can also show the range, of cost values with the distribution of the values within that range. Figure 4.8 shows the cost range (bounded between the two curves) for each point in the tradeoff of example 1. The PMF of the objective values for the first point and middle point is also presented showing that for the distribution of the middle point it is skewed towards the lower bound, which indicates that the probability of severe costs is small.

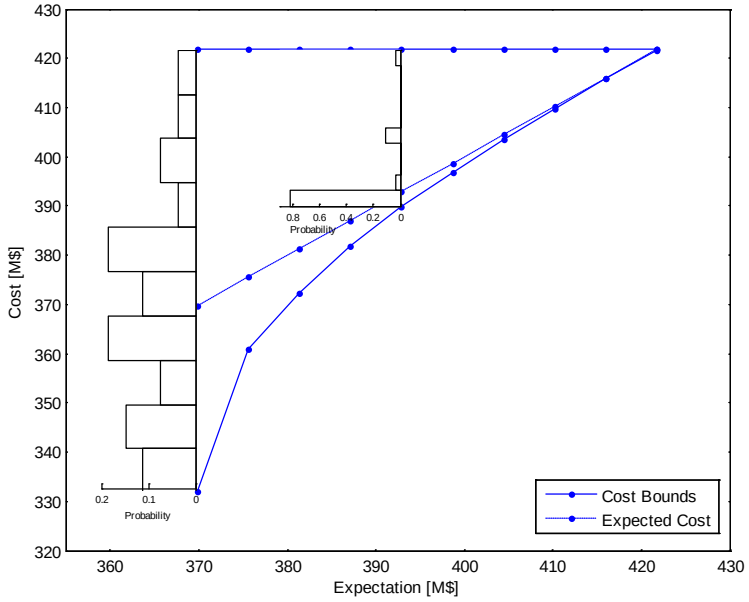

Figure 4.8: Operation cost range along the Mean-Variance tradeoff

4.6. External problem for tradeoff generation

In order to obtain the tradeoff between the expectation and the variance we do not have to solve explicitly for each E_i in the tradeoff interval. After we solve for each scenario individually, utilizing the efficiency of the deterministic model, we can define an external problem which generates the tradeoff without the need to solve many large scale optimization problems which contain all the scenario variables, $U_{indep}^{s\,\forall s}$ as in (4.13). For each E_i inner point on the tradeoff interval we can solve the following model and obtain one point on the tradeoff curve.

$$\min_{F^s \forall s} \sum_{s=1}^{S_f} p^s \cdot \left(F^s - E\right)^2$$

s.t.

$$E = \sum_{s=1}^{S_f} p^s \cdot F^s \qquad (4.14)$$

$$E \le E_i$$

$$F^s \ge \min_{U^s_{indep}} F(U^s_{indep}, R^s) \qquad \forall s$$

This model minimizes the variance while the F^s (operation cost in each scenario) is the decision variable and the constraints $F^s \ge \min_{U^s_{indep}} F(U^s_{indep}, R^s)$, $\forall s$ maintain the original problem feasibility.

4.6.1. Example

The tradeoff curve obtained by the external formulation (4.14) for the two examples in the previous Section and the curve obtained from the original problem, i.e. formulation (4.13), are compared in Figure 4.9.

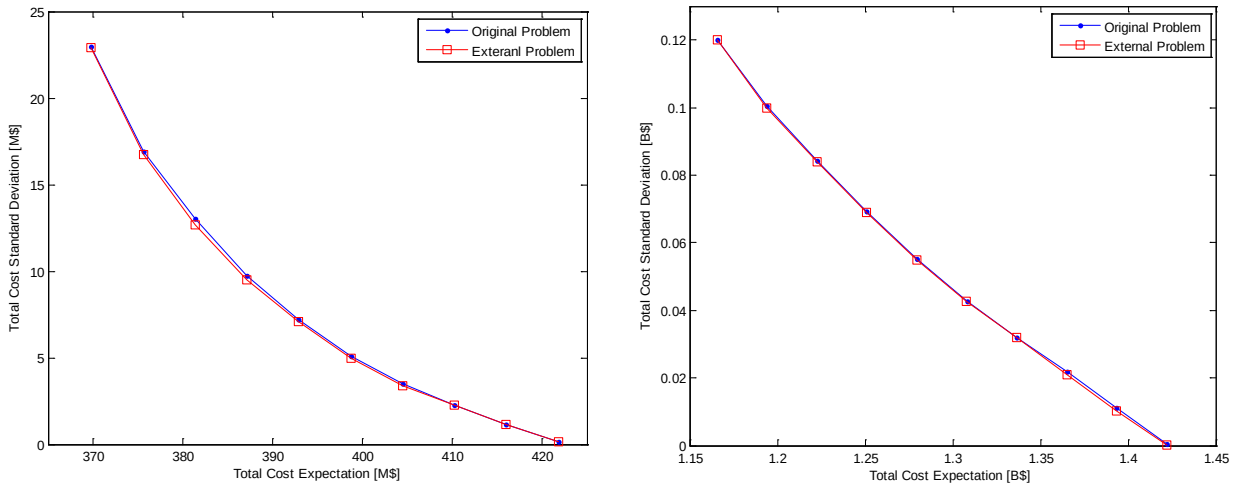

Figure 4.9: Validation of the external problem tradeoff

We can see that tradeoff curves are very close, with the curve of the external model slightly lower, i.e., better. The difference is due to lower precision in the solution of the original problem, because it is a larger model whose solution is numerically less accurate.

So, in order to obtain a point on the tradeoff of example 1 (Figure 4.9a), instead of solving formulation (4.13) (which comprised of 810 decision variables, 1944 linear constraints and 1296 nonlinear constraints) we solve formulation (4.14), which is a quadratic and easy to solve optimization problem with 27 decision variables and 28

linear constraints. In the external problem only the tradeoff itself is produced and not the decision $U^s_{indep}\ \forall s$, hence, to obtain the decision for a chosen point on the tradeoff a goal seek problem should be formulated for each scenario. The goal seek formulation to obtain the decision for a point in the tradeoff is:

$$\left.\begin{aligned} &\min_{U^s_{indep}} \ (F(U^s_{indep}, R^s) - F^{S*})^2 \\ &s.t. \\ &E[F(U^s_{indep}, R^s)] \le E_i \\ &m_2(U^s_{indep}, R^s) \le 0 \\ &\underline{U}_{dep} \le U_{dep}(U^s_{indep}, R^s) \le \bar{U}_{dep} \\ &\underline{U}_{indep} \le U^s_{indep} \le \bar{U}_{indep} \end{aligned}\right\} \forall s \qquad (4.15)$$

4.7. The Here-and-Now approach

The term Here-and-Now is used to refer to stochastic programming problems in which the decision has to be taken in advance, before a realization of the stochastic process is revealed. The extreme case is when all decisions, for all time periods, have to be made in advance, i.e. the entire problem is considered at one stage.

The single stage formulation could be considered with different statistical operators as in the Wait-and-See approach. The Mean-Variance single stage stochastic programming model can be formulated as follows:

$$\begin{aligned} &\min_{U_{indep}} \ \Sigma[F(U_{indep}, R)] \\ &s.t. \\ &E[F(U_{indep}, R^s)] \le E_i \\ &m_2(U_{indep}, R^s) \le 0 \qquad \forall s \\ &\underline{U}_{dep} \le U_{dep}(U_{indep}, R^s) \le \bar{U}_{dep} \qquad \forall s \\ &\underline{U}_{indep} \le U_{indep} \le \bar{U}_{indep} \end{aligned} \qquad (4.16)$$

In contrast to the Wait-and-See approach, here we consider a common decision for all the scenarios. Hence, we do not have the implementation problem that we had in the Wait-and-See approach. The Pareto Frontier between the variance and the mean is in the interval from the point of minimum expectation to the point of zero variance. As discussed previously, zero variance is obtained when all the objective values for all scenarios are the same. However, since the Here-and-Now approach considers only one decision for all the scenarios the zero variance can be obtained only when the stochastic part of the objective function is eliminated. In our model the stochastic part

of the objective is related to the extraction from the aquifers, hence the zero variance is obtained when the system relays only on the desalination plants without using aquifer water. This is not always feasible, which means that the tradeoff may end before the point of zero variance.

4.7.1. Example

In this approach the optimal decision vector is implementable since it is a single decision for all scenarios. For Example, the optimal solution of the minimum expected value problem of example 1 require withdrawal of [9.7 0.07 0.23] (MCM) for the three years, respectively. This decision is the same for all scenarios. The optimal decision vector is also associated with stochastic objective function and state variables (aquifer water level) which can be presented as PMFs. The PMF of the water level at the end of third year in example 1 is presented in Figure 4.10; the mean value 151 (m) and the standard deviation is $\sqrt{5000}$ (m).

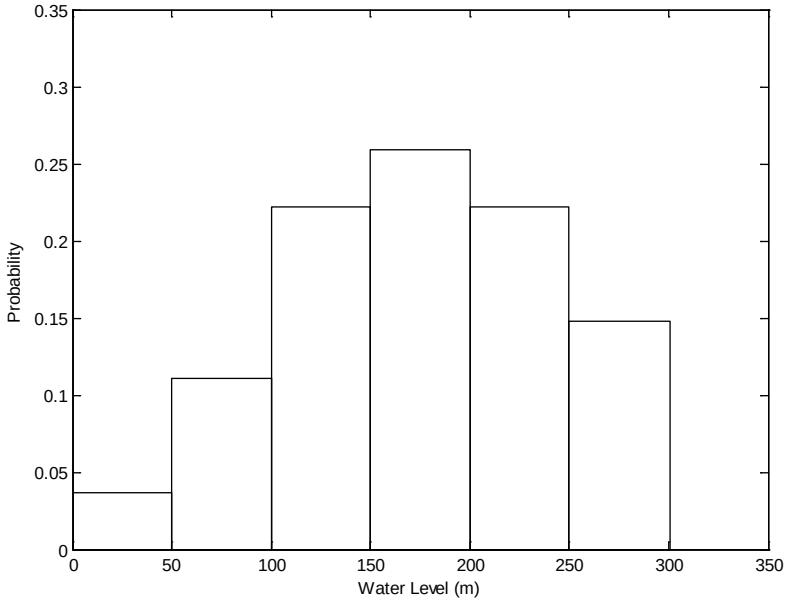

Figure 4.10: PMF of the aquifer water level at the end of the horizon

Since the decision in this approach is the same for all scenarios, the state equation of the final water level imposes an affine mapping of the stochastic recharge. Hence, the water level expectation equals the initial water level 11 (m) plus the expectations of the three years' recharges minus the three years' withdrawals 10 (MCM): $11+50\cdot 3-10=151(m)$. The variance of the water level is given by:

$$\Sigma_{Level} = [1,...,1] \cdot \begin{pmatrix} 1666.66 & 0 & 0 \\ 0 & 1666.66 & 0 \\ 0 & 0 & 1666.66 \end{pmatrix} \begin{bmatrix} 1 \\ \vdots \\ 1 \end{bmatrix} = 5000 \qquad (4.17)$$

where 1666.66 is the variance of the yearly recharge given in Table 4.1, and the ones vector is summing the yearly recharges, since the stochastic water level at the end of the horizon depends on the sum of all the yearly recharges. This demonstrates that the expectation and the variance of the final water level obtained from this analysis are identical to the expectation and the variance of the water level PMF obtained from the optimization results.

4.8. Two stage Stochastic Programming

In the two stage model we combine the Here-and-Now approach and Wait-and-See approach: the first with one decision vector for all scenarios and the second with decisions that are scenario dependent. The first approach is too conservative since it takes all decision before the process is revealed and does not take into account information which may be available after part of the decisions were implemented. On the other hand, the Wait-and-See approach provides a set of solutions which cannot be implemented. At least the decisions for first stage (in our case first year/season) are needed in order to provide operating rules for the water system.

Based on the two approaches we can define a two-stage model which takes at the first stage one decision for all scenario and scenario dependent decisions at the second stage (in our case all the years/season after the first).

The two stage model:

$$\begin{aligned} &\min_{u_{indep,t=1},\, u^{s\forall s}_{indep,t=2..T_f}} \quad E[F(u_{indep,t=1}, u^{s}_{indep,t=2..T_f}, R)] \\ &s.t. \\ &m_2(u_{indep,t=1}, u^{s}_{indep,t=2..T_f}, R^s) \le 0 \qquad \forall s \\ &\underline{U}_{dep} \le U_{dep}(u_{indep,t=1}, u^{s}_{indep,t=2..T_f}, R^s) \le \overline{U}_{dep} \qquad \forall s \\ &\underline{u}_{indep,t=1} \le u_{indep,t=1} \le \overline{u}_{indep,t=1} \\ &\underline{u}_{indep,t=2..T_f} \le u^{s}_{indep,t=2..T_f} \le \overline{u}_{indep,t=2..T_f} \qquad \forall s \end{aligned} \qquad (4.18)$$

The two stage model can also be formulated to produce the tradeoff between the expectation and the variance. In this case the tradeoff occurred in the interval, from

the point of minimum expectation until the point of minimum expectation with variance zero, as we explained previously the minimum expectation with variance zero is equal to the minimum cost of the severe scenario.

Since the two stage programming is a special case of the multi-stage stochastic programming described in the next Section we postpone the numerical examples to the next Sections.

4.9. Multi-stage Stochastic Programming (MSP)

When it is required to consider not just one decision and one observation, but sequential interactions between decisions and observations in stages, then multi-stage stochastic programming (MSP) is used. In the multistage stochastic program over time horizon T_f the stochastic process $R = (r_1 \cdots r_{T_f})$ and decision process $U = (u_1 \cdots u_{T_f})$, are interlinked into a sequence of decisions and observations is $u_1, r_1 \cdots u_{T_f-1}, r_{T_f-1}, u_{T_f}, r_{T_f}$.

The MSP distinguishes between decisions that have to be made now, before any information is revealed, and decisions at later stages when part of the information becomes available. The decisions at each stage are made while taking into account that there are opportunities for modification and corrections at later stages. The decision process is assumed to be nonanticipative or implementable, i.e., the decision vector u_t depends only on past information $R^{t-1} = (r_1 \cdots r_{t-1})$. The mathematical formulation of the MSP:

$$
\begin{aligned}
&\min \; E[F(u_{indep,1}, u_{indep,2}(r_1), u_{indep,3}(r_1, r_2), ..., u_{indep,T_f}(R), R)] \\
&s.t. \\
&m_2(u_{indep,1}, u_{indep,2}(r_1), ..., u_{indep,T_f}(R), R) \le 0 \\
&\underline{U}_{dep} \le U_{dep}(u_{indep,1}, u_{indep,2}(r_1), ..., u_{indep,T_f}(R), R) \le \overline{U}_{dep} \\
&\underline{u}_{indep,t=1..T_f} \le [u_{indep,1}, u_{indep,2}(r_1), ..., u_{indep,T_f}(R)]^T \le \overline{u}_{indep,t=1..T_f}
\end{aligned}
\qquad (4.19)
$$

When the stochastic process is given by scenarios, as it in our case, the mathematical formulation is:

$$
\begin{aligned}
&\min \; E[F(u_{indep,1}, u^s_{indep,2}, ..., u^s_{indep,T_f}, R)] \\
&s.t. \\
&m_2(u_{indep,1}, u^s_{indep,2}, ..., u^s_{indep,T_f}, R) \le 0 && \forall s \\
&\underline{U}_{dep} \le U_{dep}(u_{indep,1}, u^s_{indep,2}, ..., u^s_{indep,T_f}, R) \le \overline{U}_{dep} && \forall s \\
&\underline{u}_{indep,t=1..T_f} \le [u_{indep,1}, u^s_{indep,2}, ..., u^s_{indep,T_f}]^T \le \overline{u}_{indep,t=1..T_f} && \forall s
\end{aligned}
\qquad (4.20)
$$

where $u^s_{indep,2} = u_{indep,2}(r^s_1), ..., u^s_{indep,T_f} = u_{indep,T_f}(R^s)$ is the nonanticipativity requirement which implies that the decision must be based exclusively on the information available at decision time (i.e., it does not depend on future realizations of the stochastic data).

In the scenarios based formulation this means that every pairs of scenarios s, s' which are indistinguishable (share the same history) up to stage t must fulfill $(u^s_{indep,2}, \ldots, u^s_{indep,t}) = (u^{s'}_{indep,2}, \ldots, u^{s'}_{indep,t})$.

The introduction of the scenario tree allows us to formulate the equivalent deterministic problem (4.20), where the nonanticipativity constraints are spelled out explicitly based on the shape of the scenario tree. For example, in Figure 4.2c scenarios 1 and 4 are indistinguishable up to stage 2 thus we must impose a constraint $u^{s=1}_{indep,2} = u^{s=2}_{indep,2} = u^{s=3}_{indep,2} = u^{s=4}_{indep,2}$.

There is another approach which may be used in order to enforce the nonanticipativity constraints, an implicit approach in which the nonanticipativity constraints are fulfilled automatically by introducing a unique decision variables for each node of the tree. The implicit formulation is computationally cheaper than the explicit approach since it does not assign decision variables for each scenario at each stage. For example, in Figure 4.2c instead of the decision variables $u^{s=1}_{indep,2}, u^{s=2}_{indep,2}, u^{s=3}_{indep,2}, u^{s=4}_{indep,2}$ we have $u^{node=2}_{indep,2}$.

The general structure of the scenario tree is as follows: (a) At each time $t = 2 \ldots T_f + 1$ there are $K_t - K_{t-1}$ nodes which are denoted by $k_t = K_{t-1} + 1 \ldots K_t$ where the root of the tree is indexed by 1, i.e. $K_1 = 1$. (b) Each different value of $R^{t-1} = (r_1 \ldots r_{t-1})$ corresponds to one node at stage $t = 2 \ldots T_f + 1$, where r_t is the recharge at year t, and R^t is vector of recharges up to year t.

When the objective and the constraints are separable functions, as in our case, the equivalent deterministic problem with the implicit nonanticipativity approach leads to:

$$\min \sum_{k_2=2}^{K_2} p_{k_2} \cdot f_1(u_{indep,1}, r_1^{k_2}) + \sum_{k_3=K_2+1}^{K_3} p_{k_3} \cdot f_2(u_{indep,1}, u_{indep,2}^{k_3}, r_1^{k_3}, r_2^{k_3}) + \ldots$$
$$\ldots + \sum_{k_{T_f+1}=K_{T_f}+1}^{K_{T_f+1}} p_{k_T} \cdot f_{T_f}(u_{indep}^{k_{T_f+1}}, R^{k_{T_f+1}}) \qquad (4.21)$$

s.t.

$$m_{2,t-1}(u_{indep}^{k_t}, R^{k_t}) \le 0 \qquad \forall k_t = K_{t-1}+1 \ldots K_t \ , \ \forall t = 2 \ldots T_f + 1$$
$$\underline{u}_{dep,t-1} \le u_{dep,t-1}(u_{indep}^{k_t}, R^{k_t}) \le \overline{u}_{dep,t-1} \qquad \forall k_t = K_{t-1}+1 \ldots K_t \ , \ \forall t = 2 \ldots T_f + 1$$
$$\underline{u}_{indep,t-1} \le u_{indep}^{k_t} \le \overline{u}_{indep,t-1} \qquad \forall k_t = K_{t-1}+1 \ldots K_t \ , \ \forall t = 2 \ldots T_f + 1$$

where R^{k_t} is the data path up to node k_t at stage t; $u_{indep}^{k_t}$ is decision path up to node k_t at stage t; p_{k_t} is the data path probability up to node k_t at stage t which is obtained by multiplication of the arcs probabilities of the path.

The main issue in sequential decision making under uncertainty is the manner in which uncertainty is revealed over time; this is captured by the structure of the scenario tree which represents the stochastic process. Several possible structures of scenario trees are shown in Figure 4.2. In the fan scenario tree the uncertainty is fully revealed at the second stage, whereas in the feather-duster shape the uncertainty resides only in the final stage.

These are two cases in which the multistage stochastic programming shrinks to a two stage model. If the tree is a fan the first stage would be $t = 1$ and the second stage would be the aggregation of the remaining stages. In contrast, when the tree is a feather-duster the second stage would be $t = 4$ and the first is the aggregation of all previous stages. In contrast to these extreme cases, the balanced tree is associated with multistage model with one decision stage per stage in the tree. A more general tree shape, which is also associated with a multistage model, is the unbalanced tree in which the number of the branches at each node is not equal (Figure 4.14).

4.9.1. Implementation of MSP

In the MSP approach at any node in the multistage scenario tree the decision maker knows the exact history leading to that node, and decides how to proceed; knowing only that the future recharge is presented by each of the scenarios that emerge from the node into the future. The MSP solves for all stages simultaneously to obtain the optimal decisions (corresponding to each node) which results in minimum expectation cost over all future scenarios. However, the MSP considers only the discrete

approximation of the real-life process as a result the true realization may differ from the nodes values considered in the tree. Only the first stage (Here-and-Now) decision of the MSP can be implemented, since it is not realization dependent. The decisions of the subsequent stages (which are realization dependent) are function of the real-life realizations.

As a result, the only possible way to apply MSP in practice is to use it in the Rolling/Folding Horizon mode: at first we solve the scenario based MSP formulation in (4.21) for the entire horizon T_f and from its solution we implement the first stage optimal decision; in the second run we solve a new problem with the horizon reduced by one time period, starting from the new state of the system, again we implement the first stage of the decisions provided by the solution, etc. Examples for the MSP are presented and compared to the LMSP in the following Sections.

4.10. Limited Multistage Stochastic Programming (LMSP)

The dimension of a multistage stochastic program is often too large to be tractable by direct solution, since the dimension of the problem grows exponentially with the number of scenarios and stages. Consequently, the usual solution approach for these large scale problems is based on decomposition of the original problem into an assembly of small and easier to solve sub-problems. However, the decomposition requires assumptions concerning the convexity of the objective function and the constraints. We propose a different approach: the Limited Multistage Stochastic Program (LMSP). The LMSP is an attempt to solve without decomposition or scenario reduction techniques.

In the LMSP the number of decision variables in each stage remains constant, and thus the total number of decision variables increases linearly with the number of scenarios and stages. We begin by identifying subsets of nodes which are expected to have similar decision variables namely, which amounts to clustering by decisions; at each stage $t = 2 \ldots T_f$ we search for a predetermined number of clusters. The clustering criterion is based on the scenarios optimal decisions $v^s_{t \forall t=1..T_f} = \arg\min_{U^s_{indep}} F(U^s_{indep}, R^s)$ $\forall s = 1 \ldots s_f$ which have been obtained by solving each scenario individually. The node values corresponding to the scenarios' optimal decisions are $\overline{v^{k_t}}$ and calculated by:

$$\overline{v^{k_t}} = \frac{\left(\sum_{s \in k_t} p_s v_t^s\right)}{\left(\sum_{s \in k_t} p_s\right)} \qquad (4.22)$$

for each $t = 2 \ldots T_f$ and $k_t = K_{t-1} + 1 \ldots K_t$; where $s \in k_t$ indicates the set of scenarios which pass through the node k_t. After obtaining the nodes' values $\overline{v^{k_t}}$, we perform a clustering, by a method such as K-means on the nodes based on these values for each stage $t > 1$. Applying the clustering technique imposes more constraints in the equivalent deterministic formulation (4.21) for example $u_{indep,2}^{k_2} = x_{indep,2}^{k_2'}$ if node k_2 and node k_2' are in the same cluster. These constraints can be eliminated by algebraic substitution of variables, which reduces the total number of variables in the problem. For instance, instead of the decision variables $u_{indep,2}^{k_2}, x_{indep,2}^{k_2'}$ we define $u_{indep,2}^{cluster=1}$.

The LMSP approach implies restricting the decision maker in future decisions. The problem which should be solved in the limited version is: Given the scenario tree of the uncertain future; at each stage what are the clusters decisions and what nodes are included in each cluster such that the expectation of the objective is minimized. In the ideal solution we must address these two questions simultaneously. However, a good approximation can be obtained by solving the problem in two phases; the first answers the question: what nodes are included at each cluster? This is done by solving each scenario individually and analyzing the results. The second phase is: what are the clusters' decisions? This is answered by the optimization solver when solving the LMSP formulation.

Imposing more constraints to the MSP will obviously raise the minimum value of the optimization problem. Hence, the minimum value obtained from the LMSP will always be larger or equal to the minimum value obtained by the MSP. However, this is not a significant drawback when we solve in Rolling/Folding Horizon as described in Section 4.9.1. In the Folding mode we solve the problem repeatedly and only implement the first stage decisions. Therefore, we are most concerned about quality of the first stage decision, thus we require that the process of clustering the decision variables must not change the first stage decision significantly, as compared to the original stochastic problem.

Both the MSP and LMSP that are solved in the Folding mode framework are required to provide the first stage decisions for implementation, but they must take into account the future uncertainty and the possibility of recourse actions. The MSP considers the possibility for recourse action for each node in the scenario tree while the latter considers a smaller number of recourse actions (by clusters). These recourse actions will not be implemented in real-life and the only reason for their presence is to take into consideration the effect of the uncertain future on the first decision. Therefore, we believed that reducing the number of the recourse action in the LMSP will not significantly change the first stage decision.

4.10.1. LMSP vs. Scenarios reduction

It is most important to distinguish the clustering decision approach (LMSP) from the scenarios reduction/aggregation techniques in which the stochastic process (scenario tree) is clustered/aggregated to produce more a compact tree and a smaller optimization model. The latter techniques are applied before the model is introduced, independent of the optimization model that will be used. The size of the scenario tree is reduced by aggregating the tree nodes into separate sets to be later represented by a new node [Dupacova et al., 2003; Gulpinar et al, 2004; Latorre et al., 2007; Heitsch and Römisch, 2005; Sutiene et al., 2010]. We claim that different models may require different clustering depending on the relationship between the stochastic process and the optimization model to be solved and it is the optimization's responsibility to discover this relationship and to cluster accordingly. Hence, the clustering should be into the optimization framework, incorporating the specific model to be solved.

Another notable difference is that the LMSP keeps the scenario tree intact without reducing its size. The clustering is made only on the decisions related to the tree. The scenario tree is already an approximation of the real stochastic process, so reducing the size of the tree worsens this approximation.

To demonstrate that different models requires different clustering schemes let us consider a hypothetical problem of managing a WSS comprised of a reservoir, a desalination plant and one demand (Figure 4.11). The objective is to minimize the desalination cost over the operation horizon where the recharge is a stochastic process given in the scenario tree depicted in Figure 4.2c. Each of the nodes $2 \ldots 15$ takes the

value 0 if the node index is an odd number and 10 if the node number is even. Each arc has an equal probability of 0.5.The mathematical model of the problem:

$$
\begin{aligned}
&\min \left(\sum_{t=1}^{T_f} C_t \cdot y_t \right) \\
&s.t. \\
&\mathrm{x}_t + y_t = D_t && \forall t = 1 \ldots T_f \\
&0 \le \left(\sum_{i=1}^{t} r_i - \sum_{i=1}^{t} x_i \right) / SA \le h_{\max} && \forall t = 1 \ldots T_f \\
&\mathrm{x}_t, y_t \ge 0 && \forall t = 1 \ldots T_f
\end{aligned}
\tag{4.23}
$$

where x_t, y_t are extraction from reservoir and desalination plant, respectively; C_t desalination costs that increase with time $C_{t+1} \ge C_t \; \forall t$; D_t is the demand; r_t is the stochastic recharge; $h_{\max}$ is the maximum water level in the reservoir.

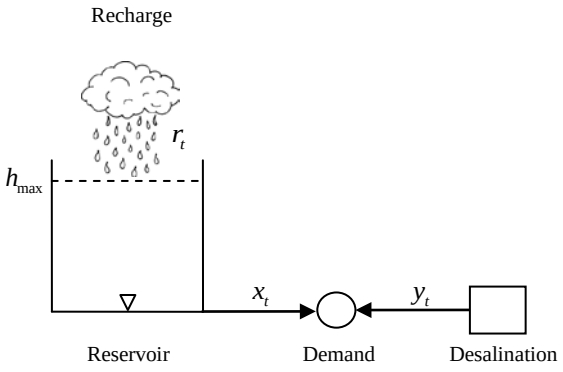

Figure 4.11: Layout of the illustrative example

When we set $h_{\max} = 10$ (the maximum yearly recharge) i.e. the reservoir cannot store water for more than one year, the optimal solution is to take the available water in each year from the reservoirs and supply the rest of the demand from the desalination plant. Hence, scenarios that have the same recharge r_t at stage t would have the same decisions at this stage. On the other hand, when we consider $h_{\max} >> 10$, the optimal solution prefers to take more reservoir water at later stages since we have higher desalination costs $C_{t+1} \ge C_t \; \forall t$, thus the optimal solution stores the recharge in the early stages for later stages. As a result, scenarios that have the same cumulative recharge $\sum_{i=1}^{t} r_i$ at stage t would have the same decisions at this stage.

The conclusion to be drawn from this example is that different management models may require different clustering; the reduction techniques would give the same clusters for both models (with and without storage capacity) because the reduction is made independently before the model is introduced.

4.10.2. K-means clustering

K-means clustering is a method for clustering given observations say $x_i, i = 1..n$ into k clusters in which each observation belongs to the cluster with the nearest mean. In the LMSP we cluster nodes according to their scenario's optimal decisions are $\overline{v^{k_t}}$. The K-means algorithm is designed to minimize an objective function J which define the within cluster sum of squares:

$$J = \sum_{j=1}^{k} \sum_{x_i \in S_j} \left\| x_i - \mu_j \right\|^2 \qquad (4.24)$$

where S_j is the set of observations included in the cluster j and μ_j is the mean of points (centroid) in S_j.

The most common algorithm uses two-phase iterative technique to minimize J:

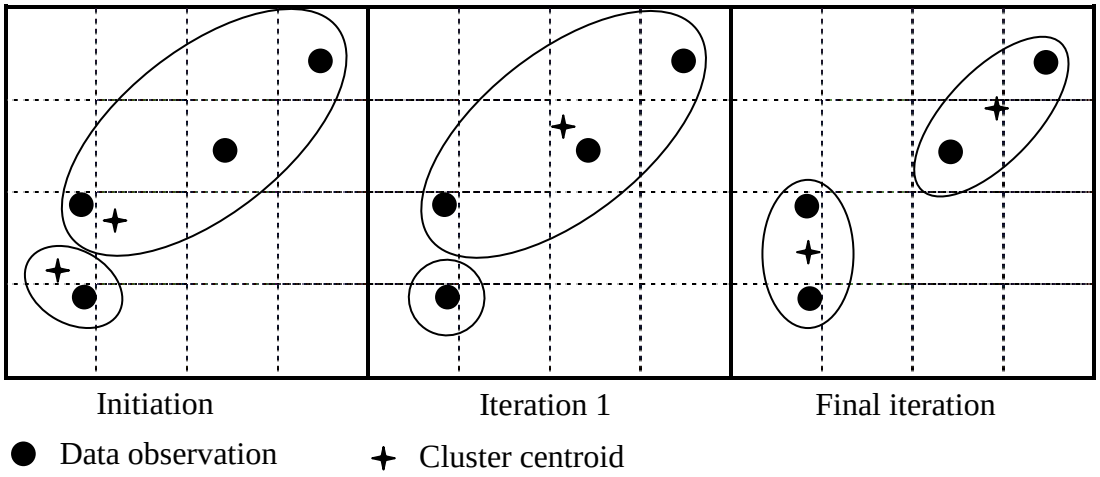

Figure 4.12: K-means clustering process

Starting from k points as initial clusters centroids μ_j, the first phase is to assign each observation to the closet centroid, after all observations are assigned the second phase is to recalculate the centroids of each cluster. The two phases are repeated until the centroids no longer move. A demonstration of the K-means algorithm on four 2D observations is illustrated in Figure 4.12.

4.10.3. Illustrative example

In this example we consider the hypothetical problem of the WSS depicted in Figure 4.11, and formulated in (4.23). Assuming $h_{\max} \to \infty$, $T_f = 3$ years and $C_{t=1..3} = [1,2,3]^T$. Substitution of the equality constraint in the objective leads to the following mathematical model:

$$\begin{aligned} &\min \left(-\sum_{t=1}^{T_f} C_t \cdot x_t \right) \\ &s.t. \\ &\sum_{i=1}^{t} r_i - \sum_{i=1}^{t} x_i \geq 0 \qquad \forall t = 1 \ldots T_f \\ &x_t \geq 0 \qquad\qquad\qquad \forall t = 1 \ldots T_f \end{aligned} \tag{4.25}$$

The MSP implicit formulation for this problem is:

$$\begin{aligned} &\min \left(-x_1 - 0.5 \sum_{k_2=2}^{3} 2x_2^{k_2} - 0.25 \sum_{k_3=4}^{7} 3x_3^{k_3} \right) \\ &s.t. \\ &r_1^2 - x_1 \geq 0 \\ &r_1^3 - x_1 \geq 0 \\ &r_1^2 + r_2^4 - x_1 - x_2^2 \geq 0 \\ &r_1^2 + r_2^5 - x_1 - x_2^2 \geq 0 \\ &r_1^3 + r_2^6 - x_1 - x_2^3 \geq 0 \\ &r_1^3 + r_2^7 - x_1 - x_2^3 \geq 0 \\ &r_1^2 + r_2^4 + r_3^8 - x_1 - x_2^2 - x_3^4 \geq 0 \\ &r_1^2 + r_2^4 + r_3^9 - x_1 - x_2^2 - x_3^4 \geq 0 \\ &r_1^2 + r_2^5 + r_3^{10} - x_1 - x_2^2 - x_3^5 \geq 0 \\ &r_1^2 + r_2^5 + r_3^{11} - x_1 - x_2^2 - x_3^5 \geq 0 \\ &r_1^3 + r_2^6 + r_3^{12} - x_1 - x_2^3 - x_3^6 \geq 0 \\ &r_1^3 + r_2^6 + r_3^{13} - x_1 - x_2^3 - x_3^6 \geq 0 \\ &r_1^3 + r_2^7 + r_3^{14} - x_1 - x_2^3 - x_3^7 \geq 0 \\ &r_1^3 + r_2^7 + r_3^{15} - x_1 - x_2^3 - x_3^7 \geq 0 \end{aligned} \tag{4.26}$$

The solution of this problem is given in Figure 4.13 which has an objective value of 270. Our proposed method (LMSP) requires solving the problem for each scenario individually to obtain the scenarios optimal solution in Table 4.3, the next step is to calculate the nodes' values (Table 4.4) by Equation (4.22).

s	R^s	v_1^s	v_2^s	v_3^s
1	10,10,10	0	0	30
2	10,10,0	0	0	20
3	10,0,10	0	0	20
4	10,0,0	0	0	10
5	0,10,10	0	0	20
6	0,10,0	0	0	10
7	0,0,10	0	0	10
8	0,0,0	0	0	0

Table 4.3: Optimal solution for each scenario (MCM), illustrative example.

Node	**Scenarios**	$\overline{v_2^{k_2}}$	$\overline{v_3^{k_3}}$
2	1,2,3,4	0	
3	5,6,7,8	0	
4	1,2		25
5	3,4		15
6	5,6		15
7	7,8		5

Table 4.4: Aggregated nodes' values (MCM).

If we want to cluster the decisions into two clusters at each stage, we apply the K-means algorithm on nodes 4-7 to represent them in two sets. Applying the K-means algorithm results in the first cluster containing nodes {4, 5, 6} and the second cluster node 7. The decisions for the clusters are denoted as $x_3^{C=1}$ and $x_3^{C=2}$ for the first and the second cluster, respectively. This results in the following model:

$$
\begin{aligned}
&\min\left(-x_1 - 0.5\sum_{k_2=2}^{3} 2x_2^{k_2} - 0.25(9x_3^{C=1} + 3x_3^{C=2})\right) \\
&s.t. \\
&r_1^2 - x_1 \geq 0 \\
&r_1^3 - x_1 \geq 0 \\
&r_1^2 + r_2^4 - x_1 - x_2^2 \geq 0 \\
&r_1^2 + r_2^5 - x_1 - x_2^2 \geq 0 \\
&r_1^3 + r_2^6 - x_1 - x_2^3 \geq 0 \\
&r_1^3 + r_2^7 - x_1 - x_2^3 \geq 0 \\
&r_1^2 + r_2^4 + r_3^8 - x_1 - x_2^2 - x_3^{C=1} \geq 0 \\
&r_1^2 + r_2^4 + r_3^9 - x_1 - x_2^2 - x_3^{C=1} \geq 0 \\
&r_1^2 + r_2^5 + r_3^{10} - x_1 - x_2^2 - x_3^{C=1} \geq 0 \\
&r_1^2 + r_2^5 + r_3^{11} - x_1 - x_2^2 - x_3^{C=1} \geq 0 \\
&r_1^3 + r_2^6 + r_3^{12} - x_1 - x_2^3 - x_3^{C=1} \geq 0 \\
&r_1^3 + r_2^6 + r_3^{13} - x_1 - x_2^3 - x_3^{C=1} \geq 0 \\
&r_1^3 + r_2^7 + r_3^{14} - x_1 - x_2^3 - x_3^{C=2} \geq 0 \\
&r_1^3 + r_2^7 + r_3^{15} - x_1 - x_2^3 - x_3^{C=2} \geq 0
\end{aligned}
\tag{4.27}
$$

The solution of this problem is given in Figure 4.13. The objective value of the MSP (270) is lower than the LMSP (277) as expected according to the explanation in Section 4.10.

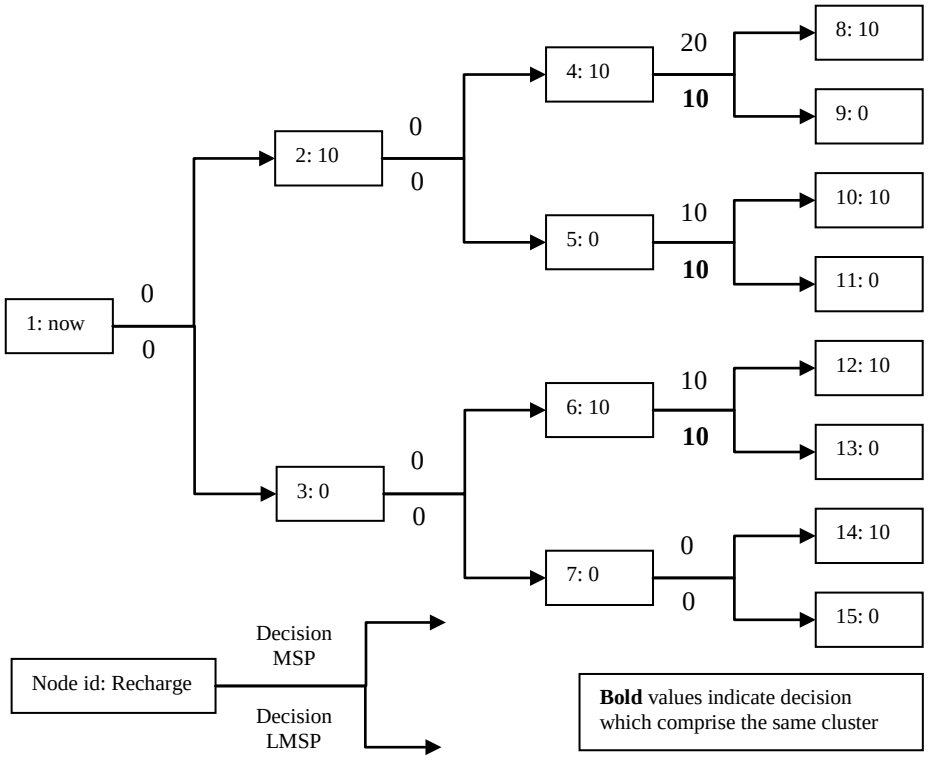

Figure 4.13: Optimal solution (MCM) of the illustrative example.

4.10.4. Example 1

In this example we solve the multi-year problem of three years horizon which is considered with the same parameters set defined in the multi-year run (Section 3.8).

The yearly aquifers recharges $R\ (MCM)$ are considered stochastic, given by the unbalanced scenario tree depicted in Figure 4.14, where each scenario has equal probability.

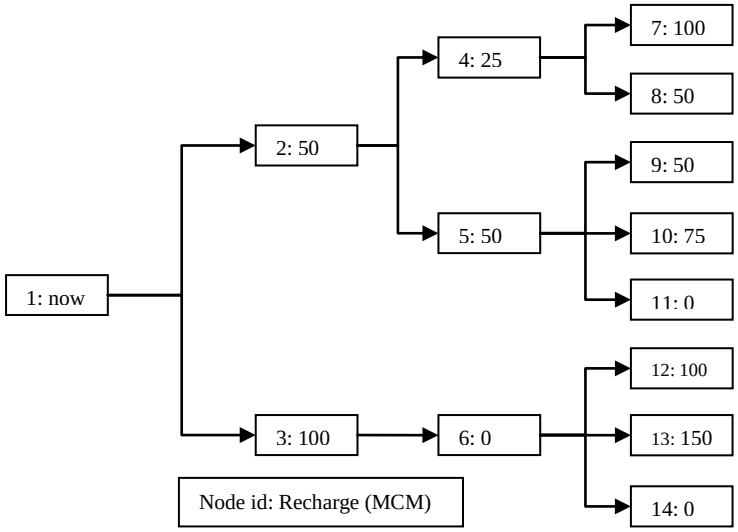

Figure 4.14: Unbalanced scenario tree of the recharge, example 1.

Each decision node 1-6 has its own decision variables; the independent decision variables for each of the node are the pipes flows $Q^1_{3,4,6,8}, Q^2_{3,4,6,8}\ (MCM)$ for season 1 and 2, respectively and the removal ratio $RR^1, RR^2\ (\%)$ for season 1 and 2, respectively.

The solution of the MSP is given in Table 4.5 where the minimum expected value of the total cost is 268.87 M$.

	Decisions in the 1st season					**Decision in the 2nd season**				
Node	Q^1_3	Q^1_4	Q^1_6	Q^1_8	RR^1	Q^2_3	Q^2_4	Q^2_6	Q^2_8	RR^2
1	19.5	19.5	12.5	12.5	99.3	14	14	12.5	12.5	99.3
2	13.7	13.7	12.5	12.5	99.3	13.5	13.5	12.5	12.5	99.3
3	15.7	15.8	12.5	12.5	99.3	15	15	12.5	12.5	99.3
4	10.8	10.9	12.5	12.5	99.3	11	11	12.5	12.5	99.3
5	18.1	18	12.5	12.5	99.3	16.3	16.3	12.5	12.5	99.3
6	15.7	15.8	12.5	12.5	99.3	15	15	12.5	12.5	99.3

Table 4.5: MSP solution, example 1. Flow (MCM), removal ratio (%).

The LMSP solution with two clusters at each stage is given by applying the following three steps:

Step 1: solve for each scenario individually (Table 4.6)

	Decisions in the 1st season						Decision in the 2nd season					
Scenario	**Year**	Q_3^1	Q_4^1	Q_6^1	Q_8^1	RR^1	Q_3^2	Q_4^2	Q_6^2	Q_8^2	RR^2	**Cost**
1	1	12.5	12.5	12.5	12.5	99.3	12.5	12.5	12.5	12.5	99.4	193.4
	2	12.5	12.5	12.5	12.5	99.4	20	20	12.5	12.5	99.3	
	3	0	0	12.5	12.5	99.6	4.7	4.7	12.5	12.5	99.6	
2	1	25	25	12.5	12.5	99.3	10.5	10.5	12.5	12.5	99.3	243.6
	2	10	10.1	12.5	12.5	99.3	12.2	12.2	12.5	12.5	99.3	
	3	12.2	12.2	12.5	12.5	99.3	12.6	12.6	12.5	12.5	99.3	
3	1	24.9	24.9	12.5	12.5	99.3	7.7	7.7	12.5	12.5	99.3	210.4
	2	7.3	7.3	12.5	12.5	99.4	10.3	10.3	12.5	12.5	99.4	
	3	10.1	10.1	12.5	12.5	99.4	9.6	9.6	12.5	12.5	99.4	
4	1	17.5	17.5	12.5	12.5	99.3	9.6	9.6	12.5	12.5	99.4	177.7
	2	9.5	9.5	12.5	12.5	99.4	8.4	8.4	12.5	12.5	99.4	
	3	5.9	5.8	12.5	12.5	99.4	6.7	6.7	12.5	12.5	99.4	
5	1	25	25	12.5	12.5	99.3	12.8	12.8	12.5	12.5	99.3	277.0
	2	12.9	12.9	12.5	12.5	99.3	14.6	14.5	12.5	12.5	99.3	
	3	15.3	15.2	12.5	12.5	99.3	14.5	14.6	12.5	12.5	99.3	
6	1	25	25	12.5	12.5	99.3	6.7	6.7	12.5	12.5	99.4	162.1
	2	6.6	6.5	12.5	12.5	99.4	6.7	6.7	12.5	12.5	99.4	
	3	2.1	2	12.5	12.5	99.6	2.9	2.9	12.5	12.5	99.6	
7	1	25	25	12.5	12.5	99.3	6.7	6.7	12.5	12.5	99.4	161.2
	2	6.5	6.6	12.5	12.5	99.4	6.7	6.7	12.5	12.5	99.4	
	3	2.1	1.9	12.5	12.5	99.6	2.7	2.7	12.5	12.5	99.6	
8	1	25	25	12.5	12.5	99.3	13.8	13.8	12.5	12.5	99.3	277.0
	2	14.3	14.3	12.5	12.5	99.3	13.8	13.8	12.5	12.5	99.3	
	3	14.3	14.3	12.5	12.5	99.3	13.8	13.8	12.5	12.5	99.3	

Table 4.6: LMSP, step 1 results of example 1. Flow (MCM), removal ratio (%).

Step 2: Calculate the nodes' values by equation (4.22) (Table 4.7)

		Decisions in the 1st season					Decision in the 2nd season				
Node	**Scenario**	Q_3^1	Q_4^1	Q_6^1	Q_8^1	RR^1	Q_3^2	Q_4^2	Q_6^2	Q_8^2	RR^2
2	1,2,3,4,5	10.4	10.4	12.5	12.5	99.36	13.1	13.0	12.5	12.5	99.3
3	6,7,8	9.1	9.1	12.5	12.5	99.37	9.0	9.0	12.5	12.5	99.3
4	1,2	6.1	6.1	12.5	12.5	99.45	8.6	8.6	12.5	12.5	99.4
5	3,4,5	10.4	10.3	12.5	12.5	99.37	10.2	10.3	12.5	12.5	99.3
6	6,7,8	6.1	6.0	12.5	12.5	99.50	6.4	6.4	12.5	12.5	99.5

Table 4.7: LMSP, step 2 results of example 1. Flow (MCM), removal ratio (%).

Step 3: Clustering the decisions (cluster size =2)

At stage 2 there are only two nodes, therefore there is no need for clustering. At stage 3 there are three nodes {4, 5 and 6} thus the decisions at this stage is clustered.

The K-means clustering method results in nodes {4, 6} in cluster 1 and node {5} in cluster 2. The results are given in Table 4.8.

	Decisions at the 1st season					**Decision at the 2nd season**				
Node	Q_3^1	Q_4^1	Q_6^1	Q_8^1	RR^1	Q_3^2	Q_4^2	Q_6^2	Q_8^2	RR^2
1	19.5	19.5	12.5	12.5	99.3	13.7	13.7	12.5	12.5	99.3
2	12.3	12.3	12.5	12.5	99.3	12.3	12.3	12.5	12.5	99.3
3	19.9	19.9	12.5	12.5	99.3	17.2	17.2	12.5	12.5	99.3
Cluster 1 {4, 6}	12.3	12.3	12.5	12.5	99.3	12.3	12.3	12.5	12.5	99.3
Cluster 2 {5}	19.9	19.9	12.5	12.5	99.3	17.2	17.2	12.5	12.5	99.3

Table 4.8: LMSP, step 3 results of example 1. Flow (MCM), removal ratio (%).

The minimum cost expectation obtained from the LMSP is 268.88 M$, somewhat higher than the obtained by the MSP (268.87 M$), since the LMSP impose more constraints than the MSP. Still, as explained previously, the first stage decision obtained from both approaches is very close as can be seen in Table 4.9.

	Decisions at the 1st season					**Decision at the 2nd season**				
	Q_3^1	Q_4^1	Q_6^1	Q_8^1	RR^1	Q_3^2	Q_4^2	Q_6^2	Q_8^2	RR^2
MSP	19.5	19.5	12.5	12.5	99.3	14	14	12.5	12.5	99.3
LMSP	19.5	19.5	12.5	12.5	99.3	13.7	13.7	12.5	12.5	99.3

Table 4.9: Comparison between the MSP and the LMSP optimal decision, example 1. Flow (MCM), removal ratio (%).

4.10.5. Example 2

In this example we solve the multi-year problem of five years horizon which is considered with the same parameters set defined in the multi-year run (Section 3.8) and maximum specific levy $\left(\overline{CE}^{\max}\right)=1 \ \ (M\$/MCM)$.

The yearly aquifers recharges $R\ (MCM)$ are stochastic, given by the balanced scenario tree with two branches at each stage. The conditional discrete probability in each year is given by the Probability Mass Function (PMF) in Table 4.10, where r_t is the recharge in year t, and R^t is vector of recharges up to year t.

	Low Recharge	High Recharge

r_t (MCM)	0	100
$\text{Prob}(r_t \mid R^t)$	0.5	0.5

Table 4.10: PMF of the recharge, example 2

In the classical MSP the number of decision nodes is 31, and the number of decision variables is $31 \cdot 10 = 310$ where 10 is the length of a single year decision vector. The minimum expected value of the MSP solution is 565 M$. Applying the LMSP with two clusters at each stage reduces the problem size to 9 decisions ($1 + 2 \cdot 4 = 9$), hence, the optimization problem has 90 decision variables. The minimum expected value of the LMSP is 570 M$ (as expected, somewhat higher than the MSP solution).

The clustering scheme to the 31 decision nodes is given in (Table 4.11) which is obtained after applying step 1 and 2 as in the previous example.

Year	**Cluster 1**	**Cluster 2**
1	NA	NA
2	2	3
3	{4,5,6}	7
4	{8,9,10,12,14}	{11,13,15}
5	{16,17,18,19,20,21,22,24,25,26,28,30}	{23,27,29,31}

Table 4.11: Clustering scheme, example 2.

The clustering results in this simple case could be verified easily. For example, examining the decision clusters at year 4, nodes 8-15 and year 5, nodes 16-31. The results of year 4 show that the nodes which have history with 100 (MCM) recharge at least twice are in the same cluster, except node 14 which has 100 (MCM) only one time. This node has been added to the first cluster in the first run, since the 100 (MCM) recharge is realized in the near past of node 14. In year 5 the same rule is valid, where node 30 has 100 (MCM) only one time. This node has been added to the first cluster, since the 100 (MCM) recharge is realized in the near past.

To compare the LMSP and the MSP we present the yearly desalination amount for each decision node. Note that each decision node has its own decision vector with 10 decision variables; however, the yearly desalination amount was chosen to present the decision characteristics as explained in Section 3.8 because of the special parameters set chosen in the example (e.g. symmetric network) the optimal solution could be easily derived after deciding on the optimal desalination amount. Table 4.12 compares the optimal desalination amount obtained from the MSP and the LMSP solution.

		MSP	LMSP	
Year	**Node**	**Des (MCM)**	**Cluster**	**Des (MCM)**
1	1	98.3	NA	98.4
2	2	34.3	1	25.3
	3	98	2	99.1
3	4	20.9	1	25.2
	5	72.2	1	25.2
	6	30.6	1	25.2
	7	97.7	2	98.7
4	8	16.9	1	43.3
	9	46.2	1	43.3
	10	23.1	1	43.3
	11	89.5	2	96
	12	20.1	1	43.3
	13	70.2	2	96
	14	23.8	1	43.3
	15	97.9	2	96
5	16	14.9	1	24.2
	17	22.1	1	24.2
	18	17.1	1	24.2
	19	90.5	1	24.2
	20	16	1	24.2
	21	62.6	1	24.2
	22	17.5	1	24.2
	23	96.2	2	98
	24	15.4	1	24.2
	25	43.4	1	24.2
	26	16.8	1	24.2
	27	93.1	2	98
	28	15.9	1	24.2
	29	72.5	2	98
	30	16.2	1	24.2
	31	98.3	2	98

Table 4.12: Comparison between the MSP and the LMSP decision, example 2.

As shown in Table 4.12, the MSP and LMSP provided very close first year decision for implementation which considers the future uncertainty and the possibility to

recourse actions in the future. MSP considers the possibility for recourse action for each node in the scenario tree while the LMSP considers a smaller number of recourse actions (clusters). These recourse actions project the uncertain future effect on the first decision. In real-life application the MSP recourse action will not be implemented since it is solved in Rolling/Folding Horizon as described in Section 4.9.1. In the Folding mode we solve the problem repeatedly and implement only the first stage decisions from each run. This brings us to an important conclusion: The LMSP is considered a good approximation of the MSP when the first stage decisions are close to one another. This is due to the fact that decision makers solve the model repeatedly and implement only the first stage decisions. As shown in Table 4.12, the first row demonstrates the yearly desalination amount suggested by both models as the first decision (first year).

4.10.6. Example 3 (Large scale example)

The large scale network presented in Section 3.9 is solved in this example. The multi-year problem of five years horizon is considered with the same parameters set defined in the multi-year run (Section 3.9). The yearly aquifers recharges $R_{a=1..3}(MCM)$ are considered stochastic, given by a balanced scenario tree with two branches at each stage. The conditional probability in each year is given in Table 4.13, where $r_{a,t}$ is the recharge in aquifer a at year t, and R_a^t is vector of recharges up to year t.

	Low Recharge	High Recharge
$r_{1,t}, r_{2,t}, r_{3,t}$ (MCM)	80, 80 ,80	200, 200 ,200
Prob$(r_{a=1..3,t} \mid R^t_{a=1..3})$	0.5	0.5

Table 4.13: PMF of the recharge, example 3.

The scenario tree in this case has 32 scenarios (paths in the tree), where each of the nodes $2\ldots63$ takes the values of the low recharge if the node index is an odd number, and the high recharge if the node number is even.

The hypothetical example in (Section 4.10.1) shows that the clustering scheme depends in the model formulation, thus we had there a different clustering scheme with and without storage capacity. The conclusion drawn from the hypothetical example is that different models may require different clustering. Example 3

demonstrates how the clustering process is affected by different parameters of the model; particularly $\left(\overline{CE}^{\max}\right)_a$ which is related to the aquifer water cost.

The large scale network is solved twice, with $\left(\overline{CE}^{\max}\right)_a = 0$, $\left(\overline{CE}^{\max}\right)_a = 0.5\ (M\$/MCM)$, respectively. In the MSP the number of the decision nodes is 31, thus the number of decision variables is $31 \cdot 62 = 1922$ where 62 is the length for each year's decision vector. The minimum expected value of the MSP solution is 173.8 and 230 M$ for the two problems Runs, respectively. Applying the LMSP with two clusters at each stage reduces the problem size to 9 decisions ($1 + 2 \cdot 4 = 9$), hence, the optimization problem has 558 decision variables. The minimum expected value of the LMSP is 175.8 and 232.9 M$, respectively, not much higher than the MSP solutions.

The clustering schemes for the 31 decision nodes in the model in Run 1 with $\left(\overline{CE}^{\max}\right)_a = 0$,and Run 2 with $\left(\overline{CE}^{\max}\right)_a = 0.5\ (M\$/MCM)$, are given in Table 4.14 which show the history of the node in each year and the corresponding clustering suggested by the LMSP. Each node belongs to cluster 1 is essentially a “rich recharge cluster” while cluster 2 is a “low recharge cluster”.

The clustering results in year 3 show that nodes which have history with 200 (MCM) at least once are considered in cluster 1 (high recharge history) when $\left(\overline{CE}^{\max}\right)_a = 0$. In contrast, the second Run with $\left(\overline{CE}^{\max}\right)_a = 0.5$ clusters the nodes that have history with 0 (MCM) recharge at least once are considered in cluster 2 (low recharge history). Hence, nodes 5 and 6 are clustered differently, caused by different run parameters.

The results for year 4 show that in both Runs, nodes which have history with 200 (MCM) at least twice are in cluster 1 except node 14 which have 200 (MCM) only once. This node has been added to the first cluster in the first Run, since the 200 (MCM) recharge is realized in the near past of node 14. In year 5 nodes which have a history with 200 (MCM) at least three times are in cluster 1 in both Runs. Node 28 which has two high recharges in the near past is also in cluster 1 in both Runs. This indicates that not only the cumulative amount matters, but also the lag from the decision node are important.

Nodes that have less than three times of 200 (MCM) histories, but have 200 (MCM) at the later year are considered in cluster 1 in the first Run. In contrast, 200 (MCM) at the later year was not enough to make these nodes first cluster members when $\left(\overline{CE}^{\max}\right)_a = 0.5$.

						Clustering Scheme	
Year	**Node**	**Node History (MCM)**				**Run 1**	**Run 2**
3	4	200	200			1	1
	5	200	80			1	2
	6	80	200			1	2
	7	80	80			2	2
4	8	200	200	200		1	1
	9	200	200	80		1	1
	10	200	80	200		1	1
	11	200	80	80		2	2
	12	80	200	200		1	1
	13	80	200	80		2	2
	14	80	80	200		1	2
	15	80	80	80		2	2
5	16	200	200	200	200	1	1
	17	200	200	200	80	1	1
	18	200	200	80	200	1	1
	19	200	200	80	80	2	2
	20	200	80	200	200	1	1
	21	200	80	200	80	2	2
	22	200	80	80	200	1	2
	23	200	80	80	80	2	2
	24	80	200	200	200	1	1
	25	80	200	200	80	2	2
	26	80	200	80	200	1	2
	27	80	200	80	80	2	2
	28	80	80	200	200	1	1
	29	80	80	200	80	2	2
	30	80	80	80	200	1	2
	31	80	80	80	80	2	2

Table 4.14: Clustering scheme, example 3.

As explained in Section 4.10, example 1 and example 2, the success of the LMSP approximation is determined by the difference in the first stage decisions of the LMSP and the MSP solution. Table 4.15 compares the total yearly desalination amount at the first year, which is obtained from the MSP and the LMSP solution for both Runs.

		Desalination (MCM)				
Run	**Approach**	**Plant 1**	**Plant 2**	**Plant 3**	**Plant 4**	**Plant 5**
1	MSP	25.0	46.6	12.1	288.6	130.5
	LMSP	25.1	47.5	35.7	290.7	133.8
2	MSP	25.0	51.2	35.9	290.7	133.9
	LMSP	29.9	55.1	36.4	293.3	134.0

Table 4.15: Comparison between the MSP and the LMSP with different extraction levy, example 3.

As shown in Table 4.15, the MSP and LMSP provided very close first year decisions for implementation, hence, solving the smaller optimization problem (558 decision variables instead of 1922) has an advantage, especially when we are solving in rolling horizon mode as explained in Section 4.9.1.

4.11. Generalized LMSP (GLMSP)

The LMSP technique described in the previous Section requires specifying the same number of clusters for each stage (constant clustering scheme), to insure linear increase in the decision variables with the number of scenarios and stages. By this clustering scheme the model resulting from the LMSP approach is somehow between the single stage Here-and-Now approach described in Section 4.7 and the classic MSP approach described in Section 4.9, see Figure 4.15 for demonstration.

The GLMSP is an approach which facilitates choosing the required position between the two approaches above. In contrast to the LMSP, in the GLMSP the user is asked to provide the clustering scheme which in turn specifies the required model along the scale in Figure 4.15. For instance, to choose the Here-and-Now approach i.e. the left point on the scale, the clustering scheme should be constant with one cluster in each stage, and to choose the MSP, i.e. the right point, the number of clusters in each stage should be equal to the number of nodes at that stage, thus each cluster contains only one node. The LMSP is a special case of the GLMSP in which the clustering scheme is constant with number of clusters at each stage larger than one.

The size of the optimization problem increases as we move along the scale in Figure 4.15, the smallest model size is the single stage model (left point) and the largest one is the MSP (right point). The decision maker is asked to select a clustering scheme, by which he specifies the size of the resulting optimization problem and the how the uncertain future is incorporated.

Consider the scenario tree in Figure 4.2c, one possible clustering scheme would be [1, 2, 4, 2] in which decision are made on the tree nodes up to stage 3 (up to stage 3 the formulation is the same as in MSP) and only in stage 4 we require clustering the 8 nodes into 2 clusters. Such a clustering scheme incorporates the detailed future up to specified stage in the horizon (say detailed representation of near future) while after this specified point an aggregation is made on the decisions (less detailed representation of far future).

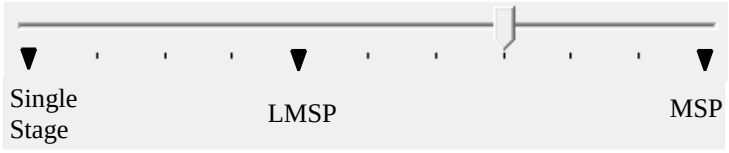

Figure 4.15: schematic description of the GLMSP scope

Note:

Refer to Section 7.2.2 for Summary and Conclusion.

5. Robust Optimization

5.1. Introduction

In this Chapter the Robust Optimization (RO) methodology [Ben-Tal et al., 2009] is applied to optimize the management of a Water Supply System (WSS) fed from aquifers and desalination plants. The water is conveyed through a network to meet specified consumptions, where the aquifers recharges are uncertain. The objective is to minimize the total cost of multiyear operation, satisfying operational and physical constraints. To apply the RO methodology we formulate a new linear model for the WSS management which only considers water quantity in the system without salinity considerations. To achieve this, some of the non-linear relations considered in the non-linear formulation in Chapter 3 were linearized.

Optimal planning and management of WSS has been studied extensively and resulted in a large number of optimization models and techniques. The parameters of early models were usually assumed perfectly known, leading to deterministic models. The results obtained by such models may perform poorly when implemented in the real world, when the problem parameters are revealed and are different from those assumed in the deterministic model.

A variety of stochastic methodologies have also been applied to WSS management, including stochastic dynamic programming [Yeh, 1985; Faber and Stedinger, 2001], implicit stochastic optimization [Lund and Ferreira, 1996; Labadie, 2004], scenarios based optimization [Pallottino et al., 2005; Kracman et al., 2006] and chance constraint methodology [Lansey at el., 1989; Sankarasubramanian et al., 2009]. In these stochastic programming methodologies the uncertain data are assumed to have a known PDF, which in reality is uncertain itself.

This Chapter employs the Robust Counterpart approach (RC) [Ben-Tal et al., 1998, 1999, 2000a, 2009], a novel methodology for optimization under uncertainty, in which the uncertainty is not described by a PDF, but is rather deterministic and known to reside within a user-defined uncertainty set. Hence, instead of immunizing the solution in a probabilistic sense, the decision maker searches for a solution that is optimal for all the possible realizations of the uncertainty set. The RC approach has been applied to variety of optimization models such as portfolio models [Ben-Tal et al, 2000b; Lobo and Boyd, 2000], inventory theory [Bertsimas and Thiele, 2006;

Bienstock and Ozbay 2008], process scheduling [Li and Ierapetritou, 2008] and network models [Mudchanatongsuk et al., 2005].

Section 5.2 presents the basics of Robust Optimization (RO). Section 5.3 contains formulation of the linear WSS management model, its objective function and constraints. Section 5.4 describes the application of the RC to the WSS model, namely structuring the model for the optimization solver. Sections 5.5-5.8 present applications of the RC on two WSS models.

5.2. Robust Counterpart (RC) approach

The RC approach is a min-max oriented methodology [Ben-Tal et al., 1998] that seeks robust feasible/optimal Here-and-Now decisions which are determined at the beginning of the time horizon, before the uncertain data are revealed. This version of the RC approach is termed "static problem".

Robust feasible decisions treat the uncertain constraints as hard constraints, i.e. constraints which have to be satisfied for all possible realizations within the given uncertainty set, while robust optimal means optimizing the guaranteed value (for a minimization problem it is the largest value) of the objective function over the uncertainty set.

The RC approach is flexible enough to allow consideration of soft constraints in which feasibility is not essential, such as demand constraints when water users can accept minor water shortages with an associated cost (penalty). This modeling of soft constraints can also be applied in the RC formulation. Mulvey et al. [1995] used the slack variables of soft constraints to penalize the objective function when soft constraints are violated. Introducing slack variables in soft constraints converts them to hard constraints which must remain feasible for all realization of the uncertainty set. The RC can also allow different ways to handle the objective function; for example, one can use the nominal values of the uncertain data in the objective while the constraints have to satisfy all the realization in the uncertainty set.

The RC solves a static problem in which the decisions for all future stages are determined Here-and-Now. As a consequence, decisions for the first stage, which are to be implemented immediately, are influenced by future information - as known or forecasted at present, including: planned or already committed modifications of the

supply system, future cost figures, forecasted demands, and hydrological forecasts. In practice, the model will be run again at the end of the first stage, with whatever information has been added or updated and starting with the actual state of the system at that time. This process is captured by the "Folding RC" approach (FRC) [Ben-Tal et al., 2000b] that will be addressed in Section 5.6.2.

5.2.1. Robust counterpart of an uncertain linear program

Consider the following problem subject to data uncertainty:

$$\min_y \left\{ c_0{}^T y : A_0 y \le b_0 \right\} \tag{5.1}$$

We assume without any loss of generality that the data uncertainty only affects the elements in the coefficient matrix. If there is uncertainty in the objective or in the Right Hand Side (RHS), we can rewrite the Linear Programming (LP) problem as:

$$\min_x \left\{ c^T x : Ax \le 0 \right\} \tag{5.2}$$

Where $x = [z, y, 1]^T$ (the last element is 1 to represent the RHS); $A = \begin{pmatrix} -1 & c_0^T & 0 \\ 0 & A_0 & -b_0 \end{pmatrix}$ and $c = [1, 0, ..., 0]^T$.

The Robust Counterpart (RC) of problem (5.2) is

$$\min_x \left\{ c^T x : Ax \le 0, \forall A \in U \right\} \tag{5.3}$$

where U is a user-defined uncertainty set. According to Ben-Tal et al. [2009, page 11] an LP with a certain objective is a constraint wise problem, which means that the RC solution does not change if the uncertainty set is extended to the product of its projections on the subspaces of the constraints, i.e. instead of solving (5.3) one can solve:

$$\min_x \left\{ c^T x : a_i^T x \le 0, \forall i, \ \forall a_i \in U_i \right\} \tag{5.4}$$

Where a_i^T is row i in matrix A and U_i is the projection of U on the space of the data of a_i.

Worst case oriented methodologies can lead to overly conservative solutions, as is Soyster's [1973] approach, which considers interval and column-wise uncertainties in

the LP, where every uncertain parameter takes its worst case value in the uncertainty set. To address over-conservativeness the RO methodology introduces a way to reduce the uncertainty set to reflect the fact that the coefficients of the constraints are not expected to be simultaneously at their worst values. There are various ways to eliminate from the uncertainty set parts which are considered to be "rare", for example cutting off "corners" where multiple uncertain variables all take extreme values. We adopt here the ellipsoidal method, in which the uncertainty set is defined by an affine mapping of a ball of radius θ:

$$U_i = \left\{ a_i : \hat{a}_i + \Delta\varsigma, \|\varsigma\| \le \theta \right\} \tag{5.5}$$

where $\hat{a}_i$ a selected nominal value, usually the expected value, Δ is the mapping matrix, and the parameter θ is a subjective value chosen by the decision maker to reflect his attitude towards risk. Ben-Tal et al. [1999] show that the RC of the LP then becomes

$$\begin{aligned} & \mathrm{a}_i^T x \le 0 \quad \forall a_i \in \left\{ \hat{a}_i + \Delta\varsigma, \|\varsigma\| \le \theta \right\} \\ & \Leftrightarrow \\ & \max_{\|\varsigma\| \le \theta} \left[\hat{\mathrm{a}}_i^T x + \left(\Delta\varsigma\right)^T x \right] \le 0 \\ & \Leftrightarrow \\ & \hat{\mathrm{a}}_i^T x + \theta \left\| x^T \Delta \right\| \le 0 \end{aligned} \tag{5.6}$$

which is a convex tractable optimization problem that can be solved by polynomial time interior point algorithms. When only part of the parameters are uncertain, e.g. a_{i1} is a vector of certain parameters and a_{i2} a vector of uncertain parameters in row i of the matrix A, the RC is

$$\begin{aligned} & a_{i1}^T x_1 + a_{i2}^T x_2 \le 0 \quad \forall a_{i2} \in \left\{ \hat{a}_{i2} + \Delta_2 \varsigma_2, \|\varsigma_2\| \le \theta \right\} \\ & \Leftrightarrow \\ & a_{i1}^T x_1 + \hat{a}_{i2}^T x_2 + \theta \left\| x_2^T \Delta_2 \right\| \le 0 \end{aligned} \tag{5.7}$$

where x_1, x_2 are the elements of x corresponding to a_{i1}, a_{i2} respectively. A special case is when the only uncertainty is on the right hand side, in vector b_0. In this case $x = [z, y, 1]^T$ in (2) is separated into $x_1 = [z, y]^T$ and $x_2 = 1$, hence we obtain a linear RC of the form

$$a_{i1}^T x_1 + \hat{a}_{i2}^T + \theta \left\| \Delta_2 \right\| \le 0 \tag{5.8}$$

5.2.2. Why ellipsoidal uncertainty?

Several considerations lead to the selection of an ellipsoidal uncertainty set: (a) it leads to an explicit convex tractable RC which can be solved by polynomial time methods such as interior-point, (b) an ellipsoidal uncertainty set is defined by the subjective safety (reliability) parameter θ ; this enables solving the RC with a set of values of θ, and obtaining the tradeoff between robustness and performance (value of the objective function), and (c) using an ellipsoidal uncertainty set can be stochastically justified, even though no underlying PDF is assumed to be known for the uncertain parameters.

Some information on the uncertain data is usually available and can be used in defining the ellipsoid. Simple probabilistic arguments such as 1st and 2nd moments (expectation and variance) of the stochastic variables can be used to replace stochastic uncertainty by the ellipsoidal deterministic uncertainty. To demonstrate this let us consider the linear constraint:

$$\mathrm{a}_1^T x_1 + \mathrm{a}_2^T x_2 \le 0 \tag{5.9}$$

where a_2 is a random vector with expectation vector μ_{a_2} and covariance matrix Σ_{a_2}. Thus, the left hand side of the constraint is a stochastic random variable with expectation μ_l and variance Σ_l defined as:

$$\mu_l = \mathrm{E}\left[\mathrm{a}_1^T x_1 + \mathrm{a}_2^T x_2\right] = \mathrm{a}_1^T x_1 + \mu_{a_2}^T x_2 \tag{5.10}$$

$$\Sigma_l = Var\left[\mathrm{a}_1^T x_1 + \mathrm{a}_2^T x_2\right] = x_2^T \Sigma_{a_2} x_2 = x_2^T \Delta\Delta^T x_2 = \left\| x_2^T \Delta \right\|^2 \tag{5.11}$$

where $\Sigma_{a_2} = \Delta\Delta^T$. The matrix Δ can be obtained by Cholesky decomposition. If we define the "safe" version of the constraint as the realization of the stochastic left side when perturbed by θ standard deviations, we obtain:

$$\begin{aligned} &\mu_l + \theta \left\| x_2^T \Delta \right\| \le 0 \\ &\mathrm{a}_1^T x_1 + \mu_{a_2}^T x_2 + \theta \left\| x_2^T \Delta \right\| \le 0 \end{aligned} \tag{5.12}$$

which is the same as the robust counterpart with ellipsoidal uncertainty set:

$$U_{a_2} = \left\{ a_2 = \mu_{a_2} + \Delta\varsigma, \left\|\varsigma\right\| \le \theta \right\} \tag{5.13}$$

Hence, if we solve the linear robust counterpart in which the coefficients belong to the ellipsoidal uncertainty set defined above it is the same as saying that we are immunized against θ standard deviations of the constraints.

Note that the stochastic vector a_2 with expectation μ_{a_2} and covariance matrix Σ_{a_2} can be described as a linear transformation of the random vector ξ with expectation $\mu_\xi = 0$ and covariance matrix $\Sigma_\xi = I$:

$$a_2 = \mu_{a_2} + \Delta \cdot \xi \tag{5.14}$$

Since $\mu_{a_2} = \mu_{a_2} + \Delta \cdot \mu_\xi = \mu_{a_2}$ and $\Sigma_{a_2} = \Delta \Sigma_\xi \Delta^T = \Delta\Delta^T$

Thus, the construction of the ellipsoidal uncertainty set replaces the stochastic variables ξ by the perturbation vector ς varying in the perturbation set $\text{Ball}_\theta = \{\|\varsigma\| \le \theta\}$

5.2.3. Probability guarantees of RC

In the RC methodology no underlying stochastic information of the data is assumed to be known, although such knowledge may be used to obtain more justified and representative uncertainty sets or to provide probabilistic guarantees for the robust solution, which can be computed a priori, depending on the structure and size of the uncertainty set.

Ben-Tal et al. [2009] considered several cases where partial knowledge of the uncertain stochastic parameters can help to decide a-priori on the degree of immunization. Consider the uncertain (stochastic) constraint parameterized by random variables ξ:

$$\mathrm{a}_1^T x_1 + \mathrm{a}_2^T x_2 \le 0 \quad \forall a_2 = \mu_{a_2} + \Delta \cdot \xi \tag{5.15}$$

Where all we know about ξ is that (a) the elements of ξ are independent, (b) the expectation vector is $\mu_\xi = 0$, and (c) the elements of ξ are bounded $|\xi_l| \le 1 \ \forall l$. Given this information we can say that replacing the stochastic vector ξ by a perturbation vector ς varying in the perturbation set $\text{Ball}_\theta = \{\|\varsigma\| \le \theta\}$ insures reliability of $1 - \exp(-\theta^2 / 2)$:

$$\text{Prob}\left\{\underbrace{a_1^T x_1 + a_2^T x_2}_{orginal} \le \underbrace{a_1^T x_1 + \mu_{a_2}^T x_2 + \theta\left\|x_2^T \Delta\right\|}_{RC} \le 0\right\} \ge 1 - e^{\frac{-\theta^2}{2}} \qquad (5.16)$$

This allows the decision maker to choose the safety parameter θ, i.e. the radius of the ellipsoidal uncertainty set, based on a level of probabilistic protection. The relation between unreliability and the ellipsoidal uncertainty set is $\theta = \sqrt{2\ln(1/\varepsilon)}$ where ε is the unreliability level. E.g. when the prescribed unreliability is set to $\varepsilon = 0.05$, the corresponding radius is $\theta = 2.45$.

Hence, the ambiguous (unknown distribution) chance constraint:

$$\text{Prob}\left\{a_1^T x_1 + a_2^T x_2 \le 0\right\} \ge 1 - e^{\frac{-\theta^2}{2}}$$

can be replaced by the approximation:

$$a_1^T x_1 + \mu_{a_2}^T x_2 + \theta\left\|x_2^T \Delta\right\| \le 0$$

One might be misled to believe that this guarantees that 0.95 of the distribution support (all possible realizations of ξ) is covered by the uncertainty set defined as a ball of radius 2.45. To demonstrate that this is a wrong intuition we consider the (rather extreme) case where the elements of ξ are two dimensional Bernoulli independent random variables $\{-1,1\}$ with probability 0.5 each, which satisfies the conditions (a)-(c) listed above. Replacing ξ by a perturbation vector ς varying in the perturbation set $\text{Ball}_1 = \left\{\left\|\varsigma\right\| \le 1\right\}$ insures reliability of $1 - \exp(-1/2) = 0.393$ while the uncertainty set does not contain a single realization of ξ, since a circle with radius 1 does not contain any corner of the box defined by [-1 1].

5.3. Management model of a Water Supply System (WSS)

We consider management of a WSS where water is taken from sources, conveyed through a conveyance and distribution network to consumers. Mathematical optimization models have proven their usefulness in dealing with such problems [Loucks et al., 1981]. Various types of models can be applied to WSS, depending on the time horizon and time steps, ranging from long-term development of large systems, to detailed operation of smaller parts. Thus models range from highly aggregate versions of an entire water system to much more detailed models in space

and time [Shamir, 1971]. The short-term (weekly to annual) or long-term (years, decades) operation of a large scale water supply system can be captured in a model of medium aggregation that is used to manage simultaneously both the sources and the network [Fisher et al., 2002; Draper et al., 2003, 2004; Jenkins et al., 2004; Watkins et al., 2004; Zaide, 2006].

In this work we consider an optimization model with a medium aggregation level; water is taken from sources, which include aquifers, reservoirs and desalination plants, conveyed through a distribution system to consumers who require certain quantities of water, see Figure 5.1 (small system, for which we provide detailed analysis) and Figure 3.11 (large system, only major results). The time horizon covers several years, with an annual time step. The operation is subject to constraints such as water levels in the aquifers, capacities of the pumping stations, carrying capacities of the distribution system and production capacity of the desalination plants. The objective is to operate the system with minimum total cost of desalination and pumping, plus a depletion penalty for ending below a prescribed final level in the aquifers, which becomes a reward if the final state is higher than this level.

The network representation in the model can be classified according to the physical laws that are considered explicitly in the model constraints [Ostfeld and Shamir, 1993; Cohen et al., 2000]. According to this classification the proposed model is flow model which only considers the balance of the flows without explicit inclusion of the hydraulics. The inherent assumption of this flow model is that the detailed hydraulic operation of the system to deliver the quantities prescribed by the model is feasible. A further consideration included in the proposed model is sustainability of the management plan. This implies meeting the needs of the present without reducing the ability of the next generation to meet its needs [Loucks, 2000]. This is represented by a relatively long time-horizon with specified state conditions at its end. A general aspect of multi-year WSS management relates to uncertainty, including, among others, [Ajami et al., 2008], climate change [Brekke et al., 2009; Yates et al., 2005], population growth [Kasprzyk et al., 2009], the decline of water quality in the sources, and the economic parameters in the objective function. In the current work only the replenishment into the natural resources is taken as uncertain. Possible inclusion of the salinity in the model and extensions to other sources of uncertainty will be brought up in the final Chapter of the thesis.

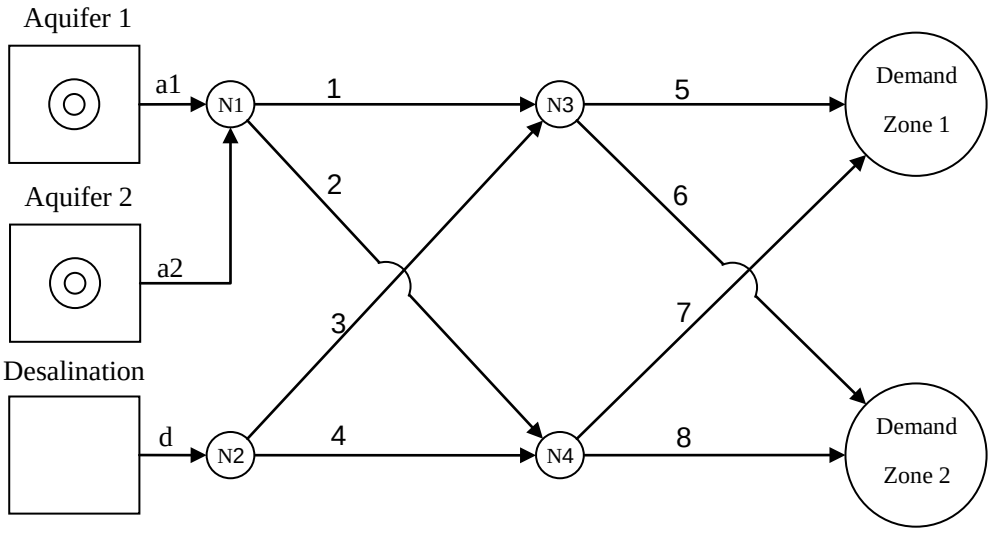

Figure 5.1: Network layout

5.3.1. Mathematical model

Objective Function

The objective is to operate the system with minimum total cost comprised of desalination and conveyance costs over the operation horizon T_f years, and a penalty/reward related to the final state of the aquifers at the end of the planning horizon. This term depends on the deviation of the final water level from a prescribed value: being below it incurs a penalty while being above results in a reward. Henceforth all values are in million cubic meters per year ($MCM / year$) and the costs are in ($\$/MCM$), where a , d , l , z and t denote aquifer, desalination, link, demand zone and year, respectively. The objective is:

$$\sum_{t=1}^{T_f}\left[\sum_{d} des_{d,t}\cdot Q_{d,t}+\sum_{l} C_{l,t}\cdot Q_{l,t}\right]+\sum_{a}\left[(\hat{h}_a-h_{a,T_f})\cdot E_a\right]\rightarrow \min \qquad (5.17)$$

where $des_{d,t}$ is the cost of desalinated water per MCM ($\$/MCM$); $Q_{d,t}$ is desalinated water amount ($MCM / year$); $C_{l,t}$ is cost of transportation per MCM ($\$/MCM$); $Q_{l,t}$ is flow in the link ($MCM / year$); $h_{a,t}$ is the water level (m) in the aquifer at the end of year *t*; $\hat{h}_a$ is the prescribed final water level (m); E_a is penalty per unit deviation ($\$/m$).

Constraints

Water Conservation Law

The distribution system is represented as a directed graph consisting of N nodes connected by M edges. The nodes can be grouped into two sub-groups: N_1 are source nodes, desalination plant and aquifers, with one outgoing link from each source node, and N_2 intermediate and demand nodes, where two or more edges meet. The M edges represent the links between two nodes; links in which the direction of flow is not fixed are represented by two edges, one in each direction. The topology of the network is represented by the junction node connectivity matrix G, where $G \in \mathbf{R}^{N_2 \times M}$ has a row for each node and a column for each edge. The nonzero elements in each row are $+1$ and -1 for incoming and outgoing edges respectively. The first columns in G correspond to the links which leave source nodes (aquifers and desalination plants), while the last rows correspond to the demand nodes. For each year t the following linear equation system insures water conservation at the network nodes.

$$G \cdot Q_t = S_t \tag{5.18}$$

where $Q_t = [Q_{natural,t}, Q_{desalination,t}, Q_{links,t}]^T$; $S_t = [0, Q_{demand,t}]^T$; $Q_{natural,t}$ is the vector of elements $Q_{a,t}\ \forall a$; $Q_{desalination,t}$ is the vector of elements $Q_{d,t}\ \forall d$; $Q_{links,t}$ is the vector of elements $Q_{l,t}\ \forall l$; $Q_{demand,t}$ is the vector of elements $Q_{z,t}\ \forall z$ where $Q_{z,t}$ denotes demand at year t in demand zone z. The water supply network shown in Figure 5.1 has 3 source nodes, 4 intermediate nodes and 2 demand nodes. The junction node connectivity matrix $G \in R^{6\times 11}$ is given in Table 5.1. The vectors Q_t, S_t are: $Q_t = [Q_{a,t}, Q_{d,t}, Q_{1,t}, ..., Q_{8,t}]^T$ and $S_t = [0, ..., 0, Q_{z=1,t}, Q_{z=2,t}]^T$.

Node	Source			Links							
	a1	a2	d	1	2	3	4	5	6	7	8
1	1	1	0	-1	-1	0	0	0	0	0	0
2	0	0	1	0	0	-1	-1	0	0	0	0
3	0	0	0	1	0	1	0	-1	0	-1	0
4	0	0	0	0	1	0	1	0	-1	0	-1
5	0	0	0	0	0	0	0	1	1	0	0
6	0	0	0	0	0	0	0	0	0	1	1

Table 5.1: The junction node connectivity matrix for the network in Figure 5.1.

Hydrological Balance for Aquifers

The hydrological water balance insures that the change in aquifer storage equals the difference between the recharge and withdrawal during the year:

$$h_{a,t} = h_{a,0} + \frac{1}{SA_a}\left(\sum_{i=1}^{t} R_{a,i} - \sum_{i=1}^{t} Q_{a,i}\right) \quad (5.19)$$

where $Q_{a,t}$ is the extraction amount ($MCM / year$); $R_{a,t}$ is recharge ($MCM / year$); SA_a is the storativity multiplied by area (MCM / m); $h_{a,t}$ is water level in the aquifer at the end of year t (m); $h_{a,0}$ is initial water level (m).

Limits on Water Levels in the Sources

Constraints on water levels in the natural resources reflect both policy and physical/operational limits:

$$h_{a,t}^{\min} \le h_{a,t} \le h_{a,t}^{\max} \quad (5.20)$$

where $h_{a,t}^{\min}$ is minimum allowed water level (m); $h_{a,t}^{\max}$ is maximum allowed water (m)

Conveyance Capacity Constraints

The model deals with water balance and does not include explicitly the hydraulic energy equations. Still, in order to maintain feasibility of hydraulic conditions the discharges in the links are limited by capacity constraints which are calculated from hydraulic data of the pipes/links. The lower bound is set to zero since the flow direction in the links is fixed.

$$0 \le Q_{l,t} \le Q_{l,t}^{\max} \quad (5.21)$$

where $Q_{l,t}^{\max}$ is the maximum discharge allowed ($MCM / year$) .

Capacities of the Natural Sources

The extracted amount from each natural resource may be restricted by an upper bound, reflecting various hydrological and hydraulic considerations. The lower bound is set to zero as the flow from the source is one-directional.

$$0 \le Q_{a,t} \le Q_{a,t}^{\max} \quad (5.22)$$

where $Q_{a,t}^{\max}$ is the maximum admissible/feasible withdrawal ($MCM / year$)

Desalination Capacity

The amount of desalinated water from each plant is limited by an upper bound which represents plant capacity and by a lower bound that represents a condition usually set in the contract with the plant concessions (which may be zero).

$$Q_{d,t}^{\min} \le Q_{d,t} \le Q_{d,t}^{\max} \tag{5.23}$$

where $Q_{d,t}^{\max}$ is maximum supply (*MCM* / *year*); $Q_{d,t}^{\min}$ is minimum supply (*MCM* / *year*)

The resulting mathematical model is uncertain LP where the uncertainty is in the recharge parameters $R_{a,t}\ \forall a \forall t$. Hence, we can define the uncertain column vector $R = [R_{a=1..a_f,t=1}, \cdots, R_{a=1..a_f,t=T_f}]^T$ where a_f is the number of natural resources.

5.4. Applying the RC approach

5.4.1. Constructing the uncertainty set

Recharge into natural resources is usually given as historical time series, frequently of limited duration and not rich enough to describe fully the underlying stochastic process. To construct an ellipsoidal uncertainty set for the natural resources recharge we assume that the annual recharge values are independent random variables, where the recharge vector of the aquifers $R' = R_{a=1..a_f,t'}$ in each year t' is correlated with covariance matrix $\Sigma_{R'}$ and expectation vector $\mu_{R'}$, indicating positive correlation between recharge of different aquifers (e.g., a wet year is wet all over). Each row in $\Sigma_{R'}$ and $\mu_{R'}$ corresponds to an aquifer $a = 1..a_f$. The annual recharges are assumed independent over time so the recharge data is repeated for the entire horizon. Hence, the expectation vector of the overall recharge is $\mu_R = [\mu_{R'}, ..., \mu_{R'}]^T$ and covariance matrix Σ_R is a diagonal block matrix:

$$\Sigma_R = \begin{pmatrix} \Sigma_{R'} & 0 & 0 \\ 0 & \ddots & 0 \\ 0 & 0 & \Sigma_{R'} \end{pmatrix} \tag{5.24}$$

Consider the linear transformation of the stochastic vector R :

$$\begin{aligned} R &= \mu_R + \Delta \cdot \xi \\ \mu_R &= \mu_R + \Delta \cdot \mu_\xi \\ \Sigma_R &= \Delta \cdot \Sigma_\xi \cdot \Delta^T \end{aligned} \tag{5.25}$$

If we set $\mu_\xi = 0$ and $\Sigma_\xi = I$ and wish to maintain the covariance of R, then $\Sigma_R = \Delta \cdot \Delta^T$. By replacing the stochastic vector ξ with the perturbation vector ς that varies in the perturbation set $\text{Ball}_\theta = \{\|\varsigma\| \le \theta\}$, we obtain the ellipsoidal uncertainty set U of the uncertain vector R:

$$U = \{R : \mu_R + \Delta\varsigma, \|\varsigma\| \le \theta\} \tag{5.26}$$

The parameter θ determines the range of values of the uncertain R against which the optimal policy is immunized, i.e. remains feasible. A large value means immunization against more extreme values of R. θ = 0 implies that only the expected value of *R* is taken into consideration, and any deviation of its actual value from this expectation could lead to constraint violation.

The matrix $\Delta = \Sigma_R^{0.5}$ can be obtained by Cholesky decomposition. Each row in Δ corresponds to year t and aquifer a and implies $\sigma_a = \|\Delta_{t,a}\|$, where σ_a is the standard deviation of recharge in aquifer a which remains constant over the years.

5.4.2. Formulation of the RC

Formulation of a RC for the WSS model developed in Section 5.3 requires extracting the state variable $h_{a,t}$ from the uncertain equation (5.19). The resulting model, after substituting $h_{a,t}$ and converting it to the form of the LP in (5.2):

$$\begin{aligned}
&K \to \min \\
&\text{Subjecte to} \\
&(I) \quad \sum_{t=1}^{T_f}\sum_{a}\frac{E_a \cdot Q_{a,t}}{SA_a} - \sum_{t=1}^{T_f}\sum_{a}\frac{E_a \cdot R_{a,t}}{SA_a} + \sum_{t=1}^{T_f}\sum_{d} des_{d,t} Q_{d,t} + \sum_{t=1}^{T_f}\sum_{l} C_{l,t} Q_{l,t} + P_0 - K \le 0 \\
&(II) \quad \begin{cases} h_{a,0} + \dfrac{1}{SA_a}\left(\sum_{i=1}^{t} R_{a,i} - \sum_{i=1}^{t} Q_{a,i}\right) - h_{a,t}^{\max} \le 0 & \forall a \forall t \\ -h_{a,0} - \dfrac{1}{SA_a}\left(\sum_{i=1}^{t} R_{a,i} - \sum_{i=1}^{t} Q_{a,i}\right) + h_{a,t}^{\min} \le 0 & \forall a \forall t \end{cases} \\
&(III) \quad \begin{cases} G \cdot Q_t = S_t & \forall t \\ Q_{d,t}^{\min} \le Q_{d,t} \le Q_{d,t}^{\max} & \forall d \forall t \\ 0 \le Q_{a,t} \le Q_{a,t}^{\max} & \forall a \forall t \\ 0 \le Q_{l,t} \le Q_{l,t}^{\max} & \forall a \forall t \end{cases}
\end{aligned} \tag{5.27}$$

where $P_0 = \sum_a (\hat{h}_a - h_{a,0}) E_a$ is a certain constant.

Consider the vectoroized version of the uncertain constraints (I) and (II)

$$\sum_{t=1}^{T_f}\sum_{a}\frac{E_a\cdot Q_{a,t}}{SA_a}-R^T D_{SA}^{-1}v+\sum_{t=1}^{T_f}\sum_{d}des_{d,t}Q_{d,t}+\sum_{t=1}^{T_f}\sum_{l}C_{l,t}Q_{l,t}+P_0-K\le 0$$

$$h_{a,0}+R^T D_{SA}^{-1}\delta_{a,t}-\frac{1}{SA_a}\sum_{i=1}^{t}Q_{a,i}-h_{a,t}^{\max}\le 0 \qquad \forall a\forall t \qquad (5.28)$$

$$-h_{a,0}-R^T D_{SA}^{-1}\delta_{a,t}+\frac{1}{SA_a}\sum_{i=1}^{t}Q_{a,i}+h_{a,t}^{\min}\le 0 \qquad \forall a\forall t$$

where $R=[R_{a=1..a_f,t=1},\cdots,R_{a=1..a_f,t=T_f}]^T$; $v=[E_{a=1..a_f},\cdots,E_{a=1..a_f}]^T$; $\delta_{a,t}\in\mathbf{R}^{(a_f\cdot T_f\times 1)}$ has 0 and 1 values according to a,t, in order to extract the elements corresponding to the constraint from the elements of R; D_{SA} is a diagonal matrix with main diagonal vector $[SA_{a=1..a_f},\cdots,SA_{a=1..a_f}]^T\in\mathbf{R}^{(a_f\cdot T_f\times 1)}$. For example, when there are two aquifers, $\delta_{a=1,t=2}=[1,0,1,0,0,\cdots,0]^T$.

The robust version of the uncertain constraint is (see Section 5.2.1):

$$\sum_{t=1}^{T_f}\sum_{a}\frac{E_a\cdot Q_{a,t}}{SA_a}-\mu_R^T D_{SA}^{-1}v+\theta\left\|v^T D_{SA}^{-1}\Delta\right\|+\sum_{t=1}^{T_f}\sum_{d}des_{d,t}Q_{d,t}+\sum_{t=1}^{T_f}\sum_{l}C_{l,t}Q_{l,t}+P_0-K\le 0$$

$$h_{a,0}+\mu_R^T D_{SA}^{-1}X_{a,t}+\theta\left\|\delta_{a,t}^T D_{SA}^{-1}\Delta\right\|-\frac{1}{SA_a}\sum_{i=1}^{t}Q_{a,i}-h_{a,t}^{\max}\le 0 \qquad \forall a\forall t \qquad (5.29)$$

$$-h_{a,0}-\mu_R^T D_{SA}^{-1}X_{a,t}+\theta\left\|\delta_{a,t}^T D_{SA}^{-1}\Delta\right\|+\frac{1}{SA_a}\sum_{i=1}^{t}Q_{a,i}+h_{a,t}^{\min}\le 0 \qquad \forall a\forall t$$

The resulting RC is LP, since no decision variables appear in the norms and the uncertainty appears only on the RHS. Recalling that the data in μ_R and Δ are repeated each year and that $\sigma_a=\left\|\Delta_{t,a}\right\|$ we obtain $\mu_R^T D_{SA}^{-1}\delta_a^t=\frac{t\cdot\mu_{R'_a}}{SA_a}$, $\left\|\delta_{a,t}^T D_{SA}^{-1}\Delta\right\|=\frac{\sqrt{t}\cdot\sigma_a}{SA_a}$, hence, the RC of the WSS model is:

$K\to\min$

Subjected to

$$\sum_{t=1}^{T_f}\sum_{a}\frac{E_a\cdot Q_{a,t}}{SA_a}-\mu_R^T D_{SA}^{-1}v+\theta\left\|v^T D_{SA}^{-1}\Delta\right\|+\sum_{t=1}^{T_f}\sum_{d}des_{d,t}Q_{d,t}+\sum_{t=1}^{T_f}\sum_{l}C_{l,t}Q_{l,t}+P_0-K\le 0$$

$$h_{a,0}+\frac{t\cdot\mu_{R'_a}}{SA_a}+\theta\frac{\sqrt{t}\sigma_a}{SA_a}-\frac{1}{SA_a}\sum_{i=1}^{t}Q_{a,i}-h_{a,t}^{\max}\le 0 \qquad \forall a\forall t$$

$$-h_{a,0}-\frac{t\cdot\mu_{R'_a}}{SA_a}+\theta\frac{\sqrt{t}\sigma_a}{SA_a}+\frac{1}{SA_a}\sum_{i=1}^{t}Q_{a,i}+h_{a,t}^{\min}\le 0 \qquad \forall a\forall t \qquad (5.30)$$

$$G\cdot Q_t=S_t \qquad \forall t$$

$$Q_{d,t}^{\min}\le Q_{d,t}\le Q_{d,t}^{\max} \qquad \forall d\forall t$$

$$0\le Q_{a,t}\le Q_{a,t}^{\max} \qquad \forall a\forall t$$

$$0\le Q_{l,t}\le Q_{l,t}^{\max} \qquad \forall a\forall t$$

5.5. Examples

5.5.1. Problem data

A small water supply system (Figure 5.1) is used for detailed demonstration. Summary results are later shown for a larger system (Figure 3.11) that constitutes a central part of the Israeli National Water System. The system in Figure 5.1 is fed from two aquifers and a desalination plant to supply two customers over a 10 year horizon, for which a minimum total operation cost is sought. The annual costs of transportation in the links are {0.1, 0.05} ($M\$/MCM$) for odd and even links, respectively, and the desalination cost is 1 ($M\$/MCM$). Desalinated water is purchased from a private supplier, so the construction costs are included in the cost per unit of water obtained from the plant; this is the case in Israel, where the desalination plants are developed by private industry on a Build-Operate-Transfer (BOT) basis. The same costs hold for later years $t = 2..T_f$ and are capitalized to the present (decision time) with a 5% discount rate. The penalty at the final stage is 0.3 ($M\$/m$) for being below the prescribed water level, and is positive for levels above the prescribed value. Both aquifers have identical physical properties: $SA = 0.8\,(MCM/m)$, $h_0 = 75\,(m)$, $\hat{h} = 30\,(m)$, $h_{\min} = 0\,(m)$ and $h_{\max} = 500\,(m)$ (an arbitrary high value, to insure no spill and thus simplify the demonstration). All discharges have the same bounds: 0-100 (MCM). The annual recharges are i.i.d. with a joint uniform discrete distribution {30,40,50} for aquifer 1 and {35,50,60} for aquifer 2 respectively, and remains the same for all 10 years. This distribution has mean recharges of {40, 48.33} (MCM) in aquifer 1 and 2 respectively and a covariance matrix:

$$V_{R'} = \begin{pmatrix} 66.67 & 83.33 \\ 83.33 & 105.56 \end{pmatrix} \tag{5.31}$$

The resulting uncertainty set of the annual recharge is:

$$U = \left\{ R' : \begin{pmatrix} 40 \\ 48.33 \end{pmatrix} + \begin{pmatrix} 8.17 & 0 \\ 10.21 & 1.18 \end{pmatrix} \begin{pmatrix} \varsigma_1 \\ \varsigma_2 \end{pmatrix}, \|\varsigma\| \le \theta \right\} \tag{5.32}$$

The demand in the first year is 80 (MCM) in each demand zone, and it increases by 5% in each subsequent year.

5.5.2. RC solution and Simulation results

We compare five management policies: three Robust Policies (RP1, RP2 and RP3) which are obtained from the RC solution with different values of $\theta = \{1, 2, 3\}$, respectively, a Nominal Policy (NP) which is obtained from a deterministic solution with the average recharge, and a Conservative Policy (CP) which is obtained from the worst case realization, namely minimum recharge in all years. Each of these policies determines Here-and-Now decisions which are implemented at the beginning of the planning horizon before the uncertainty is revealed.

Figure 5.2 compares the progression of annual amounts of desalinated water purchased over the planning horizon in each of these polices. The CP results in constant desalination of 120 ($MCM / year$), which is equal to the full capacity of the desalination plant. The NP results in taking as much as possible from the aquifers in the first stages while recognizing that the demand is increasing beyond the desalination capacity which leads to storing aquifer water to close the gap between the demand and the supply capacity at later stages. The conservativeness of the CP over all other policies is apparent. The robust polices RP1, RP2 and RP3 require less desalinated water than the CP, indicating that these policies are not myopic; in other words, they take advantage of the variability of recharge over time. Compared to the NP, a robust policy takes more desalinated water in the first stages, resulting in higher water level in the aquifers, which insures maneuverability within the operational limits of the aquifers in later years. The degree of conservativeness of the robust policies is noticeable - an RP with smaller θ results in less desalination but lower reliability/immunization and higher penalties, as will be shown below, where RP with $\theta = 0$ (which is the NP) is a lower bound. The vertical distance of an RP policy above the NP policy is a measure of the extra reliability that the RP requires; the vertical of an RP policy below the CP policy is a measure of the foresight of the RP in taking advantage of the variability range of the recharge in the future.

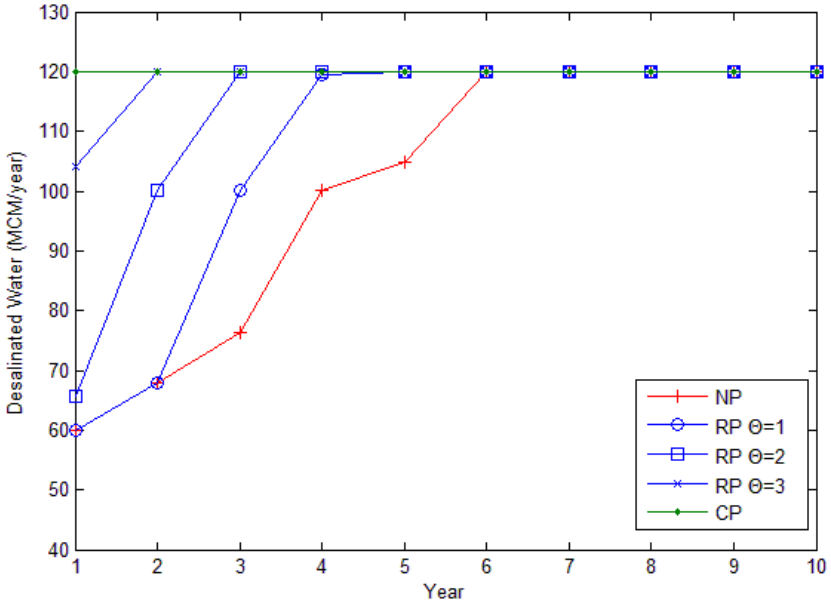

Figure 5.2: Desalination amount over years for each static policy

The performance of each policy is examined by simulation, which shows the tradeoff between the amount of desalination prescribed and the unreliability: lower desalination results in lower reliability. Each optimal policy is examined by simulation with 1,000 random samples, each with $a_f T_f = 20$ random recharge values drawn from the defined uniform discrete distribution of the recharge. Summary results for NP and RP3 are shown in Figures 5.3 and 5.4, respectively: the final water levels in the two aquifers, the total cost and the penalized cost. The feasibility of policies RP1, RP2, RP3 and NP is obviously not guaranteed for all possible realizations of the recharge, as seen by some excursions of the level to negative values. However, as seen in Figure 5.4 for RP3 these are very few; they are fewer as θ increases. In CP there are obviously no infeasibilities, as it considers only the lowest value of the recharge.

Since some of the generated samples can result in the reservoirs/aquifers becoming empty in some year it is necessary to take this into consideration in two respects: (1) continuing the path of the reservoir/aquifer beyond this point, and (2) penalizing the policy for failing to meet the specified operational limits. The two aspects are handled as follows: (a) when the reservoir goes dry and "wants" to go below the minimum level, it is set back to empty as the initial state for the next year, and (b) a penalty term is added to this simulation. The penalty is

$$\max(h_{a,t}^{\min} - h_{a,t}, 0) \cdot DC_t \qquad \forall a \forall t \qquad (5.33)$$

and the water balance is

$$h_{a,t+1} = \max(h_{a,t}^{\min}, h_{a,t}) + \frac{R_{a,t+1}}{SA_a} - \frac{Q_{a,t+1}}{SA_a} \qquad \forall a \forall t \tag{5.34}$$

where $DC_t = 3\,(M\$/m)$ is the deficit cost. Note that this is used only in evaluating the optimal solution by simulation and is not included in the optimization models. We define the total cost after applying (5.33) and (5.34) as the "penalized cost".

For the reader to see the mean shortage in (MCM) units and not via penalty; the cost increment in Table 5.2 should be divided by the deficit cost. For example the mean shortage associated with the NP is (1074.89-984.54)/3=30.11 (m) i.e. 30.11*0.8=24 (MCM).

Figures 5.3 and 5.4 demonstrate the simulation results for NP and RP3: where subfigures show the results for: (a) final water level in aquifer1 (b) final water level in aquifer2 (c) the total operation cost and (d) the penalized cost.

The NP results in almost 50% of the samples deviating from the operation limits (going negative, as if they are allowed to do so) at the final stage in both aquifers, while in RP3 there are only 4 deviations over all 1,000 simulations. Figures 5.3d & 5.4d show that almost 10% of the samples in the NP exceed the worst cost of RP3. Moreover, a very large difference in the cost variability is exposed.

Table 5.2 reports the empirical maximum, minimum, average and standard deviation of the total cost and penalized cost for each policy, along with the empirical reliability defined as the fraction of the total simulations which maintain feasibility in both aquifers in all years. The constant value of the cost standard deviation in Table 5.2 indicates that all policies run on the same sample of the recharge; this indicates that the results are obtained from a fair simulation experiment.

Policy	**Cost (M$)**				**Penalized Cost (M$)**				**Reliability %**
	min	**max**	**mean**	**std**	**min**	**max**	**mean**	**std**	
NP	916.60	1060.98	984.54	21.27	916.60	1778.32	1074.89	143.71	48.6
RP1	948.43	1092.81	1016.38	21.27	948.43	1613.35	1035.52	74.01	81.4
RP2	983.28	1127.66	1051.22	21.27	983.28	1451.40	1053.66	34.07	97.7
RP3	1021.09	1165.46	1089.03	21.27	1021.09	1289.22	1089.22	22.29	99.7
CP	1101.62	1246.00	1169.56	21.27	1101.62	1246.00	1169.56	21.27	100

Table 5.2: Simulation results for the static polices. std=standard deviation.

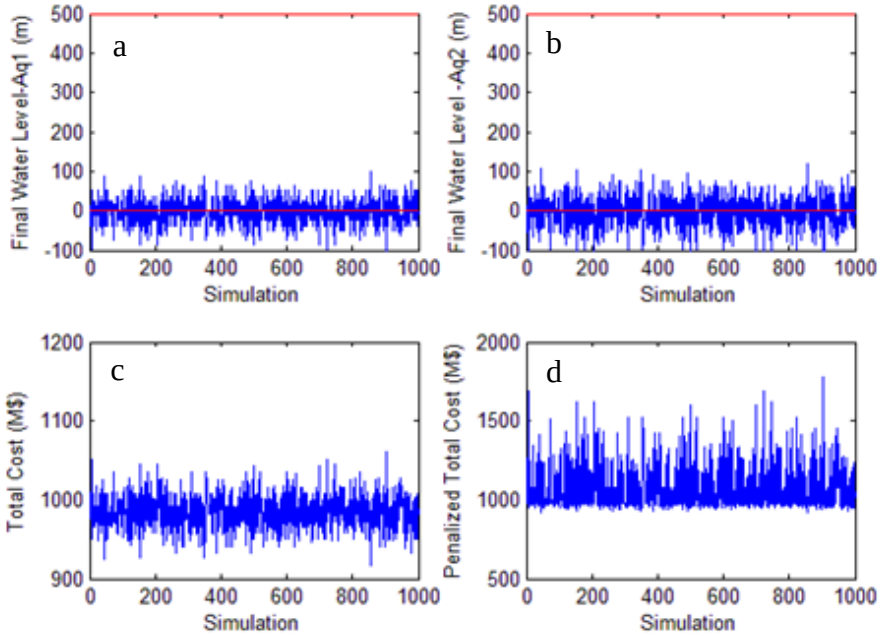

Figure 5.3: Simulation results of the NP

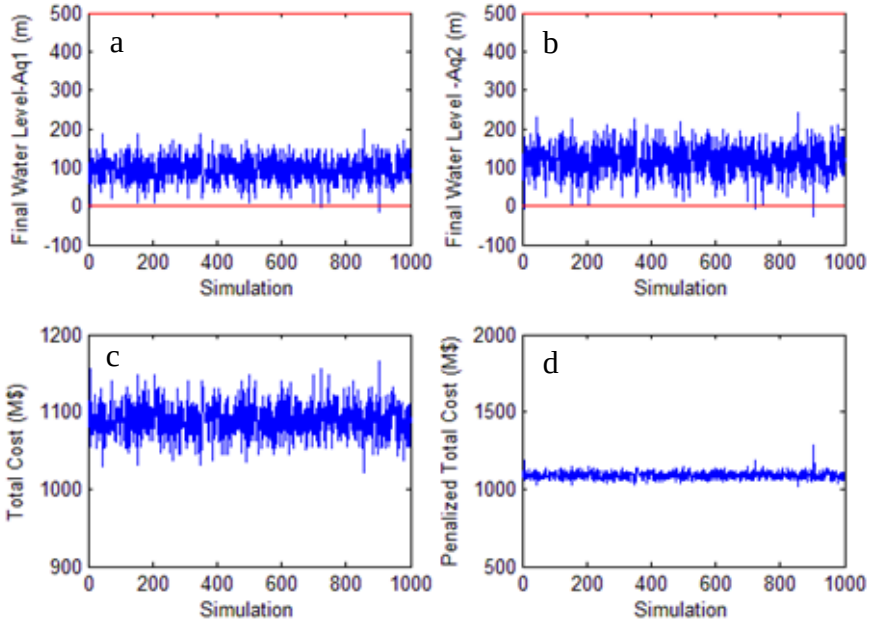

Figure 5.4: Simulation results of the RP3 policy

The results show that the cost of the NP range between 916-1061 M$ while the cost of RP3 ranges between 1021-1166 M$. The NP yields infeasible situations in 51.4% of the samples while the unreliability of RP3 is only 0.3%. The low cost of NP does not mean advantage over RP3, since there is a very large difference in the reliabilities and it is a matter of multi-objective decision making. Accounting for the constraint

violation in the cost (Figures 5.3d & 5.4d) shows clear preference of RP3 over NP for the specified value of the penalty coefficient. RP3 immunize the NP from a reliability of 48.6% to 99.7% with only 10.6% increase in the mean cost. RP3 immunizes the NP with price of robustness (mean cost increment) of 2.05 M$ for each 1% reliability, while the CP immunize it with price of robustness of 3.6 M$ for each 1% reliability. Comparing CP with RP3 shows clear preference of RP3; since the CP immunizes RP3 by getting rid of the last remaining 0.3% unreliability with an associated cost of 80.5 M$, or 268 M$ for each 1% reliability.

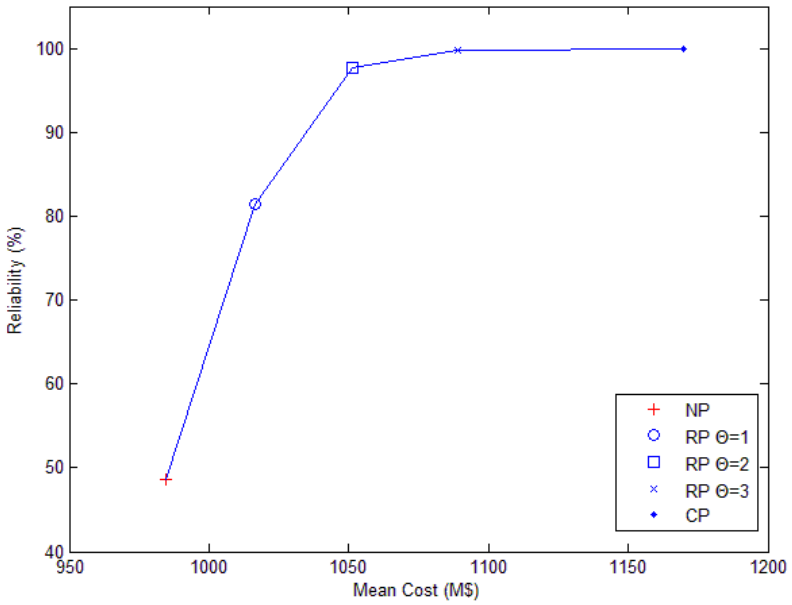

Figure 5.5: Reliability vs. Cost

Figure 5.5 shows the tradeoff between reliability and mean cost, for all policies. The tradeoff is characterized by a mild slope of the last segment connecting RP3 with CP which indicates that a large increment in the mean cost is needed in order to obtain a small increment in reliability. The question to be asked is whether it is justified to add this large cost to immunize against rare events of the recharge. In our case the answer is given by the penalized cost which quantifies the unreliability by a penalty. The CP does not violate any constraint over all realizations of the recharge; hence the cost and penalized cost are identical. In Table 5.2 the mean penalized cost of RP3 (with the assumed penalty coefficient) is 80.34 M$ less than the mean cost of CP, in contrast the CP maximum cost is 43.22 M$ less than the maximum penalized cost of RP3. However, further analysis of the cost distribution shows that only one sample in RP3 exceeds the worst cost of the CP (1246 M$) while 695 samples in RP3 are below the best cost of the CP (1101.6 M$). This results shows that implementation of the CP

would increase the mean cost by 80.34 M$ while the only gain is reduction of 43.22 M$ in the cost's upper bound, which is rarely realized.

Policies RP2 and RP3 are indeed robust, the corresponding standard deviations of the penalized cost are less by a factor of 4.2-6.4 than the NP standard deviation, indicating that these robust policies lead to stable policies without large variability in the associated costs which can be accounted as preference over other alternatives.

5.6. Folding Robust Counterpart (FRC)

The RC approach solves a static problem in which the decisions are Here-and-Now for all years, as if all future decisions are fixed in advance. This may seem a myopic approach, but in fact only the decision for the first year should be implemented and the analysis is then repeated towards the end of this year, with new information (if any) about the recharge, demands, costs, and initial system state (aquifer water levels). This is captured in the Folding Robust Counterpart (FRC) model.

At time "now" the RC solution for all years is computed, and the first stage decision is implemented. At the beginning of the next year, we solve a new problem with a new state (obtained from the first year decision and realization) and a reduced time horizon (it could also be extended by one year if desired). This is repeated over all the stages (years).

We next demonstrate and compare the Folding Robust Policy (FRP) with Folding Multistage Stochastic Programming Policy (FMSPP). The comparison is carried out for the small system in Figure 5.1 with the data listed above, where the aquifers recharge in each year is i.i.d. given by multivariate normal distribution with expectation $\mu = [40, 48.33]$ and covariance matrix V defined in (5.31).

5.6.1. Multistage Stochastic Programming (MSP)

A well studied method for solving multi-stage stochastic decision models is Multistage Stochastic Programming [Shapiro et al., 2009]. In the MSP we capture the uncertainty as a stochastic process with a known probability distribution. One variant of the MSP is scenarios based, which assumes that the distribution of the stochastic process is given by a finite number of scenarios, each with its corresponding probability p^s. Following this approach, the stochastic recharge of the example in Section 5.5.1 is modeled by a 10-stage scenario tree having three branches at each

stage with identical probabilities. This scenario tree has 3^{10} different scenarios, which at each stage t are bundled into 3^t nodes while all scenarios which share the same node at stage t have the same recharge up to this stage.

At any node in the multistage scenario tree, the decision maker knows the exact history leading to that node, and decides how to proceed; knowing only that the future recharge is presented by each of the scenarios that emerge from the node into the future. The MSP solves for all stages simultaneously to obtain the optimal decisions (corresponding to each node) which results in minimum expectation cost over all scenarios. The MSP model for the WSS model is:

$$\sum_{s=1}^{Scenarios} p^s K^s \rightarrow \min$$

Subjecte to

$$\begin{aligned}
&\sum_{t=1}^{T_f}\sum_{a}\frac{E_a\cdot Q^s_{a,t}}{SA_a}-\sum_{t=1}^{T_f}\sum_{a}\frac{E_a\cdot R^s_{a,t}}{SA_a}+\sum_{t=1}^{T_f}\sum_{d} des_{d,t}Q^s_{d,t}+\sum_{t=1}^{T_f}\sum_{l}C_{l,t}Q^s_{l,t}+P_0-K^s\le 0 && \forall s\\
&h_{a,0}+\frac{1}{SA_a}\left(\sum_{i=1}^{t}R^s_{a,i}-\sum_{i=1}^{t}Q^s_{a,i}\right)-h^{\max}_{a,t}\le 0 && \forall a\forall t\forall s\\
&-h_{a,0}-\frac{1}{SA_a}\left(\sum_{i=1}^{t}R^s_{a,i}-\sum_{i=1}^{t}Q^s_{a,i}\right)+h^{\min}_{a,t}\le 0 && \forall a\forall t\forall s\\
&G\cdot Q^s_t=S_t && \forall t\forall s\\
&Q^{\min}_{d,t}\le Q^s_{d,t}\le Q^{\max}_{d,t} && \forall d\forall t\forall s\\
&0\le Q^s_{a,t}\le Q^{\max}_{a,t} && \forall a\forall t\forall s\\
&0\le Q^s_{l,t}\le Q^{\max}_{l,t} && \forall a\forall t\forall s\\
&Q^s_t\in\mathcal{N} && \forall t\forall s
\end{aligned} \qquad (5.35)$$

where s denotes scenario; p^s is the probability associated with each scenario; $\mathcal{N}$ is the set of nonanticipativity constraints, which are the set of constraints such that $Q^{s_1}_t = Q^{s_2}_t$ for all scenarios s_1 and s_2 that are indistinguishable (share the same history) up to stage t [Shapiro et al., 2009, page 71].

In the general case of continuous distributed random data the MSP is computationally intractable; however we can apply the MSP by approximating the continuous distributions of the data by discrete sets. In our case the multivariate normal distribution is discretized. The size of the deterministic equivalent of the stochastic program depends on the number of elements considered in the discrete distribution. We use the 5-elemnent discrete distribution $\{\mu, \mu\pm\sigma, \mu\pm 2\sigma\}$ given in Table 5.3 to represent the continuous normal distribution.

With regard to the computational difficulty of solving the deterministic equivalent of the stochastic program, the nonanticipativity constraints can be eliminated by substitution of variables, this reduces the total number of constraints and variables in the problem. Still, the real computational difficulty arises due to the number of scenarios considered in the problem since the size of the deterministic program increases rapidly with the number of scenarios. For the example considered in Section 5.5.1 with a 5-value distribution of the recharge as given in Table 5.3, the 10-stage problem would result in 36,621,091 variables and 141,601,544 inequality constraints even after elimination of the nonanticipativity constraints, while the RC of the10-stage example has only 111 variables and 381constraints. To reduce the computational burden for this presentation, we compare the performance of the three dynamic methodologies: FRP and FMSPP on a 5-stage example, in which the MSP results in 11,716 variables and 45,299 constraints while the RC results in 56 variables and 191 constraints.

$R_{a=1,t}, R_{a=2,t}$	23.67, 27.79	31.84, 38.06	40, 48.33	48.17, 58.61	56.33, 68.88
Prob	0.06	0.22	0.44	0.22	0.06

Table 5.3: Discrete approximation of the multivariate normal distribution.

5.6.2. Folding horizon simulation

To evaluate these policies for the example outlined in Section 5.5 with 5-stages, we simulate their optimal solutions with 1,000 random samples of $a_f T_f = 10$ random members each, drawn from the multivariate normal distribution of the recharge.

The MSP is a sequential decision making approach; hence it provides the optimal decision at each stage according to the history up to that stage. However, the MSP only considered the discrete approximation of the continuous distribution. Hence, the MSP is also applied in folding mode, since the realization of the recharge could be different from the values in the discrete approximation.

To apply the folding horizon, for each of the samples we start by solving a 5-stage problem. From the 5-stage solutions we only adopt the first stage optimal solution according to each policy, i.e. RP and MSPP. Then we use the first member of the sample as if it is the actual realization of the recharge at the first stage. The new state of the system at the end of the first stage is calculated, given the decisions and the realization of the first stage.

After this stage is fully covered, a 4-stage problem is solved with the initial state corresponding to each of the states obtained at the end of the first stage. We continue with this process until we solve the problem of the 5^{th} stage for all its possible initial states. At the end of the horizon we can calculate the total cost of each policy corresponding to the sample. Applying this procedure for each of the 1,000 samples we obtain the simulation results for comparing the methodologies.

5.6.3. Simulation results

Table 5.4 reports the simulation results for the three dynamic decision making policies the static policy RP with $\theta = 3$, the FRP with $\theta = 3$, and FMSPP . It contains the maximum, minimum, average and standard deviation of the total cost and the penalized cost for each policy, along with the empirical reliability defined as the fraction of the total simulations which maintain feasibility in all aquifers and at all stages.

The advantage of the adjustable dynamic RP over the static one is apparent. Both policies have a high reliability of 99.9% but the dynamic policy results in a narrower cost range of 301-569 M$ instead of 393-604 M$ and a lower mean cost of 418 M$ compared to 451 M$. The lower standard deviation of the static RP is the result of the non-adjustability of the decision, namely in the folding mode the decisions depend on the realization and hence the standard deviation can be expected to increase.

The FRP produces a more reliable solution than the FMSPP. The FRP immunizes the FMSP with price of robustness (mean cost increment) of 2.47 M$ for each 1% reliability. Comparing the penalized cost which quantifies the unreliability by the penalty, shows that the mean penalized cost of the FMSPP is 7.9 M$ (1.9%) less than that obtained in the FRP, however the worst and best cost of the FRP are less than in the FMSPP by 10.3% and 4.7%, respectively and the standard deviation of the cost is smaller. Thus, in addition to better reliability, the FRP has greater flexibility to take advantage of opportunities (lower best cost) and to optimize in severe cases (lower worst cost).

The RP3 solution could be a legitimate choice based on these results, but it is recommended that further statistical analysis of the penalized cost over longer periods and more simulations is required to determine preference. Still, the large size of the MSP model compared to the RP, could tip the scales toward using the RP.

The decisions in the folding mode are realization dependent and hence each of decision variables starting from the second stage could take on as many values as the number of states obtained at the end of the previous stage.

Figure 5.6 shows the maximum and mean desalination amount in each year according to each folding policy along with the desalination amount of the static policy (which is not realization dependent). The mean desalinated amount of the FRP is lower than in the other policies, starting from the second year. The FMSPP starts with low desalination, but immediately in the second stage fixes the desalination amount sharply to exceed the maximum desalination obtained from the FRP. However, both of the folding methodologies utilize the full capacity of the desalination plant starting from the third year.

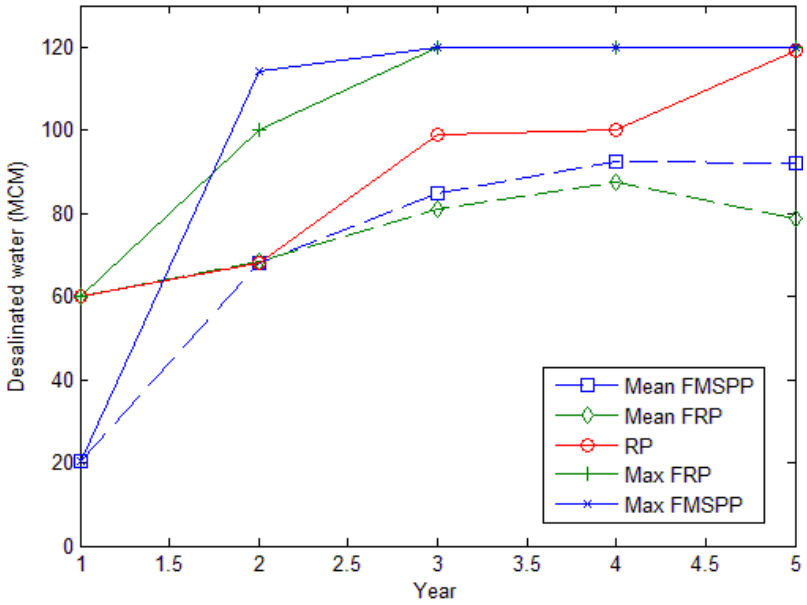

Figure 5.6: Desalination amount over years for each dynamic policy

Policy	Cost (M$)				Penalized Cost (M$)				Reliability %
	min	max	mean	std	min	max	mean	std	
RP3	393.45	508.65	451.24	15.03	393.45	603.80	451.34	15.68	99.9
FRP3	301.17	568.42	418.67	31.21	301.17	568.42	418.69	31.24	99.9
FMSPP	316.25	575.14	409.78	34.41	316.25	633.79	410.79	36.73	96.3

Table 5.4: Simulation results for the dynamic polices. std=standard deviation.

5.7. Ambiguous chance constraints (Example)

In this Section we show how to estimate probability guarantees [Ben-Tal et al., 2009] that determine the degree of immunization, with partial knowledge of the uncertain

stochastic parameters. Suppose that all we adopt form the historical record of the recharge in the example discussed above is the mean recharge $\mu_{R'}$ and the fact that the distribution support is bounded within the box $\mu_{R'} \pm 2\sigma$, where $\mu_{R'} = [40, 48.33], \sigma = [8.17, 10.27]$ (MCM). (Distribution support is the smallest closed set such that the probability to obtain a value outside of this set is zero).

According to Section 5.2.3, the RC with the following uncertainty set

$$U = \left\{ R' : \begin{pmatrix} 40 \\ 48.33 \end{pmatrix} + \begin{pmatrix} 16.34 & 0 \\ 0 & 20.54 \end{pmatrix} \begin{pmatrix} \varsigma_1 \\ \varsigma_2 \end{pmatrix}, \|\varsigma\| \le \sqrt{2\ln(1/\varepsilon)} \right\} \tag{5.36}$$

is an approximation of the ambiguous (unknown distribution) chance constraints formulation of the WSS model defined in (5.27):

$$\begin{array}{ll} K \to \min & \\ \text{Subjected to} & \\ \text{Prob}\{\text{consraint } I\} \ge 1-\varepsilon & \\ \text{Prob}\{\text{consraints } II\} \ge 1-\varepsilon & \forall a \forall t \\ \text{consraints } III & \forall a \forall t \forall d \end{array} \tag{5.37}$$

With only this partial knowledge of the recharge (bounds and mean, and no information about the distribution) one can use the RC with the uncertainty set U in (5.36) to solve (5.37). To test this approximation let us consider asymmetric distributions (all with mean $\mu_{R'}$ and the same bounds) which give Pmax of the values on the upper bound and the rest are uniformly distributed close to the lower bound. Figure 5.7 shows the distributions supports for different Pmax values. The test is applied on the example of 10-stage WSS with the uncertainty set U from (5.36) with a desired reliability of 0.95. The empirical reliability according to 10,000 simulations obtained by solving the RC approximation of the chance constraints model is reported in Table 5.5. The results show that the empirical reliability is above the desired reliability of 95% even for the extreme case when the recharge can take only minimum and maximum values.

Pmax	**Reliability (%)**
0.35	100
0.4	100
0.45	99.7
0.5	97.2

Table 5.5: Simulation results for the ambiguous chance constraints example.

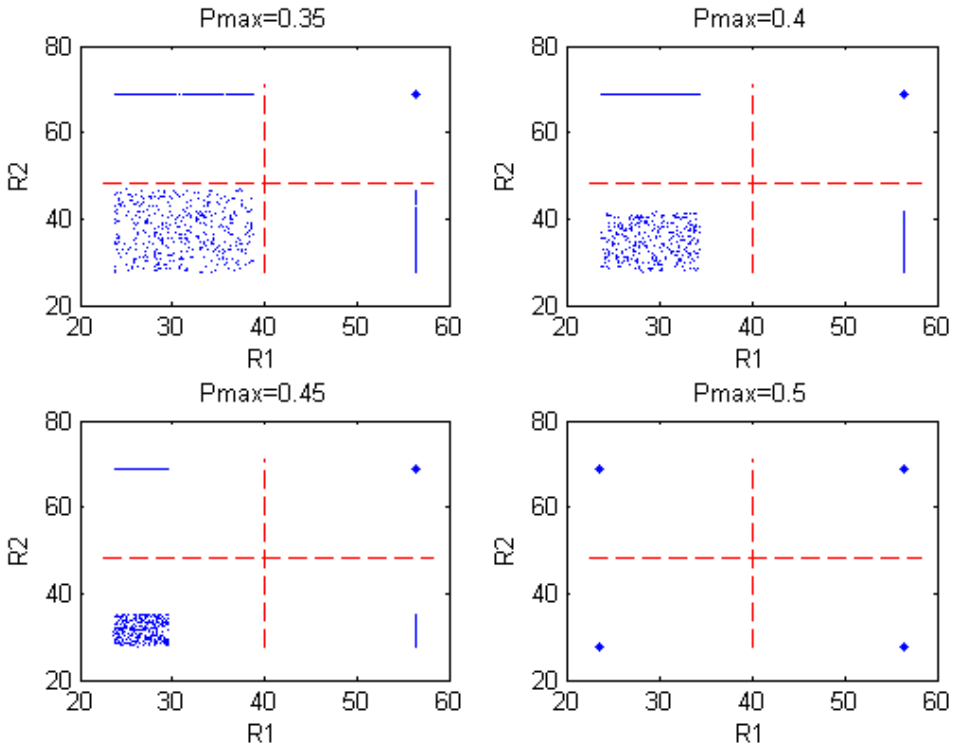

Figure 5.7: Distributions support for different Pmax values

5.8. Application to the large WSS system

A water system shown in Figure 3.11 has 9 demand zones, 3 aquifers, 5 desalination plants and 49 pipes and approximates the central part of the Israeli National Water System. The full recharge record of the 3 aquifers has 78 annual values (1932-2009, Israeli Hydrological Service). We demonstrate the RC approach based on part of this historical record (1932-2004) and then simulate the RC approach in folding mode to imitate the adoption of a Folding Robust Policy (FRP) in 2005. The results are also compared to the Folding Nominal Policy (FNP).

The ellipsoidal uncertainty set for the RC model is based on the computed means and covariance matrix of the recharge into the three aquifers:

$$\mu_{R'} = \begin{pmatrix} 210 \\ 100 \\ 81 \end{pmatrix}, \quad V_{R'} = \begin{pmatrix} 3702 & 1585 & 4576 \\ 1585 & 1255 & 3428 \\ 4576 & 3428 & 9813 \end{pmatrix} \tag{5.38}$$

According to Section 5.4.1 the uncertainty set of the annual recharge is:

$$U = \left\{ R' : \begin{pmatrix} 210 \\ 100 \\ 281 \end{pmatrix} + \begin{pmatrix} 60.84 & 0 & 0 \\ 26.05 & 24 & 0 \\ 75.2 & 61.17 & 20.34 \end{pmatrix} \begin{pmatrix} \varsigma_1 \\ \varsigma_2 \\ \varsigma_3 \end{pmatrix}, \|\varsigma\| \le \theta \right\} \tag{5.39}$$

Figure 5.8 shows the water level of the 3 aquifers according to each of the two policies. In Aquifer 1 the RP raises the water level by an almost constant increment each year. In aquifer 3 the gap between the water level obtained by the RP and the one form NP increases over time to such an extent that the water level of the NP is below the minimum water level allowed.

In aquifer 2 both policies result in the same water level over years; this is due to the limitation of the network topology associated with this aquifer, since aquifer 2 can supply only to demand zone 2, as can be seen in Figure 3.11.

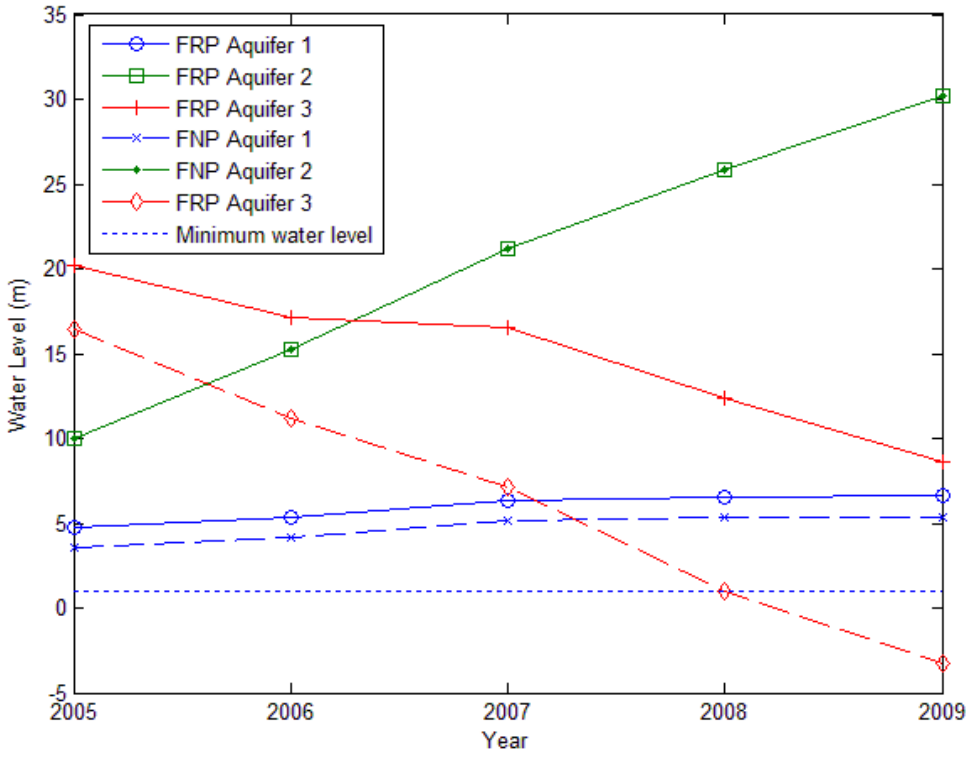

Figure 5.8: Aquifers water levels in the large system

Note:

Refer to Section 7.2.3 for Summary and Conclusion.

6. Info-Gap model

6.1. Introduction

In this Chapter we introduce the application of the Info-Gap methodology for the WSS developed in Chapter 3. As described in Chapter 2 the Info-Gap decision theory [Ben-Haim, 2006] is a non-probabilistic decision theory seeking to maximize robustness to failure instead of minimizing the objective function. Hence, the optimization problem is to find the decision x such that it will be feasible with as many as possible realizations of the uncertain parameters set.

For the model developed in this work the failure criteria are:

1. Water level in the aquifer below the minimum level.
2. Water level in the aquifer above the maximum level.
3. Operating cost is above the given budget.

The robustness analysis evaluates each feasible decision by asking: how much deviation from the replenishment estimate we can tolerate and still leads to performance within requirements. In other words the robustness of a decision is the maximum deviation allowed without failure.

This Chapter presents preliminary results for the Info-Gap application. Discussion for further research on the application of the methodology and its hybrid probabilistic version is presented in Section 7.3.4.

6.2. One year model

The Info-Gap methodology defines an uncertainty model as nested subsets $U(\alpha)$ around a point estimate $\tilde{R}$ of a parameter and range of uncertainty α: with no uncertainty, the estimate is correct, and as uncertainty increases, the subset grows, in general without bound, however in our case the recharge must have non-negative value.

The uncertainty model in this Chapter for the WSS defined in Chapter 3 is defined as:

$$U(\alpha)=\left\{R: R\geq 0, \left|R-\tilde{R}\right|\leq \alpha\right\}\ \alpha\geq 0$$
$$U(\alpha)=\left\{R:\ \max\left[0,\tilde{R}-\alpha\right]\leq R\leq \tilde{R}+\alpha\right\}\alpha\geq 0 \qquad (6.1)$$

$\tilde{R}$ – Estimated recharge

α – Uncertainty parameter

$U(\alpha)$ is a nested subset hence: $U(\alpha) \subseteq U(\beta)$ if $\alpha \le \beta$. The robustness to failure for each of the three conditions is expressed by the limit of recharge (MCM/year) that is required to meet the specified condition:

$$
\begin{aligned}
&\hat{\alpha}_1 = \max\left\{\alpha : \left(\max_{R\in U(\alpha)} \text{cost}(x,R)\right) \le \textit{Budget}\right\}\\
&\hat{\alpha}_2 = \max\left\{\alpha : \left(\max_{R\in U(\alpha)} h_f(x,R)\right) \le h_{\max}\right\}\\
&\hat{\alpha}_3 = \max\left\{\alpha : \left(\min_{R\in U(\alpha)} h_f(x,R)\right) \ge h_{\min}\right\}\\
&\hat{\alpha} = \min\left(\ \hat{\alpha}_1\ ,\ \hat{\alpha}_2\ ,\ \hat{\alpha}_3\ \right)
\end{aligned}
\qquad (6.2)
$$

x – vector of decision variables

h_f – water level in the aquifer

$\hat{\alpha}_1$ – maximum deviation which satisfy: cost ≤ Budget

$\hat{\alpha}_2$ – maximum deviation which satisfy: $h_f \le h_{\max}$

$\hat{\alpha}_3$ – maximum deviation which satisfy: $h_f \ge h_{\min}$

$\hat{\alpha}$ – maximum deviation which satisfy the 3 constrains

By satisfying all α constraints we guarantee that the decisions are such that the minimum and maximum limits on aquifer levels and the maximum limit on budget are satisfied.

6.2.1. Robustness functions

Maximum and minimum water level

The water level in the aquifer is:

$$h_f(Q_{aq}, R) = \frac{R - Q_{aq}}{SA} + h_0 \qquad (6.3)$$

For fixed Q_{aq}, $h_f(Q_{aq}, R)$ is a linear function with respect to R, thus:

$$
\begin{aligned}
&\max_{R\in U(\alpha)} h_f = \frac{\tilde{R} + \alpha - Q_{aq}}{SA} + h_0\\
&\min_{R\in U(\alpha)} h_f = \frac{\max\left[0, \tilde{R} - \alpha\right] - Q_{aq}}{SA} + h_0
\end{aligned}
\qquad (6.4)
$$

Maximum cost

The yearly operation cost is comprised of conveyance and desalination cost (not function of R) and extraction levy (function of R):

$$\text{cost}(x,R) = \text{cost(x)} + \left(1 - \frac{h_f - h_{\min}}{h_{\max} - h_{\min}}\right) \cdot CE^{\max} \cdot \text{Q}_{aq} \qquad \textbf{(6.5)}$$

For fixed x, $\text{cost}(x,R)$ is a linear function with respect to R, thus:

$$\max_{R \in U(\alpha)} \text{cost}(x,R) = \begin{cases} \text{cost}(x,R) = \text{cost(x)} + \left(1 - \dfrac{h_f^* - h_{\min}}{h_{\max} - h_{\min}}\right) \cdot CE^{\max} \cdot Q_{aq} \\ h_f^* = \dfrac{\max\left[0, \tilde{R} - \alpha\right] - Q_{aq}}{SA} + h_0 \end{cases} \qquad (6.6)$$

The robustness of staying within the budget is:

$$\hat{\alpha}_1 = \max_{\alpha \geq 0} \left\{ \alpha : \left(\underbrace{\max_{R \in U(\alpha)} \text{cost}(x,R)}_{M_1(\alpha)} \right) \leq Budget \right\} \qquad (6.7)$$

Let $M_1(\alpha)$ denotes the inner maximum, which increases with α. The robustness $\hat{\alpha}_1$ is the largest α for which $M_1(\alpha) \leq Budget$. Thus, $\hat{\alpha}_1$ is the largest solution for α of $M_1(\alpha) = Budget$. In other words, $\hat{\alpha}_1(Budget)$ is the inverse of $M_1(\alpha)$, obtained from:

$$M_1(\alpha) = \begin{cases} h_f^* = \dfrac{-Q_{aq}}{SA} + h_0 \;\; ; \;\; \text{cost(x)} + \left(1 - \dfrac{h_f^* - h_{\min}}{h_{\max} - h_{\min}}\right) \cdot CE^{\max} \cdot Q_{aq} = \text{cost}^0 \;\; ; \;\; \alpha \geq \tilde{R} \\ \\ h_f^* = \dfrac{\tilde{R} - \alpha - Q_{aq}}{SA} + h_0 \;\; ; \;\; \text{cost(x)} + \left(1 - \dfrac{h_f^* - h_{\min}}{h_{\max} - h_{\min}}\right) \cdot CE^{\max} \cdot Q_{aq} \;\; ; \;\; 0 \leq \alpha \leq \tilde{R} \end{cases} \qquad (6.8)$$

$$\hat{\alpha}_1(Budget) = \begin{cases} \infty & ; \; Budget \geq \text{cost}^0 \\ \left[\dfrac{\left(Budget - \text{cost}(x)\right) \cdot \left(h_{\max} - h_{\min}\right)}{CE^{\max} \cdot Q_{aq}} + h_0 \right] \cdot SA + \tilde{R} - Q_{aq} & ; M_1(0) \leq Budget \leq \text{cost}^0 \end{cases} \qquad (6.9)$$

$\hat{\alpha}_1 - \text{maximum deviation which satisfy the} \quad \text{cost} \leq \text{Budget}$

The robustness against failure of meeting a specified $h_{\max}$ is:

$$\hat{\alpha}_2 = \max_{\alpha \geq 0} \left\{ \alpha : \left(\underbrace{\max_{R \in U(\alpha)} h_f(x,R)}_{M_2(\alpha)} \right) \leq h_{\max} \right\} \qquad (6.10)$$

Let $M_2(\alpha)$ denote the inner maximum, which increases with α. The robustness $\hat{\alpha}_2$ is the largest α for which $M_2(\alpha) \le h_{\max}$. Thus, $\hat{\alpha}_2$ is the largest solution for α of $M_2(\alpha) = h_{\max}$ .In other words, $\hat{\alpha}_2(h_{\max})$ is the inverse of $M_2(\alpha)$.

$$M_2(\alpha) = \frac{\tilde{R} + \alpha - Q_{aq}}{SA} + h_0 \;\; ; \alpha \ge 0 \tag{6.11}$$

$$\hat{\alpha}_2(h_{\max}) = \left(h_{\max} - h_0\right) \cdot SA + Q_{aq} - \tilde{R} \;\; ; \;\; h_{\max} \ge M_2(0)$$
$$\hat{\alpha}_2 - \text{maximum deviation which satisfy } h_f \le h_{\max} \tag{6.12}$$

The robustness against failure of meeting a specified $h_{\min}$ is:

$$\hat{\alpha}_3 = \max_{\alpha \ge 0} \left\{ \alpha : \left(\underbrace{\min_{R \in U(\alpha)} h_f(x,R)}_{M_3(\alpha)} \right) \ge h_{\min} \right\} \tag{6.13}$$

Let $M_3(\alpha)$ denote the inner minimum. $M_3(\alpha)$ decreases as α increases. The robustness $\hat{\alpha}_3$ is the greatest α at which $M_3(\alpha) \ge h_{\min}$. Thus, $\hat{\alpha}_3$ is greatest solution for α of $M_3(\alpha) = h_{\min}$ .In other words, $\hat{\alpha}_3(h_{\min})$ is the inverse of $M_3(\alpha)$.

$$M_3(\alpha) = \begin{cases} \left(\dfrac{-Q_{aq}}{SA} + h_0 \right) = h^* & ; \alpha \ge \tilde{R} \\ \dfrac{\tilde{R} - \alpha - Q_{aq}}{SA} + h_0 & ; 0 \le \alpha \le \tilde{R} \end{cases} \tag{6.14}$$

$$\hat{\alpha}_3(h_{\min}) = \begin{cases} \infty & ; h_{\min} \le h^* \\ \tilde{R} - Q_{aq} - \left(h_{\min} - h_0\right) \cdot SA & ; h^* \le h_{\min} \le M_3(0) \end{cases} \tag{6.15}$$
$$\hat{\alpha}_3 - \text{maximum deviation which satisfy } h_f \ge h_{\min}$$

The robustness for against all three failures is:

$$\hat{\alpha}(x, Budget, h_{\max}, h_{\min}) = \min(\hat{\alpha}_1, \hat{\alpha}_2, \hat{\alpha}_3)$$
$$\hat{\alpha} \;\; - \text{maximum deviation which satisfy the 3 constrains} \tag{6.16}$$

By satisfying all α constraints we guarantee that the decisions are such that the minimum and maximum limits on aquifer levels and the maximum limit on budget are satisfied.

6.2.2. Example 1

In this example we solve the small network in Figure 3.1, with the parameter set defined in Section 3.8. The estimated aquifer recharge is set to $\tilde{R} = 50$ (MCM) and the maximum specific levy is set to $\left(\overline{CE}^{\max}\right) = 1 \ \ (M\$ / MCM)$.

The Info-Gap formulation above does not consider uncertainty in the salinity balance equation, as it considers only the uncertain recharge in the water level equation of the aquifer. To overcome this drawback the recharge salinity was set to $C_R = 180 \ (mgcl / lit)$, equal to the initial salinity. Since the recharge salinity is equal to the initial salinity the aquifer salinity remains constant $180 \ (mgcl / lit)$ for all values of the recharge.

Comparing operation rules

In this Section we compare the robustness of two possible operation rules $x_1 \ and \ x_2$, for explaining the workings of the Info-Gap approach.

Operation rule x_1: extract 10 (MCM) from the aquifer and as a consequence, given the yearly demand of 100 (MCM), the desalination amount is 90 (MCM). Recalling that the aquifer salinity is constant $180 \ (mgcl / lit)$, we set the salinity at the demand nodes to the maximum admissible value $C_z = 190 \ (mgcl / lit)$ and to insure this value at the demand nodes the desalinated water salinity at the plant has been set to $C_d = 191.1 \ (mgcl / lit)$ i.e., $RR_d = 99.29 \ (\%)$. The aquifer water is equally distributed in pipes 1, 2 since these are identical, $Q_{1,2} = 10 / 2 = 5 \ (MCM)$. In the same manner, the desalinated water is equally distributed $Q_{3,4} = 90 / 2 = 45 \ (MCM)$. Each of the intermediate nodes 3 and 4 has $45 + 5 = 50 \ (MCM)$, recalling that since pipes 5-8 have identical parameters this results in $Q_{5-8} = 25 (MCM)$

Operation rule x_2: extract 30 (MCM) from the aquifer and as a consequence, given yearly demand of 100 (MCM), the desalination amount is 70 (MCM). Following the same explanation as above, $C_d = 194.3 \ (mgcl / lit)$, i.e., $RR_d = 99.28 \ (\%)$, $Q_{1,2} = 15 \ (MCM)$, $Q_{3,4} = 35 \ (MCM)$, $Q_{5-8} = 25 \ (MCM)$

Figure 6.1 shows the robustness functions $\hat{\alpha}_{1,2,3}$ and the overall robustness $\hat{\alpha}$ (when $h_{\min} = 1, h_{\max} = 100$) for both operation rules x_1 and x_2. The alphas $\hat{\alpha}_{1,2,3}$ are the limits of

the recharge that satisfy the constraint on the maximum budget and on the maximum and the minimum levels, respectively.

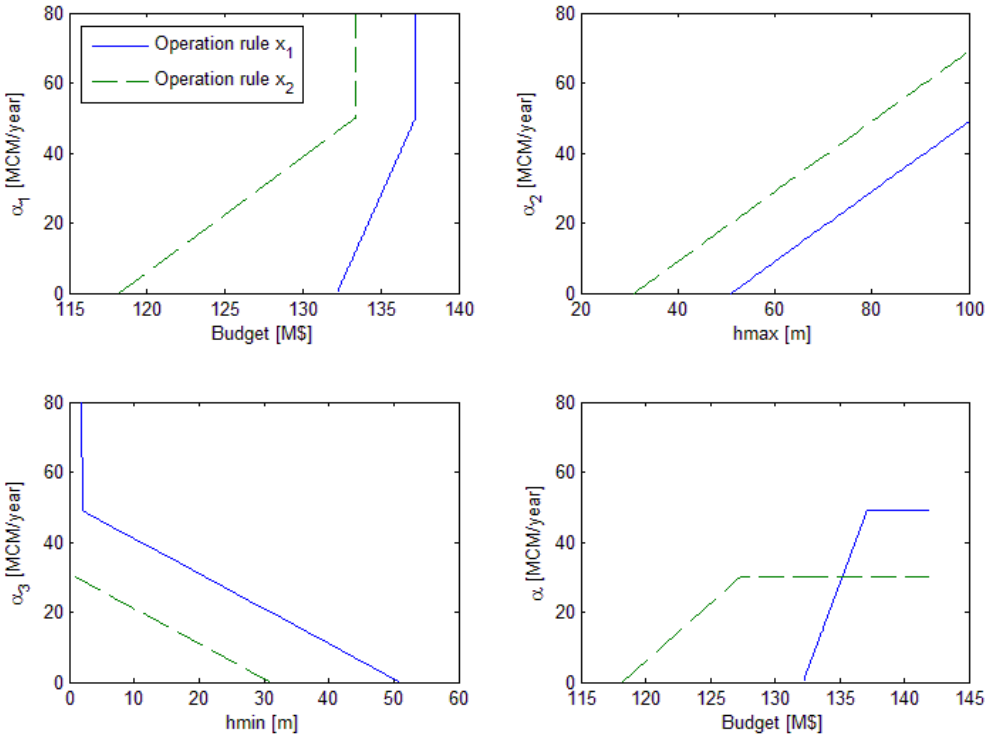

Figure 6.1: Example 1, robustness for: (a) budget (b) maximum water level (c) minimum water level (d) overall system.

The overall robustness $\hat{\alpha}$ is defined as: $\min(\hat{\alpha}_1, \hat{\alpha}_2, \hat{\alpha}_3)$, since $h_{\min} = 1, h_{\max} = 100$ (m) $\hat{\alpha}_2^{x_1} = 49$, $\hat{\alpha}_2^{x_2} = 69$, $\hat{\alpha}_3^{x_1} = \infty$ and $\hat{\alpha}_3^{x_2} = 30$ (MCM).

For operation rule x_1 the maximum robustness is 49 (MCM) which is obtained as a result of $\hat{\alpha}_2^{x_1} = 49$. The maximum robustness for x_2 is 30 (MCM) which is obtained as a result of $\hat{\alpha}_3^{x_2} = 30$. Comparing the overall robustness shows that the operation rule x_2 is preferred for budget bellow 135.2 (M$), since its robustness is higher. The robustness curves for the cross over at this value. For budget above 135.2 (M$), x_1 result in higher robustness and thus it may be preferred to x_2. Deciding to allocate a budget above 135.2 (M$) is a subjective matte. For example, the operation rule x_2 provides robustness of 30 (MCM) with budget 127.5 (M$) while x_1 provides maximum robustness 49 (MCM) with budget 137.1 (M$). Hence, the decision maker should decide whether it is justified to add 9.6 (M$) in order to get 19 (MCM) of robustness.

Note that the operation rule x_1 is not even feasible below a budget of 132.1 (M$), since the budget with $\hat{\alpha} = 0$ indicates the cost associated with the estimated recharge (without uncertainty).

6.2.3. Optimization

For predefined $(Budget, h_{\max}, h_{\min})$ we can search for the maximum allowed deviation $\hat{\alpha}$. In this optimization problem we must satisfy all the constraints of the original model plus the constraints from the Info-Gap formulation.

$$\begin{aligned} &\max_{x} \quad \left[\min(\hat{\alpha}_1, \hat{\alpha}_2, \hat{\alpha}_3)\right] \\ &\text{s.t.} \\ &M_1(0) \le Budget \\ &M_2(0) \le h_{\max} \\ &M_3(0) \ge h_{\min} \\ &x \in C(x) \end{aligned} \tag{6.17}$$

6.2.4. Example 2

Consider the WSS in Figure 6.2 which includes one aquifer, one desalination plant and one demand zone with demand of 100 MCM.

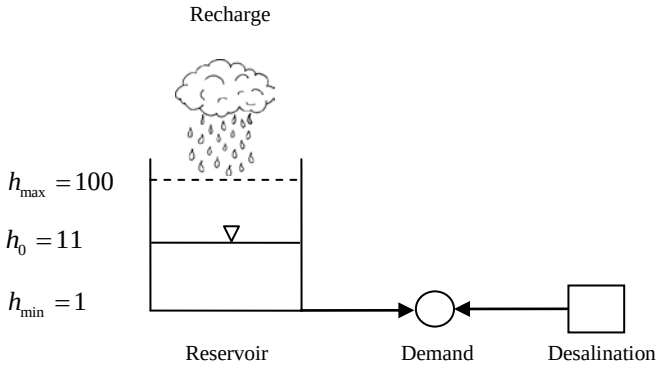

Figure 6.2: Example 2, WSS layout

The total operation cost is comprised of linear desalination cost and an extraction levy. Hence, the deterministic formulation for this model is:

$$\begin{aligned} &\min_{Q_{aq}} \left[des \cdot (100\text{-}Q_{aq}) + \left(1 - \frac{h - h_{\min}}{h_{\max} - h_{\min}}\right) \cdot CE^{\max} \cdot Q_{aq} \right] \\ &s.t. \\ &h = 11 + \frac{R - Q_{aq}}{SA} \\ &h_{\min} \le h \le h_{\max} \\ &0 \le Q_{aq} \le 100 \end{aligned} \tag{6.18}$$

Following the Info-gap model developed above with $des = 1.41(M\$/MCM)$, $CE^{\max} = 1(M\$/MCM)$, $SA = 1(MCM/m)$ and estimated recharge $\tilde{R} = 50(MCM)$ the optimization problem for the Info-Gap (6.17) has one decision variable Q_{aq}. The required functions for formulation of the optimization problem are:

$$\hat{\alpha}_1(Budget) = \left[\frac{\left(Budget - 1.42 \cdot (100\text{-}Q_{aq})\right) \cdot 99}{Q_{aq}} + 11 \right] + 50 - Q_{aq} \tag{6.19}$$

$$\hat{\alpha}_2(h_{\max} = 100) = 39 + Q_{aq} \tag{6.20}$$

$$\hat{\alpha}_3(h_{\min} = 1) = 60 - Q_{aq} \tag{6.21}$$

$$M_2(0) = M_3(0) = 61 - Q_{aq} \tag{6.22}$$

$$M_1(0) = 1.42 \cdot (100\text{-}Q_{aq}) + \left(1 - \frac{60 - Q_{aq}}{99}\right) \cdot Q_{aq} \tag{6.23}$$

Figure 6.3, shows the overall robustness function $\hat{\alpha}(Q_{aq}, Budget)$ for different values of the budget. The last subfigure includes range of budget form 115-140 M$ by step of 1 M$. The tradeoff “maximum robustness vs. aquifer withdrawal” and the tradeoff of the “maximum robustness vs. budget” are given in Figure 6.4.

The first tradeoff (Figure 6.4a) shows that the robustness decreases as we extract more form the aquifer. The tradeoff is divided into two ranges, the first (left) is the range in which the aquifer withdrawal is not high, and hence the optimal points in Figure 6.3d are on the line $\hat{\alpha}_3(h_{\min} = 1) = 60 - Q_{aq}$, the second range (right) is where the aquifer withdrawal is high and the optimal points in Figure 6.3d are on the nonlinear function $\hat{\alpha}_1(Budget)$ not on the intersection with $\hat{\alpha}_3(h_{\min} = 1)$.

The second tradeoff (Figure 6.4b) shows also almost linear relation between the budget and the robustness. This is because, the vertical distance between the optimal points in Figure 6.3d is almost constant, hence the slope of the tradeoff is almost constant (linear). The last segment in the tradeoff is constant at value 49.5 (MCM) this is because beyond budget 137 M$ all the robustness functions have the same optimal point which is the intersection of the two linear lines $\hat{\alpha}_3(h_{\min} = 1)$ and $\hat{\alpha}_2(h_{\max} = 100)$.

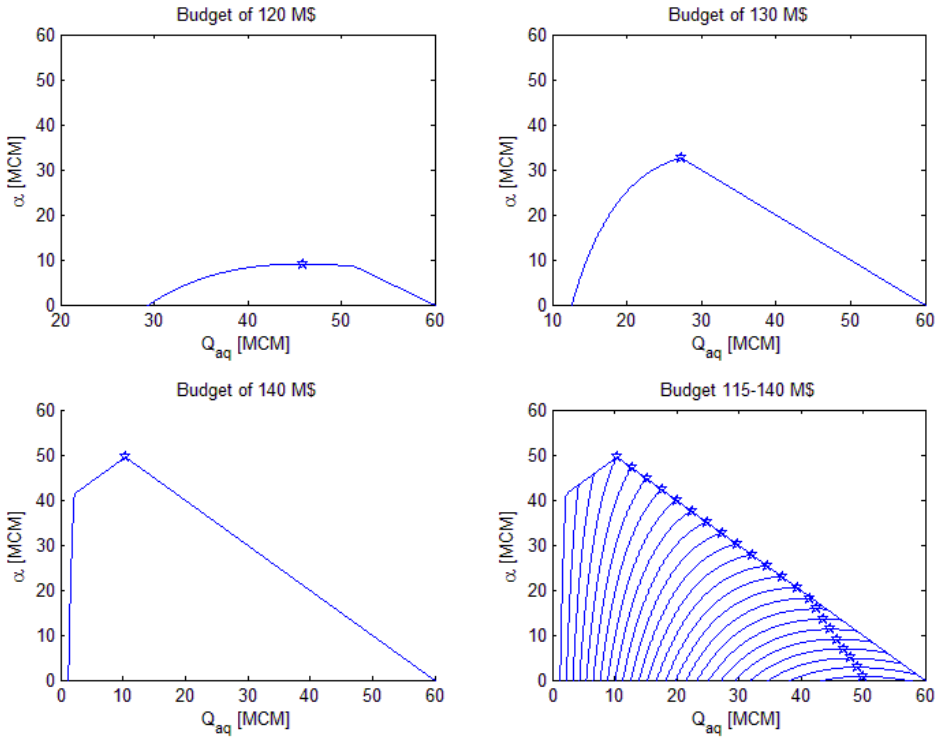

Figure 6.3: Example 2, robustness as a function of the aquifer withdrawal with different values of budget.

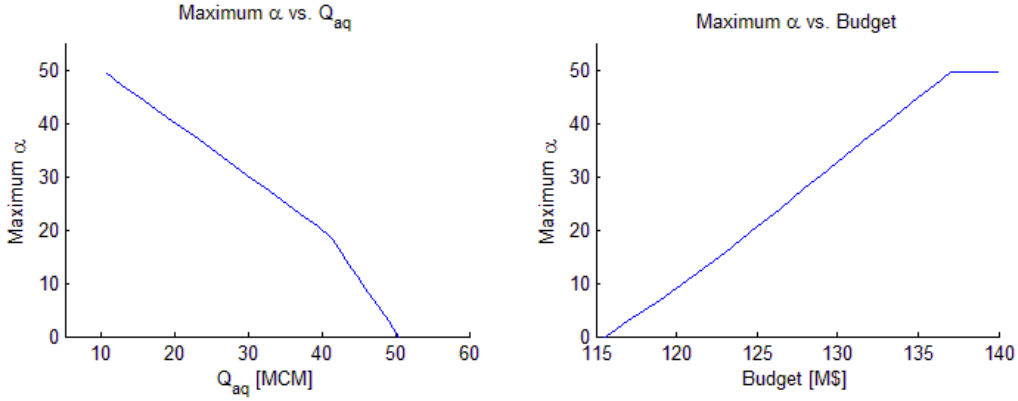

Figure 6.4: Example 2, maximum robustness tradeoffs: (a) maximum robustness vs. aquifer withdrawal (b) maximum robustness vs. budget

When the budget is very high the robustness is given by $\hat{\alpha} = \min(\hat{\alpha}_2, \hat{\alpha}_3)$. The maximum of α is obtained at the intersection point of $\hat{\alpha}_2, \hat{\alpha}_3$ since the first is increasing linearly and the second is decreasing linearly with the decision variable Q_{aq}. The solution of $\hat{\alpha}_2(h_{\max}) = \hat{\alpha}_3(h_{\min})$ for Q_{aq} results in the optimal aquifer extraction for high (or unlimited) budget. The solution is:

$$Q_{aq}^{*} = \tilde{R} - \frac{\left(h_{\min} + h_{\max} - 2h_0\right) \cdot SA}{2} \qquad (6.24)$$

In the above example $Q_{aq}^{*} = 10.5(MCM)$ as shown in Figure 6.3d.

6.2.5. Example 3

Further to example 1 for the WSS in Figure 3.1, we can show that the two decision rules x_1 and x_2 are not optimal for every given budget. To obtain the optimal decision rule for a specified budget we have to solve the optimization problem (6.17). This optimization problem has a vector of decision variables, hence we cannot show the graphs of the robustness as we did in example 2. Instead we can solve the optimization problem numerically. The problem was solved by the interior-point algorithm within FMINCON in Matlab, after an auxiliary variable was introduced to replace the minimum operator in the objective function.

Figure 6.5, shows the tradeoff between the maximum robustness and the budget for optimal decisions, along with tradeoff of operation rule x_1 and operation rule x_2.

The optimal operation line in Figure 6.5 shows the maximum robustness obtained from the optimization model (6.17). Hence, it outperforms the pre-determined operation rules from example 1. Note that for each point on the optimal operation line there is different decision rule.

As shown in the Figure 6.5, the decision x_1 resulted in lower robustness for all values of the budget. In contrast, decision x_2 is optimal solution when the budget is equal to 127.3 M$ and only in this situation, since it resulted in lower robustness in the remaining points.

For each point in the optimal robustness tradeoff we have the decision vector corresponding to that point. For any given budget the optimization problem (6.17) provides the optimal extraction, the optimal water distribution in the network and the optimal removal ratio which maximize the robustness of the system operation.

The maximum robustness obtained at a budget of 137 (M$), increasing the budget beyond this value will not increase the robustness since it is no longer the limiting factor. In this case the optimal robustness is obtained by considering $\hat{\alpha} = \min(\hat{\alpha}_2, \hat{\alpha}_3)$.

The optimal robustness in this case obtained when $\hat{\alpha}_2, \hat{\alpha}_3$ which will result in optimal aquifer extraction of Q_{aq}^* in Equation (6.24) as explained in the previous example.

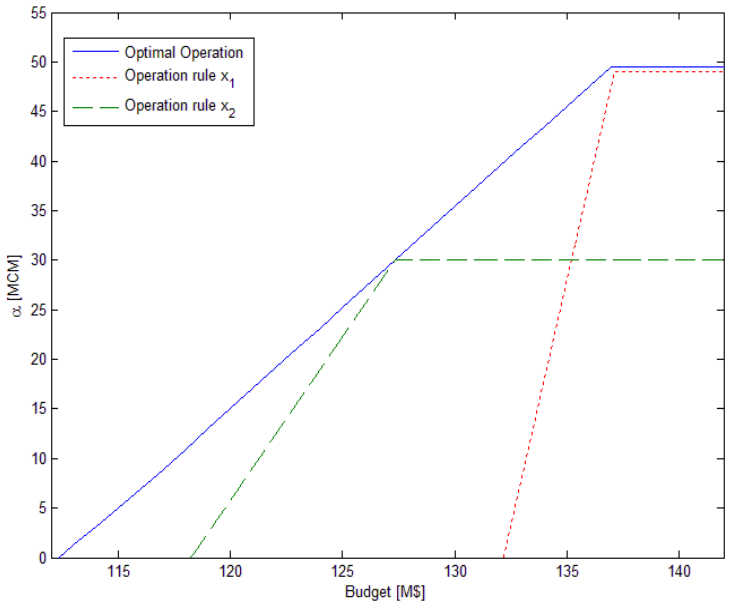

Figure 6.5: Example 3, maximum robustness vs. budget

As discussed in Section 3.8, because of the parameter set chosen for the network, the conveyance costs are not a significant portion of the objective function and for this reason the conveyance aspect did not change the optimal solution significantly. To show the influence of the conveyance cost on the optimal tradeoff, all pipes diameters were set to 15 (in) instead of 50 (in) as in the original run. Figure 6.6a compares the optimal robustness tradeoff from Figure 6.5 with the tradeoff after increasing the conveyance cost.

The tradeoff is also highly dependent on the other parameters in the objective function, for example the maximum specific extraction levy $CE^{\max}$. Figure 6.6b show this influence of the extraction levy by modifying the original parameters of the example to $CE^{\max} = 1.5(M\$)$.

Decreasing the pipes' diameters increases the conveyance cost, and as a result the tradeoff is shifted to the right. Moreover, since the conveyance cost is calculated by the non-linear Hazen Williams Formula, the tradeoff imposes more non-linearity. Increasing the maximum extraction levy coefficient results in more weight for the extraction cost in the objective function, as a result the tradeoff is shifted to the right and it is imposes more non-linearity since the extraction cost is non-linear (quadratic).

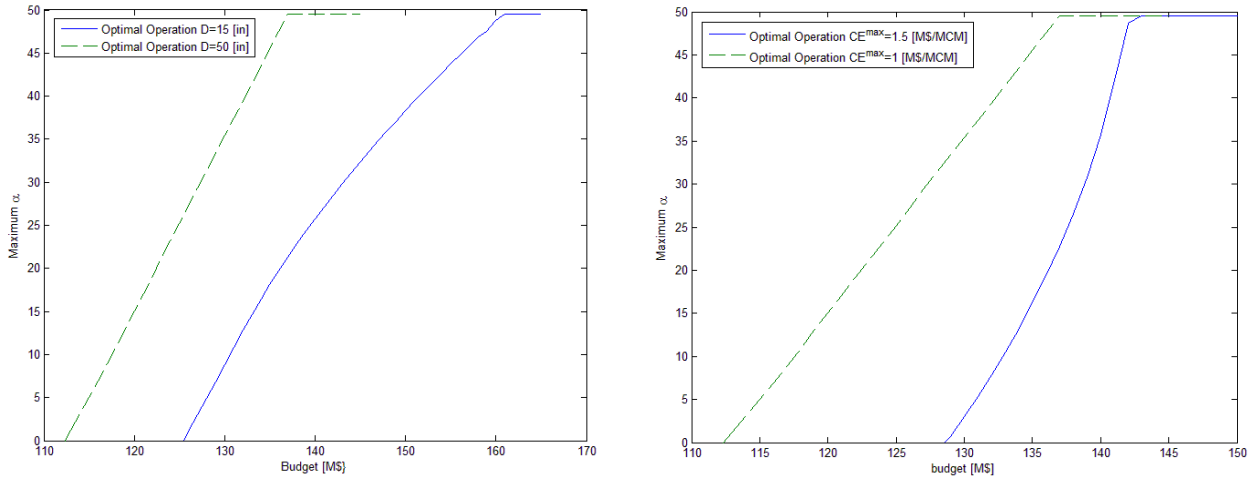

Figure 6.6: Example 3, maximum robustness vs. budget: (a) influence of the network parameters (b) influence of the aquifer parameters

6.3. Multi-year model

The multi-year uncertainty model in this Chapter is defined as:

$$
\begin{aligned}
&U(\alpha) = \left\{ R^t : R^t \geq 0, \left| R^t - \tilde{R}^t \right| \leq \alpha \ \forall t \right\} \ \alpha \geq 0 \\
&U(\alpha) = \left\{ R^t : \ \max\left[0, \tilde{R}^t - \alpha\right] \leq R^t \leq \tilde{R}^t + \alpha \ \forall t \right\} \ \alpha \geq 0 \\
&\tilde{R}^t - \text{Estimated recharge at year } t = 1..T \\
&\alpha - \text{Maximum deviation}
\end{aligned}
\qquad \textbf{(6.25)}
$$

6.3.1. Robustness functions

$$
\begin{aligned}
&\hat{\alpha}_1 = \max\left\{ \alpha : \left(\max_{R^t \in U(\alpha)} \cos t(x, R^{t=1..T}) \right) \leq Budget \right\} \\
&\hat{\alpha}_2^{t=1..T} = \max\left\{ \alpha : \left(\max_{R^t \in U(\alpha)} h_f^t(x, R^{i=1..t}) \right) \leq h_{\max} \right\} \\
&\hat{\alpha}_3^{t=1..T} = \max\left\{ \alpha : \left(\min_{R \in U(\alpha)} h_f^t(x, R^{i=1..t}) \right) \geq h_{\min} \right\} \\
&\hat{\alpha} = \min\left(\ \hat{\alpha}_1 \ , \ \hat{\alpha}_2^{t=1..T} \ , \ \hat{\alpha}_3^{t=1..T} \ \right)
\end{aligned}
\qquad (6.26)
$$

In the previous Section we showed that the water level is a linear function with respect to R, thus:

$$
\begin{aligned}
&\max_{R \in U(\alpha)} h_f^t = \sum_{i=1}^{t} \left(\frac{\tilde{R}^i + \alpha - Q_{aq}^i}{SA} \right) + h_0 \\
&\min_{R \in U(\alpha)} h_f^t = \sum_{i=1}^{t} \left(\frac{\max\left[0, \tilde{R}^i - \alpha\right] - Q_{aq}^i}{SA} \right) + h_0
\end{aligned}
\qquad (6.27)
$$

The operation cost is comprised of conveyance and desalination cost (not function of R) and extraction levy (function of R). The cost function is also a linear function with respect to R, thus:

$$\max_{R\in U(\alpha)} \text{cost}(x,R)=\text{cost(x)} - \frac{CE^{\max}}{h_{\max}-h_{\min}}\sum_{t=1}^{T}\left(\sum_{i=1}^{t}\left(\frac{\max\left[0,\tilde{R}^i-\alpha\right]-Q_{aq}^i}{SA}\right)+h_0\right)\cdot Q_{aq}^t \tag{6.28}$$

The robustness of failure for meet a specified budget is:

$$\hat{\alpha}_1=\max_{\alpha\geq 0}\left\{\alpha:\left(\underbrace{\max_{R\in U(\alpha)}\text{cost}(x,R)}_{M_1(\alpha)}\right)\leq Budget\right\} \tag{6.29}$$

Let $M_1(\alpha)$ denote the inner maximum. $M_1(\alpha)$, which increases with α. The robustness $\hat{\alpha}_1$ is the largest α for which $M_1(\alpha)\leq Budget$. Thus, $\hat{\alpha}_1$ is the largest solution for α of $M_1(\alpha)=Budget$. In other words, $\hat{\alpha}_1(Budget)$ is the inverse of $M_1(\alpha)$. To write an explicit expression for $M_1(\alpha)$ we define a vector δ with elements δ^t $t=1..T$ where:

$$\delta^t=\begin{cases}0\ ;\ \alpha\geq\tilde{R}^t\\ 1\ ;\ \alpha<\tilde{R}^t\end{cases} \tag{6.30}$$

$$M_1(\alpha)=\begin{cases}\text{cost(x)} - \dfrac{CE^{\max}}{h_{\max}-h_{\min}}\displaystyle\sum_{t=1}^{T}\left(\sum_{i=1}^{t}\left(\frac{-Q_{aq}^i}{SA}\right)+h_0\right)\cdot Q_{aq}^t=\text{cost}^0\ ;\ \text{if}\ \sum_{t=1}^{T}\delta^t=0\\ \text{cost(x)} - \dfrac{CE^{\max}}{h_{\max}-h_{\min}}\displaystyle\sum_{t=1}^{T}\left(\sum_{i=1}^{t}\left(\frac{\delta^i\left(\tilde{R}^i-\alpha\right)-Q_{aq}^i}{SA}\right)+h_0\right)\cdot Q_{aq}^t\ ;\ \text{if}\ \alpha\geq 0\ \text{and}\ \sum_{t=1}^{T}\delta^t\neq 0\end{cases} \tag{6.31}$$

$$\hat{\alpha}_1(Budget)=\begin{cases}\infty & ;\ Budget>\text{cost}^0\\ \left[\begin{array}{l}\dfrac{\left(Budget-\text{cost}(x)\right)\cdot\left(h_{\max}-h_{\min}\right)}{CE^{\max}}+....\\ ...+\displaystyle\sum_{t=1}^{T}h_0\cdot Q_{aq}^t+\sum_{t=1}^{T}\left(\sum_{i=1}^{t}\frac{\delta^i\tilde{R}^i-Q_{aq}^i}{SA}\right)\cdot Q_{aq}^t\end{array}\right]\cdot\dfrac{SA}{\displaystyle\sum_{t=1}^{T}\left(\left(\sum_{i=1}^{t}\delta^i\right)\cdot Q_{aq}^t\right)} & ;\ M_1(0)\leq Budget\leq\text{cost}^0\end{cases} \tag{6.32}$$

In the same manner the robustness for failure in the water level limits are:

$$M_2^t(\alpha)=\sum_{i=1}^{t}\left(\frac{\tilde{R}^i+\alpha-Q_{aq}^i}{SA}\right)+h_0\ \ ;\ \forall t=1..T \tag{6.33}$$

$$\hat{\alpha}_2^t(h_{\max})=\frac{\left(h_{\max}-h_0\right)\cdot SA-\displaystyle\sum_{i=1}^{t}\left(\tilde{R}^i-Q_{aq}^i\right)}{t}\ \ ;\ h_{\max}\geq M_2^t(0)\ \ ;\ \forall t=1..T \tag{6.34}$$

$$M_3^t(\alpha)=\begin{cases}\sum_{i=1}^{t}\left(\dfrac{-Q_{aq}^i}{SA}\right)+h_0=h_*^t & ;\text{ if } \sum_{t=1}^{T}\delta^t=0\\ \sum_{i=1}^{t}\left(\dfrac{\delta^i\left(\tilde{R}^i-\alpha\right)-Q_{aq}^i}{SA}\right)+h_0 & ;\text{ if } \alpha\geq 0 \text{ and } \sum_{t=1}^{T}\delta^t\neq 0\end{cases} \tag{6.35}$$

$$\hat{\alpha}_3^t(h_{\min})=\begin{cases}\infty & ;\ h_{\min}<h_*^t\\ \dfrac{\sum_{i=1}^{t}\left(\delta^i\tilde{R}^i-Q_{aq}^i\right)-\left(h_{\min}-h_0\right)\cdot SA}{\sum_{i=1}^{t}\delta^i} & ;\ h_*^t\leq h_{\min}\leq M_3^t(0)\end{cases} \tag{6.36}$$

The robustness for the three kinds of failure for all years is:

$$\hat{\alpha}(x,Budget,h_{\max},h_{\min})=\min\left(\ \hat{\alpha}_1\ ,\ \hat{\alpha}_2^{t=1..T}\ ,\ \hat{\alpha}_3^{t=1..T}\ \right) \tag{6.37}$$

6.3.2. Example

In this example we solve the small network in Figure 3.1, for 4 years. The estimated recharge for the 4 years is $\tilde{R}^{t=1..4}=[5,10,15,20](MCM)$.The same physical parameters of the network from example 1 are considered with maximum specific levy is set to $\left(\overline{CE}^{\max}\right)=1\ \ (M\$/MCM)$. The storativity is $SA=0.8(MCM/m)$, and the two demands are set to 15 (MCM) each. The initial, minimum and maximum water levels in the aquifer are 25, 0 and 50 (m), respectively.

Comparing operation rules

Using the robustness functions we can compare the robustness of different operation rules. Two operation rules $x_1\ and\ x_2$ are compared in this example: the first x_1 is extracting 10 (MCM) from the aquifer in each of the 4 years, while the second is extraction 5 (MCM) in each year. The distribution of the sources water in the network follows the explanation in example 1.

Figure 6.7, show the robustness $\hat{\alpha}_3(Budget)$ for the defined level limits $h_{\max}=50(m)$ and $h_{\min}=0(m)$. For instance, when the budget is 18.5 (M$) the operation rule x_1 allows a deviation of 6.3 (MCM/year) without exceeding the budget constraint, while operation rule x_2 allows only a deviation of 3.5 (MCM/year). The budget for which the robustness is infinite is the one which corresponds to the cost of relying only on the initial storage of the aquifer, without any recharge.

As shown in Figure 6.7 when the budget is below 19 (M$) operation rule x_1 allows more deviation in the recharge than the rule x_2, and it is preferred in terms of robustness to budget failure. However, there are other failure criteria which along with the robustness to budget failure determine the overall robustness of the decision rule. Thus, we cannot conclude yet, which operation rule is preferred in terms of overall robustness.

Note that the breakpoints in the tradeoff are not a result of coarse resolution in the budget axis. These are actual breakpoints obtained because of the presence of the vector δ in Equation (6.32) which includes the binary variables depending on the value of budget.

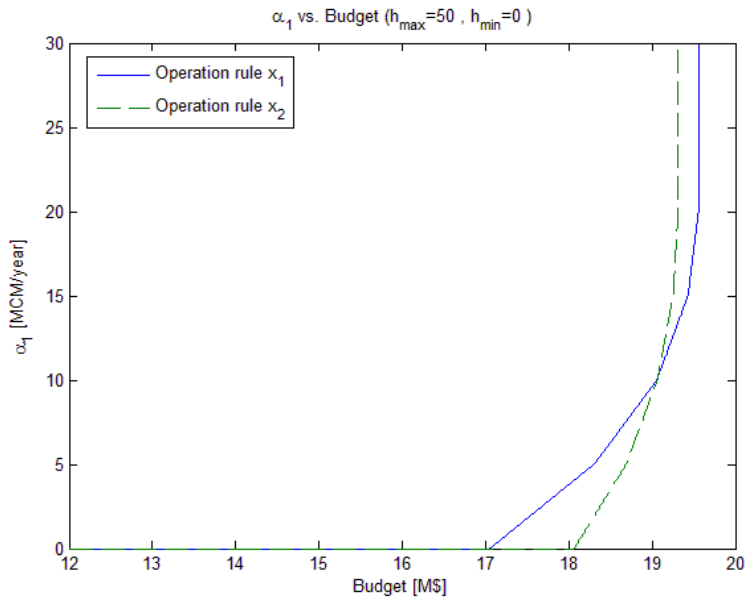

Figure 6.7: Multi-year example, robustness for budget violation

Figure 6.8 shows the robustness $\hat{\alpha}_2^t(h_{\max})$ and $\hat{\alpha}_3^t(h_{\min})$ for each of the 4 years, respectively. For the rule x_1 when $h_{\min}=0$ the deviation allowed in the third year is the minimum among all years, hence the yearly deviation of $\hat{\alpha}_3^{x_1}$ is 7.5 (MCM/year) insures no failure in the minimum water level constraints for all years.

For operation rule x_2, the robustness $\hat{\alpha}_3^{x_2}=\infty$, meaning that no matter how large the deviation is, no failure will occur in the minimum water level constraints for all years. For the maximum water level failure $h_{\max}=50(m)$, yearly deviation of $\hat{\alpha}_2^{x_1}=2.5$ insures no failure in all years when operation rule x_1 is applied. In contrast, there is no yearly

deviation which insures no failure at all years, hence $\hat{\alpha}_2^{x_2} = 0$ (MCM/year) as a result of $\hat{\alpha}_2^4 = 0$ at $h_{\max} = 50(m)$. From this analysis, we can conclude that the overall robustness of x_2 is zero i.e. $\hat{\alpha}^{x_2} = 0$, while the overall robustness of x_1 is positive value $\hat{\alpha}^{x_1} = \min(\hat{\alpha}_1(budget), 2.5)$.

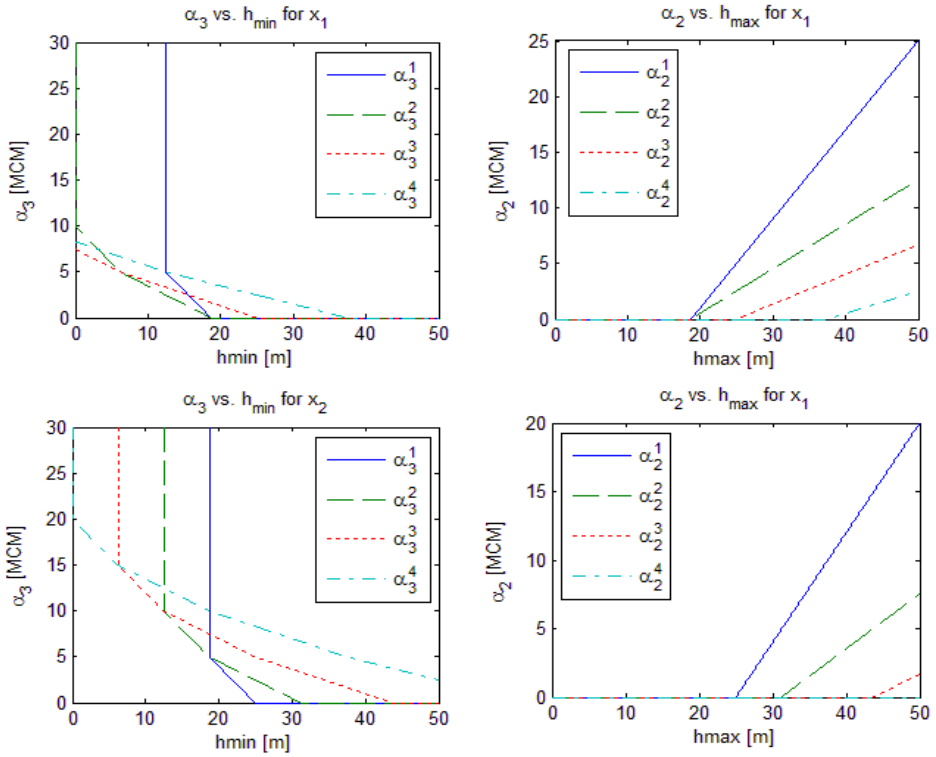

Figure 6.8: Multi-year example, robustness for: (a) minimum water level, decision 1 (b) maximum water level, decision 1 (c) minimum water level, decision 2 (d) maximum water level, decision 2.

For predefined $(Budget, h_{\max}, h_{\min})$ we can search for the maximum robustness $\hat{\alpha}$ by an optimization problem similar to (6.17). This optimization problem includes $\hat{\alpha}_2^t(h_{\max})$ and $\hat{\alpha}_3^t(h_{\min})$ for each $t = 1..T$.

Figure 6.9, shows the tradeoff between the maximum robustness and the budget for different runs, each with different time horizon. The optimal tradeoff for the 4 year horizon along with robustness of the tradeoff operation rule x_1 are shown in the Figure 6.9d. The results show that the operation rule x_1 was not optimal, since for each budget in the interval there is higher robustness which obtained by the optimizing the decision variables.

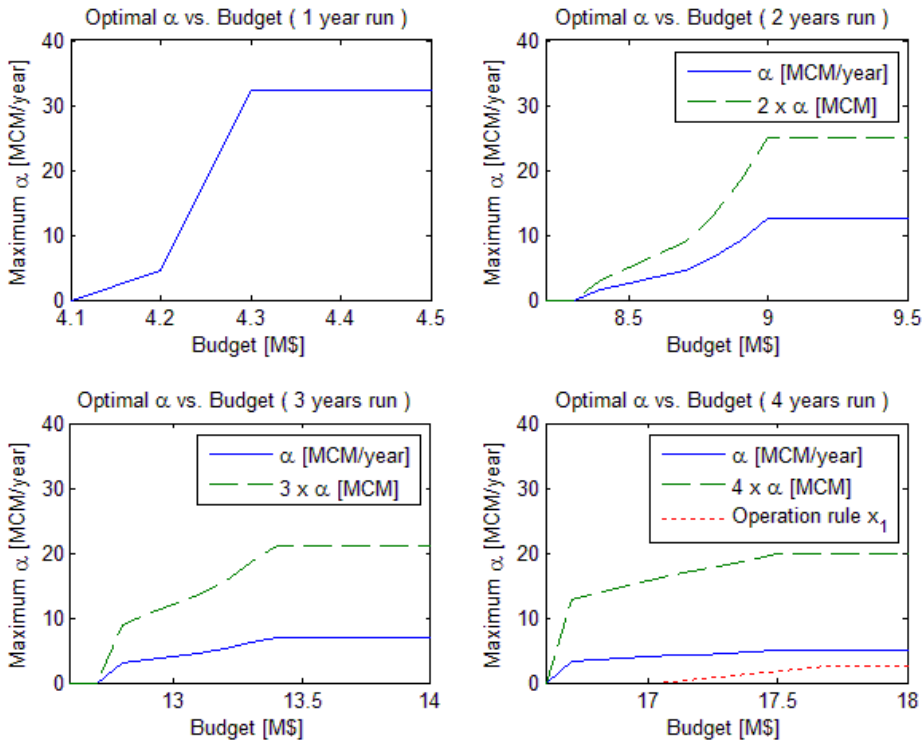

Figure 6.9: Multi-year example, maximum robustness for: (a) 1 year horizon (b) two years horizon (c) three years horizon (d) 4 years horizon.

Comparing the different tradeoffs obtained for different horizons shows that the budget tradeoff shrinks when the operation horizon is increased. For instance, when we solve a 4 year problem, the maximum (constant value) is almost obtained close to left side of the tradeoff interval. The conclusion to be drawn is that the budget is becoming less limiting in determining the robustness as the operation horizon increases. This can also be concluded from the definition of the robustness, since as the horizon increases more $\hat{\alpha}_2^t(h_{\max})$ and $\hat{\alpha}_3^t(h_{\min})$ are involved in the minimum operator, hence, there will be less profit from increasing the budget.

Note that, in the multi-year runs the robustness is the deviation allowed for each year in the horizon, the deviation for the entire horizon is given by the robustness multiplied by the operation horizon length as shown on Figure 6.9.

6.4. Discussion 1

The Info-Gap methodology as described by Ben-Haim [2006] involves the following components: (a) defining the failure criteria (b) solving for the inner

maximum/minimum in the robustness functions, Equations (6.8), (6.11), (6.14) (c) finding the robustness by extracting the failure indices from the robustness functions, i.e., find the inverse of the functions from the second step Equations (6.9), (6.12), (6.15) (d) defining the overall robustness by (6.16).

When the Info-Gap model is used to compare different alternatives the explicit closed forms of the robustness functions (6.9), (6.12) and (6.15) can be used. However, we claim that these steps are not essential when we solve the Info-Gap model within optimization problem such as (6.17). The maximum robustness of the system could be obtained without explicit definition for each failure as individual function, and more important with no need to define the inverse functions.

To demonstrate this claim the optimization problem (6.17) is transformed to another optimization problem. In the objective functions we have $\min(\hat{\alpha}_1, \hat{\alpha}_2, \hat{\alpha}_3)$ which could be formulated as the following maximization problem by using auxiliary variable $\hat{\alpha}$:

$$\begin{aligned} &\max_{\hat{\alpha}} \ \hat{\alpha} \\ &\text{s.t.} \\ &\hat{\alpha} \le \hat{\alpha}_1 \\ &\hat{\alpha} \le \hat{\alpha}_2 \\ &\hat{\alpha} \le \hat{\alpha}_3 \end{aligned} \tag{6.38}$$

By applying the functions $M_{1..3}$ for each of the constraints, respectively, and recalling that $\hat{\alpha}_i \equiv M_i^{-1}$ we obtain:

$$\begin{aligned} &\max_{\hat{\alpha}} \ \hat{\alpha} \\ &\text{s.t.} \\ &M_1(\hat{\alpha}) \le \mathit{Budget} \\ &M_2(\hat{\alpha}) \le h_{\max} \\ &M_3(\hat{\alpha}) \ge h_{\min} \end{aligned} \tag{6.39}$$

Inserting (6.39) into (6.17) results in:

$$\begin{aligned} &\max_{x,\hat{\alpha}} \ \hat{\alpha} \\ &\text{s.t.} \\ &M_1(\hat{\alpha}) \le \mathit{Budget} \\ &M_2(\hat{\alpha}) \le h_{\max} \\ &M_3(\hat{\alpha}) \ge h_{\min} \\ &\hat{\alpha} \ge 0 \\ &x \in C(x) \end{aligned} \quad \Leftrightarrow \quad \begin{aligned} &\max_{x,\hat{\alpha}} \ \hat{\alpha} \\ &\text{s.t.} \\ &\max_{R \in U(\alpha)} \ \mathrm{cost}(x,R) \le \mathit{Budget} \\ &\max_{R \in U(\alpha)} \ h(x,R) \le h_{\max} \\ &\min_{R \in U(\alpha)} \ h(x,R) \ge h_{\min} \\ &\hat{\alpha} \ge 0 \\ &x \in C(x) \end{aligned} \tag{6.40}$$

The second form in (6.40), shares various elements with the Robust Optimization (RO) formulation. The second discussion raises this point.

6.5. Discussion 2

In discussion 1 we have shown that there is no need to formulate the robustness functions for each function individually, and there is no need to formulate the inverse functions either, and we have introduced another formulation which gives the same results. This version of the Info-Gap has many common similarities with the RO formulation of the problem. In fact we claim that in certain conditions the Info-Gap model is the inverse formulation of the RO. Inverse in the sense that, instead of minimizing the worst case cost for a given uncertainty set (with given shape and size), in the Info-Gap we solve for maximizing the uncertainty set size given the worst case cost (budget). The RO formulation of the problem is given in (6.41), which could be further transformed to another formulation by using the auxiliary variable "budget" to move the objective into the constraints.

$$\begin{aligned} &\min_{x}\left[\max_{R\in U(\alpha)} \text{cost}(x,R)\right] \\ &\text{s.t.} \\ &\max_{R\in U(\alpha)} h(x,R) \le h_{\max} \\ &\min_{R\in U(\alpha)} h(x,R) \ge h_{\min} \\ &x \in C(x) \end{aligned} \quad \Leftrightarrow \quad \begin{aligned} &\min_{x,budget}\left[budget\right] \\ &\text{s.t.} \\ &\max_{R\in U(\alpha)} \text{cost}(x,R) \le budget \\ &\max_{R\in U(\alpha)} h(x,R) \le h_{\max} \\ &\min_{R\in U(\alpha)} h(x,R) \ge h_{\min} \\ &x \in C(x) \end{aligned} \tag{6.41}$$

It should be noted that in the second form of the RO formulation (6.41), the first constraint will always be binding in the optimal solution.

Comparing formulation (6.41) of the RO and formulation (6.40) of the Info-Gap shows that the only difference is in the objective function where the first minimizes the budget for given α and the second maximizes α for given budget.

Formulation (6.40) is the inverse of formulation (6.41), whenever solving the first with a given $budget^*$ results in x^* and α^*, while solving the second with given α^* results in the same $budget^*$ and x^*.

Recalling that the budget constraint has to be binding at the final solution x^*, if the solution from the Info-Gap formulation does not imply binding budget constraint then it is not the inverse of the RO formulation.

To demonstrate this let us consider the yearly formulation of the Info-Gap. For fixed decision vector x, the constraints in formulation (6.40) are linear with α as could be seen from Section 6.2.1. Figure 6.10 shows schematic representation of these constraints at the optimal point of the Info-Gap problem in case (a) budget constraint is not binding (b) budget constraint is binding

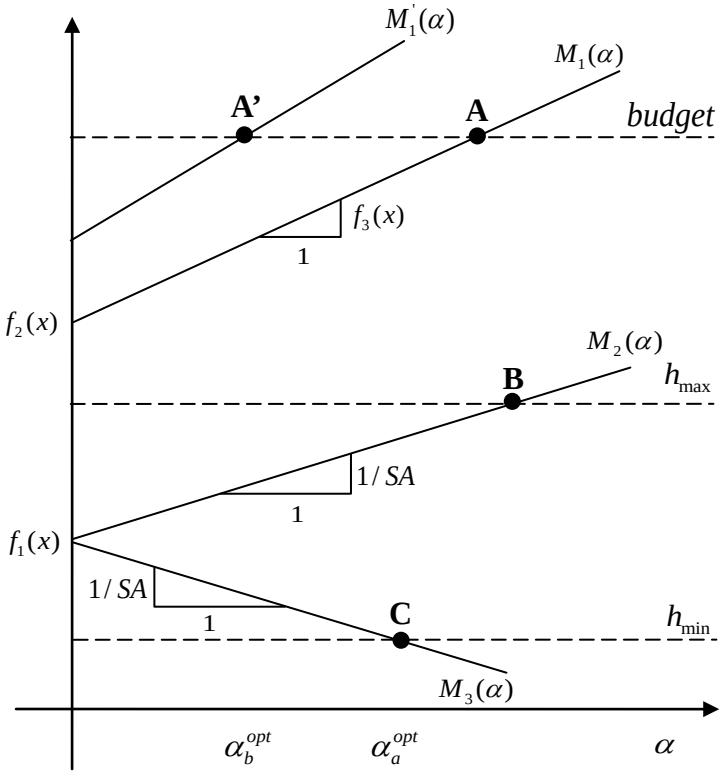

Figure 6.10: Schematic presentation of the Info-Gap formulation

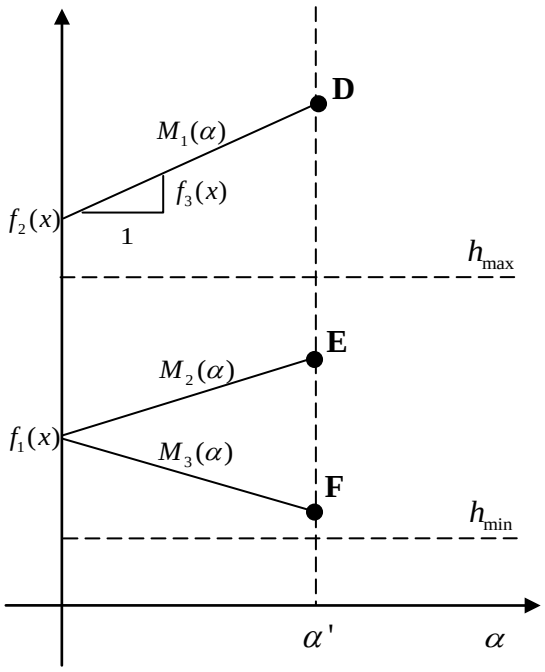

Figure 6.11: Schematic presentation of the RO formulation

Both functions $M_2(\alpha)$ and $M_3(\alpha)$ share the same point at $\alpha = 0$, the value of that point is a function of the decision (particularly the aquifer extraction), where the slopes does not depend on x. For $M_1(\alpha)$ both the intersection point $M_1(0)$ and the slope depend on the decision x. The maximum α which maintain feasibility for all constraint is the smallest α among the three intersection points (A, B, C).

The optimization problem of the Info-Gap (6.40), seeks intersections points $f_1(x)$, $f_2(x)$ and slope $f_3(x)$ such that the critical α corresponds to one of the points (A, B, C) is maximized.

In the RO formulation for a given level of α, say α' (Figure 6.11), the optimization problem seeks intersection points $f_1(x)$, $f_2(x)$ and slope $f_3(x)$ such that points E, F are within the bounds and the value of point D is minimized.

When the budget constraint is not binding (Figure 6.10, $M_1(\alpha)$), if we solve the RO with the optimal value α_a^{opt} we will not get the same x^*. Where if the budget constraint is binding (Figure 6.10, $M_1^{'}(\alpha)$), then solving the RO with optimal value α_b^{opt} will result in the same x^* because we know that there is no decision which could result in a point lower than A' , since if such decision exist, the Info-Gap optimization should find before because it results in larger α.

7. Conclusions

7.1. Research Contributions

7.1.1. Water Supply System (WSS) model

- Developed a WSS management model for seasonal multi-year management of water quantities and salinities of large scale WSS comprised of aquifers, reservoirs, desalination plants, demand zones and conveyance network. The model has a user friendly interface which facilitates constructing and solving different networks without the need for further programming. The model also generates an automatic report, including tabular (Figure 3.19) results and schematic figures (Figure 3.11) of the network with optimal distributions of water quantities and qualities. The model is formulated and solved with selected values of the stochastic variables, which can be the expected values or a more pessimistic or optimistic value that reflects the decision maker's attitude to risk. (Chapter 3).

7.1.2. Optimization

- To increase the efficiency of the optimization, a set of manipulations reduces the model size, and an efficient finite differences scheme has been developed for calculating the derivatives that are required by the optimization algorithm for the model's multi-stage structure, titled Time-Chained-Method (TCM). As seen in Figure 3.18 the TCM reduced the run time for 10 year problem by a factor of 6.5. (Section 3.10).
- As a byproduct of my work a Search Method for Box Optimization (SMBO) was developed. SMBO is a heuristic population based search methodology which solves global optimization problems by representing the population as a Probability Density Functions (PDF) within the problem bounds. The performance of SMBO is compared with old and recent genetic algorithms (GA). The results show that SMBO performs equally or better than theses GAs in both comparisons. (Appendix 1).

7.1.3. Optimization under uncertainty

- Stochastic programming approaches were applied to the WSS model. These include the Wait-and-See approach, the Here-and-Now approach, the two-stage approach, and the Multi-stage approach. The formulation and application of these approaches for various objectives were presented. (Chapter 4).
- The results of the stochastic programs were presented as Mean-Variance tradeoff. This presentation can be associated with the stochastic (scenario) based robust methodology suggested by Mulvey et al. [1995]. However, we suggest a new external problem formulation (small size and easy to solve optimization problem) which is solved to obtain the tradeoff without the need to solve the original large scale problem. (Section 4.6).
- Developed the Limited Multi-Stage Programming (LMSP) in which the total number of decision variables increases linearly with the number of scenarios and-stages. In this approach, titled Decision Clustering, we begin by identifying subsets of nodes which are likely to have similar decisions. The LMSP is a way to solve smaller optimization models without scenario reduction techniques. (Section 4.10).
- Applied the Robust Optimization (RO) methodology [Ben-Tal et al., 2009] to WSS management models. RO is a non-probabilistic min-max oriented decision methodology for optimization under uncertainty. (Chapter 5).
- Applied the Info-Gap decision theory [Ben-Haim, 2006], that is a non-probabilistic decision methodology, seeking to maximize robustness to failure under uncertainty. (Chapter 6).

7.2. Summary and Conclusions

7.2.1. Deterministic Model

The model developed in Chapter 3 determines the optimal flow and salinity distribution in each season of a multi-year planning horizon for a WSS that is fed from aquifers (could also be lakes or reservoirs) and desalination plants and supplies to consumers through a hydraulic system. The objective is to minimize the total present value of the cost, which includes the cost of water at the sources and the cost

of conveyance to supply prescribed quantities within salinity limits to all consumers. The algorithm handles a non-linear objective function, so objectives other than the one formulated in Section 3.4 can also be considered.

Flexibility in model building, ease of use, and computational efficiency are important properties for its application in the deterministic form presented herein for evaluation of proposed system developments. These properties are even more important when the model is used for management of the WSS under uncertainty, where very many optimization solutions are required with changing data.

Computational efficiency of the optimization model has been achieved through mathematical development and implementation of several strategies: (a) extracting dependent and resultant variables, thereby reducing the size of the system matrix, (b) matrix formulation of the dilution constraints which allows extraction of the quality variables (Section 3.5), (c) extraction of the dependent discharges, which facilitates their scaling to ensure solvability, (d) an efficient scheme of evaluating the objective and constraints, (e) a novel and efficient scheme for calculating the gradients of the objective and the Jacobian matrix in a time-dependent inventory problem (called Time-Chained-Method, TCM). It is shown that these strategies, combined, result in a model that is tractable even for a large water system. Due to this efficiency, the time horizon can be expanded and/or the year can be subdivided into more periods, for example four seasons per year, at the cost of a linearly increasing computation time (as seen in Figure 3.18). Since the model examines a long time horizon it facilitates the search for sustainable management policies.

General efficacy and applicability of the model is achieved by a user-oriented front-end processor; it receives the system data in a concise format and "spreads out" the model. This enables easy evaluation of modifications and expansions of the system, using the difference in the optimal cost between the new/proposed system and the existing one to determine the justification for the proposed addition/expansion/change. As a consequence, the model can be used in interactive mode with the decision maker to evaluate alternatives.

The development of the model is demonstrated on a small system, and its efficacy is proven on a large WSS that mimics the central part of the Israeli National Water System with several aquifers and desalination plants, using a 10-year historical time

series of aquifer recharge. Sensitivity runs are used to indicate the robustness of the methodology and its application for testing proposed modifications in the system.

7.2.2. Stochastic Models

Starting from the deterministic model developed in Chapter 3 and the efficient optimization procedure developed, Chapter 4 introduces various stochastic formulations in which the recharge of the natural resources is considered stochastic and presented by a scenario tree.

Various stochastic programming approaches have been aggregated into one formulation, so that the user can select the approach to be adopted by choosing certain statistical operators (Section 4.2). The implicit stochastic programming formulation was solved for various numerical examples. These examples show how the implicit approach can be used to formulate the proper explicit stochastic program, and its inability to provide decisions for implementation. In the implicit stochastic program an external optimization problem was formulated to reduce the computation burden when producing the Mean-Variance tradeoff (Section 4.6); this formulation provides the same tradeoff as obtained from the original optimization problem, with greatly reduced computational efforts. Various explicit stochastic formulations were introduced, including one-stage, two-stage and multi-stage programs.

An approximation of the MSP is presented in Section 4.10, the LMSP, to approximate the MSP formulation by restricting the number of recourse decisions. This restriction is performed by means of a clustering procedure of the decision nodes of the scenario tree. The logic of the LMSP and its application for our model are demonstrated. The LMSP solution was compared to the original problem of the MSP. The results show that the LMSP provides a good approximation for the MSP solution. A generalization of LMSP (GLMSP) is developed in Section 4.11, in which the user can customize his preference along a "scale" that spans between a single-stage model and a classical MSP. Several examples were solved using the GLMSP to determine its sensitivity to different points along the scale (Figure 4.15). However, not all the results were presented as they would require more space than can be allowed in this work.

7.2.3. RC Methodology

To facilitate the formulation of the RC problem, a new model, differing from the model developed in Chapter 3, is introduced in Chapter 5: it does not include salinity and is therefore linear.

The underlying concepts of the RC methodology introduced in Chapter 5. RC allows the decision maker to express his attitude to risk through the selection of a single parameter, θ that defines the domain of uncertainty in which the solution remains feasible, and generates Robust Policies (RPs) for specified values of θ. This approach shows considerable promise, regarding the tractability of the models and the value of the results obtained. The results demonstrate the advantage of being able to replace the stochastic behavior of the uncertainty by specifying a user-defined set within which the resulting policies are immunized (remain feasible), as well as being able to show the trade-off between reliability and cost.

The methodology and its dynamic variant, the Folding RC (FRC), were applied to the small WSS as a test-bed, and to the central part of the Israeli National Water System to yield FRC policies (FRPs). While the advantage of the RP over the NP and CP is apparent, as demonstrated in Section 5.2., the advantage over multistage stochastic programming (MSP) is not apparent. On the one hand, the FRP obtains better reliability and has greater flexibility to take advantage of opportunities (lower best cost) and to optimize in severe cases (lower worst cost). On the other, the stochastic programming solution has lower mean cost. The small size of the RP model compared to the MSP is a remarkable advantage of the robust methodology.

As we will discuss in Section 7.3.3 a variety of RO based methodologies, [Ben-Tal et al., 2009], including Adjustable Robust Counterpart (ARC), Affine Adjustable Robust Counterpart (AARC) may be also applied to this model. The non-linear model may be approximated or decomposed to be tackled by RO this is one of the topics considered in Section 7.3.3.

7.2.4. Info-Gap Methodology

Chapter 6 presents a preliminary application of the Info-Gap methodology; one year formulation and multi-year formulation of the small WSS were solved and analyzed. The resulting application of the Info-Gap methodology demonstrates the advantage of

being able to replace the stochastic behavior of the uncertainty by an uncertainty set. The Info-Gap min-max oriented methodology seeks to maximize the robustness to failure. The robustness to failure is determined by the largest uncertainty set in which no failure will occur. By defining the uncertainty model we are essentially defining the shape of the uncertainly set without specifying its size. The optimization problem seeks the maximum size for the uncertainly set for a predefined level of performance.

The Info-Gap requires a formulation of the mathematical model that seems non-intuitive. Usually, we formulate the mathematical model to reflect the performance and the underlying physics of the problems as a function of the input variables (for instance, in our case the cost and the water level as a function of the recharge), in the Info-Gap methodology we formulate the inverse problem in which the input is a function of the performance indices. On the other hand, the resulted output of the info-gap model is very intuitive to comprehend. The decision maker specifies his preferred performance indices, and the method provides how far from the estimated recharge he can handle. The methodology can also be used without an optimization framework for comparing and evaluating alternatives as presented in example 1, Section 6.2.2.

A very interesting conclusion stems from the one year optimization model of the Info-Gap formulation: when the budget is unlimited the optimal aquifer withdrawal (which maximizes the overall robustness) is given by the closed form (6.24) which depends only on the aquifer parameters. However, in spite of the fact we have the closed form (6.24), we still have to solve optimization problem (6.17), since the obtained aquifer withdrawal from (6.24) may not be feasible, because of conveyance constraints. It is important to notice that equation (6.24) is valid only for the underlying uncertainty model considered.

In the multi-year example the results indicate over-conservativeness as discussed: increasing the problem horizon shrinks the budget tradeoff, showing that the budget is becoming less limiting in determining the robustness. The over-conservativeness may be a result of the simple uncertainty set, i.e. the interval uncertainty set used to demonstrate the methodology in Chapter 6. The drawback of conservativeness may be overcome by choosing another shape of the uncertainty set, for example see in Section 5.2.2, justification of an ellipsoidal shape uncertainty set.

Chapter 6 introduces the basics of the methodology as applied on the small example, which leads to recommendations for further research in the Info-Gap methodology and its hybrid-probabilistic version in (Section 7.3.4).

7.2.5. Main Conclusions

- The results demonstrate the importance of introducing uncertainty into deterministic models, as the solution can change dramatically when recharge uncertainty is considered.
- Combined management of the quality and the quantity can change the optimal solution compared to quantity considerations alone.
- The optimal solution of multi-year WSS management (even in the deterministic case) is difficult to predict; even understanding the optimal solution may require substantial effort.
- In the Wait-and-See approach, it is possible to formulate an external optimization problem to obtain the mean-variance tradeoff; this problem is smaller and easier to solve than the original stochastic program.
- The LMSP provides a good approximation of the stochastic approaches.
- The results obtained from the non-probabilistic approaches (RC and Info-Gap) are very promising, they result in a smaller mathematical problem and they obtain competitive results in term of robustness and tractability compared to the classical probabilistic methods. This conclusion demonstrates the advantage of being able to replace the stochastic detail of the uncertainty by an uncertainty set.
- The definition of the solution's robustness differs between the methodologies. In the Mean-variance approach which can be attributed to the scenario based robust optimization suggested by Mulvey et al. [1995], a robust solution is defined as one that results in low variability. In the RO methodology, a robust solution is one that remains feasible for all possible values of the uncertain variables within in a given uncertainty space, while optimizing a guaranteed value of the objective. In the Info-Gap methodology the robustness is defined as the maximum deviation of the uncertain parameter form a given nominal value without a system failure.

7.3. Future Research

7.3.1. Deterministic Model

- Incorporating broad economic considerations into the model, in particular demand functions (consumers' willingness to pay) in order to transform the model objective from minimum operation cost to maximum net benefit.
- Incorporating better modeling of the aquifers, which projects the hydrological behavior. It is worth mentioning that in the early stages of this research the aquifers were presented by a finite differences scheme. While this was found possible in principle, it was not pursued as it was not considered in the main stream of this research.
- Refining the data and the topology of the INWSS example.
- This model in its general form can be used for projecting climate change impacts on water resources systems. Thus, it could be integrated with climate driven models.
- The TCM, methodology introduced in Chapter 3 is a generic technique which can be used for any optimization problem which shares the same stages structure. In the water resources field there are many problems which have this structure, such as reservoir management, hydropower optimization and WSS rehabilitation. It may also serve in other domains, for instance supply chain management models.

7.3.2. Stochastic models

- Constructing scenario trees from the historical record of the recharge data, which would be used to perform more realistic runs for the INWSS.
- In Chapter 4 we have developed the external problem which efficiently produces the Mean-Variance tradeoff of the objective. However, we have shown that the cost variability (variance) is not always a good measure of robustness. Further research is needed to identify such situations.
- The LMSP technique developed in this work provides a good approximation of the MSP. However, in the LMSP we need to solve each scenario separately in order to cluster the decision nodes. We claim that in this phase (solving scenarios) the solution need not be accurate. Since it is only used to determine the clusters members. Further research is needed to verify this assumption.

- The GLMSP is a tool which reflects the decision maker's preference along the "scale" between the single-stage stochastic programming and the MSP. Choosing the clustering scheme determines the position along this scale (Figure 4.15). Further research is needed to provide rules for choosing the proper point on the scale.

7.3.3. Robust Optimization

- We cannot underestimate the importance of incorporating more uncertainties in the model, such as: demands, desalination costs, conveyance costs and extraction levy. Incorporating more uncertainties into the RO formulation of the WSS in Chapter 5 will neither increase the model size nor its solvability. We strongly recommend future research on the application of the RO methodology with more uncertainties than the recharge.
- The RO methodology is applied to the linear WSS system which only considers only water quantity in the system, without salinity consideration. Moreover, some of the non-linear relations considered in the non-linear formulation in Chapter 3 were linearized. We suggest the following research directions in order to incorporate the nonlinearity with the RO methodology:
    - The non-linear extraction levy could be approximated by a convex piecewise linear function. Thus, since we consider minimization problem, the model could be reformulated as a linear program.
    - Incorporating the salinity in the model introduces bi-linear relations. This means that (a) fixing the salinity variables makes the problem linear with respect to the flows (b) fixing the flows makes the problem linear with respect to the salinities. Therefore, decomposition of the problem facilitates the application of the RO. In the decomposition framework the flow variables and the salinity variables are solved separately.
    - The non-linear RO model could be solved by Sequential Linear Programming (SLP) algorithm. The SLP consists of linearizing the objective and constraints in a region around a nominal operating point by a Taylor series expansion. The resulting linear programming problem is then solved by the RC approach.

- Only the static version of the RO methodology was applied in Chapter 5. Application of the dynamic version of the RO methodology is needed. This version considers the multi-stage decision making where the first-stage decision should be implemented before the true data is obtained and later stage decisions should be implemented after realization of the data in earlier stages. Thus, the decisions of each stage depend on all parts of the data which have already been realized up to that stage. The Affine Adjustable Robust Counterpart (AARC) approach could be applied to the WSS model formulated in Chapter 5. In AARC the dependence of the adjustable decision variables on past realized data is restricted to be linear; this restriction is imposed to achieve tractability. The Matlab code for the AARC has been developed and several runs were performed for the WSS model in Chapter 5. However, since further work is needed to finalize the results it was not included in this thesis.

7.3.4. Info-Gap Model

- Chapter 6 presents only a preliminary application of the Info-Gap methodology. The results obtained from this application are promising. We strongly recommend future research in this direction.
- The results obtained from the Info-Gap methodology indicate over-conservativeness of the solution. We believe that this may be the result of the simple interval uncertainty set which was used to demonstrate the methodology. The drawback of conservativeness could by overcome by choosing another shape of the uncertainty set, for example see in Section 5.2.2., justification of an ellipsoidal shape uncertainty sets. Testing different uncertainty sets within the Info-Gap methodology is a matter for future research.
- Another approach which could be applied for the WSS is the Hybrid Info-Gap methodology [Ben-Haim, 2006], in which the uncertain parameters of the model are formulated in hybrid probabilistic and non-probabilistic measures. The uncertain parameters are associated with PDFs in which the tails of the distribution are dealt with in a different manner. In fact the Hybrid Info-Gap methodology takes a PDF estimator to the real PDF with unknown extreme values.

8. Appendix 1

A new box-constrained optimization methodology and its application for a water supply system model

Mashor Housh[1], Avi Ostfeld[2] and Uri Shamir[3]

[1] PhD student, Faculty of Civil and Environmental Engineering, Technion – Israel Institute of Technology, Haifa 32000, Israel; PH: +972-4-8295943; FAX: 972-4-8228898; E-mail: mashor@tx.technion.ac.il (corresponding author)

[2] Associate Professor, Faculty of Civil and Environmental Engineering, Technion – Israel Institute of Technology, Haifa 32000, Israel; PH: +972-4-8292782; FAX: 972-4-8228898; E-mail: ostfeld@tx.technion.ac.il

[3] Emeritus Professor, Faculty of Civil and Environmental Engineering, Technion – Israel Institute of Technology, Haifa 32000, Israel; PH: +972-4-8292239; FAX: 972-4-8228898; E-mail: shamir@tx.technion.ac.il

Abstract

This study introduces a new search method for box-constrained optimization problems titled Search Method for Box Optimization (SMBO). SMBO is a population heuristic based search method which solves global optimization problems. SMBO represents the population as Probability Density Function (PDF) inside the problem bounds. The PDF shape is dynamically adapted during the process to guide to a "good" search domain. The applicability and the efficiency of the method are demonstrated using two benchmark sets, which include unimodal, multi-modal, expanded and hybrid composition functions. The performance of SMBO is compared with several genetic algorithms (GAs); the first benchmark compares it with nine codes of traditional/classic GAs, and the second compares SMBO with two recent variants of genetic algorithms. The results show that SMBO performs as well as or better than the GAs in both comparisons. The method is also applied to optimize a nonlinear model for management of a Water Supply System (WSS), and the results are compared to the commercial GA toolbox of MATLAB.

Index Terms— Evolutionary Algorithms, Genetic Algorithms, Global Optimization, Search Methods

A2: 1. Introduction

Many heuristic techniques were proposed to solve multidimensional global optimization problems (Ahrari et al., 2009; Georgieva and Jordanov, 2009; Regis and Shoemaker, 2007) among them genetic algorithms (GAs) (Harik et al., 1999; Holland, 1975; Tu and Lu, 2004) which are based on the genetic evolution of biological organisms. Essentially, each variable is represented as a gene, while the vector of variables is represented as a chromosome that combines all the genes.

The GA starts with an initial population in which each individual has its own chromosome. The population evolves over generations by means of random selection based on the fitness of the individuals. Pairs of individuals are selected out of the current generation and their chromosomes are recombined by a crossover operator. To ensure diversity, Mutation can be applied to some individuals. Generally, the efficiency of GAs depends on the values of the algorithm parameters, such as population size, initial population, selection scheme, the mutation fraction, and retention of elite members for the next generation (Tvrdík, 2009).

This work presents a search method for global optimization of box-constrained problems. SMBO is based on representing the population of each generation as Probability Density Function (PDF) defined within the problem bounds, where each gene has its own triangular shape PDF.

The details of this method and performance comparison using two benchmark sets are given in the next sections. In section 2, the method and its algorithm are presented, including a 2D example to demonstrate its propagation towards the optimal solution. Section 3 contains comparisons with results obtained by other search methods and section 4 demonstrates the application of SMBO for a WSS model.

A2: 2. Searching Method for Box Optimization (SMBO)

A2: 2.1. Outline of the method

The following optimization problem is considered:

$$\min_{x} f(x) \text{ subject to } LB \le x \le UB \tag{8.1}$$

where $x \in \Re^m$ is the variables vector, f is the objective function, and $LB \in \Re^m, UB \in \Re^m$ represent the lower and the upper bounds respectively.

Population based search methods can be defined as follows:

$$P^{new} = G\left(P^{old}, f\left(P^{old}\right)\right) \tag{8.2}$$

where P^{old} is a subset of solutions inside the search domain, which we call population, f is an objective function which returns the fitness for each population member and G is a manipulation function which creates a new population evolved from the previous one.

For instance, in GAs the manipulation function is defined by the operators applied to the old population to create the new one, such as: selection, mutation, crossover, etc.

SMBO is a population heuristics based search method in the form of equation (8.2) where each gene of a population member is represented by a PDF. For each gene the PDF is represented as an isosceles triangle inside the problem bounds, which is defined by a center point and base length. With regard to the manipulation function, SMBO draws n independent samples taken from the previous PDF, evaluates these samples and defines the new population (PDF).

To define the new population: (a) the new center points of the triangular PDFs are calculated as a mean of the elite members of the previous population sample (b) the new bases lengths of the triangles are reduced in order to achieve convergence.

Since SMBO deals with box optimization problems, the manipulation function must guarantee that all new population members are within the feasible domain. Therefore, when the vertices of the triangle are outside the problem bounds, the triangle is truncated at the bounds and normalized again to ensure a new population within the given bounds. Figure 1 shows the shape of the PDF and Figure 2 contains the pseudo code of the sampling algorithm from the triangular shape PDF.

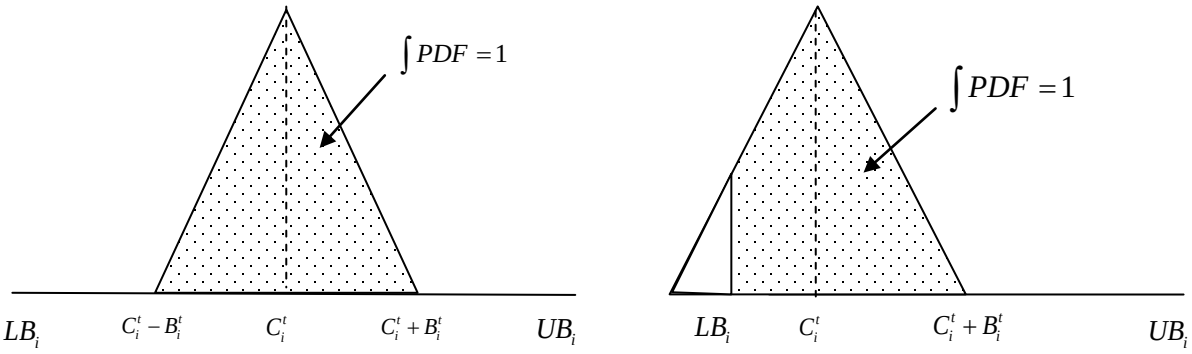

a. The triangular shape is inside the bounds b. Part of the triangular shape is outside the bounds

Figure 1: PDF of variable *i* at iteration *t*

1) **given** $C \in \Re^m$ – Triangle center points, $B \in \Re^m$ – Half triangle bases
$LB \in \Re^m$ – Lower bound and $UB \in \Re^m$ – Upper bound

2) **generate** m **PDFs, one for each gene**

for $i := 1$ *to* m *do*

$\underline{R}_i = \max\left(LB_i, C_i - B_i\right), \overline{R}_i = \min\left(UB_i, C_i + B_i\right)$

define the shape Δ_i *using the coordinates*:

$$\left(\underline{R}_i, 0\right), \left(\underline{R}_i, \underline{R}_i - (C_i - B_i)\right), (C_i, B_i), \left(\overline{R}_i, -\overline{R}_i + (C_i + B_i)\right), \left(\overline{R}_i, 0\right)$$

define the PDF $\hat{\Delta}_i = \dfrac{\Delta_i}{\int_{\underline{R}_i}^{\overline{R}_i} \Delta_i}$

3) **generate** n **randomly distributed feasible samples** (Rubinstein, 1981)

for $s := 1$ *to* n *do*

for $i := 1$ *to* m *do*

draw x_i^s *by the inverse transform method out of the PDF* $\hat{\Delta}_i$

Figure 2: Sampling Algorithm

A2: 2.2. Base reduction scheme

Four parameters are considered in controlling the base reduction: *Warming*, *Refining*, $B_{\min}$ – Minimum half base and α – Linear reduction factor. *Warming* and *Refining* are control parameters which are fractions of the total generations in which there is no base reduction. *Warming* is defined for the first generations, e.g. the first 10% of the total generations and *Refining* is defined for the last generations, e.g. the last 5% of the total generations. Figure 3 shows the pseudo code of the SMBO algorithm.

$$B_i^t = \begin{cases} B_i^0 & t \le W \cdot TG \\ B_{\min} & t \ge (1 - RE) \cdot TG \\ \alpha g_1 + (1-\alpha) g_2 & else \end{cases}$$

$$g_1 = B_i^0 - \frac{\left(B_i^0 - B_{\min}\right)}{RG} \cdot \left(t - W \cdot TG\right) \qquad (8.3)$$

$$g_2 = B_i^0 \cdot \left(\frac{B_{\min}}{B_i^0}\right)^{\frac{(t - W \cdot TG)}{RG}}$$

where

TG – *Total Generation*, RE – *Refining*, W – *Warming*,

$RG = \left(1 - W - RE\right) \cdot TG$ and $B_i^0 = \dfrac{UB_i - LB_i}{2}$

1) **given** n – Number of samples in each generation, EC – Elite count, TG -Total generation, $B_{\min}$ – Minimum base, α - Linear reduction factor, W – Warming, Re - Refining, LB – Lower bound, UB – Upper bound,

2) **initialize the algorithm**

- set $t = 0$, $B^0 = \frac{UB - LB}{2}$, $X_{\min} = C^0$, $f_{\min} = f(X_{\min})$ where C^0 is a random vector uniformly distributed within the problem bounds.

3) **generate feasible samples**

- apply the Sampling Algorithm in Figure 2 on C^t and B^t
- add the obtained n samples to a set P^t
- add the vectors C^t, $\overline{R}^t$, $\underline{R}^t$ and $X_{\min}$ to the set P^t

4) **evaluate the samples**

- evaluate the members in the set P^t, and sort them in ascending order based on their objective values.
- define X_{best} as the first vector of the sorted vectors, and $f_{best} = f(X_{best})$
- if $f_{best} \le f_{\min}$ do $X_{\min} = X_{best}$, $f_{\min} = f_{best}$

5) **define the new parameters of the PDFs**

- define C^{t+1} as the average of the first EC vectors of the sorted vectors.
- evaluate B^{t+1} based on equations (3)

10) if $t \le TG$ do $t = t + 1$, back to step 3
else return $X_{\min} = X_{best}$, $f_{\min} = f_{best}$

Figure 3: SMBO Algorithm

A2: 2.3. Propagation to the optimal solution (using a 2D example)

Consider the problem:

$$\begin{aligned} & x \cdot e^{(-x^2 - y^2)} + \frac{(x^2 + y^2)}{20} \to \min \\ & \text{subject to} \\ & -10 \le x \le 10 \\ & -10 \le y \le 10 \end{aligned} \tag{8.4}$$

The optimal solution of (8.4) is $x_{\min} = -0.67$, $y_{\min} = 0$. SMBO starts from an initial population defined by a triangular PDF with centers $C_x^0 = -9.2$, $C_y^0 = -7.8$, $B^0 = 10$ for both variables. Figure 4 shows the propagation of the algorithm towards the optimal solution, Figure 4a shows the first and second PDFs representing the initial and the second populations during the solution process. Figure 4b shows all the PDFs during the search process. The final PDFs are concentrated on the optimal solution, since the base of the triangles at the final iteration is 0.02, after normalization they have a height of 100 where the triangles heights at the earlier iterations have relativity small heights which are represented by the flat part along axes x and y in Figure 4b.

The parameters set considered in this small example are defined in Table 1.

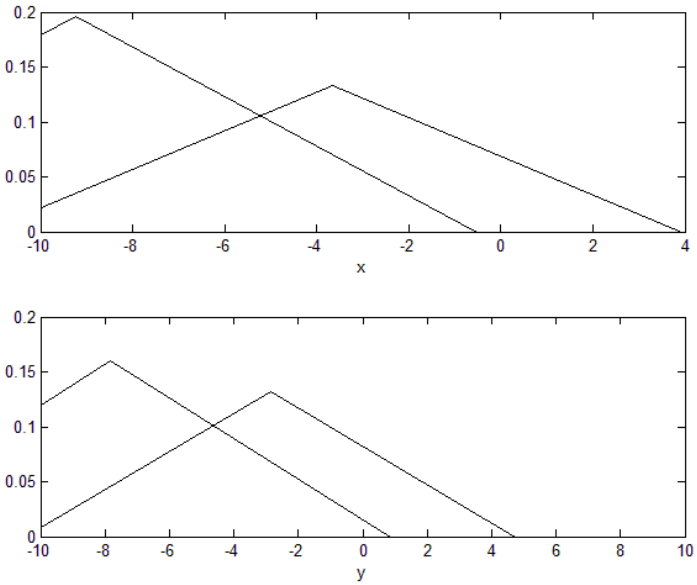

a. The PDFs at the first (left) the second (right) iterations

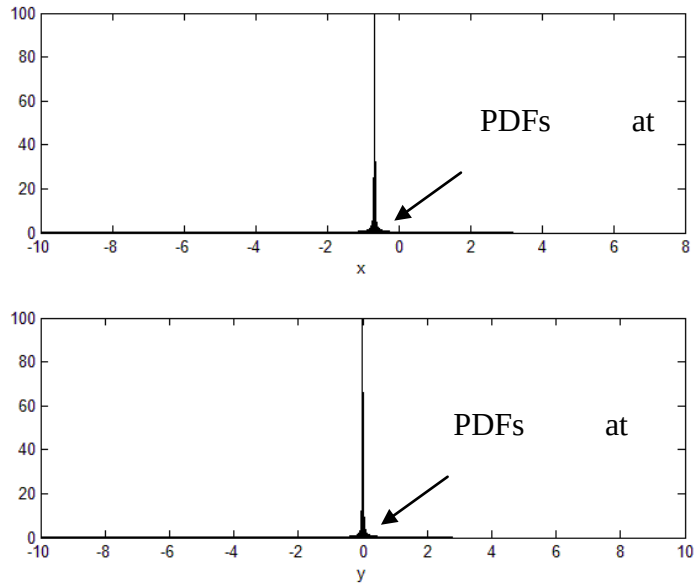

b. PDFs at the end of the search process

Figure 4: Example (2D)

A2: 3. Comparison of test results with GAs

To test the ability of the proposed method to find the global or at least local minimum efficiently, two suits of benchmark functions are optimized by SMBO, using the parameters given in Table 1.

A2: 3.1. De Jong's test suite

De Jong's suite contains five test functions (De Jong, 1975) which are listed in the Appendix. F1 is a unimodal function. F2 is a multimodal function. F3 is discontinuous. F4 is unimodal padded with noise. F5 is a function with many local optima. The performance of SMBO is compared with that obtained in Colorado et al., (1993) which used nine GA codes. For comparison purposes our algorithm was executed 30 times on all the test functions, each time we have used 400 evaluations at each generation and total generations $TG = 1000$, as was done in Colorado et al., (1993).

The stopping criterion $\left(f^{obtained} - f^{optimal}\right) \le \varepsilon$ was set as in Colorado et al., (1993) where $\varepsilon = 0.01$ except for the function F3 in which $\varepsilon = 0$ and F4 in which $\varepsilon = -2.5$. Table 2 reports the average number of function evaluations and its standard deviation that each algorithm takes in order to solve the De Jong's functions.

Table 1: SMBO Parameters

De Jong's test suite	**2D-Example**	**CEC'05 test suite**
$RE = \{F1, F2, F3, F4 = 0.95\}, \{F5 = 0\}$ $W = 0$ $\alpha = 0.5$ $B_{\min} = 0.01$ $n = 397$ $EC = \min\left[\left\lceil 0.1 \cdot (n+3)\right\rceil, 10\right]$	$TG = 50$ $RE = 0$ $W = 0$ $\alpha = 0$ $B_{\min} = 0.01$ $n = 100$ $EC = 10$	$RE = 0.1$ $W = 0$ $\alpha = 0$ $B_{\min} = 0.01$ $n = 147$ $EC = \min\left[\left\lceil 0.1 \cdot (n+3)\right\rceil, 10\right]$

Table 2: De Jong's test suite results*

F1		
Algorithm	**E_ev**	**Std_ev**
SMBO(400)	2760	881
Genitor	6800	1640
I-Genitor	9280	2120
pCHC	11360	2600
ESGA	11560	2720
SGA	12280	2960
I-ESGA	12920	3040
Cellular	13000	3200
I-pCHC	13280	2960
I-SGA	16520	4480

F2		
Algorithm	**E_ev**	**Std_ev**
SMBO(400)	2013	817
I-pCHC	31200	22800
I-ESGA	32400	16000
ESGA	33200	22000
Cellular	42000	37600
I-Genitor	44800	37600
pCHC	61200	55600
Genitor	76000	64000
SGA	113600	79200
I-SGA	166800	101200

F3		
Algorithm	**E_ev**	**Std_ev**
SMBO(400)	1747	222
Genitor	3280	840
I-Genitor	4920	1440
ESGA	6120	1640
SGA	6680	1680
pCHC	6760	1480
Cellular	7160	1840
I-ESGA	7320	2000
I-pCHC	7520	1760
I-SGA	8800	2120

F4		
Algorithm	**E_ev**	**Std_ev**
SMBO(400)	10427	1807
Genitor	54000	26800
ESGA	61200	19600
SGA	64400	16000
I-Genitor	83200	64800
pCHC	89200	41600
I-ESGA	150000	78800
Cellular	158800	81600
I-SGA	162000	76800
I-pCHC	198000	95600

F5		
Algorithm	**E_ev**	**Std_ev**
Genitor	3160	1000
I-Genitor	4480	1480
I-ESGA	5520	1880
ESGA	5720	17600
SGA	5840	1760
Cellular	6120	1720
pCHC	6400	1560
I-pCHC	6520	2120
SMBO(400)	8107	7763
I-SGA	8120	2760

*E_ev, Std_ev are average and standard deviation of function evaluations respectively.

A2: 3.2. CEC-05 test suite

In this section SMBO is applied to a subset of the benchmark functions provided by CEC-05 special session on real parameter optimization (Suganthan et al., 2005). The chosen subset includes four groups: unimodal, multi-modal, expanded and hybrid composition functions. All the test functions are listed in the appendix.

The performance of SMBO is compared with that obtained in Hsieh et al., (2009) by means of two recent variants of GAs on eighteen test functions with 30 dimensions. For comparison purposes the number of function evaluations was set to 150,000 and each of the test functions was run 30 times. In SMBO we set the evaluations at each generation to 150 and the total generations to 1000. Table 3 reports the mean value and the standard deviation of the objective function that each algorithm obtained after 150,000 evaluations. In each function the algorithm with minimum mean value is shown bold.

The results show that SMBO obtained better results (lower mean value) than HTGA (Tsai et al., 2004) in all the test functions except for functions f8 and f11. Moreover, SMBO outperforms SEGA (Hsieh et al., 2009) in fourteen out of the eighteen functions considered, i.e. (78%) of the test set.

With regard to the function f12, despite the fact that SMBO obtained lower mean value in the third decimal place, both SMBO and SEGA are shown in bold. However,

one can argue that SEGA obtained better result because of the lower standard deviation.

Table 3: CEC-05 test suite results*

Function	Algorithm		
	SEGA	HTGA	SMBO
f1	-4.49E+02 ± 1.34E-02	-4.41E+02 ±4.92E+00	**-4.50E+02 ± 2.63E-06**
f2	8.24E+02 ±4.33E+02	1.51E+04 ±1.46E+03	**-4.50E+02 ± 2.86E-05**
f3	1.28E+07 ±3.81E+06	1.64E+07 ±2.66E+06	**1.09E+07 ±5.39E+07**
f4	1.94E+04 ±7.87E+03	3.15E+04 ±3.30E+03	**-4.50E+02 ± 4.97E-05**
f5	**8.90E+02 ±1.18E+03**	4.05E+03 ±2.32E+03	1.98E+03 ±2.81E+03
f6	4.52E+03 ± 1.18E-02	4.52E+03 ± 6.75E-02	**-1.80E+02 ± 7.15E-07**
f7	-1.19E+02 ± 6.32E-02	-1.19E+02 ± 8.85E-02	**-1.20E+02 ± 9.34E-02**
f8	**-3.29E+02 ± 5.40E-03**	-3.27E+02 ±1.35E+00	-3.02E+02 ±1.09E+01
f9	-2.73E+01 ±9.60E+01	2.65E+01 ±6.75E+01	**-3.05E+02 ±7.55E+00**
f10	1.24E+02 ±3.42E+00	1.24E+02 ±2.24E+00	**9.38E+01 ±3.19E+00**
f11	**2.01E+04 ±1.37E+04**	2.87E+04 ±1.57E+04	4.53E+04 ±1.55E+05
f12	**-1.29E+02 ± 2.13E-01**	-1.28E+02 ± 3.82E-01	**-1.29E+02 ± 9.68E-01**
f13	-2.87E+02 ± 2.40E-01	-2.87E+02 ± 2.97E-01	**-2.89E+02 ±1.04E+00**
f14	4.97E+02 ±1.09E+02	4.57E+02 ±8.27E+01	**4.39E+02 ±2.66E+02**
f15	**1.14E+03 ±3.40E+02**	1.71E+03 ±3.04E+02	1.24E+03 ±3.41E+01
f16	1.53E+03 ±7.43E+01	1.51E+03 ±4.49E+01	**8.94E+02 ± 2.54E-04**
f17	8.17E+02 ±5.06E+02	9.86E+02 ±5.24E+02	**4.60E+02 ± 3.37E-04**
f18	1.55E+03 ±6.79E+01	1.60E+03 ±3.25E+01	**1.23E+03 ±8.00E+00**

HTGA-Hybrid Taguchi Genetic Algorithm (Tsai et al., 2004)
SEGA-Sharing Evolution Genetic algorithm (Hsieh et al., 2009)
* The values have been rounded to 3 significant digits

A2: 4. Solving a WSS problem

A seasonal multi-year model for management of water quantities and salinity for the WSS shown in Figure 5 was solved. Water is taken from sources, which include aquifers, reservoirs and desalination plants, conveyed through a distribution system to consumers who require certain quantities of water under specified salinity constraints.

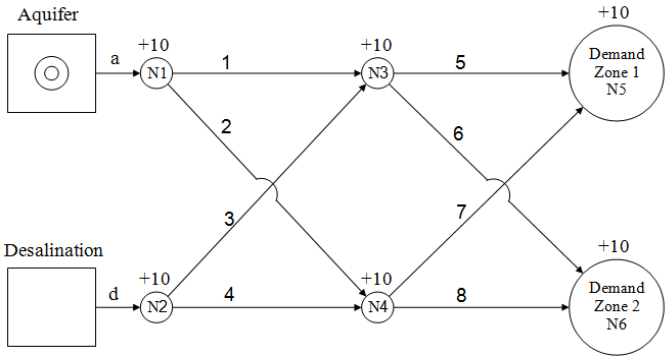

Figure 5: Network Layout

The objective is to operate the system with minimum total cost of desalination, pumping, delivery, and an extraction levy in the aquifers. The objective function and some of the constraints in the model are nonlinear, leading to a nonlinear optimization problem.

The objective is to minimize the operation cost over a period of five years, where each year has two seasons. The optimization problem is:

$$\text{cost}=\sum_{Y=1}^{5}\sum_{S=1}^{2}\left(\underbrace{\sum_{p=1}^{8}\omega_p^{S,Y}\cdot\left(Q_p^{S,Y}\right)^{2.852}}_{Conveyance}+\underbrace{(\alpha+\beta\cdot h_a^{S,Y})\cdot Q_a^{S,Y}}_{Extraction\ Levy}+\underbrace{(\gamma+\left(C_d^{S,Y}\right)^{-\delta})\cdot Q_d^{S,A}}_{Desalination}\right)\rightarrow \min \qquad (8.5)$$

Subject to

State equation for water level in the aquifers $\forall S\forall Y$:

$$R_a^{S,Y}-Q_a^{S,Y}=SA_a\cdot(h_a^{S,Y}-h_a^{(S,Y)-1})$$

State equation for water salinity in the aquifers $\forall S\forall Y$:

$$\left(C_R\right)_a^{S,Y}\cdot R_a^{S,Y}-C_a^{(S,Y)-1}\cdot Q_a^{S,Y}=SA_a\cdot\left(C_a^{S,Y}\cdot h_a^{S,Y}-C_a^{(S,Y)-1}\cdot h_a^{(S,Y)-1}\right)$$

Desalinated water salinity $\forall S\forall Y$:

$$C_d^{S,Y}=C_{sea}\cdot\left(1-RR_d^{S,Y}\right)$$

Water balance in the network $\forall S\forall Y$:

$$A\cdot Q^{S,Y}=0$$

Salinity (mass) balance in the network $\forall S\forall Y$:

$$A\cdot\Delta_{Q^{S,Y}}\cdot C^{S,Y}=0$$

Full dilution in the network nodes $\forall S\forall Y$:

$$B\cdot C^{S,Y}=0$$

Bounds $\forall S\forall Y$:

$$\left(h_{\min}\right)_a^{S,Y}<h_a^{S,Y}<\left(h_{\max}\right)_a^{S,Y}$$
$$\left(C_{\min}\right)^{S,Y}<C^{S,Y}<\left(C_{\max}\right)^{S,Y}$$
$$\left(Q_{\min}\right)_{Sources}^{S,Y}<Q_{Sources}^{S,Y}<\left(Q_{\max}\right)_{Sources}^{S,Y}$$
$$\left(Q_{\min}\right)_{Pipes}^{S,Y}<Q_{Pipes}^{S,Y}<\left(Q_{\max}\right)_{Pipes}^{S,Y}$$
$$\left(RR_{\min}\right)_d^{S,Y}\le RR_d^{S,Y}\le\left(RR_{\max}\right)_d^{S,Y}$$

where p,a,d,z,S,Y denote pipe, aquifer, desalination plant, demand zone, season and year, respectively.

Model parameters:

$\omega_p^{S,Y}, \alpha, \beta, \gamma, \delta$ are cost parameters; $R_a^{S,Y}$ is recharge (m^3); SA_a is the storativity multiplied by area (m^2); $(C_R)_a^{S,Y}$ is salinity of the recharge water ($mgcl/lit$); C_{sea} is sea water salinity ($mgcl/lit$); A is the graph matrix of the network; B full dilution matrix which indicates equal salinity for two outgoing pipes which share the same node; $Q_{Demand} = [Q_{z=1}, Q_{z=2}]$ (m^3); lower and upper bounds.

Model variables:

$Q_{Sources} = [Q_a, Q_d]$, $Q_{Pipes} = [Q_1, ..., Q_8]$ are discharges from sources and in pipes, respectively; $C = [C_a, C_d, C_1, \ldots, C_8, C_{z=1}, C_{z=2}]^T$ is vector combines salinity in the system sources, pipes and demand zones; $RR_d^{S,Y}$ is removal ratio in the desalination plant; $h_a^{S,Y}$ is water level in the aquifer; Δ_Q is diagonal matrix with main diagonal $Q = [Q_{Sources}, Q_{Pipes}, Q_{Demand}]^T$.

To reduce the model size we extracted one dependent decision variable from each equality constraint. Then, the dependent variables are substituted in the objective function and the inequality constraints. For the model defined above, extracting all the dependent variables leads to the following mathematical model which has 50 decision variables, 120 linear constraints, 80 nonlinear constraints and 50 bounds:

$$\sum_{Y=1}^{5}\sum_{S=1}^{2} \text{cost}(Q_{Indep}^{S,Y}, RR_d^{S,Y}) \rightarrow \min \qquad (8.6)$$

Subject to

Inequality linear constraints $\forall S \forall Y$:

$$\underbrace{K^{S,Y} \cdot Q_{Indep}^{S,Y}}_{(KQ)^{S,Y}} \le 0$$

Inequality nonlinear constraints $\forall S \forall Y$:

$$g_i(Q_{Indep}^{S,Y}, RR_d^{S,Y}) \le 0 \quad \forall i = 1 \cdots 8$$

Bounds $\forall S \forall Y$:

$$(Q_{\min})_{Indep}^{S,Y} < Q_{Indep}^{S,Y} < (Q_{\max})_{Indep}^{S,Y}$$

$$(RR_{\min})_d^{S,Y} \le RR_d^{S,Y} \le (RR_{\max})_d^{S,Y}$$

where $Q_{Indep}^{S,Y} = [Q_3^{S,Y}, Q_4^{S,Y}, Q_6^{S,Y}, Q_8^{S,Y}]^T$.

The mathematical model in (8.6) was solved by SMBO where all inequality constraints except the bounds where added to the objective as penalty terms with penalty factor P. After introducing the penalty terms the model is a box constrained optimization problem:

$$\sum_{Y=1}^{5}\sum_{S=1}^{2}\left[\text{cost}(Q_{Indep}^{S,Y}, RR_d^{S,Y}) + \text{P}\cdot\sum_{j=1}^{12}\max(0,(KQ)_j^{S,Y}) + \text{P}\cdot\sum_{i=1}^{8}\max(0, g_i^{S,Y})\right] \rightarrow \min$$

$$\text{Subject to} \quad \forall S \forall Y \tag{8.7}$$

$$(Q_{\min})_{Indep}^{S,Y} < Q_{Indep}^{S,Y} < (Q_{\max})_{Indep}^{S,Y}$$

$$(RR_{\min})_d^{S,Y} \le RR_d^{S,Y} \le (RR_{\max})_d^{S,Y}$$

Problem (8.7) with penalty factor $\text{P} = 1\text{E}6$ (very high value compared to the values in the cost function), was solved by SMBO and the commercial GA solver of MATLAB. In both algorithms the evaluations at each generation and the total generations were set to 200 and 1000, respectively. Both solvers were run without special tuning, the parameters of SMBO are the same as those for the CEC-05 (Table 1) where for the MATLAB GA we used the default options for creation, selection, crossover and mutation.

The solvers were run 10 times each, and the best run results are reported in Figure 6. SMBO obtained a feasible solution (value below 400 M$) at generation 58 while the GA obtained it only at generation 183. The final solution obtained by SMBO (64.51 M$) is also better than that obtained by the GA (65.55 M$). The best known solution for problem (8.6) (the original constrained problem) is 64.12 M$. This solution was obtained by the interior point algorithm of the FMINCON solver within the commercial MATLAB optimization toolbox.

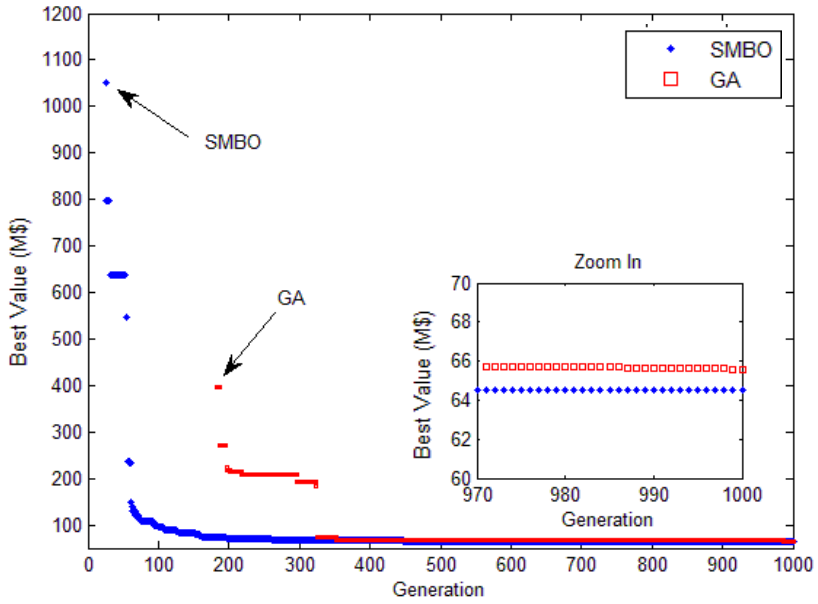

Figure 6: Progress of the SMBO and GA Solutions

A2: 5. Conclusions

A new method for box constrained global optimization – SMBO has been presented. The algorithm searches for the global minimum with competitive performance compared with other methods. The algorithm was tested on two benchmark problem sets. The number of evaluations needed to obtain the global minimum in De Jong's test suite was the smallest in four functions. Moreover, SMBO achieved closer solution to the global minimum in most of the CEC'05 test suite problems.

In reference to the WSS management model SMBO obtained better results than the commercial GA solver of MATLAB and achieved close results to the best known solution obtained by the gradient optimization solver within the commercial optimization toolbox of MATLAB.

These results demonstrate the promising potential of the method, especially for expensive functions in which each evolution is time-consuming.

In the second test the control parameters of the algorithm were given the same values for all the tasks, without any tuning. Further research is needed for improving the algorithm performance through its parameters selection for example; in the first test suite further analysis shows that 400 evaluations at each generation, which is specified in the comparison, is too large for SMBO to attain the best performance in the test suite problems. This analysis show that SMBO obtained even better results when low values of E were selected in the 5 test functions.

Further research to modifying SMBO to a hybrid global optimization method that combines it with local search algorithms is also considered.

A2: 6. Appendix

This appendix presents all the test problems used in both comparisons. Table 4 and Table 5 present the functions of the first and the second test respectively.

Table 4: De Jong's test suite (De Jong, 1975)

Function name	Interval	Function	Global Min
F1 (Sphere)	$x \in [-5.12, 5.12]^3$	$f(x) = \sum_{i=1}^{3} x_i^2$	$f_{\min} = 0$
F2 (Rosenbrock)	$x \in [-2.048, 2.048]^2$	$f(x) = 100 \cdot (x_1^2 - x_2)^2 + (1 - x_1)^2$	$f_{\min} = 0$
F3 (Step)	$x \in [-5.12, 5.12]^5$	$f(x) = \sum_{i=1}^{5} \lfloor x_i \rfloor$	$f_{\min} = -30$
F4 (Stochastic)	$x \in [-1.28, 1.28]^{30}$	$f(x) = \sum_{i=1}^{30} i \cdot x_i^4 + Gauss(0,1)$	$f_{\min} = 0$

F5 (Foxholes)	$x \in [-65.536, 65.536]^2$	$f(x) = \left[0.002 + \sum_{j=1}^{25} \frac{1}{j + \sum_{i=1}^{2} (x_i - a_{ij})^6} \right]^{-1}$	$f_{\min} = 0.998$

Table 5: CEC'05 test suite (30D problems) (Suganthan et al., 2005).

Function name	Interval	Function	f_{bias} *
Uni-modal Functions			
f1-Sphere	$x \in [-100,100]$	$f(x) = \sum_{i=1}^{30} z_i^2 + f_{bias}$, $z = x - o$ *	-450
f2-Schwefel 1.2	$x \in [-100,100]$	$f(x) = \sum_{i=1}^{30} \left(\sum_{j=1}^{i} z_j \right)^2 + f_{bias}$, $z = x - o$	-450
f3-Rotated high conditioned elliptic	$x \in [-100,100]$	$f(x) = \sum_{i=1}^{30} (10^6)^{\frac{i-1}{29}} \cdot z_i^2 + f_{bias}$, $z = (x - o) \cdot M$ M-Orthogonal Matrix	-450
f4-Schwefel 1.2 with noise	$x \in [-100,100]$	$f(x) = \left(\sum_{i=1}^{30} \left(\sum_{j=1}^{i} z_j \right)^2 \right) \cdot (1 + 0.4 \lvert N(0,1) \rvert) + f_{bias}$ $z = x - o$	-450
Multi-modal Functions			
f5-Rosenbrock	$x \in [-100,100]$	$f(x) = \sum_{i=1}^{29} (100 \cdot (z_i^2 - z_{i+1})^2 + (z_i - 1)^2) + f_{bias}$ $z = x - o + 1$	390
f6-Rotated Griewank		$f(x) = \sum_{i=1}^{30} \frac{z_i^2}{4000} - \prod_{i=1}^{30} \cos\left(\frac{z_i}{\sqrt{i}} \right) + 1 + f_{bias}$ $z = (x - o) \cdot M$ M-Linear Transformation Matrix, Condition Number = 3	-180
f7-Rotated Ackley with optimum on bounds	$x \in [-32,32]$	$f(x) = -20 \exp\left(-0.2 \sqrt{\frac{1}{30} \sum_{i=1}^{30} z_i^2} \right) - \exp\left(\frac{1}{30} \sum_{i=1}^{30} \cos(2\pi z_i) \right) + 20 + e + f_{bias}$ $z = (x - o) \cdot M$ M-Linear Transformation Matrix, Condition Number = 100	-140
f8-Rastrigin	$x \in [-5,5]$	$f(x) = \sum_{i=1}^{30} z_i^2 \cdot (z_i^2 - 10\cos(2\pi z_i) + 10) + f_{bias}$ $z = z - o$	-330
f9-Rotated Rastrigin	$x \in [-5,5]$	$f(x) = \sum_{i=1}^{30} z_i^2 \cdot (z_i^2 - 10\cos(2\pi z_i) + 10) + f_{bias}$ $z = (x - o) \cdot M$ M-Linear Transformation Matrix, Condition Number = 2	-330

f10-Rotated Weierstrass	$x \in [-0.5, 0.5]$	$f(x) = \sum_{i=1}^{30} \left(\sum_{k=0}^{k_{\max}} \left[a^k \cos(2\pi b^k (z_i + 0.5)) \right] \right)$ $- 30 \sum_{k=0}^{k_{\max}} \left[a^k \cos(2\pi b^k \cdot 0.5) \right] + f_{bias}$ $z = (x - o) \cdot M, a = 0.5, b = 0.3, k_{\max} = 20$ M-Linear Transformation Matrix, Condition Number = 5	90
f11-Schwefel 2.13	$x \in [-100, 100]$	$f(x) = \sum_{i=1}^{30} \left(A_i - B_i(x)^2 \right)^2 + f_{bias}$ $A_i = \sum_{j=1}^{30} \left(a_{ij} \sin(\alpha_j) + b_{ij} \cos(\alpha_j) \right)$ $B_i(x) = \sum_{j=1}^{30} \left(a_{ij} \sin(x_j) + b_{ij} \cos(x_j) \right)$ A, B are two 30×30 matrices. a_{ij}, b_{ij} integer random numbers in the range [-100,100] α_j are random numbers in the range $[-\pi, \pi]$	-460
Expanded Functions			
f12-Griewank+ Rosenbrock	$x \in [-3, 1]$	$f_a(x) = \frac{x^2}{4000} - \cos(x) + 1$ $f_b(x_1, x_2) = 100 \cdot (x_1^2 - x_2)^2 + (1 - x_1)^2$ $f(x) = f_a(f_b(z_1, z_2)) + f_a(f_b(z_2, z_3)) + \ldots$ $+ f_a(f_b(z_{29}, z_{30})) + f_a(f_b(z_{30}, z_1)) + f_{bias}$ $z = x - o + 1$	-130
f13-Rotated expanded Scaffer	$x \in [-100, 100]$	$f_a(x_1, x_2) = 0.5 + \frac{\sin^2(\sqrt{x_1^2 + x_2^2}) - 0.5}{\left(1 + 0.001(x_1^2 + x_2^2)\right)^2}$ $f(x) = f_a(z_1, z_2) + f_a(z_2, z_3) + \ldots + f_a(z_{29}, z_{30})$ $+ f_a(z_{30}, z_1) + f_{bias}$, $z = (x - o) \cdot M$ M-Linear Transformation Matrix, Condition Number = 3	-300
Hybrid Composition Functions**			
f14-Rotated hybrid composition 1 with noise	$x \in [-5, 5]$	$f_1(x)$ is composed using ten function:, two Weierstrass, two Rastrigin, two Ackley, two Griewankand two Sphere functions.** $f(x) = f_1(x) \cdot \left(1 + 0.2 \left| Gauss(0,1) \right|\right) + f_{bias}$	120
f15-Rotated hybrid composition 3	$x \in [-5, 5]$	$f(x)$ is composed using ten functions: two rotated expanded Scaffer, two (Griewank+ Rosenbrock), two Weierstrass, two Rastrigin and two Griewank functions.**	360
f16-Rotated hybrid composition 3 with high condition number matrix	$x \in [-5, 5]$	The previous function with high condition number matrices in the composition process.	360
f17-Rotated hybrid composition 4	$x \in [-5, 5]$	$f(x)$ is composed using ten functions: rotated expanded Scaffer, non-continuous expanded Scaffer, Weierstrass, (Griewank+ Rosenbrock), Ackley, Rastrigin, non-continuous Rastrigin,	260

		Griewank, high conditioned Elliptic and Sphere function with noise.**	
f18-Rotated hybrid composition 4		The same as the previous function	260
* All the following problems are in 30D and shifted to $f_{\min} = f_{bias}$, o – is the shifted global optimum ** For more information about composition functions see [10], pages 18-38. (http://www.ntu.edu.sg/home/EPNSugan/index_files/CEC-05/CEC05.htm			

A2: 7. References

Ahrari, A., Shariat-Panahi, M., Atai, A.A. (2009). "Gem: A novel evolutionary optimization method with improved neighborhood search." *Applied Mathematics and Computation*, vol. 210, no. 2, pp. 376–386

Colorado, S.G., Gordon, V.S., Whitley, D. (1993). "Serial and parallel genetic algorithms as function optimizers." *Proceedings of the Fifth International Conference on Genetic Algorithms*, pp. 177–183

De Jong, K.A. (1975). "*An analysis of the behavior of a class of genetic adaptive systems*". Ph.D. dissertation, Ann Arbor, MI, USA

Georgieva, A., Jordanov, I. (2009). "Global optimization based on novel heuristics, low-discrepancy sequences and genetic algorithms." *European Journal of Operational Research*, vol. 196, no. 2, pp. 413–422

Harik, G.R., Lobo, F.G., Goldberg, D.E. (1999). "The compact genetic algorithm." *IEEE Transactions on Evolutionary Computation*, vol. 3, no. 4, pp. 287–297

Holland, J.H. (1975). "*Adaptation in Natural and Artificial Systems*." Ann Arbor, MI, USA: University of Michigan Press

Hsieh, S., Sun, T., Liu, C. (2009). "Potential offspring production strategies: An improved genetic algorithm for global numerical optimization." *Expert Systems with Applications*, vol. 36, no. 8, pp. 11 088–11 098

Regis, R.G., Shoemaker, C.A. (2007). "Parallel radial basis function methods for the global optimization of expensive functions." *European Journal of Operational Research*, vol. 182, no. 2, pp. 514–535

Rubinstein, R.Y. (1981). "*Simulation and the Monte Carlo Method*." New York, NY, USA: John Wiley & Sons, Inc

Suganthan, P.N., Hansen, N., Liang, J.J., Deb, K., Chen, Y.P., Auger, A., Tiwari, S. (2005). "Problem definitions and evaluation criteria for the CEC'05 2005 special session on real parameter optimization." Nanyang Technological University, Tech. Rep. http://www.ntu.edu.sg/home/epnsugan

Tsai, J.T., Liu, T.K., Chou, J.H. (2004). "Hybrid Taguchi-genetic algorithm for global numerical optimization." *IEEE Trans. Evolutionary Computation*, vol. 8, no. 4, pp. 365–377

Tu, Z., Lu, Y. (2004). "A robust stochastic genetic algorithm (STGA) for global numerical optimization." *IEEE Transactions on Evolutionary Computation*, vol. 8, no. 5, pp. 456–470

Tvrdík, I. (2009). "Adaptation in differential evolution: A numerical comparison." *Applied Soft Computing Journal*, vol. 9, no. 3, pp. 1149–115

9. Appendix 2

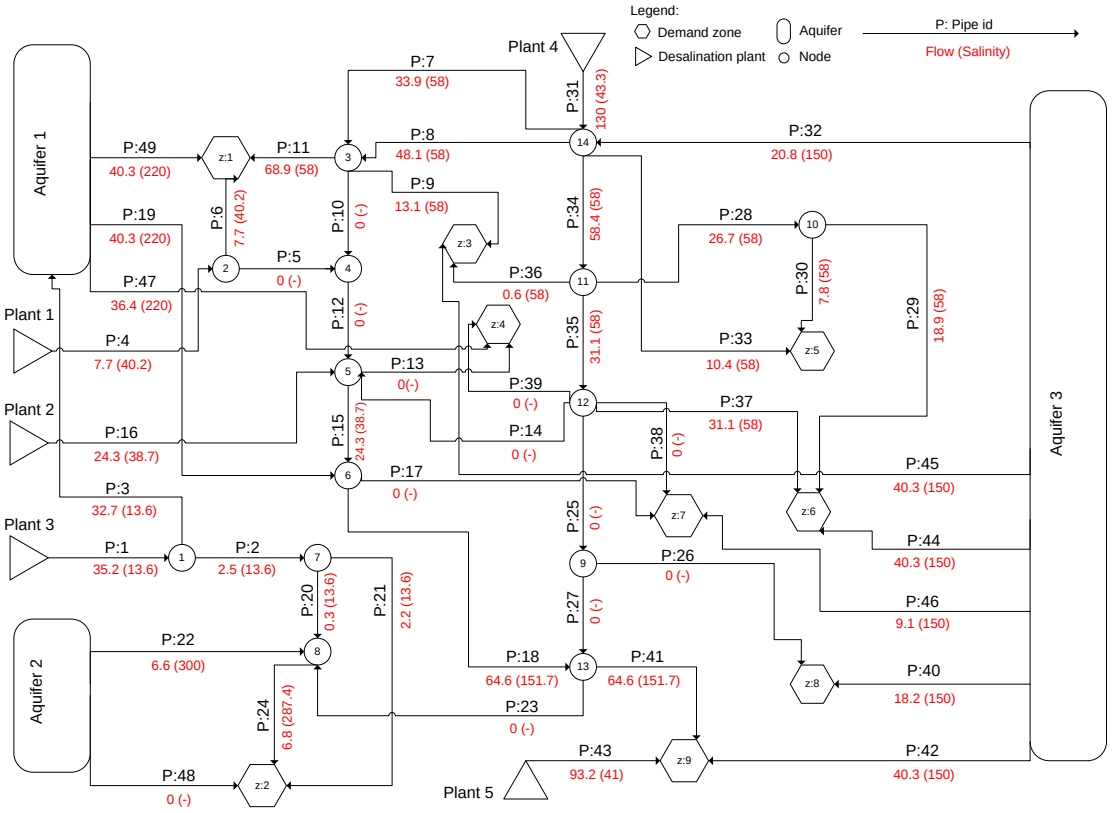

Figure 1: SA1, Season 1 results - flow (MCM) and salinity $(mgcl/lit)$ distribution. (All values have been rounded to one decimal place)

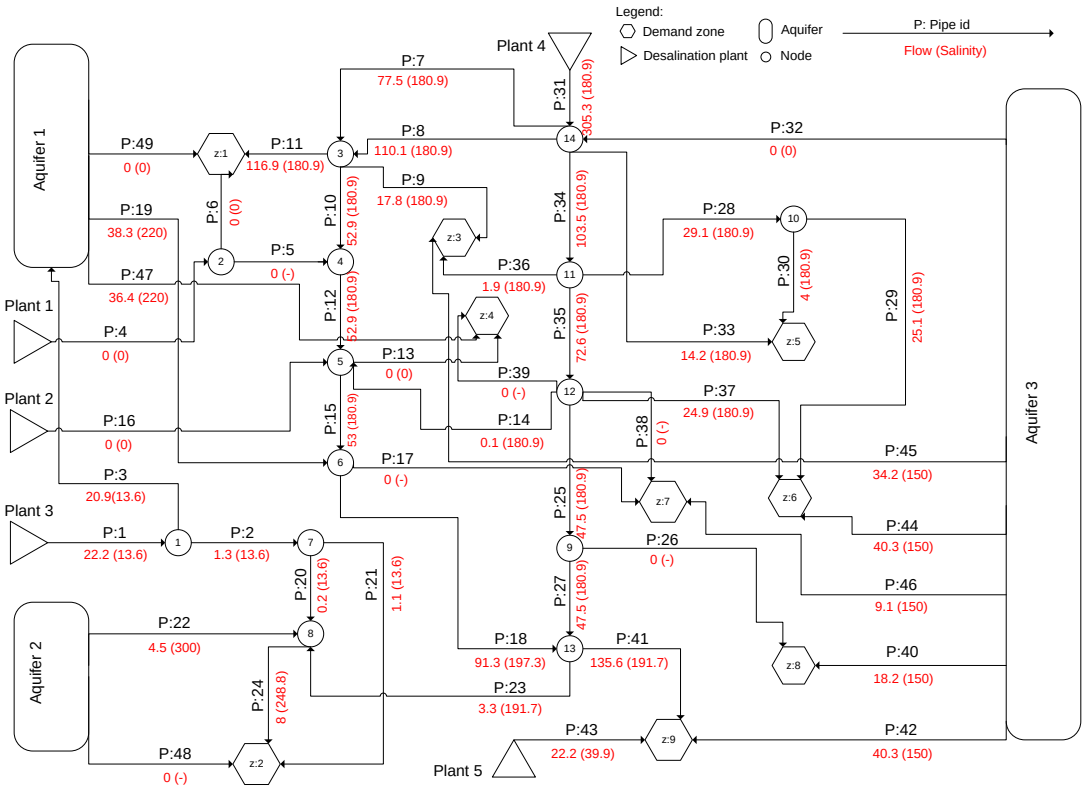

Figure 2: SA2, Season 1 results - flow (MCM) and salinity $(mgcl/lit)$ distribution. (All values have been rounded to one decimal place)

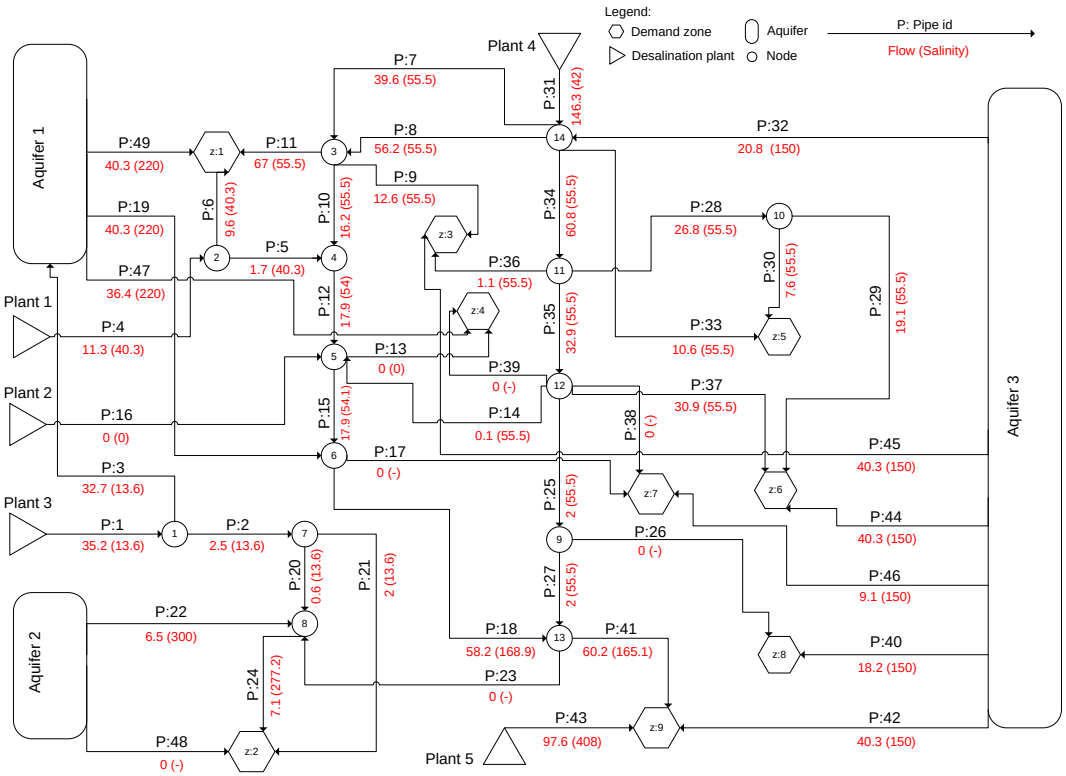

Figure 3: SA3, Season 1 results - flow (MCM) and salinity $(mgcl/lit)$ distribution. (All values have been rounded to one decimal place)

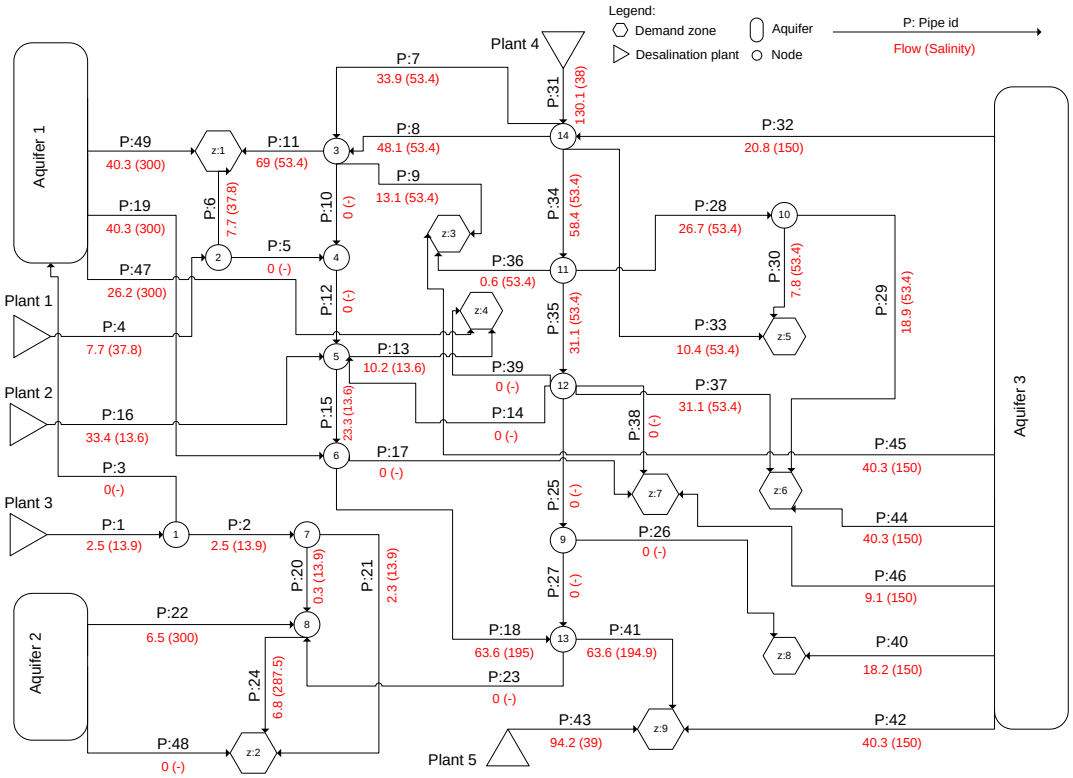

Figure 4: SA3, Season 1 results - flow (MCM) and salinity $(mgcl/lit)$ distribution. (All values have been rounded to one decimal place)

10. References

Ajami, N.K., Hornberger, G.M., and Sunding, D.L., (2008), Sustainable water resource management under hydrological uncertainty, *Water Resources Research*, 44(11).

Babayan, A.V., Savic, D. A., Walters, G.A., and Kapelan, Z.S., (2007), Robust Least-Cost Design of Water Distribution Networks Using Redundancy and Integration-Based Methodologies, *Journal of Water Resources Planning and Management*, 133(1), 67–77.

Babayan, A.V., Savic, D.A., Walters, G.A., and Kapelan, Z.S., (2005), Least-Cost Design of Water Distribution Networks under Demand Uncertainty, *Journal of Water Resources Planning and Management*, 131(5), 375–382.

Barros, M., Tsai, F., Yang, S.-L., Lopes, J., and Yeh, W., (2003), Optimization of large-scale hydropower system operations, *Journal of Water Resources Planning and Management*, 129(3), 178–188.

Benders, J.F., (1962), Partitioning procedures for solving mixed variables programming problems, *Numerische Mathematik*, 4, 238-252.

Ben-Haim, Y., (2006), Info-Gap Decision Theory: Decisions Under Severe Uncertainty, *2nd edition, Academic Press*, London.

Ben-Tal, A., and Nemirovski, A., (1998), Robust Convex Optimization, *Mathematics of Operation Research*, 23(4), 769-805.

Ben-Tal, A., and Nemirovski, A., (1999), Robust solutions to uncertain linear programs, *Operations Research Letters*, 25, 1-13.

Ben-Tal, A., and Nemirovski, A., (2000a), Robust solutions of linear programming problems contaminated with uncertain data, *Mathematical Programming*, 88, 411-421.

Ben-Tal, A., El Ghaoui, L., and Nemirovski, A., (2009), Robust Optimization, *Princeton University Press*.

Ben-Tal, A., Margalit, T., and Nemirovski, A., (2000b), Robust modeling of multi-stage portfolio problems, Chapter 12 in High Performance Optimization, H. Frank et al. (eds.), Kluwer Academic Press, Potterdam, 303-328.

Bertsimas, D., and Thiele, A., (2006), A robust optimization approach to supply chain management, *Operations Research*, 54(1), 150-168.

Betts, J.T., (2004), Practical methods for optimal control using nonlinear programming. *SIAM 2001*, Philadelphia

Bienstock, D., and Ozbay, N., (2008), Computing robust base stock levels, *Discrete Optimization*, 5(2), 389-414.

Birge, J.R., and Louveaux, F.V., (1997), Introduction to Stochastic Programming, *Springer-Verlag*, New York.

Boulos, P., and Altman, T., (1991), A graph-theoretic approach to explicit nonlinear pipe network optimization. *Applied Mathematical Modelling*, 15(9), 459-466.

Boulos, P.F., Lansey, K.E., and Karney, B.W., (2006). Comprehensive water distribution systems analysis handbook for engineers and planners. *MWH Soft.*

Brekke, L.D., Maurer, E.P., Anderson, J.D., Dettinger, M.D., Townsley, E.S., Harrison, A., and Pruitt T., (2009), Assessing reservoir operations risk under climate change, *Water Resources Research*, 45(4).

Byrd, R.H., Gilbert, J.C., and Nocedal, J., (2000), A trust region method based on interior point techniques for nonlinear programming. *Mathematical Programming*, Series B, 89(1), 149-185.

Cai, X., McKinney, D., and Lasdon, L., (2001), Solving nonlinear water management models using a combined genetic algorithm and linear programming approach, *Advances in Water Resources*, 24(6), 667–676.

Chan, P., Hui, C., Li, W., Sakamoto, H., Hirata, K., and Li, P., (2006), Long-term Electricity Contract Optimization with Demand Uncertainties, *Energy*, 31(13), 2133-2149.

Cohen, D., Shamir, U., and Sinai, G., (2000), Optimal operation of multi-quality water supply systems-I: Introduction and the Q-C model, *Engineering Optimization*, 32(5), 549-584.

Crawley, P., and Dandy, G., (1993), Optimal operation of multiple reservoir system, *Journal of Water Resources Planning and Management*, 119(1), 1–17.

Draper, A.J., Jenkins, M.W., Kirby, K.W., Lund, J.R., Howitt, R.E., (2003), Economic-engineering optimization for California water management, *Journal of Water Resources Planning and Management*, 129(3), 155-164.

Draper, A.J., Munévar, A., Arora, S.K., Reyes, E., Parker, N.L., Chung, F.I., Peterson, L.E., (2004), CalSim: Generalized model for reservoir system analysis, *Journal of Water Resources Planning and Management*, 130(6), 480-489.

Dupačová, J., (1995). Multistage Stochastic Programs: the State–of–the–Art and Selected Bibliography. *Kybernetika*, 31(2), 151–174.

Dupačová, J., Consigli, G., and Wallace, S.W., (2000), Scenarios for Multistage Stochastic Programs, *Annals of Operations Research*, 100, 25–53.

Dupačová, J., Gröwe-Kuska, N., and Römisch, W., (2003), Scenario Reduction in Stochastic Programming, *Mathematical Programming*, 95(3), 493–511.

Dupačová, J., and Sladký, K., (2002), Comparison of multistage stochastic programs with recourse and stochastic dynamic programs with discrete time, *ZAMM-Zeitschrift fur Angewandte Mathematik und Mechanik*, 82, 753-765.

Dupačová, J., Gaivoronski, A., Kos, Z., and Szantai, T., (1991), Stochastic programming in water management: A case study and a comparison of solution techniques, *European Journal of Operational Research*, 52, 28–44.

Faber, B.A., and Stedinger, J.R., (2001), Reservoir optimization using sampling SDP with ensemble stream flow prediction forecasts, *Journal of Hydrology*, 249(1-4), 113-133.

Filion, Y.R., Adams, B.J., and Karney, B.W., (2007), Stochastic Design of Water Distribution Systems with Expected Annual Damages, *Journal of Water Resources Planning and Management*, 133(3), 244–252.

Fisher, F.M., Arlosoroff, S., Eckstein, Z., Haddadin, M., Hamati, S.G., Huber-Lee, A., Jarrar, A., Jauuousi, A., Shamir, U., and Wesseling, H., (2002), Optimal water management and conflict resolution: The middle east water project, *Water*

Resources Research, 38(11), 251-2517.

Fletcher, R., (1985), Practical methods of optimization. Constrained Optimization, Vol. 2. *John Wiley & Sons*, New York.

González, J., Romera, R., Carretero, J., and Perez, J., (2006), Optimal Railway Infrastructure Maintenance And Repair Policies To Manage Risk Under Uncertainty With Adaptive Control, *Statistics and Econometrics Working Papers*, Universidad Carlos III.

Grantz, K., Rajagopalan, B., Zagona, E., and Clark, M., (2007), Water management applications of climate-based hydrologic forecasts: Case study of the Truckee-Carson river basin, *Journal of Water Resources Planning and Management*, 133(4), 339-350.

Gülpinar, N., Rustem, B., and Settergren, R., (2004), Simulation and optimization approaches to scenario tree generation, *Journal of Economic Dynamics and Control*, 28, 1291-1315.

Heitsch, H., and Romisch, W., (2005), Generation of multivariate scenario trees to model stochasticity in power management, *IEEE St. Petersburg Power Tech*.

Hiew, K., Labadie, J., and Scott, J., (1989), Optimal operational analysis of the Colorado-Big Thompson project, *Computerized decision support systems for water managers*, J. Labadie et al., eds., ASCE, Reston, Va., 632–646.

Hipel, K.W., and Ben-Haim, Y., (1999), Decision making in an uncertain world: Information-gap modeling in water resources management, *IEEE Transactions on Systems*, 29(4), 506-517.

Huang, G. H., Chi, G.F., and Li, Y.P., (2005), Long-term planning of an integrated solid waste management system under uncertainty-I model development, *Environmental Engineering Science*, 22(6), 823-834.

Huang, G.H., Baetz, B.W., and Patry, G.G., (1994), Grey dynamic programming for solid waste management planning under uncertainty, *Journal of Urban Planning and Development*, 120(3), 132–156.

Jenkins, M.W., Lund, J.R., Howitt, R.E., Draper, A.J., Msangi, S.M., Tanaka, S.K., Ritzema, R.S., and Marques, G.F., (2004), Optimization of California's water supply system: Results and insights, *Journal of Water Resources Planning and Management*, 130(4), 271-280.

Jido, M., Otazawa, T., and Kobayashi, K., (2008), Optimal repair and inspection rules under uncertainty. *Journal of Infrastructure Systems*, 14(2), 150-158.

Kapelan, Z., Savic, D.A., and Walters, G.A., (2005), Multiobjective Design of Water Distribution Systems under Uncertainty, *Water Resources Research*, 41, W11407, doi:10.1029/2004WR003787.

Kasprzyk, J.R., Reed, P.M., Kirsch, B.R., and Characklis, G.W., (2009), Managing population and drought risks using many-objective water portfolio planning under uncertainty. *Water Resources Research*, 45(12).

Kracman, D.R., McKinney, D.C., Watkins Jr., D.W., and Lasdon, L.S., (2006), Stochastic optimization of the highland lakes system in Texas, *Journal of Water Resources Planning and Management*, 132(2), 62-70.

Labadie, J. W., (2004), Optimal operation of multi-reservoir systems: State-of-the-art

review, *Journal of Water Resources Planning and Management*, 130(2), 93-111.

Lal, A.M.W., Obeysekera, J., and Van Zee, R., (1997), Sensitivity and uncertainty analysis of a regional simulation model for the natural system in south Florida, paper presented at the 27th Congress of the IAHR and the ASCE, San Francisco, pp. 560-565.

Lansey, K.E., Duan, N., Mays, L.W., and Tung, Y.K., (1989), Water distribution system design under uncertainties, *Journal of Water Resources Planning and Management*, 115(5), 630-645.

Latorre, J.M., Cerisola, S., and Ramos, A., (2007), Clustering algorithms for scenario tree generation: Application to natural hydro inflows, *European Journal of Operational Research*, 1339-1353.

Li, Y.P., Huang, G.H., and Baetz, B.W., (2006), Environmental management under uncertainty - an internal-parameter two-stage chance-constrained mixed integer linear programming method, *Environmental Engineering Science*, 23(5), 761-779.

Li, Z., and Ierapetritou, M.G., (2008), Robust optimization for process scheduling under uncertainty, *Industrial & Engineering Chemistry Research*, 47, 4148-4157.

Liik, O., Valdma, M., Keel, M., and Tammoja, H., (2004), Optimization of electricity production capacity under uncertainty, *International Energy Workshop*, International Energy Agency (IEA), Paris, France.

Lobo, M.S., and Boyd., S., (2000), The worst-case risk of a portfolio, Working Paper

Loucks, D.P., (2000), Sustainable water resources management, *Water International*, 25(1), 3-10.

Loucks, D.P., Stedinger, J.R., and Haith, D.A., (1981), Water resource systems planning and analysis, *Prentice-Hall*, Englewood Cliffs, N.J.

Lund, J.R., and Ferreira, I., (1996), Operating rule optimization for Missouri river reservoir system, *Journal of Water Resources Planning and Management*, 122(4), 287-295.

Markowitz, H., (1959), Portfolio Selection, *Yale University Press*, New Haven, Connecticut.

Mehrez, A., Percia, C. and Oron, G., (1992), Optimal operation of a multisource and multiquality regional water system, *Water Resources Research, 28*(5), 1199-1206.

Minville, M., Brissette, F., and Leconte, R., (2010), Impacts and Uncertainty of Climate Change on Water Resource Management of the Peribonka River System (Canada), *Journal of Water Resources Planning and Management*, 136, 376, doi:10.1061/(ASCE)WR.1943-5452.0000041

Mudchanatongsuk, S., Ord´onez, F., and Zhao, J., (2005), Robust solutions for network design under transportation cost and demand uncertainty, *Technical report*, University of Southern California.

Mulvey, J.M., and Ruszczynski, A., (1995), A new scenario decomposition method for

large-scale stochastic optimization, *Operation Research*, 43(3), 477-490.

Mulvey, J.M., Vanderbei, R.J., and Zenios, S.A., (1995), Robust Optimization of Large-Scale Systems, *Operations Research*, 43(2), 264-281.

Nicklow, J., Reed, P., Savic, D., Dessalegne, T., Harrell, L., Chan-Hilton, A., Karamouz, M., Minsker, B., Ostfeld, A., Singh, A., and Zechman, E., (The ASCE Task Committee on Evolutionary Computation in Environmental and Water Resources Engineering), 2010. State of the art of genetic algorithms and beyond in water resources planning and management, *Journal of Water Resources Planning and Management, 136(4), 412-432*.

Ostfeld, A., and Shamir, U., (1993), Optimal operation of multi-quality networks. I: Steady-state conditions, *Journal of Water Resources Planning and Management*, 119(6), 645-662.

Pallottino, S., Sechi, G.M., and Zuddas, P., (2005), A DSS for water resources management under uncertainty by scenario analysis, *Environmental Modelling and Software*, 20(8), 1031-1042.

Peng, C.S., and Buras, N., (2000), Practical estimation of inflows into multireservoir system, *Journal of Water Resources Planning and Management*, 126(5), 331–334.

Philbrick, C.R., and Kitanidis, P.K., (1999), Limitations of deterministic optimization applied to reservoir operations, *Journal of Water Resources Planning and Management*, 125(3), 35–142.

Rockafellar, R.T., and Wets, R.J.B., (1991), Scenarios and policy aggregation in optimization under uncertainty, *Mathematics of Operations Research*, 16, 119-147.

Sahinidis, N.V., (2004), Optimization under uncertainty: State-of-the-art and opportunities, *Computers and Chemical Engineering*, 28(6), 971-983.

Sankarasubramanian, A., Lall, U., Souza, F., Filho, A., and Sharma, A., (2009), Improved water allocation utilizing probabilistic climate forecasts: Short-term water contracts in a risk management framework, *Water Resources Research*, 45, W11409

Schwarz, J., Meidad, N., and Shamir, U., (1986), Incorporation of quality in the TKUMA Model, TAHAL Report for the Water Commission (Hebrew).

Seifi, A., and Hipel, K., (2001), Interior-point method for reservoir operation with stochastic inflows, *Journal of Water Resources Planning and Management*, 127(1), 48–57.

Shamir, U., (1971), A Hierarchy of Models for Optimizing the Operation of Water Systems, *Symposium on The Water Environment and Human Needs*, MIT.

Shapiro, A., Dentcheva, D., and Ruszczynski, A., (2009), Lectures on Stochastic Programming: Modeling and Theory, *SIAM, Philadelphia*.

Soyster, A.L., (1973), Convex Programming with Set-Inclusive Constraints and Applications to Inexact Linear Programming, *Operations Research* 1154-1157.

Sutiene, K., Makackas, D., and Pranevičius, H., (2010), Multistage K-Means

Clustering for Scenario Tree Construction, *Informatica*, 21(1), 123-138.

Tol, R.S.J., (1998), Short-term decisions under long-term uncertainty. Energy Economics, 20(5), 557-569.

Tu, M., Tsai, F.T. and Yeh, W.W., (2005), Optimization of water distribution and water quality by hybrid genetic algorithm. *Journal of Water Resources Planning and Management, 131*(6), 431-440.

Vasiliadis, H., and Karamouz, M., (1994), Demand-driven operation of reservoirs using uncertainty-based optimal operating policies, *Journal of Water Resources Planning and Management*, 120(1), 101–114.

Wagner, B.J., (1999), Evaluation of data worth for ground water management under, *Journal of Water Resources Planning and Management*, 125(5), 281–288.

Waltz, R.A., Morales, J.L., Nocedal, J., and Orban, D., (2006), An interior algorithm for nonlinear optimization that combines line search and trust region steps. *Mathematical Programming*, 107(3), 391-408.

Water Commission, Planning Division, (2002), National Master Plan (Transition) 2002-2010 (Hebrew).

Water Commission, Planning Division, by TAHAL, (2003), Aggregative Model for Management the Israeli Water Sector (Hebrew).

Watkins Jr., D.W., Kirby, K.W., and Punnett, R.E., (2004), Water for the everglades: Application of the south Florida systems analysis model, *Journal of Water Resources Planning and Management*, 130(5), 359-366.

Watkins, D. W., and McKinney, D. C., (1997), Finding Robust Solutions to Water Resources Problems, *Journal of Water Resources Planning and Management*, 123(1), 49-58.

Wendt, M., Li, P., and Wozny, G., (2002), Nonlinear Chance-Constrained Process Optimization under Uncertainty, *Industrial & Engineering Chemistry Research*, 41(15), 3621–3629.

Wong, H.S., and Yeh, W.W., (2002), Uncertainty analysis in contaminated aquifer management. *Journal of Water Resources Planning and Management, 128*(1), 33-45.

Wu, J., Zou, R., and Yu, S.L., (2006), Uncertainty analysis for coupled watershed and water quality modeling systems. *Journal of Water Resources Planning and Management, 132*(5), 351-361.

Xu, C., and Goulter, I. C., (1998), Probabilistic model for water distribution reliability, *Journal of Water Resources Planning and Management*, 124(4), 218–228.

Yamout, G.M., Hatfield, K., and Romeijn, H.E., (2007), Comparison of new conditional value-at-risk-based management models for optimal allocation of uncertain water supplies, *Water Resources Research*, (119).

Yates, D., Sieber, J., Purkey, D., and Huber-Lee, A., (2005), WEAP21 - A demand priority and preference-Driven water planning model. part 1: Model characteristics. *Water International, 30*(4), 487-500.

Yeh, W., (1985), Reservoir management and operations models: A state-of-the-art

review. *Water Resources Research*, 21(12), 1797-1818.

Young, G., (1967), Finding reservoir operating rules, *Journal of Hydraulics Division*, 93(6), 297–321.

Zaide, M., (2006), A model for multiyear combined optimal management of quantity and quality in the Israeli national water supply system. M.Sc thesis, Technion – I.I.T. http://urishamir.wri.technion.ac.il/

Zhao, T., and Fu, C.C., (2006), Infrastructure development and expansion under uncertainty: A risk-preference-based lattice approach, *Journal of Construction Engineering and Management*, 132(6), 620-625.